

**UNIVERSITY OF SOUTHAMPTON**

FACULTY OF MEDICINE

Cancer Sciences Unit

Volume 1 of 1

**Impact of Target Antigen Properties on Antibody Effector Mechanisms**

by

**Kirstie Lorraine Siân Cleary**

Thesis for the degree of Doctor of Philosophy

September 2015



UNIVERSITY OF SOUTHAMPTON

## **ABSTRACT**

FACULTY OF MEDICINE

Biomedicine

Thesis for the degree of Doctor of Philosophy

### **IMPACT OF TARGET ANTIGEN PROPERTIES ON ANTIBODY EFFECTOR MECHANISMS**

Kirstie Lorraine Siân Cleary

Monoclonal antibody (mAb) immunotherapy has proven effective in the treatment of haematological malignancies. Antibodies towards unique epitopes within the same antigen can engage different effector mechanisms to facilitate cell clearance. Understanding what drives the engagement of these mechanisms is important for the development of new therapeutics. This thesis investigated the role of the antigen, in particular the epitope bound by a mAb in defining the effector mechanisms engaged. Specifically, the role of distance between the epitope and the target cell membrane in relation to the engagement of the effector mechanisms; complement dependent cytotoxicity (CDC), antibody dependent cellular phagocytosis (ADCP) and antibody dependent cellular cytotoxicity (ADCC) were assessed.

A panel of model antigens were generated; incorporating the same epitope for a clinically relevant mAb attached to the N-terminus of various CD137 constructs. Extracellular domains of CD137 were removed or added in order to change the distance of the clinically relevant epitope from the cell membrane. These constructs were transfected into CHO-S and A20 cells and tested *in vitro* to assess the engagement of the three aforementioned effector mechanisms. It was found that the engagement of CDC and ADCC was diminished when targeting the largest (8-domain) construct (therefore most distal from the membrane), whilst ADCP was impaired with the smallest (membrane-flush) construct and required the presence of at least one extracellular domain for activity. However, ADCP engagement was restored when the membrane-flush epitope was tethered to the membrane via a GPI anchor rather than a transmembrane peptide domain. These findings were confirmed using two separate epitopes targeted by rituximab and CAMPATH-1H antibodies.

Finally, the therapeutic response when targeting either the membrane-flush or 8-domain constructs was investigated *in vivo*. Mice who received A20 cells expressing the membrane-flush construct exhibited clearance of tumour in the spleen following antibody therapy, whilst those that received tumours expressing the 8-domain construct did not respond to therapy. Together the work in this thesis demonstrates how the effector mechanisms engaged by a mAb can be altered dependent on the position of the epitope in relation to the cell membrane.



# Table of Contents

<b>Table of Contents</b>	<b>i</b>
<b>List of Figures</b>	<b>v</b>
<b>List of Tables</b>	<b>viii</b>
<b>Declaration of Authorship</b>	<b>ix</b>
<b>Acknowledgements</b>	<b>x</b>
<b>Abbreviations</b>	<b>xi</b>
<b>Chapter 1: Literature Review</b>	<b>1</b>
<b>1.1 Cancer as a Disease:</b>	<b>1</b>
1.1.1 Associated risk factors:	2
1.1.2 Hallmarks of cancer:	3
<b>1.2 The Immune System:</b>	<b>7</b>
1.2.1 B cells:	8
1.2.2 T cells:	10
1.2.3 Natural Killer cells:	11
1.2.4 Monocytes and Macrophages:	12
1.2.5 Dendritic Cells:	13
1.2.6 Neutrophils:	13
<b>1.3 Cancer Therapy:</b>	<b>14</b>
<b>1.4 Immunotherapy:</b>	<b>16</b>
1.4.1 Active immunotherapy:	16
1.4.2 Passive immunotherapy:	18
1.4.2.1 Cytokine therapy:	18
1.4.2.2 Adoptive cell therapy:	18
1.4.2.3 Monoclonal antibody immunotherapy:	19
<b>1.5 Monoclonal Antibodies:</b>	<b>20</b>
1.5.1 Antibody structure and nomenclature:	20
1.5.2 Generation of antibody diversity:	23
<b>1.6 Monoclonal Antibody Production:</b>	<b>25</b>
1.6.1 Immunisation and hybridoma technology:	25
1.6.2 Recombinant engineering / cell transfection:	26
1.6.3 Immunisation of humanised mice:	27
1.6.4 Phage display library:	28

1.6.5 Post-translational modification of antibodies:	28
<b>1.7 Direct Targeting mAb Effector Mechanisms:</b>	<b>29</b>
1.7.1 Cell-intrinsic effector mechanisms:	30
1.7.2 Cell signal disruption:	31
1.7.3 Direct cell death:	31
1.7.4 Cell-extrinsic effector mechanisms:	33
1.7.5 Fc receptor independent mechanisms:	33
1.7.5.1 Complement cascade:	33
1.7.5.2 Regulation of the complement cascade:	36
1.7.5.3 Complement Dependent Cytotoxicity in mAb immunotherapy:	37
1.7.6 Fc receptor dependent mechanisms:	39
1.7.7 Fcγ receptors:	39
1.7.7.1 FcγR polymorphisms:	41
1.7.7.2 FcγR in mAb immunotherapy:	43
1.7.7.3 FcγR signalling:	43
1.7.8 Antibody Dependent Cellular Cytotoxicity:	44
1.7.9 Antibody Dependent Cellular Phagocytosis:	45
<b>1.8 CD20 and its Antibodies:</b>	<b>46</b>
1.8.1 Human CD20:	46
1.8.2 Rituximab:	48
1.8.3 Type I and II anti-CD20 mAbs:	48
<b>1.9 CD52 and CAMPATH-1H:</b>	<b>50</b>
1.9.1 Human CD52:	50
1.9.2 CAMPATH-1H	51
<b>1.10 Antigen Properties Which May Influence mAb Engagement of Effector Mechanisms:</b>	<b>52</b>
1.10.1 Antigen density:	54
1.10.2 Distance of epitope from cell membrane:	54
1.10.3 Properties of the antibody:epitope interaction:	56
1.10.4 Antigen mobility within the cell:	56
1.10.4.1 Lipid raft localisation:	56
1.10.4.2 Internalisation/Modulation:	57
<b>1.11 Hypothesis and Aims of Thesis:</b>	<b>58</b>
<b>Chapter 2: Methodology</b>	<b>61</b>
<b>2.1 Cell culture:</b>	<b>61</b>

2.1.1 Tissue culture conditions:	61
2.1.2 Differentiation of bone marrow derived macrophages (BMDM)	62
2.1.3 Peripheral Blood Mononuclear Cell isolation	62
2.1.4 Serum preparation from whole blood:	62
<b>2.2 Molecular biology techniques:</b>	<b>62</b>
2.2.1 cDNA templates:	62
2.2.2 Polymerase Chain Reaction (PCR)	63
2.2.3 DNA Sequencing	63
2.2.4 Site-directed mutagenesis	64
2.2.5 Agarose Gel electrophoresis	64
2.2.6 DNA gel extraction and purification	65
2.2.7 Restriction enzyme digests	65
2.2.8 Ligations	65
2.2.9 Heat Shock Transformation	65
2.2.10 Plasmid DNA miniprep and maxipreps	66
<b>2.3 Protein expression and analysis:</b>	<b>66</b>
2.3.1 Mammalian cell transfections	66
2.3.2 Nucleofection:	66
2.3.3 Electroporation:	67
2.3.4 Antibody Fluorescein-Isothiocyanate (FITC) conjugation:	67
2.3.5 Antibody labelling of cells for flow cytometry	68
2.3.6 Data acquisition by flow cytometry	68
2.3.7 Preparation of mammalian cell lysates:	68
2.3.8 Bradford Assay:	68
2.3.9 SDS-PAGE:	69
2.3.10 Western Blot	69
<b>2.4 Functional assays to assess antibody efficacy:</b>	<b>69</b>
2.4.1 Complement Dependent Cytotoxicity (CDC) assay	69
2.4.2 Antibody dependent Cellular Phagocytosis (ADCP) assay	70
2.4.3 Antibody Dependent Cellular Cytotoxicity (ADCC) assay	70
<b>2.5 In vivo techniques:</b>	<b>71</b>
2.5.1 A20 Cell Passage	71
2.5.2 A20 tumour immunotherapy	71
2.5.3 Short term cell transfer	71
<b>2.6 Buffer compositions:</b>	<b>72</b>

<b>Chapter 3: Generation of Model Antigen Constructs to Investigate Distance on mAb Effector Mechanisms</b>	<b>73</b>
3.1 Introduction:	73
3.2 Cloning of Constructs:	75
3.3 Protein expression in mammalian cells:	81
3.4 Troubleshooting the CD52 peptide:CAMPATH-1H interaction	86
3.5 Alternative Epitopes:	92
3.6 Generation of rituximab binding (Rp3-CD137-) constructs:	94
3.7 Chapter Discussion:	98
<b>Chapter 4: <i>In vitro</i> functional assessment of fusion proteins</b>	<b>103</b>
4.1 Expression of constructs in target cells for functional assays:	103
4.2 Complement Dependent Cytotoxicity:	103
4.2.1 293F cells as targets:	103
4.2.2 CHO-S as target cells:	105
4.2.3 Optimising CDC assay:	107
4.3 Phagocytosis assay:	111
4.4 ADCC assay:	116
4.5 Corroborating datasets – Alternative Antibody:Epitope	118
4.6 Production of Stably Transfected Cell Lines:	121
4.7 Chapter Discussion:	127
<b>Chapter 5: Understanding why human CD52 is an effective target for ADCP</b>	<b>133</b>
5.1 Introduction:	133
5.2 CAMPATH-1H is able to phagocytose cells expressing WT-CD52	135
5.3 Investigating the contribution CD52 glycosylation has on the susceptibility to ADCP	137
5.4 Investigating the contribution of the GPI anchor on the susceptibility of CD52 to engage ADCP	139
5.5 Chapter Discussion:	144
<b>Chapter 6: <i>In vivo</i> investigation of the mAb distance from the cell surface hypothesis</b>	<b>147</b>
6.1 Introduction:	147
6.2 Short Term Tracking of A20 cells:	148
6.3 A20 tumour passage:	149
6.4 Antibody Immunotherapy Model:	153
6.5 Chapter Discussion:	158
<b>Chapter 7: Discussion and Future Work</b>	<b>161</b>



<b>Appendices:</b>	<b>169</b>
<b>Appendix A: Primer sequences used for the generation and DNA sequencing of fusion constructs</b>	<b>169</b>
<b>Appendix B: pcDNA4/HisMaxB vector map</b>	<b>171</b>
<b>References:</b>	<b>173</b>

## List of Figures

Figure 1.1: B cell maturation stages and phenotypic markers .....	8
Figure 1.2: General antibody structure.....	21
Figure 1.3: V(D)J recombination and class switch recombination for formation of complete immunoglobulin heavy chain.....	25
Figure 1.4: Schematic of depletion mechanisms that are potentially engaged after cells are bound by a mAb.....	30
Figure 1.5: Schematic of Classical Complement Pathway: .....	34
Figure 1.6: Alternative complement pathway diagram.....	35
Figure 1.7: Summary of FcγR family in humans and mice .....	41
Figure 1.8: Illustration of ADCC activation of FcγR engagement .....	45
Figure 1.9: Illustration of CD20 structure .....	47
Figure 1.10: Epitopes of therapeutic anti-CD20 mAbs .....	49
Figure 3.1: Model of CD137 and the proposed fusion proteins for use throughout thesis project .....	75
Figure 3.2: Schematic of overlap PCR technique to produce CD52- CD137 fusion constructs...	76
Figure 3.3: Generation of fusion proteins by overlap PCR .....	77
Figure 3.4: pCR-Blunt II-TOPO cloning vector map .....	78
Figure 3.5: EcoRI digest of JM109 colonies transformed with CD52-137 fusion genes ligated into TOPO-Blunt vector.....	79
Figure 3.6: pcDNA3.1/- expression vector map.....	80
Figure 3.7: Generation of the CD52-137-8d construct by overlap PCR .....	81
Figure 3.8: Gating strategy used to analyse cell surface expression of proteins in transfected 293F cells.....	83
Figure 3.9: Summary data of fusion protein expression on the surface of 293F cells 24 hours after transfection .....	84

Figure 3.10: Measuring CAMPATH-1H binding of 293F cells transfected with CD52-137 fusion proteins .....	85
Figure 3.11: CAMPATH-1H recognises wild type CD52 expressed on Raji and Ramos cell lines	86
Figure 3.12: Generation of CD52-flush and CD52-His-4d constructs by overlap PCR .....	88
Figure 3.13: Surface expression of CD52-flush and CD52-His-4d constructs on 293F cells. ....	89
Figure 3.14: Expression of His-CD52-137-4domain on transfected 293F cells.....	90
Figure 3.15: DNA sequencing traces confirming point mutations to create the proline mutants SADPL and SPDAL .....	91
Figure 3.16: 293F cells transfected with either CD52-SADPL or CD52-SPDAL mutants .....	92
Figure 3.17: Restriction digest confirming Cp11-CD137 fusion protein ligation into expression vector pcDNA3.1/-.....	93
Figure 3.18: CAMPATH-1H binds Cp11-CD137 fusion proteins expressed in 293F cells.....	94
Figure 3.19: Illustration of rituximab epitope containing constructs, Rp3-CD137.....	95
Figure 3.20: Rp3-CD137 fusion protein surface expression in 293F cells. ....	97
Figure 3.21: Western Blot for Rp3-CD137 fusion proteins from transfected CHO-S cell lysates	98
Figure 4.1: Gating used to analyse flow cytometry data from CDC assay.....	104
Figure 4.2: Serum titration of Rp3-CD137-4d transfected 293F cells. ....	105
Figure 4.3: Serum titration of pcDNA3.1/- transfected CHO-S cells.....	106
Figure 4.4: Rp3-CD137 constructs expressed in CHO-S cells.....	106
Figure 4.5: Rp3-CD137-4d transfected CHO-S cells produce an antibody dependent response in CDC assay.....	107
Figure 4.6: Serum titration of Rp3-CD137-4d transfected CHO-S cells opsonised with rituximab .....	108
Figure 4.7: Transfection efficiency for CHO-S cells with each of the Rp3-CD137 fusion proteins. ....	109
Figure 4.8: Normalisation of data to allow inter-assay comparison .....	110
Figure 4.9: Collated CDC assay results from CHO-S transfected cells after rituximab opsonisation. ....	111
Figure 4.10: BMDM differentiation from mouse bone marrow .....	112
Figure 4.11: Gating used to analyse flow cytometry data collected from ADCP assay.....	113
Figure 4.12: Effect of incubation time on the phagocytosis of Rp3-CD137-4d transfected CHO-S cells.....	114
Figure 4.13: Dose dependent phagocytosis assay using CHO-S cells transfected with Rp3-CD137-4d construct.....	115

Figure 4.14: Collated ADCP assay results from CHO-S transfected cells after rituximab opsonisation.....	116
Figure 4.15: Analysis of ADCC assay data from fluorescence units into percentage of maximum lysis.....	117
Figure 4.16: ADCC results for CHO-S cells transfected with Rp3-CD137 fusion proteins .....	118
Figure 4.17: CDC Assay Results for CHO-S cells transfected with Cp11-CD137 fusion proteins. ....	119
Figure 4.18: ADCP Assay Results for Cp11-CD137 constructs in CHO-S cells .....	120
Figure 4.19: ADCC Assay results for Cp11-CD137 transfected CHO-S cells .....	121
Figure 4.20: Expression of Rp3-CD137 fusion proteins on A20 cells after transfection and selection .....	123
Figure 4.21: Confirmation of protein expression in A20 stable transfectants.....	124
Figure 4.22: <i>In vitro</i> assessment of CDC with stable transfected A20 cells expressing Rp3-CD137 constructs.....	125
Figure 4.23: Assessment of ADCP using Rp3-CD137 stable expressing A20 cells.....	125
Figure 4.24: Assessment of ADCC using Rp3-CD137 stable expressing A20 cells.....	126
Figure 4.25: ADCC assay of A20 cells using murine NK cells as effectors .....	127
Figure 5.1: Comparison of Cp11-flush and CD52 mature peptides: .....	135
Figure 5.2: CAMPATH-1H is able to engage ADCP when targeting human B cells .....	136
Figure 5.3: Susceptibility for ADCP is different between CD52 and Cp11-flush .....	137
Figure 5.4: Generation and expression of CD52-NQ in CHO-S cells.....	138
Figure 5.5: ADCP assay results of Cp11-flush, CD52 and CD52-NQ transfected CHO-S cells following CAMPATH-1H opsonisation .....	139
Figure 5.6: Generation and expression of Cp11-GPI construct in CHO-S cells: .....	140
Figure 5.7: Confirmation of Cp11-GPI anchoring by PI-PLC treatment.....	141
Figure 5.8: Attaching Cp11 peptide to GPI anchor is able to restore ADCP engagement. ....	142
Figure 5.9: Attachment of the Rp3 peptide to a GPI anchor also restores susceptibility towards ADCP. ....	143
Figure 6.1: Short term Tracking of CFSE labelled A20 cells in whole blood.....	149
Figure 6.2: Phenotype of Rp3-CD137-4d transfected A20 cells by flow cytometry .....	150
Figure 6.3: Example of flow cytometry analysis used to quantify A20 cell line passage .....	151
Figure 6.4: Surface expression of Rp3-CD137 fusion constructs on A20 tumour cells following <i>in vivo</i> passage .....	152
Figure 6.5: A20 tumour formation after passage into WT BALB/c mice .....	153
Figure 6.6: Transfected A20 cells response to rituximab therapy in WT BALB/c mice.....	155

Figure 6.7: Tracking A20 clearance in response to rituximab therapy at days 10, 16 and 24...	157
Figure 7.1: Summary of how distance from the cell membrane impacts the mAb effector mechanisms engaged .....	167

## List of Tables

Table 1.1: Incidence of haematological malignancies within the United Kingdom .....	2
Table 1.2: Hallmarks of Cancer .....	4
Table 1.3: Human FcγR specificity towards human IgG isotypes .....	42
Table 1.4: Mouse FcγR affinity towards mouse IgG antibodies .....	43
Table 1.5: Clinically approved mAbs for cancer immunotherapy .....	53
Table 2.1: Culture conditions for cells used throughout the thesis .....	61
Table 2.2: Thermocycler conditions used for DNA amplification methods .....	63
Table 2.3: Nucleofection conditions for mammalian cell lines .....	67
Table 2.4: Composition of Buffers used throughout thesis.....	72
Table 3.1: Structural modifications made to the CD52-137-4d construct in order to resolve binding of CAMPATH-1H .....	87
Table 3.2: Comparison of human CD52, the modified CD52 peptide present in the fusion protein and the alternative CAMPATH-1H epitope, Cp11 .....	93
Table 3.3: Alignment of gene sequence for the CD52 peptide and Rp3 peptide used to design the mutagenesis primer .....	96
Table 3.4: Viable amino acid substitutions that allow CAMPATH-1H binding .....	100
Table 4.1: Summary of data collated within Chapter 4.....	128

# Declaration of Authorship

I, **Kirstie Lorraine Siân Cleary**, declare that this thesis and the work presented in it are my own and has been generated by me as the result of my own original research.

## **Impact of Target Antigen Properties on Antibody Effector Mechanisms**

I confirm that:

1. This work was done wholly or mainly while in candidature for a research degree at this University;
2. Where any part of this thesis has previously been submitted for a degree or any other qualification at this University or any other institution, this has been clearly stated;
3. Where I have consulted the published work of others, this is always clearly attributed;
4. Where I have quoted from the work of others, the source is always given. With the exception of such quotations, this thesis is entirely my own work;
5. I have acknowledged all main sources of help;
6. Where the thesis is based on work done by myself jointly with others, I have made clear exactly what was done by others and what I have contributed myself;
7. Parts of this work have been published as stated below:

Figures 1.4, 1.9 and 1.10 were originally published as part of a CD20 review article, although they have been modified for presentation within this thesis.

Oldham, R. J., Cleary, K. L. S. & Cragg, M. S. (2014) CD20 and Its Antibodies: Past, Present, and Future. *Forum on Immunopathological Diseases and Therapeutics* **5**: 7-23, doi:10.1615/ForumImmunDisTher.2015014073

Signed: .....

Date:.....

# Acknowledgements

First and foremost I would like to thank my supervisors: To Prof Mark Cragg, for his unstoppable enthusiasm for research and guidance over the years; thank you for never saying “that’s a stupid question” no matter what has been asked, especially when proof-reading reports I have written. Thanks also to Dr Claude Chan, who provided supervision and training in the world of molecular biology, particularly when starting out.

Second to the members of the BRF for training and technical assistance with the *in vivo* experiments performed. A special thanks goes to Vikki Field, for her patience and perseverance when training me to handle mice, I never thought I’d have the confidence to complete it! For a whole variety of reasons, from providing feedback in meetings and presentations, to teaching me the ropes in the laboratory, and generally making it a welcoming place to work, I would like to thank all members of the Antibody & Vaccine group; I have really appreciated the support you have provided.

With regards to supplying reagents used in this thesis I would like to thank Dr Martin Pule and Dr Brian Philip for providing the DNA templates used for the alternative rituximab and CAMPATH-1H epitopes within this project. I would also like to thank Prof Ronald Levy for supplying the A20 anti-Id antibody used. This work would not have been possible without the funding provided by the BBSRC.

For listening (or at least letting me talk at you about science!) I would like to thank my family, who have always been there for me throughout the years. Thanks for all of the support you have given me, providing pep talks, humour and the confidence to pursue a PhD no matter what life has had in store. Last, but by no means least, I would like to thank Ruth, Robert and Muchaala for their support and multiple tea (or capri sun) sessions over the years which have been invaluable to surviving. It wouldn’t have been the same without our catan evenings and the annual Bake off Bake off!

## Abbreviations

ADCC	Antibody dependent cellular cytotoxicity
ADCP	Antibody dependent cellular phagocytosis
AID	activation-induced cytidine deaminase
ALL	Acute Lymphocytic leukaemia
AML	Acute Myeloid Leukaemia
APC	antigen presenting cell
BCR	B cell receptor
BiTE	bispecific T cell engager
BMDM	Bone Marrow Derived Macrophages
BSA	Bovine Serum Albumin
β2M	beta-2 microglobulin
C	Constant domain
CAR	Chimeric antigen receptor
CD	Cluster of Differentiation
CDC	Complement dependent cytotoxicity
cDNA	complementary DNA
CDR	Complementarity Determining Regions
CFSE	Carboxyfluorescein succinimidyl ester
CHOP	cyclophosphamide, doxorubicin, oncovin and prednisolone
CHO-S	Chinese Hamster Ovary Suspension cells
CLL	Chronic lymphocytic leukaemia
CML	Chronic Myeloid Leukaemia
CMV	Cytomegalovirus
CRUK	Cancer Research UK
CSR	class switch recombination
CTLA-4	Cytotoxic T-Lymphocyte Associated Protein 4; CD152
CVF	Cobra Venom Factor
D	diversity domain
DC	Dendritic cell
DCD	Direct cell death
dH <sub>2</sub> O	Distilled Water
DLBCL	Diffuse large B cell Lymphoma
DMEM	Dulbecco's Modified Eagle Medium
DNA	deoxyribose nucleic acid
dNTP	deoxynucleotide triphosphate
DR	death receptor
DRM	Detergent Resistant Microdomains
DZ	dark zone of germinal centre
EBV	Epstein Barr Virus
ECL	enhanced chemiluminescent substrate
EDTA	Ethylene-diamine-tetra-acetic acid
EGFR	Epidermal Growth Factor Receptor
EMA	European Medicines Agency

F(ab)	Fragment, Antigen binding
FACS	fluorescent activated cell sorting
FADD	Fas Activating death domain
Fc	Fragment, Crystallisable
FcγR	Fc gamma Receptor
FcR	Fc Receptor
FCS	Foetal Calf Serum
FDA	Food and Drug Administration
fDC	follicular dendritic cell
FITC	fluorescein isothiocyanate
FL	Follicular Lymphoma
FRET	Förster resonance energy transfer
GC	Germinal Centre
GeoMFI	Geometric Mean Fluorescence Intensity
GM-CSF	granulocyte macrophage - colony stimulating factor
GP	Glutamine and Sodium pyruvate (media supplement)
GPI	Glycosylphosphatidylinositol
GvHD	Graft vs Host disease
HAMA	human anti-mouse antibody
hCD_	human CD protein
HEK	Human embryonic kidney
HPV	Human papilloma virus
ICE	ifosfamide, cisplatin, etoposide
Id	Idiotypic
IFN	interferon
Ig	Immunoglobulin
IL	interleukin
i.p.	intraperitoneal
ISO	Isotype control – same heavy IgG constant domain
ITAM	immunoreceptor tyrosine activation motif
ITIM	immunoreceptor tyrosine inhibitory motif
i.v.	intravenous
J	Junctional domain
KO	Knock-out
LN	Lymph Node
LPS	lipopolysaccharide
LZ	light zone of germinal centre
mAb	monoclonal antibody
MAC	Membrane Attack Complex
MACS	Magnetic-activated cell sorting
MASP	MBL associated serine protease
MBL	Mannose binding lectin
MCA	Methylcholanthrene
mCD_	mouse CD protein
M-CSF	macrophage – colony stimulating factor
MHC	major histocompatibility complex



MHC-I	MHC class I
MHC-II	MHC class II
mRNA	messenger RNA
MZL	Marginal Zone Lymphoma
NETs	neutrophil extracellular traps
NHL	Non-Hodgkin lymphoma
NHS	National Health Service
NK	Natural killer
NO	nitrous oxide
NOD	non-obese diabetic
n.s.	non-significant result after t-test statistical analysis
NSCLC	Non-small cell lung cancer
ORF	open reading frame
PBMC	peripheral blood mononuclear cells
PBS	Phosphate Buffered Saline
PCR	polymerase chain reaction
pDC	plasmacytoid DC
PE	phycoerythrin
PI	Propidium iodide
PI-PLC	Phosphoinositide phospholipase C
PMA	phorbol-myristate-acetate
PS	Penicillin and Streptomycin
RNA	ribose nucleic acid
ROS	reactive oxygen species
RPMI	Roswell Park Memorial Institute (Media)
RR-MS	Relapse-remitting multiple sclerosis
RSS	recombination signal sequence
RT	Room temperature
RT-PCR	Reverse transcriptase polymerase chain reaction
RTX	rituximab
ScFv	Single chain Variable Fragment
SCID	Severe combined immunodeficiency
SD	Standard deviation
SDS-PAGE	Sodium dodecyl-sulfate - Polyacrylamide Gel Electrophoresis
SHM	somatic hypermutation
SLE	Systemic Lupus Erythematosus
SNP	Single nucleotide polymorphism
SRBC	sheep red blood cell
TCR	T cell receptor
T <sub>CM</sub>	Central memory T cell
T:E	Target to effector cell ratio
T <sub>EM</sub>	Effector memory T cell
T <sub>FH</sub>	Follicular helper T cell
TGFβ	transforming growth factor beta
TLR	Toll-like receptor
TNFα	tumour necrosis factor-alpha

TNFR	tumour necrosis factor receptor
T <sub>reg</sub>	Regulatory T cell
UV	Ultraviolet
V	Variable domain
VEGF	Vascular endothelial growth factor
WB	western blot
WHO	World Health Organisation
WT	Wild type
YFP	Yellow fluorescent protein
293F	HEK 293F suspension line – adapted to Life Technologies FreeStyle™ media

# Chapter 1: Literature Review

In the UK fifty percent of the population within their lifetime will be diagnosed with cancer <sup>1</sup>. Cancer encompasses a vast number of different diseases, which are phenotypically unique from one another, that arise as a culmination of mutations which lead to the uncontrolled proliferation of cells and eventually death if left untreated. Presentation of the disease is heterogeneous, where it can remain undetectable until the late stages (such as pancreatic cancer <sup>2</sup>) or in other cases result in clear physical changes that can lead to quick identification and treatment, such as skin pigmentation changes evident with melanoma <sup>3</sup>. A good prognosis for the disease is typically dependent on both the type and subset of cancer, and the progression of the disease at diagnosis; earlier detection results in an improved chance of survival <sup>1</sup>. Current cancer research looks into both understanding the biological basis underpinning the disease as well as identifying effective therapeutic strategies.

## 1.1 Cancer as a Disease:

Cancer is a clonal disease, resulting in the accumulation of cells caused by uncontrolled proliferation. Due to the clonality of the disease, the tumour cells often retain the identity of the tissue of origin, even after it has metastasised, thereby leading to a classification system that is based on the precursor tissue. For example, lymphoma and leukaemia refer to cancers which arise from lymphocytes and leukocytes, whereas colorectal carcinomas arise from the epithelial cells present in the colon.

Clinically cancers are classified by severity (or tumour burden) and morphological changes within the cell (aggressiveness). In the UK and America the severity of solid tumours can be defined using a systematic approach known as the TMN system. The TMN system, grades the Tumour burden (T), invasion of the lymph node (N) and presence of metastases (M) on individual scales <sup>4</sup>. For tumours that do not primarily form defined masses, for example with haematological malignancies such as leukaemia, an alternative system which takes into account the percentage and number of lymphocytes present in the blood is used, the cell phenotype as well as any invasion into secondary lymphoid tissue <sup>5,6</sup>. Using this system provides a unique code which provides more information to the practitioner than the initial classification of the disease. This allows an informed decision on the disease severity and prognosis to be made, along with providing a framework with regards to which available therapeutic strategies would be beneficial.

Haematological malignancies refer to those that arise from cells of the immune system or from the tissue involved in haematopoiesis, such as the bone marrow. In 2008 the World Health Organisation (WHO) issued refined guidance on the classifications of these malignancies <sup>7,8</sup>. These guidelines were able to classify the different subsets of haematological diseases based on their phenotype, morphology, clinical presentation and underlying genetics <sup>7</sup>. Based on the available 2011/2012 data for the UK, Non-Hodgkin lymphoma (NHL) was the 6<sup>th</sup> most prevalent cancer. Leukaemia was the 11<sup>th</sup> most prevalent cancer. Within both of these diseases there are a number of different subsets which differ in their frequency and severity across the population; these details are summarised in Table 1.1.

Disease	Subset	Acronym	Incidence within group
Non-Hodgkin Lymphoma	Diffuse Large B cell Lymphoma	DLBCL	48%
	Marginal Zone Lymphoma	MZL	20%
	Follicular Lymphoma	FL	19%
	Others	-	13%
Leukaemia	Chronic Lymphocytic Leukaemia	CLL	38%
	Acute Lymphoblastic Leukaemia	ALL	8%
	Acute Myeloid Leukaemia	AML	34%
	Chronic Myeloid Leukaemia	CML	8%

**Table 1.1: Incidence of haematological malignancies within the United Kingdom**

The incidence of leukaemia and lymphomas in the UK along with the most common subsets as recorded for 2011/2012 by Cancer Research UK (CRUK) <sup>9,10</sup>.

### 1.1.1 Associated risk factors:

Due to an aging population the incidence of cancer is increasing, and the prevalence of cancer across the world – not just the western countries – was described by the WHO as “the global epidemic of cancer and noncommunicable diseases” (where cardiovascular disease, diabetes and chronic respiratory disease were included) <sup>11</sup>. As such prevention strategies, as well as direct therapies, are of great interest to the field where an understanding on the origins of cancer can be comprehended and appropriate steps to tackle the cause can be undertaken. A preventative strategy is more likely to reduce the overall burden on the healthcare services by reducing the number of cases of preventable cancers from developing <sup>1</sup>.

As cancer is a disease of accumulated mutations, avoiding the causes of these lesions is desirable. Mutations can occur during cellular stress and also in response to particular

chemicals (referred to as carcinogens), therefore exposure to these compounds increase the risk of developing cancer. Common sources of carcinogens in everyday life include tobacco (linked to the development of lung cancer<sup>12</sup>), asbestos (reported to increase the risk of lung cancer<sup>13</sup>) and exposure to the ultraviolet (UV) rays from sunlight (which increases the risk of developing melanoma<sup>14</sup>).

Alongside these chemical associated risks there are genetic elements which determine the relative risk of a person developing cancer. These heritable traits are controlled at both the genetic and epigenetic level, and although inheriting the element does not guarantee the development of cancer, it does increase an individual's risk<sup>15</sup>. An example of a well-studied genetic element is in the *BRCA1/BRCA2* tumour suppressor genes. Mutations within these genes are associated with a 10-15% increase in breast and ovarian cancer – particularly in those who have a family history<sup>15-17</sup>. As such, understanding an individual's family history and genetic status of key oncogenes can influence the treatment; from recommending earlier screening to catch early-stage disease, to larger scale surgical interventions in the event of disease development<sup>18</sup>.

Viral infections have been reported to alter a person's risk towards developing specific cancers. Exposure to viral infections has been linked with an increased risk to develop certain specific type of cancer. Viral replication in the host cells can induce mutations into the germline DNA via recombination events or translocations as a result of insertion, resulting in transformed cells. These mutations may be inert for some time, however subsequent mutations as a result of aging or DNA replicative errors add to these resulting in a malignant phenotype. For example, exposure to Epstein-Barr virus (EBV) has been linked to Burkitt lymphoma, whilst infection with Hepatitis virus is correlated with an increased incidence of liver cancers<sup>7,19</sup>. Most notable in terms of current public health management is the relationship between the human papilloma virus (HPV) and the increased risk of developing cervical cancer. This observation has allowed a prophylactic vaccination to be developed against the HPV (types 16 and 18) and a nationwide immunisation programme within the UK to be established, vaccinating girls between the age of 10-13 years against contracting the virus<sup>20</sup>.

### **1.1.2 Hallmarks of cancer:**

As the increasing complexity of cancer has been revealed in recent decades, where so many individual diseases that are classed as cancer, with differences present across morphology,

phenotype and genetic elements, it seemed unlikely that they could be seen as a single condition. In 2000 Hanahan and Weinberg attempted to collate the disparate features reported across cancer and define the key elements, known as the Hallmarks of Cancer <sup>21</sup>. This work was updated in 2011 to take into account the expanded knowledge and breakthroughs made in the subsequent decade, in particular with regards to the improvement in gene sequencing and genome mapping <sup>22</sup>. The current hallmarks can be separated into two groups; those that contribute to the survival of the cell and those that result in the adaptation to the tumour microenvironment (summarised in Table 1.2).

Overcoming the normal cell cycle	Adaptation to the microenvironment
<ul style="list-style-type: none"> <li>• Genomic instability and mutation</li> <li>• Evading growth suppressors</li> <li>• Resisting cell death</li> <li>• Sustaining proliferative signalling</li> <li>• Enabling replicative immortality</li> <li>• Deregulating cellular energetics</li> </ul>	<ul style="list-style-type: none"> <li>• Inducing angiogenesis</li> <li>• Activating invasion and metastasis</li> <li>• Avoiding immune destruction</li> <li>• Tumour-promoting inflammation</li> </ul>

**Table 1.2: Hallmarks of Cancer**

The Hallmarks of Cancer – as defined by Hanahan and Weinberg – can be separated into two categories based on final outcome; those that contribute to overcoming the normal cell cycle, and those that contribute to the alteration and adaptation of the microenvironment and supports metastasis <sup>21,22</sup>.

The life cycle of a cell is a tightly regulated process that goes through a number of phases with checkpoints to ensure only healthy cells are able to proliferate <sup>23</sup>. During G<sub>1</sub> phase, cells increase production of cellular components, such as organelles and proteins, and become enlarged <sup>24</sup>. Following this is the S phase where DNA replication occurs in preparation for mitosis <sup>25</sup>. G<sub>2</sub> phase follows where the cell checks for any errors in the replication of DNA, and ensures that all of the cellular components have been duplicated; once these checks have been confirmed the cell is able to undergo mitosis. After mitosis the cell may enter G<sub>0</sub>, a senescent/quiescent stage, or continue the cycle again by entering G<sub>1</sub> <sup>26</sup>.

Throughout this cycle there are checkpoints and regulators, particularly at the transition between phases, which ensure the cell remains stable and healthy before proliferation <sup>27</sup>. Failure to meet the required checkpoint conditions results in the cell moving into a senescent phase, or in some cases initiate apoptosis in order to remove any potentially detrimental cells from establishing themselves <sup>23</sup>. Dysregulation of the cell cycle results in the proliferation of cells which would otherwise have not been ready or contain too many genetic coding errors, leading to cells which have incorporated genomic instability and eventually cancer <sup>22,23</sup>.

Mutations in the checkpoint regulators have been reported for a number of cancers, for example with the regulator p53 (encoded by the *TP53* gene)<sup>28</sup>. p53 controls entry into the S phase<sup>24</sup>. In many incidences of cancer it is found to be inactivated or inhibited, preventing the activation of apoptosis or senescence in response to cellular stress from occurring<sup>28</sup>. In cases of DLBCL, the presence of *TP53* mutations was present in approximately 20% of cases and correlated with poorer survival in a retrospective cohort study<sup>29</sup>. As well as affecting the checkpoint regulators, the cell cycle can also be overridden by mutations in key cell signalling pathways, resulting in a constitutively activated cell in the absence of any ligands. A group of proteins commonly reported as mutated in cases colon carcinomas are the Ras family<sup>30,31</sup>. K-RAS is a GTPase that is downstream of the epidermal growth factor receptor (EGFR). Common mutations are found to alter the conformation of K-RAS into its active form in a constitutive irreversible manner, whereby it promotes the entry into the cell cycle independently of external growth signals. Tumours which gain K-RAS mutations have a poorer prognosis, and are less sensitive to therapy, as reported for non-small cell lung carcinoma (NSCLC)<sup>32</sup>.

The net expansion of cells through uncontrolled proliferation alone is not sufficient for the establishment of cancer, an ability to avoid death and immune destruction is also required<sup>21</sup>. Physiologically, the main form of cell death observed is apoptosis. Apoptosis removes damaged, potentially harmful or unnecessary cells from the body in a controlled fashion which does not release harmful agents which could damage the surrounding microenvironment<sup>33</sup>. It is a tightly regulated system that can be activated both intrinsically and extrinsically, and is controlled by a balance between pro- and anti-apoptotic proteins<sup>34,35</sup>. Bcl2 is a pro-survival protein that prevents entry into the apoptotic pathway. Translocation of the Bcl2 gene, resulting in the upregulation of this protein, is a key feature of follicular lymphoma<sup>36</sup>. This event leads to an increase in the survival of the cell; however it requires the addition of other oncogenes – such as c-myc – to develop into immortalised cells, pivotal for the establishment of cancer<sup>37</sup>. Overexpression of this protein has been reported for patients with DLBCL, where these cells are able to overcome apoptotic stimulus and can induce resistance to chemotherapy drugs<sup>38,39</sup>. Overcoming these means of drug resistance and tumour survival is a potential therapeutic strategy, although most inhibitors currently developed are toxic to all cells, not just the malignant tissue, and as such need refining in order to deliver a targeted approach.

Resources, such as oxygen and glucose, can become a limiting factor during the development of tumour masses as cells further away from the capillaries are unable to collect the nutrients required via diffusion<sup>21</sup>. In order to overcome this limitation there are a number of

adaptations, either to the cell itself or within the tumour, have been reported. Changes in metabolism to adapt to restricted resources have been reported, where an increase in glycolysis in the cytoplasm of the cell, noted by an increase in pyruvate – but without the same oxidation seen in the mitochondria – occurs <sup>22</sup>. This phenomenon is known as the Warburg effect, and can be measured by a notable increase in the presence of lactic acid <sup>40,41</sup>.

Angiogenesis is the process whereby new blood vessels are formed within the tumour. This process can be triggered under hypoxic conditions, and requires the production of vascular endothelial growth factors (VEGF) to promote the differentiation and proliferation of endothelial cells into diffuse capillaries <sup>42</sup>. This is commonly seen with tumours that form large masses, such as breast and colon carcinomas, and as such is often looked at as a potential target to reduce expansion. Unfortunately, if VEGF is disrupted, a number of non-vascular roles such as haematopoiesis and wound healing would also be affected as well <sup>43</sup>.

A common feature associated with severe and late stage cancers is the presence of secondary cancers that are distal from the primary tumour site. These are referred to as metastases, and represent a vast process of adaptation of the primary tumour cell in order to survive and become established away from the primary growth <sup>44</sup>. The malignant cells have to be able to survive in the periphery – either via the lymph or blood system – and convert themselves back to an adherent phenotype where it can colonise a new location <sup>45</sup>. Throughout this process it is exposed to new immune sensors and different microenvironments and as such is under constant stress <sup>22</sup>.

The importance of a complete immune system for the prevention and control of cancer development was illustrated through a number of mouse knock-out (KO) models <sup>46</sup>. Mice which did not express Rag2 (therefore had no functional B or T lymphocytes) were more susceptible to carcinogen (methylcholanthrene, MCA) induced tumours compared to wild type (WT) controls. In the same report, mice that were STAT1 deficient (a protein that lies downstream of the interferon (IFN)- $\gamma$  pathway) demonstrated a similar sensitivity to MCA exposure. Together this report presents a role for the lymphocytes in the control and clearance of spontaneous tumour development. Avoiding recognition of these cells, through the downregulation of molecules such as the major histocompatibility complex (MHC), would remove the malignant cells from this control and allow them to proliferate outside of the confines of the immune system <sup>47,48</sup>. Many other approaches to immune avoidance have been described in different malignancies; for example through the upregulation and secretion of anti-inflammatory cytokines such as interleukin (IL)-10 and IL-4 <sup>49</sup>. These cytokines are known



to suppress the cytotoxic response of T cells, as well as skew macrophages towards a regulatory phenotype (discussed later in section 1.2) <sup>50,51</sup>.

Even though the immune system has proven to be sufficient to eradicate pre-cancerous benign cells during the early stages of disease (as described above), there comes a point where the immune response becomes overwhelmed. Examples of this immune avoidance has been provided above, however the transformation from being susceptible towards the immune response to immune evasion has been termed immunoediting <sup>44,52</sup>. There are three stages for this process known generally as the “three Es”; Elimination, Equilibrium and Escape <sup>48</sup>. The elimination stage refers to the removal of pre-cancerous cells, resulting in a pro-inflammatory environment, where immune effector cells (such as T cells, Dendritic cells (DC) and Natural Killer (NK) cells) infiltrate <sup>48</sup>. Whilst the pro-inflammatory environment is conducive to immune activation, it can also form a barrier where the cancerous cells are protected from the immune effector cells <sup>53</sup>. A dynamic equilibrium, the second phase, becomes established, where the tumour cells within the protective niche persist, but the rest of the cells are still removed by the immune response <sup>48</sup>. Within this niche, the tumour cells are able to mutate, this is an iterative process where cells which become less immunogenic are positively selected for and persist <sup>54</sup>. The final stage of the immunoediting process is termed Escape; this refers to either the uncontrolled expansion of low-immunogenic tumour cells which are no longer recognised by the immune response or the release and colonisation of new sites <sup>44,45,55</sup>. It is these clones, which have been selected for that proliferate and lead to the establishment of malignant disease.

## 1.2 The Immune System:

As discussed above, the immune system is important for the clearance and control of tumour growth. Classically, the immune system has typically been organised into two separate arms – the adaptive and innate system – however as our understanding of the immune response has grown the distinction between these two classes has become less distinct. Generally speaking the innate immune system consists of the primary immune response, has broad specificity towards antigens and is unable to generate an immune memory <sup>27</sup>. In contrast the adaptive system provides a highly specific response to the antigen. Although it takes longer to act compared to the innate system, it is able to generate a memory of the infection/pathogen allowing the host to establish a more potent and timely response in the event of a secondary infection <sup>56</sup>. The complement system (discussed in section 1.4.7.1) and NK cells, along with the

myeloid cells, are typically grouped as members of the innate system, whilst B and T lymphocytes mediate the adaptive immune response.

### 1.2.1 B cells:

B cells are responsible for the production of antibodies which opsonise and neutralise foreign particles or infected cells. These cells develop from progenitor haematological stem cells (HSCs) within the bone marrow. The key stages of development are summarised in Figure 1.1<sup>57</sup>. The generation of the B cell receptor (BCR) is pivotal to the maturation of the cell, and occurs in defined stages<sup>27</sup>. Initially, the heavy chain of the receptor is formed via VDJ recombination of germline variable region gene elements (described in section 1.5.2) to form a Pre-B cell, where the heavy chain remains expressed intracellularly and is stabilised by a surrogate light chain<sup>58</sup>. The light chain of the BCR is then generated via the VJ recombination of the light chain variable gene locus to generate a complete BCR which is expressed on the surface of the naïve B cell<sup>27</sup>.

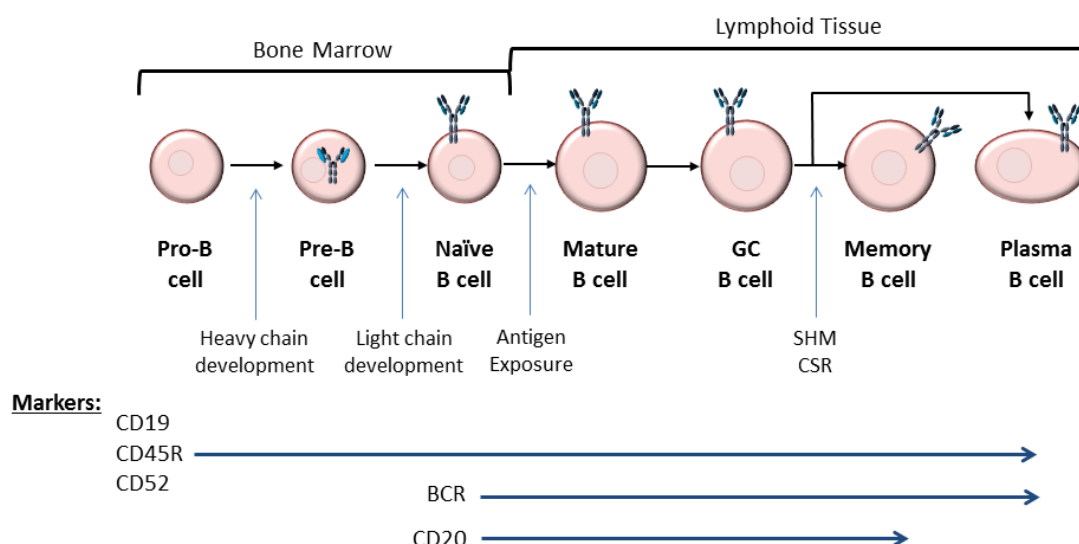


**Figure 1.1: B cell maturation stages and phenotypic markers**

B cells mature from haematopoietic stem cells within the bone marrow where they undergo V(D)J recombination to produce a B cell receptor (BCR) expressed on the surface of the cell, referred to as a naïve B cell. After this point, the naïve B cell migrates to the secondary lymphoid organs, such as the spleen, where it becomes exposed to antigens via the draining lymph node. A positive interaction between an antigen and B cell triggers the antigen-dependent maturation stage, where it enters germinal centres (GC), and the binding kinetics of the BCR is optimised by Somatic Hypermutation (SHM), and alternative antibody heavy chains can be selected via Class Switch Recombination (CSR). This process ultimately results in the production of antibody secreting plasma cells, and long term memory cells (which maintain the heavy chain Ig class) for a more rapid response in the event of re-infection. Key stages of maturation along with commonly used markers for identification are illustrated. Figure adapted from<sup>59,60</sup>.

B cell development is tightly regulated in order to prevent self-reactive B cells from entering the periphery. Auto-reactive naïve B cells, which respond strongly to self-antigens, are

eliminated before exiting the bone marrow in a process known as central tolerance, or undergo receptor editing in order to select for a specificity with a lower affinity, but this process is not absolute and some self-reactivities remain <sup>56</sup>. Once naïve B cells pass this checkpoint they migrate towards the lymph nodes and spleen where they are exposed to antigens supplied by antigen presenting cells (APCs).

Recognition of an T-cell dependent antigen by a B cell, which results in BCR activation, leads to further maturation within cellular structures present within the lymphoid tissue known as germinal centres (GC) <sup>61</sup>. GC contain a number of supporting cells such as follicular dendritic cells (section 1.2.5) and a class of T cell known as T follicular helper cells (section 1.2.2) which together facilitate the selection of the modified BCR. The specificity of the BCR is altered via the highly mutagenic process of somatic hypermutation (SHM, discussed in section 1.5.2) resulting in variations which tend to cluster within the complementarity determining regions <sup>62,63</sup>. This is an iterative process, where cells which have a higher affinity towards the antigen are allowed to be generated, whilst those that no longer respond to the presented antigen by the supporting cells are removed, or return to the GC for further mutation <sup>64</sup>. In addition to affinity maturation, a second process known as class-switch recombination (CSR, section 1.5.2) occurs, where antibodies with different heavy chain classes are produced (the classes of heavy chain are summarised in section 1.5.1) <sup>65</sup>. These cells, dependent on selection pressures then terminally differentiate into antibody secreting plasma cells or memory B cells (which retain the optimised specificity and antibody class) to respond in the case of recurrent infection.

Haematological malignancies arise from the individual stages of B cell development, and are can be described in relation to that stage. For example FL are proposed to arise from follicular B cells, whilst CLL arises from naïve B cells or mature B cells which have either undergone SHM (classified based on the mutational status of the BCR) <sup>66</sup>. Based on this information, understanding the stages of B cell development provide phenotypic clues to the precursor cell of a malignancy, as well as provide surface markers which may prove useful for identifying the tumour 5.

As well as having an active role in the opsonisation and clearance of infection there are also a subset of B cells that display a regulatory function. These cells (referred to as either B10 or B<sub>reg</sub> cells) are reported to produce anti-inflammatory cytokines such as IL-10 which create a suppressive microenvironment; diminishing both antibody production and T cell activation <sup>49,67</sup>. There is no fully defined phenotype to identify these cells, however they are generally found as a proportion of CD1d<sup>high</sup>CD5<sup>+</sup> cells <sup>68</sup>. These cells are not as well studied as their

antibody producing counterparts, however it is worth bearing in mind the potential role they have when examining the immune response as a single entity.

### 1.2.2 T cells:

T cells differentiate from haematopoietic stem cells present within the thymus. These cells are responsible for the adaptive immune response and influence all stages of immunity from direct killing of infected cells to immune regulation. T cells are classified by expression of CD3 followed by the expression of CD4 or CD8. CD8<sup>+</sup> T cells are classically referred to as the cells responsible for the cytotoxic clearance of cells, following activation by APC such as dendritic cells<sup>69</sup>. CD4<sup>+</sup> cells in response to antigen recognition differentiate into a number of different populations dependent on the exposure to cytokines. Naïve CD4<sup>+</sup> cells can develop a Th1, Th2 and Th17 response, which all have different roles within the adaptive immune system<sup>70</sup>. Th1 cells typically produce the pro-inflammatory cytokines IFN- $\gamma$ , tumour necrosis factor (TNF)- $\alpha$  and IL-2 which support the activation of surrounding effector cells. Th2 cells support the survival and proliferation of immune effector cells through the production of IL-4, IL-5 and IL-13, and in some cases can also produce the pro-inflammatory cytokine TNF- $\alpha$ . Th17 are distinct from the Th2 subset due to a dependence on transforming growth factor (TGF)- $\beta$  for differentiation and production of IL-17A and IL-17F which support the regulation of the inflammatory response<sup>71,72</sup>. In addition to these are a regulatory subset of CD4<sup>+</sup> T cells referred to as T<sub>reg</sub><sup>73</sup>. These cells are phenotypically diverse, however can typically be identified by the expression of the transcriptional regulator FoxP3<sup>73,74</sup>. T<sub>reg</sub> are involved in controlling the T cell mediated responses in order to protect the host against self-reactive cytotoxicity or excessive inflammatory damage<sup>50</sup>.

T cell activation results in the clonal expansion of reactive T cells in response to antigen recognition presented via MHC by APC. There are two classes of MHC; MHC Class I (MHC-I) are recognised by CD8<sup>+</sup> cells, and consists of a single chain to form the peptide binding domain and the association of a  $\beta$ 2 microglobulin ( $\beta$ 2M) to stabilise the conformation<sup>75</sup>. MHC class 2 (MHC-II) are expressed by APC, and present peptides to CD4<sup>+</sup> cells<sup>76</sup>. The MHC-II protein consists of two peptide chains to form the peptide binding domain. Following expansion and the eradication of infected/damaged cells, the CD8<sup>+</sup> and CD4<sup>+</sup> cells are able to further differentiate into memory populations of cells<sup>77,78</sup>. These are recognised through the downregulation of CD45RA and the expression of CD45RO<sup>77</sup>. Effector memory T (T<sub>EM</sub>) cells are able to induce a cytotoxic response upon recognition of the antigen – in the case of reinfection – whereas central memory T (T<sub>CM</sub>) cells upon antigen recognition differentiate into cytotoxic

populations in order to elicit any effector functions.  $T_{CM}$  and  $T_{EM}$  can be further differentiated by the chemokine receptor CCR7 – which controls the migration of cells towards lymphoid organs.  $T_{CM}$  cells are CCR7<sup>+</sup> as they require movement into the lymphoid organs to further differentiate into effector cell populations whilst  $T_{EM}$  are CD45RO<sup>+</sup> CCR7<sup>-</sup>.

Alongside supporting CD8<sup>+</sup> effector cells, CD4<sup>+</sup> T cells are also required for the support of B cell differentiation from mature B cells into plasma cells and memory B cells. This subset is known as Follicular Helper T ( $T_{FH}$ ) cells, and are distinguished from other CD4<sup>+</sup> cells by the expression of CXCR5, ICOS, PD-1 and IL-21 as well as other markers <sup>62</sup>.  $T_{FH}$  cells perform a variety of roles throughout the formation of germinal centres through to supporting class-switch recombination and differentiation of mature B cells into plasma cells. These differential roles are instigated by the expression and production of different cytokines and receptors, for example, the expression of CD40L and IL-4 supports B cell proliferation when they undergo somatic hypermutation <sup>62</sup>; whilst they can also induce Bcl-6 expression in B cells to instigate entry into GC for affinity maturation (section 1.5.2) <sup>61</sup>.

### 1.2.3 Natural Killer cells:

NK cells are lymphoid cells which are found to perform both innate and adaptive immune responses. They are responsible for the clearance of infections and host cells that exhibit stress, and as such express a range of different receptors which support this multifaceted role <sup>79</sup>. For example, NK cells express Toll-like receptors (TLR) which are able to recognise bacterial motifs such as lipopolysaccharide (LPS), or viral RNA (via TLR8) <sup>80</sup>; they can bind MICA (induced upon cellular stress) to remove damaged cells <sup>81</sup> and express Fcγ receptors (FcγR) to respond to antibody opsonised cells (discussed in section 1.7.7) <sup>82</sup>.

In humans, NK cells are characterised as CD3<sup>-</sup> CD56<sup>+</sup> cells, which can be further classified into CD56<sup>dim</sup> and CD56<sup>bright</sup> populations which perform different immune functions. CD56<sup>dim</sup> are the cytotoxic population of NK cells which can mediate perforin/granzyme-mediated death in a similar manner to T cells, and have been reported to instigate cytotoxic roles without the need for prior activation or priming <sup>79</sup>. In contrast, CD56<sup>bright</sup> cells do not express perforin and are unable to elicit a cytotoxic response, however they are able to produce pro-inflammatory cytokines such as IFN-γ and IL-2 to activate the neighbouring immune responses <sup>81</sup>. Another population are known as the NKT cells, these are CD56<sup>+</sup> but also express a semi-invariant T cell receptor (TCR) which recognises lipid antigens on the MHC-like molecule CD1d <sup>83</sup>. They are

able to recognise glycosphingolipids expressed on bacterial ceramides found on gram negative bacteria.

#### **1.2.4 Monocytes and Macrophages:**

Monocytes are the myeloid precursors for the professional APCs macrophages and dendritic cells. Alongside this they are also able to perform immune effector functions for the clearance of bacterial infections or wound healing via cytotoxic processes – such as Reactive Oxygen Species (ROS) and nitrous oxide (NO) induced death – and phagocytosis to remove infected cells<sup>84,85</sup>. Typically monocytes are present in the periphery – where they form approximately 10% of the leukocyte population – and once they migrate towards tissue or sites of inflammation, they are able to differentiate into the more specialised myeloid cells<sup>86</sup>.

As a cell population monocytes are identified as CD14<sup>+</sup> but do not express the classical lymphocyte markers CD3, CD19; they are heterogeneous and can be further categorised into subsets based on the expression of the Fcγ receptor CD16. CD14<sup>+</sup> CD16<sup>−</sup> monocytes are the most abundant in the periphery of human blood which also express the chemokine receptor CCR2 (responsible for migration towards inflammatory sites)<sup>84</sup>. These cells are APCs but also produce IL-10. However, in response to TLR activation they are able to produce TNF-α<sup>85</sup>. CD14<sup>+</sup> CD16<sup>+</sup> monocytes are pro-inflammatory able to produce TNF-α, and induce NO after TLR stimulation. These cells are also reported to express the other FcγRs, CD64 and CD32a, therefore are able to respond to antibody activation in addition to the innate stimuli detailed above<sup>86</sup>.

Once monocytes migrate out of the periphery into the tissue (or site of inflammation) they are able to differentiate into macrophages<sup>87</sup>. Macrophages can fulfil both inflammatory and anti-inflammatory functions dependent on the cytokine milieu present. Differentiation of macrophages under the presence of IFN-γ and LPS results in a 'classical' M1 phenotype<sup>88,89</sup>. These are responsible for the phagocytic and cytotoxic killing of apoptotic and infected cells via TNF-α and NO release. M2 skewed macrophages are akin to the Th2 responding cells and further separated into three groups<sup>90,91</sup>. M2a differentiate in response to the prototypic Th2 cytokines IL-4 and IL-13, and induce Arginase mediated defence mechanisms<sup>91</sup>. M2b are more skewed by the presence of TLR ligands such as LPS, and immune complexes to induce an anti-inflammatory response with high production of IL-10 and IL-6<sup>92</sup>. M2c macrophages play a greater regulatory role than the others, are induced by IL-10, and involved in altering the extracellular matrix rather than directly acting on cells<sup>90,93</sup>.

### 1.2.5 Dendritic Cells:

Dendritic cells are derived from the same common myeloid precursor as monocytes and macrophages mentioned previously<sup>86</sup>. They are critical in the priming and activation of the adaptive cellular responses through their function as APC<sup>94</sup>. Through the expression of MHC class I and II on the surface of cells they are able to directly interact with CD8<sup>+</sup> and CD4<sup>+</sup> T cells in the lymphoid tissue thereby priming and supporting the maturation of these cells<sup>94</sup>. Under physiological conditions, DC are able to traverse the periphery where they can collect and present both endogenous and extracellular antigens via MHC, as well as respond to opsonised particles via the expression of many other immune receptors (such as Fc Receptors and CD1 molecules).

Plasmacytoid dendritic cells (pDC) originate from the bone marrow and can be found in peripheral blood<sup>87</sup>. Here they are exposed to antigens and able to sample the environment, before migrating towards lymph nodes where they are able to prime T cells<sup>95</sup>. Activated pDC, in response to viral or bacterial challenge, results in the production of type 1 interferons which are able to activate NK cells<sup>96</sup>. Other functions of pDC include supporting the maturation of B cells<sup>97</sup>. Follicular dendritic cells (fDC) are found in the light zone of germinal centres. These cells act as APC and participate in the positive selection for the high affinity BCR that are generated during the maturation of B cells<sup>64,98</sup>. These cells are different from pDC as they do not arise from a lymphoid progenitor cell<sup>87</sup> but instead can arise from the stroma<sup>99</sup>.

### 1.2.6 Neutrophils:

Neutrophils are large granular cells which are important in the innate inflammatory response to infection or damage<sup>27</sup>. They are a heterogeneous cell population which are able to alter their inflammatory responses dependent on the stimuli present<sup>43</sup>. For example, they are able to migrate towards inflammatory sites via chemotaxis in response to complement component C5a where the neutrophil adopts a pro-inflammatory phenotype<sup>100</sup>. In wound healing, neutrophils are able to produce a number of supporting components that are able to interact with the extracellular matrix and microenvironment, from metalloproteases (which are able to promote vascularisation) and cytokines to recruit monocytes or augment the adaptive immune response<sup>43</sup>.

Neutrophils are able to cause death of pathogens using a number of different pathways. They are highly phagocytic and take up microbes where they are destroyed by exposure to the intracellular granules present, thereby exposing the cell to a variety of destructive

components, such as proteases and ROS <sup>101</sup>. As well as removing microbes via intracellular processes, they are able to form fibrous structures referred to as neutrophil extracellular traps (NETs). These NETs consist of chromatin and anti-microbial components that were previously contained in the granules <sup>101</sup>. This is able to induce a highly inflammatory environment for the eradication of infection, although if uncontrolled it has been associated with autoimmune conditions such as systemic lupus erythematosus (SLE), and may promote tumour progression <sup>102,103</sup>.

### **1.3 Cancer Therapy:**

Due to the vast diversity within cancer, a “one-treatment-fits-all” approach has not been successful. Traditionally there are three approaches that are employed dependent on the severity, accessibility and nature of the disease; these are surgical intervention, radiotherapy and chemotherapy. Combining individual techniques are a common strategy in order to provide the best prognosis, for example surgical excision to remove the bulk of the tumour followed by a course of chemotherapy is a standard approach in the treatment of early stage breast cancer. Each approach has its own advantages and limitations towards the efficacy of the therapy.

Surgery is able to physically excise tumours from the patient – however it is limited by the accessibility of the primary tumour, and is ineffective at treatment of haematological malignancies. Another limitation is upon the accuracy and confirmation that all of the malignant cells have been removed – with minimal damage to surrounding healthy tissue. Technology to improve the accuracy of surgical intervention is being implemented, for example by analysing the cells excised during the surgery by a form of mass spectrometry (rapid evaporative ionisation mass spectrometry) to define the healthy/cancerous cells known as the “intelligent knife” <sup>104</sup>. However the cost of applying this technology to the National Health Service (NHS) is vast and any inaccessible tumours or those which have metastasised are unable to be removed by this approach alone, leading to an increased incidence of secondary cancers.

Radiotherapy refers to the application of ionising energy in order to induce DNA damage and subsequent cell death. This can be used as both a monotherapy or in conjunction with surgery (to either shrink tumours, or remove residual cells post-surgery) or chemotherapy (in order to sensitise the cancerous cells towards therapy). However, exposure to radiation energy is able to induce damage to both healthy and malignant cells resulting in toxicities and non-specific



treatment. As seen in surgery, improvement in technology such as focusing energy beams and locating tumours have been effective in improving the efficacy of this approach <sup>105</sup>. For example multiple doses of energy from different angles aimed at the same location, increases the relative radiation dose achieved at the tumour compared to that of the surrounding normal tissue <sup>105</sup>. Lastly, radiotherapy can be combined with drugs able to disrupt the DNA damage repair process, or sensitise the malignant cells in comparison to healthy tissue <sup>106</sup>.

Chemotherapy refers to the application of chemicals to induce cell death. There are many classes of chemotherapy agents which function via different mechanisms of action. They became an established course of therapy for haematological malignancies during the 1960's–70's <sup>107</sup>. Successful chemotherapy agents include alkylating agents which inhibit DNA synthesis, such as cyclophosphamide and ifosfamide; compounds which arrest the cell cycle, such as etoposide, and antibiotics like the anthracycline, doxorubicin <sup>108-110</sup>. Since then the use of chemotherapy has expanded to solid tumours such as the use of cyclophosphamide for colon carcinomas and etoposide for ovarian cancers <sup>111,112</sup>.

Although they can be used as monotherapy, the best responses are seen when used in combination with other agents, for example DLBCL is treated with a regimen referred to as CHOP therapy – consisting of cyclophosphamide, doxorubicin, oncovin and prednisolone. Another regimen, known as ICE, consists of ifosfamide, cisplatin and etoposide, and is used in the treatment of NHL and refractory cases of leukaemia. These combinations provide a multifaceted response, eliminating the highly replicative cells by a number of approaches in order to reduce the possibility of leaving behind any malignant cells. Both of these regimens are now combined with the anti-CD20 monoclonal antibody rituximab (discussed in 1.8.2) where a clear improvement in both the progression free survival and overall survival were reported <sup>113,114</sup>.

The current limitations to chemotherapy regimen are the associated toxicity, which has a cumulative effect for each additional reagent added to a regime, coupled to the broad specificity of the therapeutic – targeting a pathway but not the malignancy alone. As our understanding of the molecular nature of cancer develops, more specific therapies with lower toxicities are required. Immunotherapy provides this as it is possible to utilise the host immune system to remove cancerous cells, and in some cases develop memory cells to provide long term protection.

## 1.4 Immunotherapy:

Immunotherapy refers to the activation or manipulation of the immune system to elicit a response against targeted cells. Active immunotherapy seeks to activate the endogenous immune system to mount an anti-tumour response whereas passive immunotherapy involves the introduction of immune elements (such as cells or antibodies) in order to deplete tumour cells.

### 1.4.1 Active immunotherapy:

Vaccinations, in cancer therapy, aim to prime the immune response to oncogenic elements (such as viruses or mutated proteins) allowing protection against associated cancers. There are many types of vaccinations employed and investigated in relation to cancer immunotherapy, from whole cell to DNA based vaccines. As mentioned earlier infection with particular viruses increases the associated risk of developing cancer, due to the genetic instability caused in response to the replicating virus or due to an elevated proliferation drive or inflammation triggered by the virus <sup>19,53</sup>. By targeting the virus, an inbuilt immunity is developed within the host which reduces the chance of infection and the subsequent development of cancer. This is best represented with the anti-HPV vaccine, Cervarix, given to females between 13-15 years old are protected from the HPV-16 and HPV-18 strains of the virus which are associated with an increased risk of developing cervical cancer <sup>115</sup>. Since this has been rolled out a decrease in the of viral induced cervical cancer has been reported <sup>20</sup>.

Vaccinations against tumour-specific proteins (such as mutated oncogenes) have been less successful in clinical trials, although pre-clinical data has been promising <sup>116,117</sup>. This has been investigated using different approaches from the use of tumour antigens to DNA vaccines which encode antigenic peptides. Direct immunisation against tumour antigens, coupled to an adjuvant such as LPS, has been investigated in the context of developing an anti-idiotypic (Id) response in B cell lymphomas <sup>118</sup>. One trial involved coupling the BCR isolated from the patient with NHL to the adjuvant, keyhole limpet hemocyanin (KLH), and co-administered with granulocyte macrophage-colony stimulating factor (GM-CSF) to stimulate an immune response <sup>119</sup>. Although in the phase II trial durable responses were seen, a Phase III clinical trial, using the same approach in developing anti-Id vaccinations resulted in no improvement in antibody titre compared to a control vaccine (containing just the adjuvants) <sup>117,120</sup>.

DNA vaccines involve the injection of plasmid DNA which contains multiple segments encoding tumour associated peptides, or whole proteins. The principle behind this approach is that the

plasmid DNA would be taken up by cells at the site of injection, where the cell would translate these proteins and allow presentation to T cells via MHC molecules. Alternatively the transfected cells would be phagocytosed by APC, where the tumour antigens are processed and presented in lymphoid tissue to generate an antibody response.<sup>121</sup> This has been investigated in the treatment of haematological diseases, via intra-muscular injections, although achieving high enough transfection to elicit a response has been an obstacle in this approach<sup>122</sup>. An additional approach to increase the immunogenicity of the peptide is the development of fusion genes. These constructs fuse the desired tumour peptide (such as the peptide derived from the cancer testis antigen PASD-1 found in multiple myeloma<sup>123</sup>) to a bacterial element such as fragment C of tetanus toxin<sup>124,125</sup>. This approach has been shown to increase the amount of tumour-specific cytotoxic CD8<sup>+</sup> cells in mice, as well as providing protection upon secondary tumour challenge<sup>125</sup>.

An alternative approach investigated is by loading oncogenic peptides to APC in order to present and activate the patient's own immune response towards the malignancy. This approach requires the isolation and *ex vivo* expansion of the patient's own cells and peptides are loaded by culturing the cells with cancer cell lysates, where peptides are able to be presented via the MHC-II cross-presentation pathway<sup>126</sup>. This approach has the advantage of not requiring identification of tumour-specific peptides prior to APC loading, allowing a polyclonal response to be generated and administered to the patient.

Given the potential of vaccinations to produce patient specific therapies, which are able to generate multifaceted responses to their own cancerous cells, there are downsides which make this, currently, an unviable approach. The generation of patient specific vaccines is costly, as these cannot be mass-produced and stored for widespread administration across the population. The logistics and infrastructure of supplying this type of therapy is complicated, as specialists centres that can reliably produce and distribute these therapies to patients are required<sup>127,128</sup>. There would also be a higher level of variability between responses in patients due to the uniqueness of each vaccine, making the establishment of controls required for large clinical trials difficult, and may explain the poor trial responses reported.

Passive immunotherapy provides an alternative approach to the active immunotherapies discussed which overcomes some of these limitations. They provide tumour specific (but not patient specific) therapies which are amenable to batch-production and administration to a larger cohort of patients.

#### **1.4.2 Passive immunotherapy:**

##### **1.4.2.1 Cytokine therapy:**

The use of cytokines to activate the anti-tumour response could be seen as an active therapeutic, as it has no pre-determined target, and functions via the endogenous immune response and selected tumour antigens of the patient. Successes have focussed on the use of cytokines to promote the expansion of immune cells, such as IL-2 in the treatment of metastatic melanoma to expand cytotoxic T cells <sup>129</sup>. This has proven successful, and resulted in an improvement in the prognosis of patients with this severe disease; however the percentage of patients who respond accounts for only 15% of patients demonstrating that although it has potential, there is plenty of room for improvement <sup>130</sup>.

Cytokine therapy, like traditional chemotherapies, has also been investigated as adjuvants for other immunotherapies. For example, in the treatment of neuroblastoma, combining anti-GD2 antibody with both GM-CSF and IL-2 resulted in far better responses compared to patients who received just chemotherapy <sup>131</sup>. However, this study didn't compare the combination with just the antibody alone, in order to determine how much of the response was improved by the cytokines alone. Due to the non-specific nature of this approach, toxicities and side effects are common in patients. For example fever, nausea and hypotension has been reported following high-dose IL-2 administration <sup>132</sup>. Over activation of the immune system can result in the development of autoimmunity and cytokine release syndrome <sup>133</sup>.

##### **1.4.2.2 Adoptive cell therapy:**

Adoptive cell transfer involves isolating immune cells – such as the tumour infiltrating T cells – from a patient's biopsy. The theory is that these cells have already demonstrated specificity towards their cancer as they are present at the tumour site <sup>134</sup>. These cells would then be expanded *ex vivo* and stimulated with cytokines (such as IL-2) before transferring back to the patient where they can target the remaining tumour <sup>135,136</sup>. This method allows an amplification of the tumour-specific response that cannot be achieved naturally due to the low number of immune infiltrates at the tumour site, as well as avoiding the immune suppression directed by the tumour microenvironment <sup>137</sup>. In a similar manner, it allows a polyclonal response to be put back into the patient, with no potential graft vs host response, as the cells are autologous, allowing a broader range of targets.

A more sophisticated approach to adoptive cell transfer is to genetically engineer the isolated T cells from the patient. Commonly investigated approaches are to modify the TCR to recognise a tumour specific peptide, or to produce chimeric antigen receptor (CAR) expressing T cells that conveys the specificity of an antibody towards a tumour whilst retaining the cytotoxicity of a T cell <sup>138</sup>. The viability of this approach has been demonstrated in patients diagnosed with CLL and ALL, where complete response and prolonged survival was reported when using a CAR-T cell directed against the B cell antigen CD19 <sup>139</sup>. Although effective in the depletion of targeted cells the potency of this response can lead to life-threatening conditions, such as cytokine storm and tumour lysis syndrome, caused by over activation of the immune system <sup>139-141</sup>. Therefore a better understanding of how to balance a targeted cytotoxic response with fewer repercussions to the patient is required <sup>141,142</sup>. As this approach requires the transfer of T cells it is a highly individualised technique – requiring the modification and *ex vivo* expansion of autologous cells –and with current technology it is likely to be too expensive to produce for large scale clinical trials or for use in routine therapy.

#### **1.4.2.3 Monoclonal antibody immunotherapy:**

Monoclonal antibody (mAb) immunotherapy offers an alternative method of passive immunotherapy to the adoptive cell therapy. In its simplest form it consists of the production of tumour-specific antibodies which can be administered to patients to elicit an anti-tumour immune response <sup>143</sup>. These reagents offer a high specificity with the potential to distinguish between cancerous and healthy cells (provided the antigen is carefully chosen) and once bound can engage a number of mechanisms (discussed later in section 1.7) to delete the targeted cells. The generation and licensing of rituximab (Rituxan) for the treatment of NHL in 1997 was a milestone achievement for cancer immunotherapy. In the intervening 18 years the field of mAb directed immunotherapy has expanded, resulting in therapeutics directed against solid phase tumours as well as improved therapies towards haematological malignancies <sup>144</sup>.

The versatility of mAb immunotherapy is only now becoming realised and newer antibodies now seek to go beyond the direct targeting of tumour cells. For example they can be directed against immune effector cells – such as cytotoxic T cells – in order to sensitise the cells towards antigenic stimulation <sup>145</sup>. These so-called immunomodulatory mAbs target receptors present on immune cells responsible for the inhibition of suppressor signals or the activation of anergic cells <sup>145</sup>. Current receptors investigated include the costimulatory receptors CD137, OX40 and CD40, and the checkpoint blockers PD-1, PD-L1 and CTLA-4. Ipilimumab, an anti-CTLA-4 mAb, is approved for the treatment of metastatic melanoma and is proposed to work by preventing

signalling via steric inhibition of the receptor to its ligand B7-1/2<sup>146</sup>. Alternatively direct targeting mAbs have been conjugated to toxins where they function as a drug delivery system. Clinically approved mAb-conjugates include tositumomab-I<sup>131</sup> for the treatment of NHL and gemtuzumab-ozogamizin – an anti-CD33 mAb approved for AML<sup>147,148</sup>.

An advantage of mAb therapy, compared to other types of passive immunotherapeutics, is the ability to deliver anti-tumour responses without having to generate patient specific antibodies. As such, this process is amenable to batch production allowing large quantities to be produced. This has allowed for the careful regulation and development of this class of therapeutics which will be discussed in the next section.

## **1.5 Monoclonal Antibodies:**

### **1.5.1 Antibody structure and nomenclature:**

Antibodies exist as an assembly of four immunoglobulin chains, two identical light and two identical heavy chains. Each Ig chain contains a single variable domain ( $V_L$  and  $V_H$  – for light and heavy chain, respectively) followed by either a single constant domain ( $C_L$  for the light chain) or at least three constant domains (present in the heavy chain,  $C_H$ ). The chains are held together by disulphide bonds as illustrated in Figure 1.2. Each variable domain contains three hypervariable loops, known as the complementarity determining regions (CDR). Antigen specificity is defined by the association of the CDRs from the heavy and light chains, where amino acid changes can alter both the specificity and binding affinity towards an antigen.

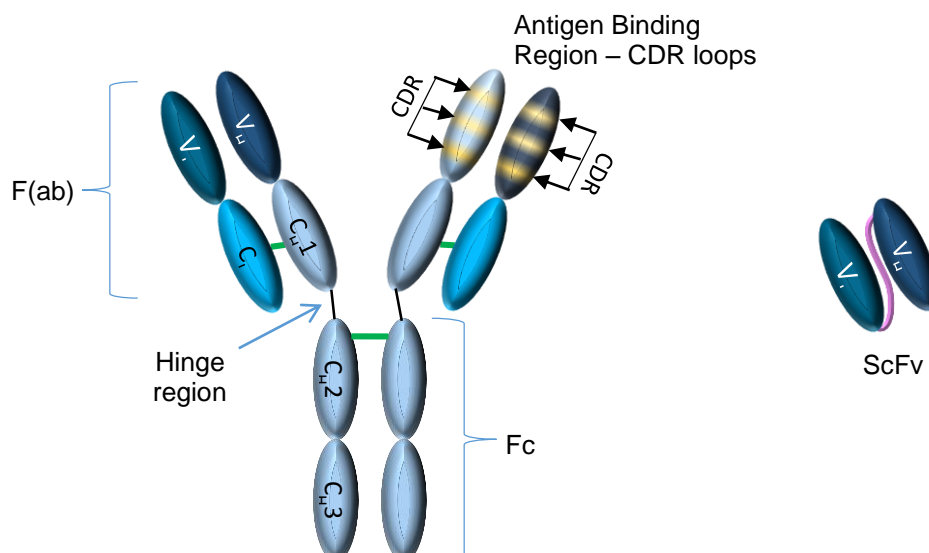


**Figure 1.2: General antibody structure**

An antibody consists of two identical heavy and two identical light immunoglobulin chains, held together by disulphide bonds (green). Each Ig chain contains a variable domain (V<sub>L</sub> or V<sub>H</sub>) which determine the antigen specificity via the three CDR loops present. Papain digestion results in three functional fragments, two F(ab) domains containing the complete light chains and the V<sub>H</sub> and C<sub>H</sub>1 domain of the heavy chain and one Fc domain which contains the C<sub>H</sub>2 and C<sub>H</sub>3 domains of the two heavy chains. ScFv (Single chain variable fragment), consists of the variable domains of both the light and heavy chain. The Hinge region is present for IgG, IgD and IgA antibodies; this domain is replaced with an additional constant domain for IgM and IgE antibodies.

When an antibody is digested with papain, three functional fragments are released. The first the two consist of a light chain associated with the V<sub>H</sub> and C<sub>H</sub>1 domain of the heavy chain held together by a disulphide bridge. These fragments are known as the antigen binding fragment – or F(ab). The remaining fragment – which consists of the C<sub>H</sub>2 and C<sub>H</sub>3 domains of both heavy chains – is known as the crystallisable fragment, or Fc domain. The Fc domain is able to interact with receptors present on the immune cells to mediate the immune response (these mechanisms are discussed in more detail in section 1.7.7). If pepsin is used to digest an antibody, the two F(ab) domains remain held together via the hinge region forming a bivalent molecule referred to as F(ab')<sub>2</sub>. A multitude of modular fragments can be derived from monoclonal antibodies<sup>149</sup>. For example, the two variable domains can be cloned as a single recombinant fragment held together with a flexible linker. These are known as single chain variable fragments, or ScFv, and are used in the development of CAR or in phage display libraries<sup>150</sup>. These fragments are summarised in Figure 1.2 for reference. Other fragments include the production of diabodies, or bispecifics, (consists of two ScFv linked covalently in closer association than that seen in a F(ab')<sub>2</sub><sup>151,152</sup>) or larger modular fragments which can contain the same antigen recognition sites (therefore increasing avidity compared to a ScFv) or

different antigens where they can bridge different cells together to elicit an immune response

153

In humans, there are five different classes of heavy chains – IgA, IgD, IgE, IgG and IgM – and two light chains -  $\kappa$  and  $\lambda$ . IgA, IgD and IgG contain a hinge region between the C<sub>H</sub>1 and C<sub>H</sub>2 domains of the heavy chain<sup>27</sup>. This domain results in a degree of flexibility between the two F(ab) domains, allowing a number of different conformations/stretching to occur for bivalent binding of an antibody to an pathogen. The number of disulphide bonds and length of the hinge regions varies between the antibody classes which can impact the flexibility and resulting function of an antibody. Recent work investigating the importance of the hinge region in human IgG2, found that the formation of the disulphide bonds in this region can change the agonistic ability of the antibody – a property important for the development of costimulatory antibodies<sup>154</sup>. IgE and IgM do not contain this region, instead having an additional constant domain, resulting in an antibody with F(ab) domains which are more fixed in relation to the Fc and with less flexibility compared to the other classes.

Each class of heavy chain has evolved to perform specific roles required by the adaptive immune response. IgA has two isotypes (IgA1 and IgA2) and can exist as either a soluble monomer or dimer, commonly found at mucosal fluids such as saliva and mucus. It protects the mucosal barrier from infections by binding pathogens to prevent their movement across the epithelial barrier<sup>155</sup>. IgM can be expressed in both a membrane bound or soluble form. In its soluble form it exists as a pentameric complex, and is able to induce cell agglutination for phagocytosis or complement fixing<sup>156,157</sup>. When bound to the membrane of B cells it forms part of the BCR, conveying its specificity during maturation. Similarly, membrane bound IgD is expressed as part of the BCR on the membrane of mature B cells – but the role of secreted IgD is unclear<sup>158</sup>. IgE is found at very low concentrations in the serum however it is linked to the allergic response<sup>159</sup>. Lastly, IgG is the most abundant Ig in the serum, has four isotypes (IgG1, IgG2, IgG3 and IgG4) is important in the adaptive immune response and of great interest in immunotherapy. These four isotypes have differences in their affinity and ability to engage in the Fc $\gamma$ R present on the immune cells. For example, IgG1 and IgG3 is able to effectively activate complement<sup>156</sup> and bind Fc $\gamma$ R<sup>160</sup>; IgG2 is unable to bind the Fc $\gamma$ R, and is important in the host response to bacterial pathogens<sup>161</sup>.

Antibodies are glycosylated proteins with the sugar residues helping to confer their structure and function. The degree of glycosylation is dependent on the heavy chain, wherein IgG contains a relatively low level of glycosylation compared to IgM<sup>162</sup>. Glycosylation helps



maintain the antibody conformation in solution, its solubility and in some cases its ability to perform its therapeutic role. In IgG, there is a conserved Asn at position 297 which sits in the C<sub>H</sub>2 domain of the Fc region. The glycosylation of this residue stabilises the structure of the Fc, and is critical for stable interactions with the FcγR on immune cells<sup>163</sup>. As well as a loss of FcγR interaction, altering this glycan can prevent complement engagement due to the loss of stability within the Fc domain<sup>164</sup>. The final composition of glycans present on an antibody is dependent on a number of factors, in particular the availability of carbohydrate processing in the endoplasmic reticulum<sup>165</sup>.

### 1.5.2 Generation of antibody diversity:

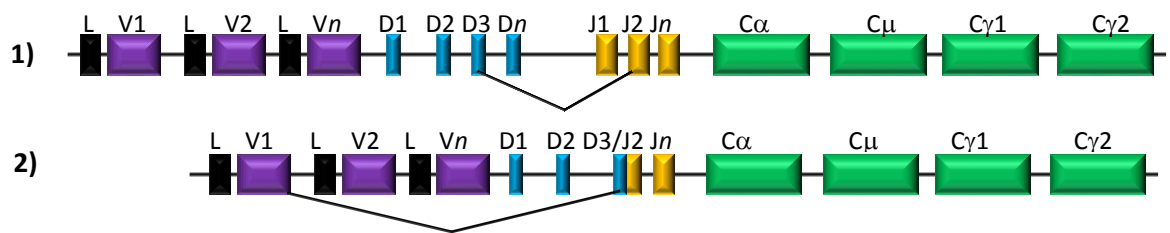
The specificity of an antibody is defined through the interaction of the CDR loops of the variable domains in the F(ab). The diversity of antigen specificity is achieved through gene rearrangement of the Ig gene locus in the germline DNA. For a complete variable domain gene, there are three separate segments for the heavy chain (only two for the V<sub>L</sub>) that need to combine together. These segments are referred to as Variable (V), Diversity (D) and Junction (J). Within the Ig locus are several variants for each individual segment which can be joined together in order to produce a single allele<sup>27</sup>. An additional segment defines the antibody class, defined as the Constant (C) segment, and is determined at the mRNA level.

Formation of the variable gene requires specific recombination events to occur which bring together a single V, D and J segment to produce a single coding region (summarised in Figure 1.3). Each segment is flanked with a conserved recombination signal sequence (RSS) which consists of a heptamer sequence followed by either a 12 or 23 nucleotide spacer followed by a conserved nonamer sequence<sup>57</sup>. Only a RSS with a 12 nucleotide spacer can join that of a 23 spacer, thereby minimising the potential for two of the same segments to join. For example, at the heavy chain locus, the V and J segments are flanked by RSS with a 23 nucleotide spacer, preventing them from joining directly to each other, whilst the D segment contain a 12 nucleotide spaced RSS<sup>27</sup>. This process requires multiple enzymes to achieve; RAG1 and RAG2 recognise and bind the RSS bringing together the two sections of DNA into close association and any DNA between the two segments form a hairpin structure<sup>57</sup>. The heptamer is then cleaved by an associated endonuclease, thereby releasing the hairpin – which forms a non-coding joint, which is degraded and lost from the genome of that individual cell – leaving the two segments in close association where they are ligated together. For the heavy chain, the recombination of the variable gene occurs in a defined order; D binds J to form DJ, then a second recombination event attaches the V to the DJ.

These recombination events provide the opportunity for additional modifications to the gene to occur as a consequence of the endonuclease and ligation process. This results in a larger number of possible unique combinations than encoded for within the genome <sup>166</sup>. Although the hairpin is cleaved at the RSS site, the exact location is not specific – in contrast to that achieved by restriction endonucleases – instead the joining sites can contain additional nucleotides resulting in insertions. Due to the single stranded nature of the initial cut, further nucleotides can be removed by exonucleases present, and during the ligation reaction free nucleotides present in the nucleus can be incorporated. Together these processes result in a hypervariable CDR3, which allows greater diversity than recombining the encoded gene segments together can provide.

The recombination events which form the variable domain occur early in the development of B cells. It is first translated along with the IgM constant region to provide the heavy chain of IgM. However after antigenic stimulation, the B cells further differentiate and mature into plasma cells via germinal centre formation <sup>61</sup>. These plasma cells have the capacity to now secrete soluble IgM. However, during the GC process further modification to the immunoglobulin gene can be undertaken through two processes referred to as somatic hypermutation and class switch recombination <sup>27</sup>. Somatic hypermutation is the result of point mutations that occur in the variable exon, which can alter the paratope of the antibody therefore changing the binding affinity and specificity towards the antigen. It is this process that provides the facility for affinity maturation; whereby randomly mutated V regions with higher affinity for the given antigen are selected for <sup>167</sup>. Additionally the class of the antibody can change in order to fulfil the appropriate role, mediated by the AID enzyme. Mice that do not express AID only express IgM antibodies, and also have a reduced ability to undergo somatic hypermutation, suggesting that the two processes are linked <sup>61</sup>. Each constant segment is flanked by a switch sequence which allows splice events to occur, looping out the intervening constant segments <sup>65</sup>. Importantly, this process of class switching is iterative and sequential such that a given B cell cannot re-express an earlier class of immunoglobulin. Within the germinal centre lies separate zones, termed the light zone (LZ) and dark zone (DZ), based on their histological appearance <sup>64</sup>. The DZ contains the proliferating B cells, and is where the recombination and DNA mutation events occur. These cells are able to migrate to the LZ – where the cells are exposed to antigenic stimulation – where the B cells are selected for with regards to antigen affinity <sup>64</sup>. Those selected for are able to cycle between these two zones allowing more variants to be tested, resulting in high affinity clones to be produced. This process is supported through the neighbouring cells such as follicular T cells and DC which produce survival signals such as Bcl-6 <sup>62,168</sup>.

### a) V(D)J Recombination



### b) Class Switch Recombination

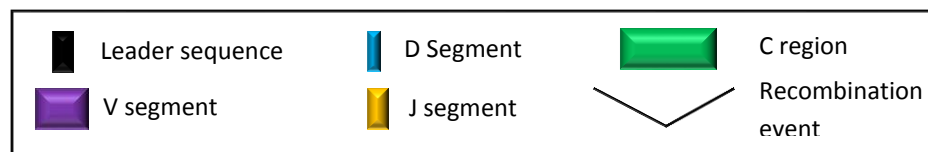
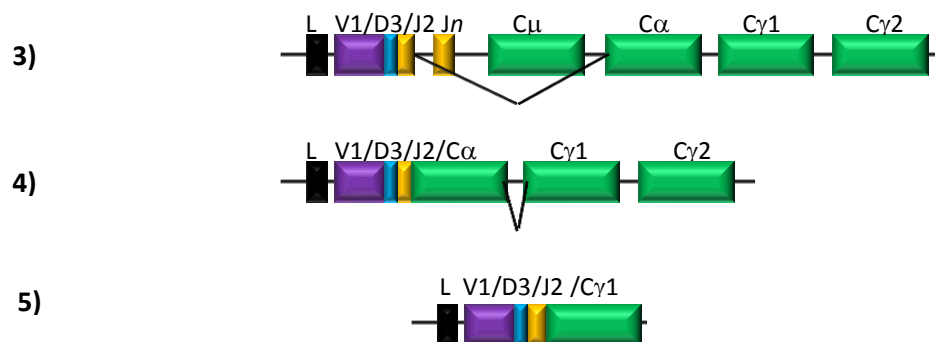


**Figure 1.3: V(D)J recombination and class switch recombination for formation of complete immunoglobulin heavy chain**

a) Gene rearrangement allows for the diversity of antibodies possible in humans via the production of hypervariable CDRs. 1) At the immunoglobulin locus (chromosome 14q32 in humans) Diversity (D) segment and Junction (J) segment recombine, in this example D3 joins J2. 2) A second recombination event occurs where a Variable (V) segment attaches to the preformed DJ segment, completing the variable domain of the antibody. B) Class switch recombination results in the selection of an alternative heavy chain Ig class. 3-4) occurs in the germline DNA in an iterative stepwise process where the recombined VDJ segment from a) is spliced against a specific constant (C) domain. 5) The resulting mRNA transcript allows for the translation of a complete immunoglobulin consisting of one VDJ adjoined to a single C segment – in the case illustrated above a human IgG1 heavy chain. A similar process occurs for the formation of the light chain, however there are only two fragments that form the variable domain (VJ) and two potential C segments ( $\kappa$  or  $\lambda$ ).

## 1.6 Monoclonal Antibody Production:

### 1.6.1 Immunisation and hybridoma technology:

Antibodies can be produced in various ways; for example they can be produced against a specific target through the immunisation of a recipient who does not already express the target, e.g. by injecting a human protein into a mouse. Immunisation results in a polyclonal

antibody response, producing multiple antibodies which differ in their epitopes and resultant binding affinities towards the antigen. Although these antibodies could be isolated from the serum for use, for example as a diagnostic or therapeutic tool, the heterogeneity of a polyclonal response typically makes polyclonal antibodies unsuitable for many purposes. Monoclonal antibodies, which contain a single antigen specificity are however, ideal for these purposes.

Producing monoclonal antibodies was made possible following the advent of hybridoma technology developed by Kohler and Milstein in 1975<sup>169</sup>. The hybridoma technology involved immunising a recipient animal with the antigen of choice (in the original paper it was Sheep Red Blood Cells (SRBC)) and collecting the splenocytes from the animal once an antibody response was generated. These splenocytes were fused to a myeloma cell line – using electroporation – and subcloned. This fusion event produced a hybridoma cell line that was able to produce antibodies towards SRBC, which could be isolated from the culture supernatant, but with the additional immortality of a cell line. It was found that the immunoglobulin genes were co-dominantly expressed – present from both the splenocyte and hybridoma – but this was subsequently overcome by using alternative myeloma cell lines that no longer produced their own antibodies<sup>170</sup>. This technology allowed the production of a monoclonal antibody in an *in vitro* system that was amenable to batch processing – thereby allowing consistency in the production of large quantities of antibody required by regulatory boards (such as the US Food and Drug Administration (FDA)) for licensing as a therapeutic<sup>171</sup>.

#### **1.6.2 Recombinant engineering / cell transfection:**

One of the early problems presented with antibodies produced using the murine hybridoma technology was the fact that patients generated a human anti-mouse antibody (HAMA) response. The HAMA response refers to the polyclonal generation of antibodies towards the non-human components of an antibody – not limited to just the Fc domain<sup>172</sup>. As a result of this response the murine antibodies were rendered inert, rapidly cleared from circulation and reinfusion was problematic, provoking adverse reactions within some patients<sup>173,174</sup>.

In order to overcome this limitation and restore the efficacy of mAb, genetic engineering of the antibody was performed, whereby the murine Ig regions were replaced with the human homologues<sup>175</sup>. This was possible through the improvement of molecular biology techniques (such as site-directed mutagenesis and recombinant gene engineering) giving rise to recombinant antibodies. Antibodies where the Variable domains of the heavy and light chain are attached to the Constant domains of a human Ig framework are referred to as chimeric

antibodies – such as rituximab. This has a far lower percentage of mouse sequence present in the final antibody sequence and is far better tolerated in multiple doses due to a reduction in the amount of anti-mouse antibodies produced <sup>174</sup>. Alternatively the CDRs of the murine antibody can be spliced onto a completely human antibody framework; these antibodies are referred to as humanised, as is the case with CAMPATH-1H <sup>176</sup>.

The recombinant genes for these antibodies are cloned into expression vectors which are transfected into antibody secreting cell lines in a similar manner to the hybridoma process (section 1.6.1). Chinese Hamster Ovarian (CHO) cell line are commonly used for this approach, instead of a murine myeloma cell line, as they are able to produce antibodies which undergo a similar post-translational modification such as the glycan structures that are added but do not themselves express native Ig molecules <sup>165,177</sup>.

### **1.6.3 Immunisation of humanised mice:**

Immunising mice with human antigens is an effective approach to generate tumour specific antibodies. However, as mentioned earlier, mouse antibodies are not ideal for long-term therapy in humans due to the HAMA response. These can be overcome through recombination with human immunoglobulin frameworks introduced above; however this process is not completely or always successful. In some cases the attachment of CDR loops required for humanised antibodies can alter the final affinity and specificity of the original antibody <sup>176</sup>. To work around this, transgenic mice which have been genetically altered to no longer produce mouse immunoglobulin but instead only generate fully human antibodies in response to immunisation with tumour antigens was required.

These humanised mice were successfully developed in 1994 by two independent groups, where the murine light and heavy chain genes were disrupted, and the loci for human immunoglobulin chains were incorporated <sup>178,179</sup>. This approach allows completely human antibodies to be produced, and coupled with the hybridoma technique, tumour specific antibodies were able to be isolated, immortalised and produced in large quantities. Panitumumab, an anti-EGFR antibody, was produced by this method and was approved in 2006/2007 for treatment of colon carcinomas <sup>144,178</sup>. Further developments to these mice with larger human repertoires are continually being developed <sup>180</sup>.

#### 1.6.4 Phage display library:

Fully human mAb can also be identified and generated in a completely *in vitro* process, termed phage display. Here, the immunoglobulin loci corresponding to both heavy and light chains are isolated from human B cells, or generated synthetically (allowing production of degenerate sequences) and cloned into bacteriophage<sup>181,182</sup>. The heavy and light chains are modified to recombine as a ScFv, or as a complete F(ab) which is able to be expressed on the surface of the bacteria, after inoculation with the bacteriophage. Potential antigens are able to be passed across the bacteria and interactions between the ScFv and antigen can be assessed. The ScFv/F(ab) DNA sequence can then be isolated from positive clones and converted into complete antibody proteins, using molecular biology techniques.

Although this process is amenable to high throughput screening, allowing the identification of potential candidates in a quicker manner than immunisation of mice, it is still a relatively expensive process, and a positive result in the first screen does not guarantee a functional antibody<sup>183</sup>. False positives are likely to arise due to the transition from the bacterial *in vitro* system to the cellular environment of the tumour cell. These hurdles include, the final affinity when grafted onto a whole Ig framework, specificity of the antibody – not all potential off-targets can be screened for *in vitro* – or even the availability of the selected epitope (a potential problem if a protein and not a cell was used in the identification of potential clones). However, due to the vast number of clones screened, many potential mAbs are identified, allowing the process to be taken forward even if the attrition level is relatively high. Critically this process is not subject to negative selection whereby self-reactive immunoglobulin expressing B cells (and antibodies) are deleted during development – allowing all possible antigens to potentially be detected.

#### 1.6.5 Post-translational modification of antibodies:

Alongside reducing the non-human component of antibodies for therapeutic mAbs, further engineering of an antibody is now being developed. An example of such engineering is through altering the glycosylation status of the hinge region and Fc domain of an antibody. Changing the final composition of the glycan attached to the Fc domain of an antibody has been shown to alter the affinity towards the FcγRs and in turn the efficacy of the depletion mechanisms engaged (discussed in section 1.7.6). This has been achieved with obinutuzumab (GA101) an anti-CD20 antibody, approved for the treatment of CLL in combination with chlorambucil<sup>184</sup>. This antibody has reduced fucose content in comparison to other anti-CD20 antibodies such as rituximab, by being produced in a cell line that does not contain the

fucosylation antibodies. This antibody is better able to engage CD16a, and as a result is more cytotoxic compared to non-glyco-engineered antibodies<sup>185,186</sup>.

## **1.7 Direct Targeting mAb Effector Mechanisms:**

Direct targeting mAb are able to engage a number of mechanisms in order to kill the targeted cell as summarised in Figure 1.4. They can be classified into cell-intrinsic mechanisms – reliant on intracellular signalling components – and cell-extrinsic mechanisms – dependent on additional extracellular components. Cell signal disruption and direct cell death (DCD) are intrinsic mechanisms whilst complement dependent cytotoxicity (CDC), antibody dependent cellular cytotoxicity (ADCC) and antibody dependent cellular phagocytosis (ADCP) are classed as extrinsic mechanisms. By understanding these mechanisms, improvements in the design and selection of immunotherapy candidates can be made which would overcome the current limitations faced in the development of antibody immunotherapy.

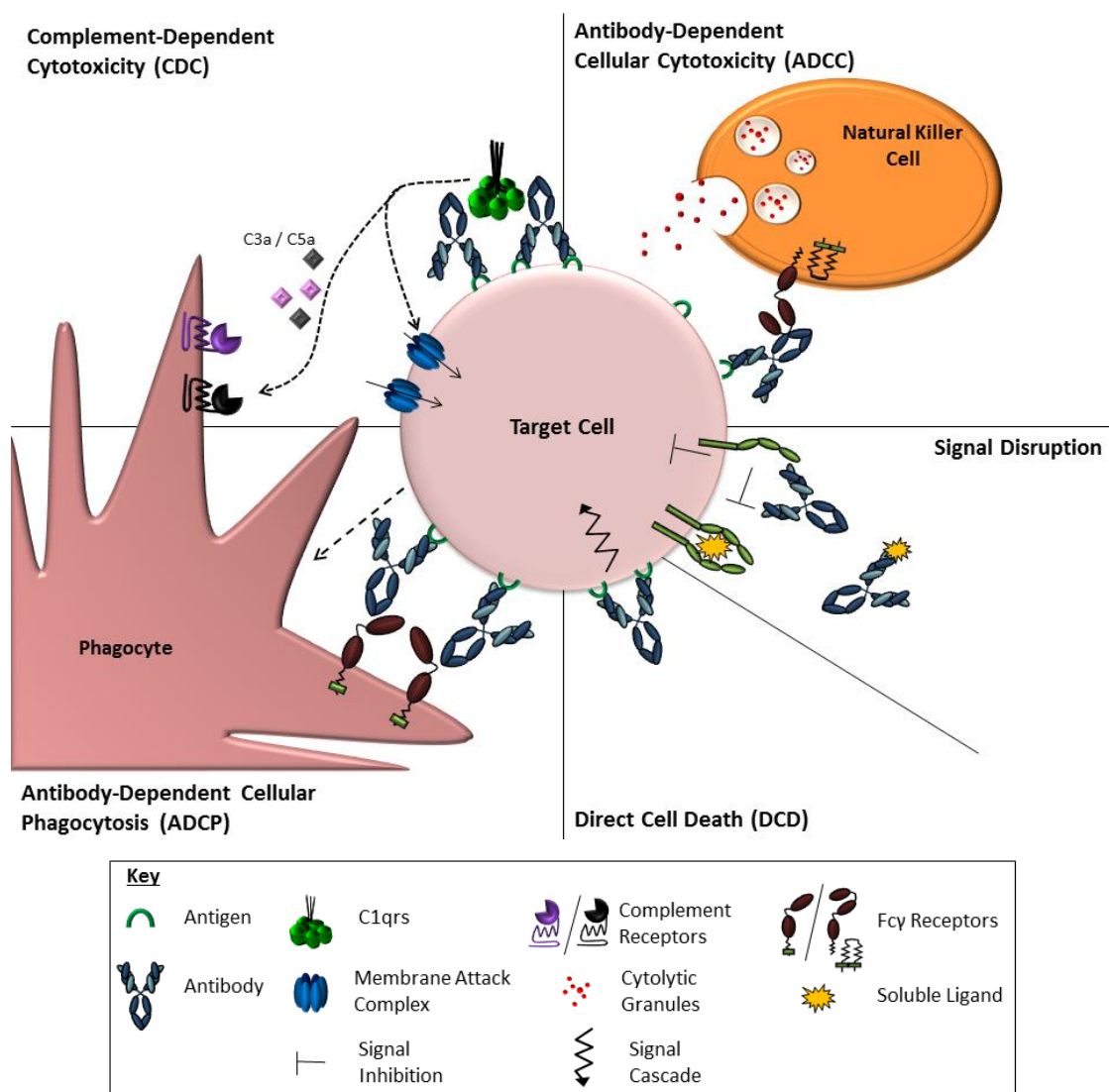


**Figure 1.4: Schematic of depletion mechanisms that are potentially engaged after cells are bound by a mAb**

When a direct targeting antibody binds the surface of a cell it can engage a number of different mechanisms resulting in the depletion of the cell. They can be independent of external factors – such as signal disruption and direct cell death (DCD) or dependent on extracellular components such as complement dependent cytotoxicity (CDC), antibody dependent cellular cytotoxicity (ADCC) and antibody dependent cellular phagocytosis (ADCP). Figure modified from CD20 review paper<sup>187</sup>.

### 1.7.1 Cell-intrinsic effector mechanisms:

Cell-intrinsic mechanisms are those which involve the antibody and the targeted cell only. Through binding alone, the antibody can initiate cell death either directly – through the engagement of death receptors or activation of the apoptotic pathway – or indirectly by interfering with signalling pathways critical for cell proliferation and survival. The ability to engage these pathways tend to be specific to the antigen selected, with a secondary reliance on the antibody isotype used.



### 1.7.2 Cell signal disruption:

When an antibody binds a receptor it can result in the inhibition of receptors or ligands critical for the survival or proliferation of the targeted cell. This property is mainly associated with the immunomodulatory antibodies which target immune effector cells, such as ipilimumab which removes T cell suppression<sup>188</sup>. Nonetheless, this property has also been observed with direct targeting mAbs which bind directly to the tumour cell.

For direct targeting antibodies, this is best exemplified with those that target the EGFR family, in particular pertuzumab and panitumumab. Pertuzumab is a humanised IgG2 mAb approved by the FDA for the treatment of Her2<sup>+</sup> metastatic breast cancer, in combination with trastuzumab and docetaxel<sup>189</sup>. It binds Her2 at the dimerisation domain, preventing ligand-dependent activation of the receptor therefore stalling cell cycle progression and proliferation in an Fc independent manner<sup>190</sup>. Similarly, panitumumab – a human IgG2 mAb for the treatment of colorectal cancer – targets the dimerisation domain of EGFR. It works in an analogous manner to pertuzumab, and due to the IgG2 isotype is less able to engage the cell-extrinsic mechanisms ADCC and CDC<sup>156</sup>. The efficacy of these mAb are dependent on the mutational status of the disease; if the cancer has gained the KRAS mutation – which results in ligand-independent receptor activation – then these mAbs are ineffective, highlighting the need for careful disease classification to identify patients that are likely to respond<sup>30</sup>.

### 1.7.3 Direct cell death:

Monoclonal antibodies are also able to induce cell death when cultured with target cells in the absence of any extracellular components<sup>191</sup>. Resistance to apoptosis is a hallmark of cancer<sup>22</sup> and as such targeting this pathway (through either the activation of pro-apoptotic components or inhibition of anti-apoptotic components) is a desirable therapeutic strategy. Further investigation has found that the type of death that is mediated upon antibody ligation can be either apoptotic or non-apoptotic in nature; similarly, the ability to engage this particular mechanism is dependent on both the antigen and the antibody involved.

Directly targeting the apoptotic pathway using agonistic antibodies is best reflected with those against the Death Receptor (DR) family of proteins – in particular DR4 and DR5. Upon ligand binding, the receptors cluster which allows the association of death-inducing signalling complexes which contains FADD (Fas Activating Death Domain) and procaspase 8<sup>35,192</sup>. FADD binding initiates the caspase cascade via activation of caspase-8 then caspase-3 activation on mitochondria, resulting in apoptosis of the cell<sup>35</sup>. DR are widely expressed on cells, and found

upregulated in epithelial carcinomas found in breast and colon tissue<sup>193</sup>. The increased expression of the receptor allows for preferential targeting with therapeutic antibodies, where the greatest dose response is found in cells expressing the most receptor – therefore most clustered/activated receptors.

Preclinical studies targeting DR4 has shown promise, where it is able to inhibit tumour growth and prolong survival<sup>194</sup>. Interrogation of the therapeutic mechanism has identified a requirement for FcγR to be present *in trans* for effective prevention of tumour growth (using mouse CD32 KO models), although whether this is required due to the resulting clustering of the receptors by cross-linking the antibodies or through an FcγR mediated mechanism is unclear<sup>195</sup>. Due to the expression profile of DR4 it was hypothesised to be toxic if given to humans, as hepatotoxicity had been reported in mice<sup>195</sup>, however a phase I dose escalation study in human patients reported that the drug was relatively well tolerated with no evidence of jaundice or liver failure, alleviating concerns of the toxicity of this drug<sup>196</sup>. Unfortunately, although low toxicity was reported, this trial did not report any significant therapeutic response contradicting the preclinical potential presented<sup>197</sup>.

An increase in cell death after antibody incubation has also been reported for antibodies which do not target the apoptosis pathway directly – for example anti-CD20 mAb<sup>198</sup>. Rituximab has been reported to engage DCD, and is more effective when cross-linked but in terms of the clinical response, this mechanism is most likely to have a supporting role in B cell depletion for this particular antibody<sup>199</sup>. The type II anti-CD20 mAbs (discussed in section 1.8.3) are better able to initiate DCD compared to rituximab, and it was found to be both independent of caspase activation, and unable to be inhibited by the overexpression of the anti-apoptotic protein Bcl-2<sup>200</sup>.

Further investigation of this caspase-independent death identified a role for actin rearrangement which led to an increase in the homotypic adhesion of cells cultured with the anti-CD20 mAb tositumomab compared to rituximab<sup>201</sup>. This cell death could be inhibited – alongside the homotypic adhesion – when an inhibitor towards actin polymerase, but not caspases, was used. The non-apoptotic death was defined as being the result of lysosomal degradation of the cytoplasm after CD20 binding<sup>201,202</sup>. This form of cell death has also been seen *in vitro* with other antibodies targeting proteins found in lipid raft microdomains, such as the BCR and HLA-DR<sup>200,201</sup>.

#### 1.7.4 Cell-extrinsic effector mechanisms:

Cell extrinsic mechanisms are those where the mAb recruits additional components – either cellular or protein in nature – in order to mediate depletion of the targeted cell. These mechanisms are mediated by the Fc region of an antibody, and can be further separated into Fc receptor (FcR)-independent and FcR-dependent mechanisms.

#### 1.7.5 Fc receptor independent mechanisms:

##### 1.7.5.1 Complement cascade:

The complement system forms part of the innate immune response to bacterial pathogens, consisting of a tightly regulated serine protease cascade. Activation of this cascade results in the formation of a membrane attack complex (MAC), which acts as a pore in the plasma membrane of a cell causing lysis and death<sup>203</sup>. There are over 30 components that contribute towards the three convergent pathways – referred to as Classical, Lectin and Alternative pathways. These three pathways all differ in their initiation but once C3 convertase is formed they follow the same stages to form the MAC.

The Classical pathway was the first elucidated, and is summarised in Figure 1.5. It is initiated when C1q binds to the Fc of antibodies bound to the cell in relatively close proximity<sup>204,205</sup>. Binding of C1q results in a conformational change that activates its associated proteins C1r and C1s; which cleave C2 and C4 into their active components<sup>206</sup>. The larger fragments, C2a and C4b, bind the target cell membrane where together they form the first main enzyme complex, C3 convertase (C2aC4b). This complex is able to cleave C3 into its active components, C3a and C3b, leading to an amplification loop, where cells become both further opsonised by C3b binding to the cell surface, as well as binding to the C2aC4b complex to create a C5 convertase multi-enzyme complex. C5 convertase facilitates the formation of the MAC with components C6-9<sup>207</sup>.

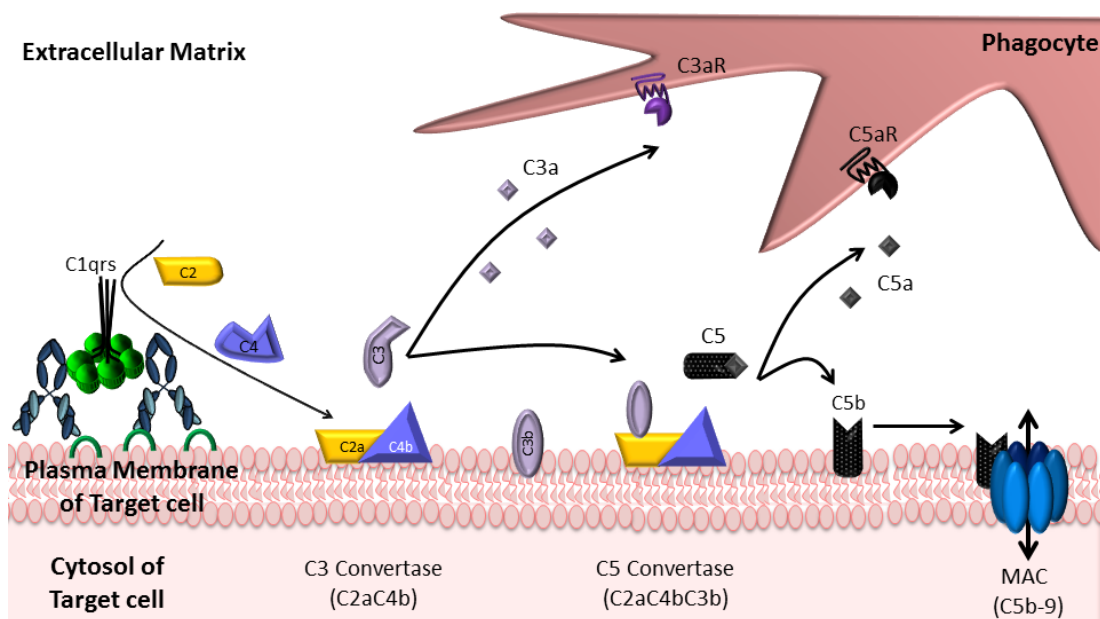


**Figure 1.5: Schematic of Classical Complement Pathway:**

The classical complement pathway requires the activation of C1 by the close association of antibody Fc regions found in immune complexes. Activation of complement results in the formation of C3 convertase leading to the formation of the membrane attack complex (MAC). The Lectin pathway is similar to the classical pathway illustrated however MBL (mannose binding lectin) which binds lectins present on the cell surface instead of C1 binding of antibodies. Complement receptors are present on phagocytes – such as macrophages and neutrophils – which are able to bind C3a and C5a resulting in activation and migration towards the opsonised target cell.

The Lectin pathway is almost identical to that of the classical pathway described above with the exception of the activation stage. Rather than relying on immunoglobulin complexes, the cascade is initiated by Mannose-binding lectin (MBL) protein, which targets the carbohydrates typically found on gram-negative bacteria or yeast <sup>208</sup>. Once bound MBL is able to activate an analogous serine protease to C1r/s, referred to as MASP (MBL-associated serine protease). MASP cleaves C2 and C4 into their active forms, allowing the cascade to continue along the pathway illustrated in Figure 1.5 <sup>209</sup>.

The third pathway, known as the Alternative pathway, is initiated by the spontaneous hydrolysis of soluble C3 in the serum into its active components C3a and C3b <sup>210,211</sup>. Free C3b is stabilised by Factor B in solution, where it is able to deposit onto the cell membrane of nearby cells – with the help of Factor D and properdin – as an alternative form of C3 convertase (C3bBb), illustrated in Figure 1.6. In a similar manner to the Classical pathway, activated C3b can then join the C3 convertase to form an alternative C5 Convertase complex (C3bBbC3b) leading to the association of the MAC <sup>212</sup>. The C3b can be produced spontaneously by this pathway, but can also come from the C3 convertase formed from the other two pathways, resulting in an amplification loop where multiple MAC can form on the targeted cell and those nearby if they do not contain complement defence molecules <sup>213</sup>. This non-targeted approach

results in the C3b component binding any nearby cells, however all cells within the body express complement defence molecules (described in section 1.7.5.2) which would prevent the formation of the MAC. Therefore it can be proposed that the alternative complement pathway provides a mechanism for the immune system to recognise non-self, by binding cells which do not express these defence molecules in an antigen independent manner.

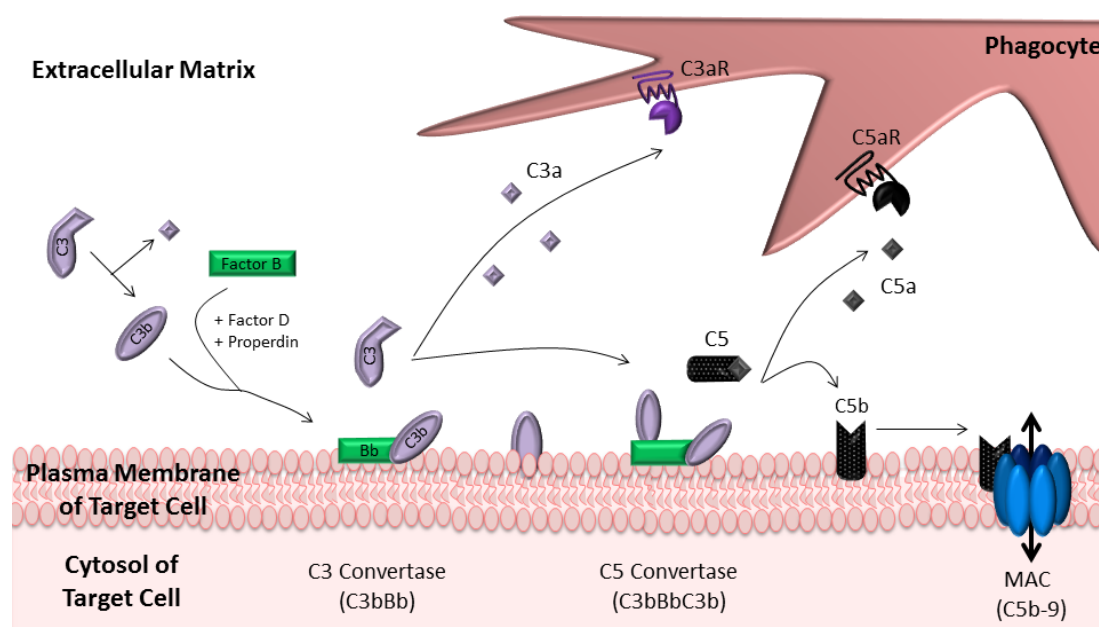


**Figure 1.6: Alternative complement pathway diagram.**

C3 can become activated by spontaneous hydrolysis (an antigen independent process) in the serum where it can be stabilised by Factor B. The stabilised C3bB complex is then cleaved by Factor D, where with the presence of properdin it can deposit on the cell surface as a C3 convertase complex. Further activation of C3 into its components leads to the formation of a high affinity C5 convertase complex (C3bBbC3b) where recruitment and formation of the Membrane Attack Complex (MAC) occurs in the same manner as the Classical complement pathway. Complement receptors are present on phagocytes – such as macrophages and neutrophils – which are able to bind C3a and C5a resulting in activation and migration towards the opsonised target cell.

As well as producing the components required for MAC formation **and** opsonins, the complement cascade also produces anaphylatoxins which are capable of recruiting immune effector cells <sup>214</sup>. These are best characterised by C5a which produces a chemotaxis gradient to promote migration of neutrophils and macrophages towards the complement opsonised cells <sup>215</sup>. Alongside their chemotaxis properties, activated complement components are able to bind complement receptors present on immune effector cells resulting in activation or augmentation of the cell function <sup>216</sup>. For example, C3b bound to the cell membrane can be further cleaved into iC3b – which is a ligand for Complement Receptor (CR) 3, found on neutrophils and macrophages. Engagement of these receptors polarise the macrophage towards a phagocytic phenotype rather than a cytotoxic one, improving the rate of clearance

<sup>217,218</sup>.

#### **1.7.5.2 Regulation of the complement cascade:**

Once activated the complement cascade is generally non-specific, therefore the potential for off-target effects is high. As a consequence of this, the complement cascade has evolved a number of regulatory systems to ensure that self-recognition is minimised. Failures in these processes can lead to increased incidences of bacterial infections or even autoimmune conditions such as SLE-like disease <sup>219</sup>.

One point of regulation is with the nature of the serine proteases. The majority exist as zymogens, which are only activated by a specific complement component prior to its position in the cascade. This mechanistic regulation results in the reduction of non-specific and unwanted proteolytic interactions from occurring <sup>220</sup>. In a similar vein, on their own, the activated components have a short half-life making them unstable; an example is with the active form of C3b which is prone to hydrolytic inactivation unless it binds to factor B, or the plasma membrane of a cell <sup>221</sup>. The key stages of the lytic pathways exist as a multi-enzyme complex resulting in a highly defined function requiring multiple steps to occur at once, once again negating the chance of spontaneous MAC formation from occurring <sup>210,212</sup>.

Alongside the serine proteases, there exist a number of soluble and membrane bound defence molecules which protect the host from the inadvertent deposition of activated complement factors. Commonly investigated complement inhibitors with regards to immunotherapy are the surface bound proteins CD46, CD55 and CD59 <sup>222</sup>. CD46 (also known as Membrane Cofactor Protein – MCP) is a membrane bound inhibitor that facilitates the inactivation of bound C4b and C3b by Factor I, however it only works *in cis* – it cannot target C4b bound to surrounding cells <sup>223</sup>. It is ubiquitously expressed in humans although the expression levels are heterogeneous across tissue <sup>224</sup>. CD55 (Decay Accelerating Factor – DAF) and CD59 (protectin) are glycosylphosphatidylinositol (GPI) linked proteins widely expressed on the surface of autologous cells <sup>225</sup>. CD55 works by destabilising the formation of C3 convertases by acting on C3b and C4b. CD59 acts on C9, thereby inhibiting the formation of the MAC and cell lysis <sup>226</sup>. Soluble regulators also exist, such as Factor I which works with the membrane bound inhibitors to inactivate C3b, although these are not as extensively investigated in relation to cancer immunotherapy.

The importance of complement for the defence and immune evasion of cancer is controversial. There is evidence that in some instances of bladder and colon carcinomas that these defence molecules are upregulated in comparison to healthy tissue <sup>227-229</sup>. However in

terms of antibody immunotherapy – discussed below – the expression levels of the defence molecules does not always correlate with therapeutic response <sup>222</sup>.

### **1.7.5.3 Complement Dependent Cytotoxicity in mAb immunotherapy:**

The lytic ability of an antibody to engage complement has been clearly demonstrated *in vitro* by a number of different groups, where target cells are opsonised with an antibody and incubated with serum (as a source of complement) <sup>230</sup>. The resultant cell lysis can be measured after as little as 5 minutes, although most *in vitro* studies use 30 minutes to measure total lysis <sup>231,232</sup>. Studies have demonstrated that opsonised cell depletion is attenuated in the presence of heat inactivated serum, and only seen with antibodies that specifically bind the cell target – not by soluble antibody present in solution (assessed with an isotype control antibody) <sup>233-235</sup>.

For antibody immunotherapy, it was found that the human IgG1 isotype was able to best lyse cells in the presence of serum, even though human IgG3 had superior binding of C1q <sup>156</sup>. IgM is also able to bind and activate complement efficiently, however with regards to the antibodies used in the clinic, IgM is not used as it is unable to engage the FcγR-mediated mechanisms (discussed in section 1.7.5) <sup>156</sup>. Close proximity of multiple Fc domains of an antibody are required for activation, with a hexameric conformation recently reported as favourable for the binding of C1q <sup>205</sup>. This clustering of Fc regions can be achieved by targeting highly expressed antigens (as seen with the anti-CD20 mAbs <sup>230</sup>) or through using a combination of antibodies towards the same antigen but target unique epitopes (demonstrated using a panel of anti-EGFR mAbs <sup>236</sup>). For haematological malignancies, CAMPATH-1H and the type I anti-CD20 mAbs are the best at engaging this mechanism in *in vitro* studies <sup>234,237,238</sup>, however, CDC has also been reported with the anti-EGFR mAb cetuximab and Herceptin <sup>239,240</sup>.

Xenograft models have previously implicated CDC as an important mechanism behind the depletion of malignant B cells by rituximab. These studies involved inhibiting complement in mice by treating with cobra venom factor (CVF) or using C1q knock-out mouse models (unable to initiate the classical pathway) – and found a reduced ability to deplete either CD20<sup>+</sup> cell lines or tumours <sup>232,241,242</sup>. These approaches did not completely prevent tumour clearance, indicating that although in these models CDC was important, it was not the only mechanism involved <sup>243</sup>. In contrast, more recent work looking at the B cell depletion of human CD20 transgenic mice with a modified rituximab antibody (mutated to prevent complement

engagement), observed little inhibition in the depletion rates of these cells when complement was impaired <sup>244</sup>. This study looked at the cell depletion in a physiologically relevant system – where the targeted cells were endogenous to the host, and not the product of a xenograft experiment (as the case of the earlier studies described) whereby only a few target cells are present. It was concluded that CDC was not a major mechanism for rituximab mediated cell depletion (in the mouse at least), leading to a change in the importance of CDC compared to alternative effector mechanisms in these models.

Clinical data supporting CDC as a mechanism for mAb-mediated depletion is more indirect, and derived from work investigating the anti-CD20 mAbs, particularly rituximab. It has been reported that complement levels in the serum were reduced following antibody therapy in CLL patients, however the extent of complement consumption did not correlate with therapeutic outcome <sup>245,246</sup>. The expression levels of the complement inhibitors CD46, CD55 and CD59 present on tumour cells did not correlate with the therapeutic resistance towards rituximab <sup>222</sup>. Work by Golay *et al.* who investigated CD55 expression on follicular lymphoma cell lines and primary tumours were able to overcome CDC resistance with rituximab if they treated the cells with an anti-CD55 antibody first <sup>247</sup>. However this work was performed *ex vivo* and the effect of blocking CD55 was best seen in the depletion of cell lines, not fresh primary samples. Whether this approach would be effective as a combination therapy to overcome resistance is yet to be validated.

The relationship between CDC and the FcγR mediated mechanism ADCC has produced conflicting observations. A complementary relationship between CDC and ADCC was proposed through a series of *in vitro* assays <sup>248</sup>. This work presented a reliance on high antigen expression levels to observe lytic effects in isolation (also reported for cetuximab <sup>249</sup>) but that an improvement in cell lysis was achieved when stimulated human peripheral blood mononuclear cells (PBMC) were used in combination with human serum as an effector source, suggesting a synergistic relationship. However the activation of the complement cascade has also been reported as antagonistic to effective ADCC. The mechanism behind this observation arises from the observation that C5 depleted serum inhibited ADCC, but C1 and C3 depleted serum had no impact, therefore concluding that the activation of C3 is important in this suppression <sup>185,250</sup>. In a separate study, C3b was found to inhibit NK cell activation (defined as a decrease in human (h)CD16 and an up-regulation of CD54) <sup>250,251</sup>. Inhibiting the C3R receptor on myeloid cells did not prevent this inhibition, ruling out a complement receptor dependent function. Furthermore, using a plate-based adhesion assay, it was reported that in the absence of serum NK cells were able to bind to rituximab coated to the plate. However, when

Page | 38



human serum was added to the rituximab coated wells prior to NK cells, this adhesion was disrupted <sup>251</sup>. Together, this information proposes that C3b can inhibit NK cell activation by directly binding hCD16 thereby preventing the Fc:FcγR interaction from occurring, diminishing ADCC activity.

It is concluded that most of the data supporting CDC as a main effector mechanism for direct targeting antibodies is indirect and primarily based on *in vitro* evidence with cell lines. As a result the overall contribution CDC has to the therapeutic efficacy of a mAb *in vivo* is unclear and likely plays a secondary role to the FcγR dependent mechanisms discussed below.

### 1.7.6 Fc receptor dependent mechanisms:

Fc receptors are a family of proteins that bind the Fc region of an antibody, and are expressed on many cells of the immune system. Within this family, the receptors are grouped dependent on the ability to bind each of the immunoglobulin heavy chains – for example FcαR binds IgA and FcγR binds IgG. As most therapeutic antibodies approved for use in the clinic have an IgG heavy chain, this section will focus on the FcγR family.

### 1.7.7 Fcγ receptors:

In humans there are six different FcγR which differ in their expression patterns, and binding to the IgG isotypes as summarised in Figure 1.7a. Humans contain one high affinity activatory receptor (hCD64; FcγRI) four low affinity activatory receptors (hCD32a, CD32c, hCD16a and hCD16b; FcγRIIA, FcγRIIC, FcγRIIIA and FcγRIIIB respectively) and one inhibitory receptor (hCD32b, FcγRIIB) <sup>160</sup>. hCD64 and hCD16a require an adaptor molecule, the common gamma-chain, for expression at the cell surface and to signal within the cell <sup>252</sup>. hCD16b is unique as it exists as an extracellular protein attached to the cell membrane via a GPI anchor. Due to its lack of intracellular domains how it is able to signal when activated is currently unclear – however it has been shown to have an activatory role and not just acting as a sink to bind soluble antibodies <sup>253</sup>.

The expression profiles of these receptors are dependent on the immune cell and to a lesser extent, the activation status of the cell. B cells predominantly only express the inhibitory receptor hCD32b, although a small population may also express hCD32c if they have the Open Reading Frame (ORF) allele <sup>254</sup>. NK cells only express the activatory receptors hCD16a and hCD32c – although again only if they express the ORF variant of hCD32c. Very rarely they may also express hCD32b through a recently discovered splice variant of hCD32c <sup>160</sup>. The myeloid

cells express a combination of inhibitory and activatory receptors, although the expression levels are dependent upon the microenvironment and stimulation of the cell.

Mice contain four FcγR which are summarised in Figure 1.7b. Akin to humans they contain one inhibitory receptor that is homologous to hCD32b (mCD32; FcγRII). They also possess one high affinity receptor – mCD64 (FcγRI) akin to hCD64 – and two low affinity activatory receptors – mCD16 and mCD16-2 (FcγRIII and FcγRIV, respectively) <sup>255</sup>. Unlike humans there are no GPI linked receptors, and all of the activatory receptors require co-expression with the mouse common γ-chain for surface expression and signalling to occur. Similar to humans, mouse B cells express only the inhibitory receptor mCD32, whilst NK cells only express the activatory receptor, mCD16. In contrast to humans, the high-affinity receptor mCD64 is expressed on macrophages and DC, whilst the rest of the myeloid population express combinations of the remaining three receptors – mCD16, mCD16-2 and mCD32 <sup>252,256</sup>.

a) Human Receptors	hCD64 (FcγRI)	hCD32a (FcγRIIA)	hCD32b (FcγRIIB)	hCD32c (FcγRIIC)	hCD16a (FcγRIIIA)	hCD16b (FcγRIIIB)
Structure						
Expressed on	Macro Mono DC (Neutro)	Macro Mono DC Neutro	Macro Mono DC B cells (NK)	Macro Mono Neutro NK cells (B cells)	NK cells Macro Mono	Neutro (DC)
Signal motif	Adaptor molecule ITAM	ITAM	ITIM	ITAM	Adaptor molecule ITAM	GPI linked
b) Mouse Receptors	mCD64 (FcγRI)	mCD16 (FcγRIII)	mCD32 (FcγRII)		mCD16-2 (FcγRIV)	
Structure						
Expressed on	DC Macro	NK cells Mono Macro DC Neutro	B cells Mono Macro DC Neutro		Neutro Mono Macro	

**Figure 1.7: Summary of FcγR family in humans and mice**

a) There are six FcγR in humans which include inhibitory and activating receptors. Signalling requirements and expression pattern is presented in the table. b) In mice there are four FcγR. They share the same nomenclature as the humans, but the similarities/homologies are not always appropriate. To reflect this mouse receptors in panel b) are ordered under the most similar human receptor to visually show analogous receptors based on function. For example mCD16 is most like hCD32a as they have similar expression patterns on immune cells, with the exception of mouse NK cells which expresses mCD16 whilst human NK cells do not express hCD32a. The cells which express each receptor has been supplied. ITAM = immunoreceptor tyrosine-based activation motif; ITIM = immunoreceptor tyrosine-based inhibition motif. Mono = monocytes; Macro = Macrophage; DC = Dendritic cells; NK = natural killer cell. Cells in parenthesis ( ) are those that occur in a small population, or demonstrates inducible expression rather than being constitutively expressed. Information for the table has been collated from review articles <sup>252,255</sup>

#### 1.7.7.1 FcγR polymorphisms:

Within the FcγR family, there are common single nucleotide polymorphism (SNP) that result in amino acid changes which alter the receptor binding affinities towards the Fc of an antibody, or its mobility on the cell surface <sup>160</sup>. Human CD16a has either a 158Val or a 158Phe allele. An

increase in the affinity towards IgG is reported for people who are either heterozygous or homozygous for the Val allele<sup>82</sup>. Human CD32a also has an allelic polymorphism which alters the affinity towards IgG, denoted by the low affinity – 131Arg – or the high affinity 131His. A human CD32b SNP results in a change in the ability to localise into lipid raft microdomains, where a switch from Ile187Thr results in a loss in this ability<sup>257</sup>. Lastly three polymorphic variants of hCD16b exist referred to as NA1 (36Arg, 65Asn, 82Asp and 106Val), NA2 (36Ser, 65Ser, 82Asn and 106Ile) and SH (NA2 variant with 78Asp). These polymorphisms change the glycosylation site within the receptor, although the phenotypic consequence of this is unknown.

Each FcγR exhibits different specificities towards the IgG isotypes resulting in unique binding profiles. Interrogation of these relationships between human Fc and FcγR has resulted in the summary present in Table 1.3<sup>255</sup>. Due to the high affinity hCD64 has to IgG, this receptor is usually bound by endogenous IgG present in circulation, as a result of this its role in mediating mAb immunotherapy is unclear, as this receptor wouldn't be freely available for the antibody to bind. However, it has been proposed that hCD64 may bind immune complexes under conditions of inflammation<sup>258</sup>.

	hIgG1	hIgG2	hIgG3	hIgG4
<b>hCD64</b>	High	No	High	High
<b>hCD32a -131His</b>	High	Med	High	Med
<b>hCD32a -131Arg</b>	High	Low	High	Med*
<b>hCD32b</b>	Low	No	Med	Low
<b>hCD32c</b>	Low	No	Med	Low
<b>hCD16a -158Val</b>	High	Low	High	Med
<b>hCD16a -158Phe</b>	Med	No	High	No
<b>hCD16b</b>	Low	No	Med	Low

**Table 1.3: Human FcγR specificity towards human IgG isotypes**

Relative binding of the human FcγR towards the Fc domain of human IgG antibodies, summarised from the work of Bruhns and colleagues<sup>160</sup>. \* binding better to Arg compared to His allele in flow cytometry experiments.

In mice, the relationship between the IgG isotype and the receptor is very different to humans – summarised in Table 1.4. The mouse IgG2a isotype is the most lytic in cell clearance, due to its ability to bind all of the FcγR, with a high affinity towards the activatory receptors, and a lower affinity towards the inhibitory receptor.

	mIgG1	mIgG2a	mIgG2b	mIgG3
mCD64	No binding	High	Low	Very poor
mCD32	Low	Low	Low	No binding
mCD16	Low	Low	Low	No binding
mCD16-2	No binding	High	High	No binding

**Table 1.4: Mouse FcγR affinity towards mouse IgG antibodies**

Relative affinity of the mouse FcγR towards the Fc domain of mouse IgG antibodies, summarised from the work of Bruhns and colleagues <sup>255</sup>.

#### **1.7.7.2 FcγR in mAb immunotherapy:**

The importance of FcγR in antibody clearance of target tumour cells was demonstrated in 2000 by Clynes and colleagues who investigated the depletion of a xenografted CD20<sup>+</sup> tumour *in vivo* using a combination of γ-chain KO and CD32 KO mice <sup>259</sup>. The γ-chain KO mouse does not express any activatory FcγR therefore only expresses the inhibitory mCD32; whilst the CD32 KO mouse would only express the activatory receptors. γ-chain KO mice were unable to clear tumour cells after rituximab treatment compared to WT mice. In contrast, CD32 KO mice responded better to mAb therapy than WT mice. Together these observations demonstrate how a combination of both the activatory and inhibitory receptors regulates the tumour clearance following mAb therapy. These observations have been reported for the depletion of endogenous B cells in response to anti-CD20 therapy, further illustrating the dependence of FcγR for effective mAb therapy <sup>242</sup>.

#### **1.7.7.3 FcγR signalling:**

Activation of the FcγR requires the receptors to cluster – achieved through binding immune complexes or multiple antibodies in close proximity due to antigen expression on the target cell <sup>257,260</sup>. With the exception of hCD16b, clustering of the activatory FcγR results in the phosphorylation of the immunoreceptor tyrosine-based activation motif (ITAM). The ITAM is present either on the intracellular tail of the receptor (for hCD32a and hCD32c) or supplied by the common γ-chain. The ITAM consists of two pairs of Tyr-X-X-Leu (where X represents any amino acid) separated by approximately 7 amino acids <sup>261</sup>.

Phosphorylation of the ITAM by Src kinases forms a docking site for Syk (a pleiotropic kinase) which is able to interact with a number of common signalling cascades, dependent on the effector cell. For example, activation of LAT, leads to the PI3K pathway – known to influence Ca<sup>2+</sup> influx thereby altering the vesicular release of cytotoxic particles, or cytoskeletal rearrangement required for phagocytosis. Similarly Syk can also activate the MAPK pathway

resulting in transcriptional changes mediated via NFκB in the nucleus, controlling the activation state of the immune cell in question <sup>252</sup>.

In both humans and mice the inhibitory receptor CD32b signals through an intracellular ITIM (immunoreceptor tyrosine-based inhibitory motif), which has a consensus sequence of Val/Ile-x-Tyr-x-x-Leu/Val <sup>252,262</sup>. As is the case for the activatory receptor, it requires receptor clustering after cross linking via an antibody or immune complex. As a consequence of receptor clustering the ITIM is phosphorylated by Src kinases, forming a docking site for SHIP-1. SHIP-1 is able to hydrolyse phosphoinositide intermediaries thereby diminishing any downstream activation pathways mediated from PI3K/PLCγ. The activation status of a cell is tightly regulated through the balance of the FcγR; CD32b can also attenuate BCR signalling pathways in response to antigen recognition <sup>263</sup>.

#### **1.7.8 Antibody Dependent Cellular Cytotoxicity:**

ADCC refers to the mechanistic release of cytotoxic particles in response to FcγR activation resulting in lysis or death of the targeted cell (Figure 1.8) <sup>264</sup>. Evidence for this mechanism as a response to mAb therapy has come primarily from *in vitro* work and the influence of FcγR polymorphisms from clinical trials. For example, a study by Cartron and colleagues, investigated the therapeutic response to rituximab in patients with NHL <sup>265</sup>. They showed that patients who were homozygous for the 158Val allele of hCD16a had far better survival compared to those that contained at least one 158Phe allele.

NK cells were proposed to be the main effector cells of ADCC due to only expressing the activatory FcγR. It is hypothesised that by expressing only activatory receptors NK cells are more sensitive to FcγR activation due to a lack of inhibitory receptors therefore would have a lower activation threshold in response to Fc binding <sup>266</sup>. NK cells were identified as the main effector cells for ADCC in an *in vitro* study. Human PBMC were able to lyse CD20<sup>+</sup> Daudi cells treated with rituximab, however this ability was lost when the NK cells were removed from the population <sup>267</sup>. Activation of hCD16 on the NK cells results in the release of perforin and granzyme, inducing apoptosis of the targeted cell, in a similar manner to that seen in T cell cytotoxicity <sup>268</sup>.

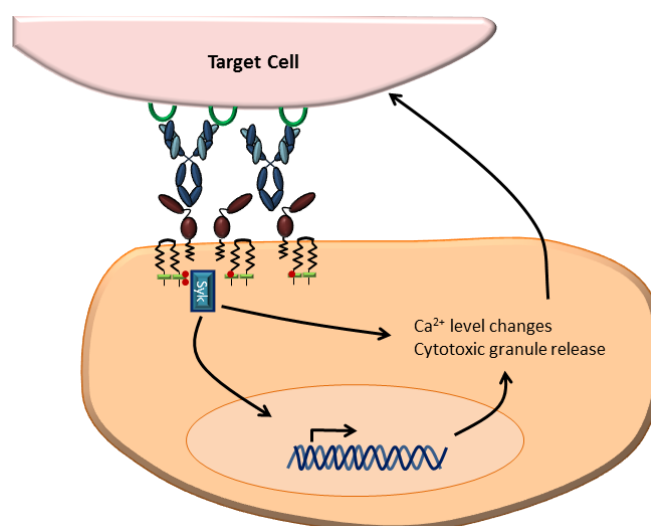


**Figure 1.8: Illustration of ADCC activation of FcγR engagement**

Antibodies bound to a target cell are able to engage with FcγR expressed on immune effector cells, such as NK cells, resulting in clustering of the receptors in the membrane. This clustering allows the ITAMs to become phosphorylated and active, becoming a docking site for Syk where different signal cascades are engaged. Together these result in activation and release of cytotoxic granules that induce apoptosis of the targeted cell.

hCD16 polymorphisms have been correlated to the therapeutic efficacy of mAbs, for example with rituximab and cetuximab<sup>265,269</sup>. Here, the presence of at least one hCD16-Val allele was sufficient to improve the lytic response with isolated human NK cells against opsonised CD20<sup>+</sup> cell lines<sup>82</sup>. In a similar manner, glycoengineered mAbs which have an afucosylated glycan, are reported to have a higher affinity towards hCD16, and produce a more potent ADCC response compared to WT antibodies *in vitro*<sup>185</sup>.

### 1.7.9 Antibody Dependent Cellular Phagocytosis:

ADCP refers to the engulfment of the targeted cell after FcγR engagement, where it is degraded by lysosomal proteins, rather than the release of cytotoxic particles. This process is mediated by FcγR engaged on myeloid cells, particularly macrophages and neutrophils. ADCP is activated in the same manner as ADCC, FcγR become clustered and phosphorylated at the ITAM, however, in this case downstream signalling events results in actin rearrangement and formation of the phagosome<sup>270</sup>.

Early work investigating the contribution of FcγR to antibody immunotherapy did not distinguish between phagocytosis and cytotoxicity. The role of macrophages and ADCP to the efficacy of therapeutic mAb is now becoming more prominent and defined. This is exemplified in a study which measured the depletion of endogenous B cells in mice following treatment with anti-mouse CD20 antibodies. The authors demonstrated that treating the mice with

clodronate – thereby removing macrophages – followed by mAb treatment resulted in diminished clearance of B cells compared to WT mice <sup>242</sup>. This inhibition was not seen when complement or NK cells were impaired, thereby concluding that macrophages were important effector cells for B cell depletion <sup>242,271</sup>.

For the *in vitro* assessment of phagocytosis, macrophages have to be derived from monocytes isolated from either human PBMC or mouse bone marrow <sup>272,273</sup>. This process produces a pure population of macrophages, which can then be used to measure phagocytosis as a direct result of an antibody in the absence of any additional opsonisation (from complement) or cell lysis (from lymphocyte based ADCC). Research into improving the engagement of this mechanism has involved looking at different isotypes of the antibodies. It has been proposed that an IgA mAb would be better at recruiting neutrophils, thereby resulting in better phagocytosis; however, this approach would remove the CDC and NK cell engagement, which may be more important for the treatment of tumours in some cases <sup>249</sup>.

## **1.8 CD20 and its Antibodies:**

### **1.8.1 Human CD20:**

CD20 is highly expressed on B cells, but lacking from early pre-B cells and the terminally differentiated plasma cells. Although the structure has not been resolved by X-ray crystallography, biochemical interrogation of the protein has resulted in its classification as a tetraspanning membrane bound protein, with an intracellular N and C terminus <sup>274</sup>. It is widely accepted that CD20 consists of an extracellular loop, held together by a disulphide bond, and a far smaller loop, which either sits flush on the membrane or just above the surface <sup>275</sup>. A summary of the 2D structure and post-translational modifications of CD20 is presented in Figure 1.9.



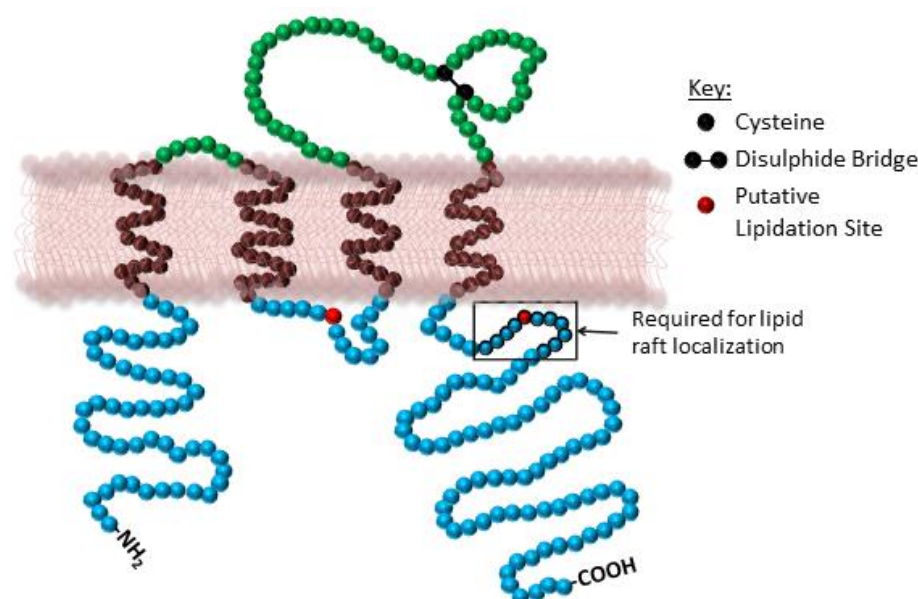


**Figure 1.9: Illustration of CD20 structure**

The current understanding for the structure of CD20 is illustrated. The protein consists of four membrane spanning regions (brown) a small and larger extracellular loop (green) held together with a disulphide bridge (denoted in black). The majority of the protein present in intracellular domains (blue), with potential sites for lipidation (in red), and involved in membrane localisation into lipid raft domains (black box) highlighted. Figure is adapted from CD20 review article <sup>187</sup>.

Even though it is an important marker of B cells, the biological role of CD20 is unclear. It contains many similarities with other proteins that are ion channels and therefore was hypothesised to be involved in the regulation of calcium flux in response to activation of the BCR. Stimulation of B cells with anti-CD20 antibodies resulted in an increase in calcium flux, similar to that seen in BCR activation <sup>276</sup>. It is more likely to be an adaptor molecule where it propagates the BCR signal, rather than an ion channel, based on studies which present a dissociation of CD20 from the BCR signalling complex after BCR activation <sup>277,278</sup>.

CD20 KO mice revealed no inherent deficiency in the differentiation of the B cell repertoire, although an impaired antibody response after vaccination with adeno-associated virus was reported <sup>279</sup>. Although rare, a case study on a person who had no CD20 reported low levels of circulating IgG and an impaired T cell independent antibody response to pneumococcal polysaccharide vaccination <sup>280</sup>. From these findings, it can be proposed that whilst not critical to B cell development, the presence of CD20 supports and enhances the generation of antibodies in response to vaccinations, and in the production of circulating IgG <sup>187</sup>.

Human CD20 shares over 70% sequence similarity with mouse CD20 (Uniprot references: P11836 and P19437) when compared using BLAST software provided by the NCBI <sup>281</sup>. Although there is high sequence similarity, one key difference lies in the rituximab binding region of the extracellular loop <sup>282</sup>. In humans this contains an -ANPS- motif, which is critical for rituximab

binding, however in mice this region contains –SNSS–<sup>231</sup>. Therefore anti-human CD20 antibodies which bind this region are unable to bind endogenous mouse CD20<sup>283</sup>.

### **1.8.2 Rituximab:**

The restricted expression of CD20 makes it highly appealing as an antigen for targeting with mAb in haematological malignancies. Rituximab is a chimeric anti-CD20 antibody containing the variable regions of the mouse antibody – 2B8 – cloned onto the constant regions of a human IgG1 heavy chain and  $\kappa$  light chain<sup>284</sup>. It has a high affinity towards CD20, and is able to effectively engage CDC, ADCC and ADCC to deplete B cells<sup>174</sup>. From the outset its ability to deplete circulating B cells, as well as those in the lymphatic system has been well documented<sup>174,285</sup>.

In 1997 rituximab (tradenames Rituxan, mAbThera) was approved for the treatment of refractory low-grade NHL as a monotherapy. Patients treated with rituximab reported a decrease in the five year mortality rates for the first time – a landmark achievement considering the rate of incidence had increased over the same period<sup>286</sup>. Since then rituximab has been approved for the treatment of CLL and ALL, and is now commonly used in combination with chemotherapy regimens where an improvement over chemotherapy is consistently reported. For example, when used in combination with the CHOP regime to treat DLBCL an improved response and survival over three and ten years post-therapy was reported, and since then R-CHOP therapy has become an established regime<sup>113,287</sup>. More recently, rituximab has been applied to autoimmune conditions, in particular rheumatoid arthritis, where B cell depletion also removes the autoreactive B cells, thereby alleviating the symptoms<sup>63</sup>. Investigation towards use for other autoimmune conditions is ongoing.

### **1.8.3 Type I and II anti-CD20 mAbs:**

The success of rituximab in the treatment of haematological malignancies has led to the development of a number of different anti-CD20 mAbs, which bind unique epitopes within the protein (summarised in Figure 1.10). Most of the anti-CD20 antibodies developed bind the carboxy-terminal end of the larger extracellular loop – presumably due to the more stable conformation maintained by the disulphide bond. The exception is ofatumumab which binds a completely separate epitope involving the small loop – and stabilised by 150Glu present on the larger loop<sup>231,288</sup>.

Although these antibodies bind the same target, and an overlapping epitope, it was concluded that not all anti-CD20 antibodies are the same functionally. Furthermore, they could be

grouped into two classes based on the effector mechanisms engaged<sup>244,289</sup>. Type I anti-CD20 mAbs (such as rituximab) are able to effectively engage CDC, ADCC and ADCC, but are poor at engaging DCD, or induction of homotypic adhesion. In contrast binding of Type II antibodies (such as tositumomab and obinutuzumab) have poor ability to engage CDC, although they are efficient at inducing DCD<sup>185,202</sup>.

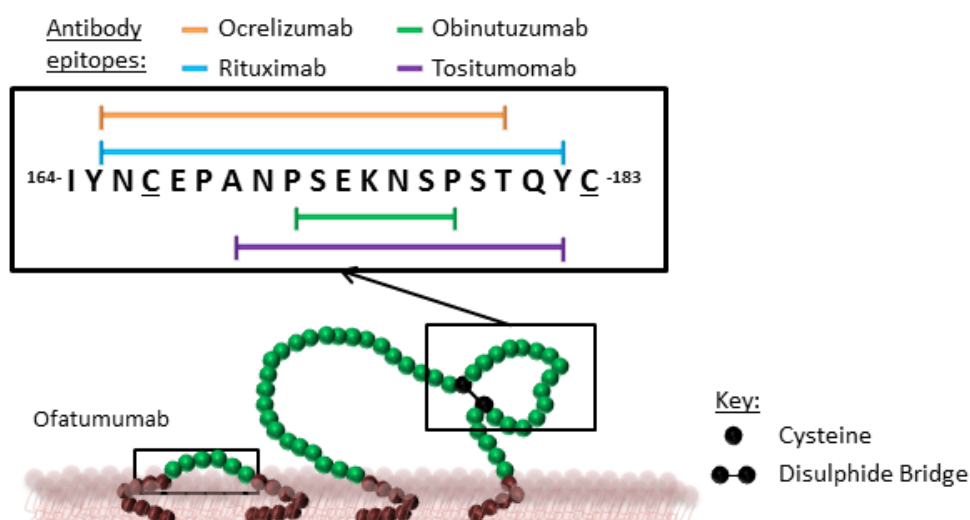


**Figure 1.10: Epitopes of therapeutic anti-CD20 mAbs**

The epitopes for the clinically approved anti-CD20 mAbs on the CD20 molecule are provided. These show that most of the antibodies bind the larger extracellular loop – with the exception of Ofatumumab. The Type I mAbs – Ocrelizumab and Rituximab – bind towards the amino-terminus of the loop, whilst the Type II mAbs – Tositumomab and Obinutuzumab – bind towards the carboxy-terminus of the loop. Figure modified from CD20 review article<sup>187</sup>.

A second defining feature of the Type I and II anti-CD20 mAb were their ability to localise CD20 into lipid rafts after binding<sup>244</sup>. Cell membranes are classified as being fluid, with the ability to alter its composition over time, either through protein turn-over, or in the development and reshuffling of membrane phospholipids<sup>290</sup>. Lipid rafts are sphingolipid rich micro-domains that are present within the plasma membrane of a cell. Due to the thicker membrane in this area (as a consequence of the fatty acid composition) they tend to attract/contain clusters of membrane bound proteins which are involved in signalling, producing a form of micro-organisation across the cell surface<sup>291</sup>. Type I antibodies (or rituximab like) are able to migrate the CD20 molecules into lipid rafts whilst Type II anti-CD20 mAbs are not able to move into raft domains<sup>200,233</sup>.

It is still unclear what physical property defines a mAb as Type I or Type II. F(ab) domains of rituximab and obinutuzumab – which bind a similar epitope (Figure 1.10) – have been resolved by X-ray crystallography using a CD20 synthetic epitope as a ligand. A comparison of these structures by Niederfellner *et al.*, revealed a difference in the angle of binding between the two antibodies in relation to the peptide<sup>292</sup>. Differences in the number of bound molecules to

CD20<sup>+</sup> cells has also been reported; twice as many Type I antibodies are able to bind CD20 compared to Type II mAbs<sup>230,233</sup>. From these observations it has been hypothesised that the orientation of the antibody can determine the ability to engage the effector mechanisms, and alter the amount of receptor cross-linking achieved<sup>289</sup>. Other reasons include potential differences in the recognition of CD20 associated tetramers present within the surface, or other conformational changes.

Lastly, the internalisation between the type I and II anti-CD20 mAbs are different. Type I mAbs are readily internalised, resulting in less on the surface of target cells for engagement by the effector mechanisms<sup>293</sup>. Type II mAbs although they bind at lower densities compared to Type I mAbs, remain on the cell surface and have a longer serum half-life<sup>271</sup>. The persistence of Type II mAbs in the serum may explain the improved responses reported when comparing B cell clearance between these classes of mAb<sup>186,244</sup>.

## **1.9 CD52 and CAMPATH-1H:**

### **1.9.1 Human CD52:**

CD52 is a small, glycosylated protein that is attached to the cell surface via a GPI anchor<sup>294,295</sup>. It is primarily found highly expressed on the surface of B and T lymphocytes, and has been reported at lower expression levels on other mononuclear cells such as monocytes, macrophages, and epithelial cells of the epididymis (where it can be translocated to the spermatozoa)<sup>296-298</sup>.

The mature peptide is unusually small, and is originally translated as a 63 amino acid pro-peptide containing a leader sequence (which traffics the protein to the surface), a 12 amino acid mature peptide, and a carboxy-terminal sequence that mediates the cleavage and attachment of the mature peptide to a GPI anchor<sup>237,299</sup>. Isolation of the CD52 protein from human spleens identified two subclasses of CD52, that varied in their hydrophobicity and sensitivity to phosphoinositide-phospholipase C (PI-PLC) digestion, denoted by either CD52-I or CD52-II<sup>296</sup>. Through a combination of biochemical analysis and mass spectrometry, it was elucidated that these two subclasses contain the same mature peptide and core glycan structure, but utilised a different GPI anchor. CD52-I, which was PI-PLC sensitive, contained a diesteroyl-phosphoinositol, whereas CD52-II contained a palmitoylated stearyl-arachidonyl-phosphoinositol. Although structurally similar, the addition of the palmitoyl group was found to inhibit the substrate site for PI-PLC resulting in a non-cleavable form<sup>296</sup>. It is unclear whether the presence of these two subclasses is cell type specific, or whether they can be co-

Page | 50

expressed. One study which treated the K422 cell line (derived from NHL) with PI-PLC reported an approximate 50% reduction in CAMPATH-1M antibody binding whereas another study showed cell specific responses to PI-PLC mediated loss <sup>295</sup>. Gene sequencing has also revealed no differences in the gene sequence of these subclasses, indicating it may be down to the GPI biosynthesis pathways available within each cell, rather than something encoded for by the genome. Although there are these minor differences in the anchor, both subclasses are able to be bound by the anti-CD52 antibody CAMPATH.

CD52 is present in other model organisms, however there is significant variation in both the sequence and length of the mature peptide, as summarised by Kirchhoff and Hale <sup>297</sup>. Human CD52 was most homologous to that found in rhesus macaques, with both the rat and mouse mature peptide being far larger and very different in the final composition of amino acid properties.

Although CD52 is too broadly expressed to be a unique cell-type specific phenotypic marker, it has far more interest as a target for immunotherapy. Its function on the cell surface is still unknown; there is no known downstream signalling due to its lack of intracellular peptide domain, however one study looked at T cell proliferation in combination with phorbol-myristate-acetate (PMA) which proposed that cross linking of GPI anchored proteins can induce an amplified T-cell response <sup>300</sup>, although this was later disputed by conflicting observations <sup>301</sup>. An alternative function is in immune defence. This is mainly from studies of spermatozoa, which postulated that CD52 is more of a scaffold for glycan attachment, which in turn protects the sperm in a glycocalyx-like role seen in bacteria to avoid destruction by the immune system <sup>297</sup>.

### 1.9.2 CAMPATH-1H

Anti-CD52 antibodies were originally raised in rats immunised with human mononuclear cells by Hale *et al* in 1983 <sup>302</sup>. CAMPATH-1 (clone YTH 66.9), a rat IgM antibody, demonstrated complement mediated lysis of B and T lymphocytes in the presence of human serum, and was subsequently used in the treatment of donor bone marrow in order to remove donor T cells and minimise graft vs host disease (GvHD) <sup>302,303</sup>. The potential for CAMPATH-1 to be used therapeutically *in vivo* was soon recognised, and a rat IgG2b isotype (denoted CAMPATH-1G) was isolated as a class-switched hybridoma <sup>294</sup>. This version maintained its lymphocyte specificity and complement fixing capabilities; however it was now able to engage FcγR mediated mechanisms <sup>304</sup>. Patient trials demonstrated anti-rat-antibody responses that

reduced the efficacy of the therapy, so finally a humanised version (denoted CAMPATH-1H) was engineered where the CDRs of the rat antibody were cloned onto a human IgG1 framework<sup>176</sup>.

As previously mentioned, CAMPATH-1H has been used in the *ex vivo* depletion of lymphocytes from bone marrow donations in order to minimise the GvHD response, reducing both transplant rejection and associated toxicities within the recipient. CAMPATH-1H (also known as alemtuzumab) has been used in the treatment of haematological malignancies such as CLL and non-refractory NHL, particularly where previous anti-CD20 therapy was ineffective<sup>305,306</sup>. For autoimmune conditions, it was identified as having a potential benefit, by removing autoreactive B and T cells in patients experiencing rheumatoid arthritis and has more recently been approved as therapy for patients with relapse-remitting multiple sclerosis (RR-MS) under the trade name, Lemtrada<sup>307,308</sup>.

Although it has been widely used, there has always been a concern over its long-term side-effects as a result of depleting most of the lymphocyte population. It has been found that the rate of lymphocyte repopulation is skewed in favour of B cells, and there is an increased incidence of patients treated developing secondary autoimmune conditions, relating to approximately 30% of patients treated, and as a result further work into the safety and associated risk factors are required<sup>306</sup>. What this work demonstrates is the care required, and potential disadvantage for utilising such potent immune targeted therapies. However, as our understanding and discovery of more specific targets is expanded, these complications should decrease in severity over time.

## **1.10 Antigen Properties Which May Influence mAb Engagement of Effector Mechanisms:**

There is a large discrepancy between the number of potentially therapeutic mAb identified in the laboratory and those that produced real clinical benefit<sup>309</sup>. As of June 2015, there were 20 approved mAbs for the treatment of cancer (summarised in Table 1.5) which target 9 different antigens, meaning that multiple antibodies are targeting the same antigen<sup>144</sup>. Comparing the antibodies that bind the same antigen has revealed differences in the engagement of the effector mechanisms, which have been widely attributed to structural differences between the antibodies.

What is less considered is whether the properties of the antigen targeted are important for the engagement of these effector mechanisms and consequently the therapeutic efficacy of an antibody. Evidence towards these features and their potential influence will be discussed in more detail within this section. Understanding what makes an effective target for direct targeting mAbs would improve the development of new therapeutics, with the potential to lower the attrition rate between the laboratory and early clinical trials.

Drug	Target	Indication	FDA approved	EU approved
Rituximab	CD20	NHL	1997	1998
Trastuzumab	Her2	Breast cancer	1998	2000
Gemtuzumab ozogamicin	CD33	Acute myeloid leukaemia	2000	N/A
Alemtuzumab	CD52	Chronic Myeloid Leukaemia	2001	2001
Ibritumomab tietan	CD20	NHL	2002	2004
Tositumomab- <sup>131</sup> I	CD20	NHL	2003	N/A
Cetuximab	EGFR	Colorectal cancer	2004	2004
Bevacizumab	VEGF	Colorectal cancer	2004	2005
Panitumumab	EGFR	Colorectal cancer	2006	2007
Ofatumumab	CD20	CLL	2009	2010
Ipilimumab	CTLA-4	Metastatic Melanoma	2011	2011
Brentuximab vedotin	CD30	Hodgkin Lymphoma	2011	2012
Pertuzumab	Her2	Breast cancer	2012	2013
Ado-Trastuzumab	Her2	Breast cancer	2013	2013
Obinutuzumab	CD20	CLL	2013	2014
Ramucirumab	VEGFR2	Gastric cancer	2014	2014
Pembrolizumab	PD1	Melanoma	2014	Pending
Blinatumomab (Bispecific)	CD19/CD3	ALL	2014	Pending
Nivolumab	PD1	Melanoma & NSCLC	2014	Pending
Dinutuximab	GD2	Neuroblastoma	2015	Pending

**Table 1.5: Clinically approved mAbs for cancer immunotherapy**

Summary of clinically approved mAbs for cancer immunotherapy in the EU and USA, adapted from the reference table produced by Janice Reichert <sup>144</sup>. N/A = not approved; NHL = Non-Hodgkin Lymphoma; CLL = Chronic Lymphocytic Leukaemia; ALL = Acute Lymphocytic Leukaemia; NSCLC = Non-Small Cell Lung Carcinoma

### 1.10.1 Antigen density:

Examining the targets of the clinically approved mAbs for cancer immunotherapy in Table 1.5 shows a trend towards favouring highly expressed antigens. CD20 and CD52 are two such targets that have demonstrated potent and effective therapeutic targets for haematological malignancies. Both of these antigens are found highly expressed on the surface of lymphocytes<sup>187,310</sup>. This high expression means that a higher density of antibody can bind a single cell, thereby resulting in an increased chance of interactions with the cell-extrinsic effector mechanisms discussed previously.

A positive correlation between the number of CD20 molecules and a patient's response to rituximab therapy was defined through the analysis of both cell lines and primary samples<sup>235</sup>. In particular, a higher antigen expression is favourable for the engagement of CDC, and to a lesser extent the FcγR-mediated mechanisms<sup>231,311</sup>. In a similar manner, it is the upregulation of EGFR which makes it an attractive target for solid tumours found in breast, colon and head and neck cancers<sup>312</sup>. Although this protein is expressed on non-malignant cells, the higher density present on malignant cells is capable of engaging the effector mechanisms, making it a form of preferentially selective therapy with reduced off-target effects<sup>249</sup>.

Derer *et al*, focussed on the impact EGFR expression levels had on the antibody effector mechanisms engaged, using a panel of cell lines with differential expression of the antigen<sup>249</sup>. They concluded that at low levels of expression, F(ab) mediated mechanisms (defined as signal inhibition and PCD) were the main method of cell death, whereas at higher expression levels the Fc mediated mechanisms (classed as CDC, ADCC and ADCP) were more effective. This paper demonstrates how a single property of an antigen can influence the effector mechanisms engaged by an antibody.

### 1.10.2 Distance of epitope from cell membrane:

Another common property of the clinically approved targets in Table 1.5 is that they are either small proteins, or that the epitope bound by an antibody lies towards the membrane proximal domains rather than further away from the cell membrane<sup>313</sup>. For example, CD20 and CD52, are both small antigens found on the surface of lymphocytes; EGFR is a far larger protein in comparison, but the epitope bound by the lytic antibody cetuximab lies on the membrane proximal domain, whilst the mAb that bind epitopes further away from the membrane in the receptor – such as panitumumab – engage the receptor signal inhibition roles<sup>189,239</sup>.



Rituximab and ofatumumab are two type I anti-CD20 mAb which are able to effectively engage CDC and ADCC, but poor at engaging PCD<sup>232,277</sup>. When comparing the CDC ability of these two antibodies *in vitro*, ofatumumab is far more effective in binding C1q and engaging CDC compared to rituximab, on both cell lines and patient samples<sup>230,314</sup>. Comparing the epitopes bound by these antibodies revealed that ofatumumab binds a unique epitope that is closer to the cell surface than rituximab (Figure 1.10)<sup>231,288</sup>. The proximity of the bound ofatumumab to the cell membrane has been proposed as an explanation for its enhanced activation of CDC since soluble complement components, once activated, have a short half-life which is stabilised once bound to a cell – a protective mechanism to protect against self-destruction<sup>27</sup>. Therefore being activated close to the target cell membrane improves the likelihood of binding the target cell, resulting in improved CDC.

This trend for targeting membrane proximal domains for effective therapeutics has been examined in chimeric antigen receptors. It was found that for anti-CD22 CAR those that targeted epitopes bound closer to the target cell membrane resulted in better T cell directed cell lysis and tumour clearance *in vivo* than those which bound further away<sup>150,315</sup>. A separate group designed a panel of Bispecific T-cell Engager (BiTE) antibodies which bound a melanoma target MCSP and CD3, and once again showed *in vitro* that improved lysis was achieved when using the BiTE antibody which was directed towards the membrane proximal domain of MCSP<sup>152</sup>. In addition, another BiTE was generated that was able to bind EpCAM. Through the use of fusion proteins which held the EpCAM domain at different distances from the cell membrane, also reported the best lysis was achieved when the EpCAM domain was bound directly to the cell membrane.

One explanation for these observations is that for effective T-cell activation, sustained phosphorylation of the TCR is required, and that to achieve this the phosphatase CD45 needs to be excluded from the immune synapse initially<sup>316,317</sup>, a facet more effectively achieved by closer cell-cell contact. A similar hypothesis could be applied to the relationship between antibody binding and engagement with effector cells through the FcγR, that there is an optimum size for the immune synapse to form that offers the best stability between the target and effector cell. However, these papers were comparing different therapeutics directed towards unique epitopes within a single antigen, which could result in more than a single variable changing which may complicate these findings.

### 1.10.3 Properties of the antibody:epitope interaction:

The position of an epitope within an antigen is likely to have an impact on the final conformation of an antibody upon binding, in a manner different to the distance hypothesis discussed above. This is best presented by investigating the physical characteristics that could define whether an anti-CD20 mAb is a Type I or Type II. Initial studies seeking to investigate this issue compared rituximab and tositumomab. As a type II mAb, tositumomab is poor at engaging CDC in comparison to rituximab. However, as these mAb had different heavy chains, rituximab was converted to a mouse IgG2a (the same isotype as tositumomab) then tested *in vitro* for the engagement of CDC and ADCC. Switching the isotype of the antibody, therefore the Fc domain, did not change rituximab into a type II, indicating that the defining property lies in the F(ab) domain of the mAb <sup>244</sup>.

Both mAb bind an overlapping epitope in CD20; however tositumomab is positioned towards the carboxy-terminus end of the loop (Figure 1.10). It was hypothesised that the orientation of the Type II antibody in relation to the antigen is more angled towards the membrane compared to rituximab, possibly reducing its ability to bind C1q favourably, therefore diminishing its activation of the complement cascade <sup>289</sup>. A similar observation – as mentioned earlier – was reported for the crystallised F(ab) of obinutuzumab, therefore it could be proposed that the angle of antibody binding can alter the availability of the Fc region and its availability to engage with the cell-extrinsic effector mechanisms <sup>292</sup>.

### 1.10.4 Antigen mobility within the cell:

#### 1.10.4.1 Lipid raft localisation:

Most of the targets for clinically approved mAbs can be found in lipid raft domains, and those that aren't (such as CD20) are able to migrate into these domains upon antibody cross-linking. Targeting an antigen that lies in these domains is linked to the antigen density property discussed earlier. An increase concentration of receptors in a relatively condensed area of a cell would increase the density of antibody molecules/Fc domains, therefore improving the ability to cluster FcγR upon engagement and for complement to bind <sup>200</sup>.

The potential of membrane localisation to impact the effector mechanisms engaged is best illustrated with the type I and II anti-CD20 mAbs as discussed earlier <sup>200,277</sup>. However, whether membrane localisation is the overriding property that explains the differences in effector mechanism engagement is still unclear, as other properties may also influence the efficacy – such as mAb orientation discussed earlier.

#### 1.10.4.2 Internalisation/Modulation:

When an antibody binds an antigen, as well as being able to engage the aforementioned effector mechanisms, it is possible to enter the cell via an endocytic process, referred to as internalisation. The possibility of this occurring is dependent both on the antibody and the antigen targeted. Some proteins are more susceptible as a consequence of high protein turnover – such as CD22 – whilst others – such as CD20 – require cross-linking with additional receptors to form an immune complex for internalisation <sup>272,318</sup>.

The internalisation of bound antibodies is variable, with some cell/cancer types more susceptible than others, and even within a subset of cancers the extent of surface antibody lost is variable <sup>272</sup>. For the Type I anti-CD20 antibodies, it has been described that a high expression of hCD32b correlated with increased internalisation of rituximab <sup>272,293</sup>. It is proposed that when rituximab bound the CD20, its Fc region was then able to bind *in-trans* hCD32b present on the cell surface as there is less internalisation observed with a F(ab')<sub>2</sub> <sup>318</sup>.

Maintaining surface binding is crucial for the efficacy of both direct targeting and immunomodulatory mAb; yet there are situations when targeting an internalising protein is beneficial. For toxin-conjugated antibodies, such as gemtuzumab ozogamicin which targets human CD33, this property is beneficial, allowing a cell specific delivery system, providing a more acute dosing strategy, with potentially fewer side effects, compared to a systemic course of chemotherapy or radiotherapy <sup>147</sup>. The ability of an antigen to internalise impacts the efficacy of a mAb *in vivo* through altering the half-life and amount of mAb present to engage the effector mechanisms described in section 1.7 <sup>271</sup>. Therefore, this characteristic of an antigen needs to be taken into consideration when assessing new therapeutic antibodies against non-established candidates.

Together, these observations highlight the importance of understanding how a particular epitope, and not just the antigen, can change the therapeutic efficacy of a mAb. Current attempts to define this has compared multiple epitopes within an antigen, so variations in the antigen:antibody interactions (such as antibody on and off rates, or the glycosylation changes in the Ig heavy chain) may affect the data collected and the conclusions drawn. Understanding how the properties of an antigen impacts mAb immunotherapy mechanisms engaged would improve the design for future therapeutic antibodies.

### 1.11 Hypothesis and Aims of Thesis:

It is hypothesised that the properties of an antigen can influence the effector mechanisms engaged by a direct targeting mAb, therefore altering the therapeutic efficacy. Previous work to understand this has investigated the impact on either a single effector mechanism, or by inferring comparisons between different antibodies towards the same antigen. This thesis aims to investigate the role that distance between the antibody epitope and the cell membrane has on the three cell-extrinsic effector mechanisms (CDC, ADCP and ADCC) by developing a controlled model where the same antibody and epitope pairing can be applied between the conditions, thereby overcoming the current limitations in the field.

In order to test this hypothesis the following objectives were set:

- 1) Develop an antigen system to model different distances between an antibody and the cell membrane.
  - a. Produce a panel of fusion proteins which all contain an epitope for a clinically relevant therapeutic mAb attached to a scaffold protein which can be manipulated to change the relative distance between the epitope and the cell membrane.
  - b. Utilise a mammalian cell expression system to confirm conformation of the fusion proteins.
- 2) Assess the impact that the distance between antibody binding and the cell membrane has *in vitro* for the three cell extrinsic effector mechanisms CDC, ADCP and ADCC.
  - a. Optimise functional assays for use with transiently transfected target cells.
  - b. Confirm findings with an alternative epitope and antibody pair.
  - c. Develop stable transfected cell lines for further corroboration in *in vitro* assays.
- 3) Investigate whether the dependence of epitope distance seen in the *in vitro* assays remains in an *in vivo* model where all of the effector mechanisms are present together in the context of a complete immune system.
  - a. Develop a tumour model which expresses the different fusion proteins and can be passaged in immune competent mice.

- b. Treat the tumours with antibody and compare tumour clearance and survival between the different fusion protein expressing models.



## Chapter 2: Methodology

### 2.1 Cell culture:

#### 2.1.1 Tissue culture conditions:

All cells used in the project were cultured using the conditions summarised in Table 2.1. Media and supplements were purchased from Life Technologies, except for foetal calf serum (FCS) which was purchased from Sigma Aldrich. On average cells were split every 2-3 days where fresh media was added. Roswell Park Memorial Institute (RPMI)-1640 and Dulbecco's modified eagle media (DMEM) was supplemented with 10% FCS, 2mM Glutamine, 1mM sodium pyruvate, 100units/mL penicillin and 100µg/mL streptomycin.

Cell line	Media	Supplemented	Cell density for culture	CO <sub>2</sub> content	Other information
A20	RPMI 1640	10% FCS, GP PS	0.5 - 1x10 <sup>6</sup> cells/mL	5%	-
BMDM	RPMI 1640	10% FCS, GP PS 50µM β-mercaptoethanol	0.5x10 <sup>6</sup> cells/mL	5%	L929 conditioned media replaced every 4 days
BWZ.36	RPMI 1640	10% FCS, GP PS 50µM β-mercaptoethanol 10mM HEPES 0.5mg/mL Hygromycin	0.1 - 1x10 <sup>6</sup> cells/mL	5%	-
CHO-S	Freestyle CHO-S	8mM Glutamine	0.5 - 2x10 <sup>6</sup> cells/mL	8%	Shaking incubator
<i>E.coli</i> JM109, TOP10	LB media (Sigma): Tryptone, yeast, salt	Either 50µg/mL kanamycin or 100µg/mL ampicillin	Grow to saturation	-	Shaking incubator
EL4	RPMI 1640	10% FCS, GP PS	0.5 - 1x10 <sup>6</sup> cells/mL	5%	-
J558L	DMEM	10% FCS, GP PS	0.5 - 1x10 <sup>6</sup> cells/mL	5%	-
NS-0, NS-1	RPMI 1640	10% FCS, GP PS	0.5 - 1x10 <sup>6</sup> cells/mL	5%	-
293F	Freestyle 293	No supplementation	0.5 - 2x10 <sup>6</sup> cells/mL	8%	Shaking incubator

**Table 2.1: Culture conditions for cells used throughout the thesis**

A summary of the conditions used within this thesis for the normal culture of cell lines. FCS = Foetal calf serum, PS = 100 units penicillin and 100µg/mL streptomycin, GP = 2mM Glutamine and 1mM sodium pyruvate.

### **2.1.2 Differentiation of bone marrow derived macrophages (BMDM)**

Bone marrow was collected from the hind legs of wild type C57BL/6 or BALB/c mice.  $4 \times 10^6$  cells were plated in flat-bottomed 6 well plates (Corning) with supplemented RPMI containing 2mM  $\beta$ -mercaptoethanol and 20% L929 conditioned media (containing Macrophage-Colony stimulating factor (M-CSF)). The media was changed on day 4 and 7, where non-differentiated cells in suspension were washed away with sterile phosphate buffered saline (PBS). Between days 8-10 the macrophages were deemed mature and ready for use in functional assays.

### **2.1.3 Peripheral Blood Mononuclear Cell isolation**

PBMC were isolated from 15mL of platelet depleted whole blood, supplied by the NHS Blood Service, using density gradient centrifugation. The blood was diluted to a total volume of 50mL in PBS containing 2mM ethylene-diamine-tetra-acetic acid (EDTA) and 10% FCS before layering 25mL over 12.5mL lymphoprep (purchased from Axis-Shield) in a 50mL tube. The blood was then allowed to separate by centrifugation at 800g for 20 minutes, with the brake off to prevent disruption of the lymphocyte layer. PBMCs were collected using a Pasteur pipette from the lymphoprep/serum interface. The cells were washed four times in 50mL PBS+2mM EDTA (spun at 300g for 5 minutes), to remove excess lymphoprep solution present. The cells were suspended in 15mL complete RPMI and counted, before diluting to  $4 \times 10^7$  cells/mL for use in an ADCC assay (section 2.4.3). The cells were kept at 37°C for no more than 4 hours between isolation and use in cytotoxic assays.

### **2.1.4 Serum preparation from whole blood:**

40mL of human blood was collected into a sterile glass centrifuge tube with no anti-coagulant present. It was mixed with a wooden stick, and incubated at room temperature (RT) to clot for 45 minutes. The tubes were centrifuged at 900g, 4°C for 20 minutes allowing separation of the coagulated blood and serum. The serum layer was transferred into 0.5-2mL aliquots in autoclaved glass tubes for storage at -80°C. No freeze thaw cycles were undertaken, once thawed the serum was used immediately in order to maintain complement activity.

## **2.2 Molecular biology techniques:**

### **2.2.1 cDNA templates:**

Template DNA for human CD137 and CD52 were previously isolated from cDNA and cloned into the pcDNA3 expression vector by Dr C. Chan. The approach used to clone and isolate both of these genes was as follows:



mRNA was isolated from human lymphocytes (known to express CD52 and CD137) using a commercially available kit (Illustra QuickPrep micro mRNA purification kit, GE). Cells were homogenised with an extraction buffer which contained an RNase inhibitor and allowed precipitation of proteins. The proteins were removed from the RNA by centrifugation, before loading the supernatant onto a column. The column was designed to bind polyadenylated mRNA present in the cell onto the column and allow all other contaminants such as DNA to be removed. Finally the mRNA was eluted with the elution buffer provided.

The mRNA was converted into cDNA using the Superscript III First-strand RT-PCR kit supplied by Invitrogen. A random hexamer was used as a primer for the mRNA. After the RT-PCR protocol, mRNA was digested using RNase H for 20 minutes. The cDNA was then used to amplify the genes of interest (in this case human CD52 and CD137). The products were ligated into a cloning vector and sequenced to confirm the selection of the gene. This was then kept for use as templates for this project.

### 2.2.2 Polymerase Chain Reaction (PCR)

Bespoke primers were produced by Invitrogen to specification (the primer sequences are provided in appendix A); PCR reagents and enzymes were supplied by Promega. 25µL reactions consisting of 4ng template DNA, 1 unit Pfu polymerase, 2.5µL 10x buffer, 100ng of both 5' and 3' primers were performed. General PCR reaction was set up using a PTC-200 thermal cycler (MJ Research) using the conditions in Table 2.2.

a) PCR			b) DNA Sequencing			c) Site-directed mutagenesis		
Step	Temp (°C)	Time (sec)	Step	Temp (°C)	Time (sec)	Step	Temp (°C)	Time (sec)
1	94	300	1	96	120	1	95	120
2	94	30	2	96	120	2	95	20
3	60	60	3	50	5	3	60	10
4	72	120	4	60	240	4	68	30/kb
Repeat 2-4 for 20-35 cycles			Repeat 2-4 for 24 cycles			Repeat 2-4 for 18 cycles		
5	72	600				5	68	600

**Table 2.2: Thermocycler conditions used for DNA amplification methods**

All reactions which required temperature cycling were performed in a PTC-200 thermal cycler with a heated lid (MJ Research). The table contains the programme information used for a) PCR, b) DNA sequencing and c) mutagenesis reactions.

### 2.2.3 DNA Sequencing

150-300ng of plasmid DNA underwent short-chain termination sequencing. For a 10µL reaction, 2µL of BigDye (pre-made mix containing DNA polymerase, dNTPs, and

dideoxynucleotides conjugated to a fluorescent dye), 5x buffer, 10ng sequencing primer and 150-300ng DNA (total reaction volume reached with dH<sub>2</sub>O) were mixed. Reaction mix underwent PCR (Table 2.2) before concentrating the DNA using ethanol precipitation. 1µL of 3M sodium acetate (pH 5.4) and 25µL of 100% ethanol was added to the sequencing reaction and incubated on ice for 5 minutes. DNA was pelleted by centrifuging at 13000rpm, 30 minutes at 4°C. Supernatant was removed, 125µL of 70% ethanol added and centrifuged for 5 minutes. Supernatant was removed and the DNA pellet air dried before suspending in 10µL formamide. The sequencing reaction was then assessed in-house using a 3130xl Genetic Analyser (Applied Biosystems). Sequencing data was analysed using SeqManPro software (DNASTar Lasergene version 8.1.5(3)).

#### **2.2.4 Site-directed mutagenesis**

Site-directed mutagenesis was carried out using Agilent Quik Lightning Site-Directed Mutagenesis kit, with bespoke primers produced to specification by Invitrogen. The sequences of the mutagenesis primers used in this thesis are available in Appendix A. 10-15 nucleotides either side of the mutation site were included in order to maximise the binding of the mismatched primer to the template DNA.

40ng of plasmid DNA was used and added to a mutagenesis reaction consisting of 250ng mutagenesis primer, 200µM dNTPs, 10x reaction buffer, 3% Quik Solution and 1µL of mutagenesis enzyme. PCR amplification was performed for 18 cycles (Table 2.2) before the parental methylated plasmid was digested with DpnI for 30 minutes at 37°C. 2µL of non-digested plasmid was then used to transform competent JM109 E.coli cells by heat-shock transformation.

#### **2.2.5 Agarose Gel electrophoresis**

0.7 agarose gels were made on the day of analysis by dissolving agarose in TAE buffer (2M Tris-base, 0.95M glacial acetic acid and 50mM EDTA (pH8) in dH<sub>2</sub>O) for 2 minutes in a microwave at full power. 5µL of Gel Red (Biotium) was added prior to pouring into a gel mould and allowed to set at room temperature. The set gel was submerged in TAE buffer in an electrophoretic tank, where samples were loaded and a constant current applied allowing charge/size dependent separation to occur. Typically the DNA gels discussed throughout the thesis were run at a constant 120V for 45-60 minutes. DNA bands were visualised with UV light and imaged using a BioRad Molecular Imager Gel Doc XR System and the associated software, Quantity One (version 4.6.7, BioRad).

### 2.2.6 DNA gel extraction and purification

DNA excised directly from an agarose gel was isolated using the QIAEX II suspension bead kit (Qiagen). In brief, a dissolving buffer and DNA binding beads were added to the gel slice and left to melt at 50°C for 10 minutes. The DNA binding beads were pelleted by centrifuging at 14500g for 30 seconds before aspirating the supernatant. The beads were washed twice in 70% ethanol to remove any residual salts. 20µL of TE solution was added and the bead suspension incubated at 50°C for 10 minutes in order to elute the bound DNA. The beads were pelleted, and the supernatant (containing DNA) was transferred to a sterile tube.

### 2.2.7 Restriction enzyme digests

Plasmid DNA was digested at 37°C in a temperature controlled heat block, for 1-2 hours. The final volume for digest reactions was either 10µL (for single enzyme) or 20µL (double enzyme). A typical reaction consisted of 1µL restriction enzyme, 1µL of 10x reaction buffer (recommended by Promega), 1µg DNA, and made up to the correct total volume with dH<sub>2</sub>O. The total volume of enzyme used was no more than 10% of the final volume in order to prevent activity inhibition due to glycerol content.

### 2.2.8 Ligations

Blunt-end ligations: 2µL of PCR product was added to 5ng of pCRII-Blunt II-TOPO vector and 0.5µL of salt solution (1.2M NaCl and 0.06M MgCl<sub>2</sub>). The ligation mix was incubated at room temperature for 20 minutes for the ligation reaction to occur.

Sticky-end ligation reactions: Ligation reactions were performed at 4°C overnight in a 30µL reaction volume. Each reaction contained 3µL of 10x ligase buffer, 3µL T4 DNA ligase added to a total volume of 24µL mix of restriction enzyme digested insert DNA and plasmid DNA (at a 3:1 ratio).

### 2.2.9 Heat Shock Transformation

Plasmid DNA was incubated on ice with 10x volume of competent JM109 cells (E.coli, from Promega) for 30 minutes. The competent cells were then heat shocked in a 42°C water bath for 35 seconds followed by incubation on ice for 2 minutes. 500µL of S.O.C. media (Invitrogen) was added and the cells were left to recover at 37°C for 1 hour before plating onto agar containing either 100µg/mL ampicillin or 25µg/mL kanamycin.

### **2.2.10 Plasmid DNA miniprep and maxipreps**

Plasmids were isolated from bacterial cultures using either the QIAprep Spin Miniprep or HiSpeed Plasmid Maxi kits (Qiagen). In brief, the cells were lysed using an alkaline solution for 5 mins before neutralisation, leading to precipitation of cellular components leaving the plasmid DNA in solution. The cell lysate was added to spin columns (miniprep) or filter tips (maxiprep) capable of binding plasmid DNA, allowing RNA, soluble proteins and other contaminants to be washed away. The plasmid DNA was eluted and ready to use in subsequent reactions. The maxiprep had an additional DNA concentration step using isopropanol to reduce the final volume.

## **2.3 Protein expression and analysis:**

### **2.3.1 Mammalian cell transfections**

HEK293F cell transfection: HEK293F cells were transfected using 293Fectin (Invitrogen). Briefly, 10µg of plasmid DNA was allowed to form complexes with the cationic lipid 293Fectin solution for 20 minutes in Opti-MEM serum free media at room temperature. This was then added drop-wise to  $1 \times 10^7$  cells cultured in 10mL Freestyle293 expression media and shaken at 37°C for 24-48 hours. Protein expression was determined using flow cytometry with fluorescently labelled antibodies (see section 2.3.5).

CHO-S cell transfection: CHO-S cells were transfected using the Freestyle Max system (Invitrogen). In brief, 10µg of plasmid DNA was mixed with the lipid Freestyle Max for 10 minutes in Opti-Pro low serum media. It was then added dropwise to  $1 \times 10^7$  cells in a 10mL culture. The cells were left at 37°C for 24-48 hours for protein expression to occur. Protein expression was determined using flow cytometry with fluorescently labelled antibodies (see section 2.3.5).

### **2.3.2 Nucleofection:**

Cells were suspended in 100µL of nucleofector solution (purchased from Lonza) into an electroporation cuvette. The cuvette was placed into the nucleofector machine (Amaxa) and shocked using the correct programme outlined in Table 2.3. The cells were removed gently by pipette into 1.5mL of pre-warmed complete RPMI media in a 12-well plate. Protein expression was assessed after 24 hours by flow cytometry (see section 2.3.5).

Cells	Number of cells	Nucleofector Kit	DNA concentration	Nucleofector Programme
A20	2x10 <sup>6</sup>	V	2µg	L-013
EL4	3x10 <sup>6</sup>	T	3µg	G-016
J558L	5x10 <sup>6</sup>	T	5µg	G-016
NS-0	2x10 <sup>6</sup>	C	2µg	T-005
NS-1	2x10 <sup>6</sup>	T	2µg	U-001

**Table 2.3: Nucleofection conditions for mammalian cell lines**

Nucleofector conditions used for the transfection of murine suspension cells as collected from the Lonza Cell and Transfection database (available at <http://bio.lonza.com/6.html> [accessed 07Jul15]).

### 2.3.3 Electroporation:

5x10<sup>6</sup> BWZ.36 cells were suspended in 800µL of non-supplemented RPMI media. 30µg of DNA was added to the cells and incubated on ice for 10 minutes. The cell and DNA suspension was transferred to a pre-chilled 4mm electroporation cuvette (Biorad) and pulsed at 0.3kV, 960µF in using Gene Pulser (BioRad). The cuvette was transferred to ice for 10 minutes, followed by a 10 minute incubation at RT. Using a pipette the cells were transferred gently into 5mL of pre-warmed media in a 6-well plate and left to culture. After 48 hours, 1mg/mL geneticin was added to the culture to select for cells which had incorporated the plasmid DNA.

### 2.3.4 Antibody Fluorescein-Isothiocyanate (FITC) conjugation:

Antibody was dialysed into PBS and concentrated to at least 2mg/mL using Vivaspins columns. 2mg/mL FITC solution was prepared in fresh bicarbonate buffer (Table 2.4). FITC solution was added to the antibody so that a final concentration of 0.2mg/mL FITC was reached. A 25°C water bath was used to incubate the sample for 45 minutes. To collect the FITC labelled fraction from the unlabelled protein by size exclusion chromatography, using a sephradex packed column (either purchased from GE Healthcare, or prepared in-house) and PBS to flush the column. The pale green fraction – observed by eye – was collected and dialysed overnight into PBS. Absorbance at 280nm and 495nm was measured using the Nanodrop in order to calculate the level of FITC labelling and final protein concentration. An F/P ratio between 0.5 and 1 was deemed suitable for use in flow cytometry.

$$F/P \text{ ratio} = \frac{\text{Absorbance at } 495\text{nm}}{\text{Absorbance at } 280\text{nm}}$$

$$\text{Protein Concentration} = \frac{A_{280\text{nm}} - (0.26 \times A_{495\text{nm}})}{1.35}$$

### **2.3.5 Antibody labelling of cells for flow cytometry**

Direct labelling:  $2 \times 10^5$  cells in PBS were incubated with  $10 \mu\text{g/mL}$  of fluorochrome-labelled antibody for 30 minutes at  $4^\circ\text{C}$ . Unbound antibody was removed by washing the cells once with FACS wash buffer (PBS containing 1% BSA and 10mM sodium azide), followed by a centrifugation step for 5 minutes at 400g to collect cells.

Indirect labelling:  $2 \times 10^5$  cells in PBS were incubated with  $10 \mu\text{g/mL}$  of non-conjugated antibody for 30 minutes at  $4^\circ\text{C}$ . The cells were washed twice with FACS wash buffer to remove unbound antibody. Non-conjugated antibodies were then detected with an appropriate fluorochrome-labelled secondary antibody for 30 minutes at  $4^\circ\text{C}$ . Cells were then washed once with FACS wash buffer.

Fluorescently labelled cells were detected using flow cytometry.

### **2.3.6 Data acquisition by flow cytometry**

All flow cytometry experiments were performed on either a FACScan or FACSCalibur machine (BD Bioscience). All experimental samples were kept on ice following antibody labelling throughout acquisition. Unless otherwise stated, 10000 events per sample were collected during acquisition in order to provide enough data for analysis.

Analysis of flow cytometry data was performed using either BD CellQuest Pro (version 4.0.2, BD Bioscience) or FCS Express (version 3.00.0825, De Novo Software).

### **2.3.7 Preparation of mammalian cell lysates:**

$6 \times 10^6$  cells were suspended in 1mL PBS in a 1.5mL tube. Cells were washed twice in chilled PBS (cells pelleted by centrifugation at 450g for 5 minutes).  $75 \mu\text{L}$  of cell lysis buffer was added to the cell pellets and left on ice for 30 minutes, and mixed halfway through to ensure complete lysis (Cell lysis buffer consists of 3mL RIPA buffer,  $30 \mu\text{L}$  protease inhibitor cocktail,  $150 \mu\text{L}$  of 1M NaF and  $7.5 \mu\text{L}$   $\text{Na}_3\text{VO}_4$ ). Cellular debris was pelleted by centrifugation at 14500g for 15 minutes at  $4^\circ\text{C}$ . The supernatant was then collected and able for use in Bradford assays or Western blots.

### **2.3.8 Bradford Assay:**

Bovine Serum Albumin (BSA) was used to prepare the standard curve, by serial diluting in  $\text{dH}_2\text{O}$  1 in 2 from  $2000 \mu\text{g/mL}$  to  $1.9 \mu\text{g/mL}$ . Samples were also prepared by diluting in  $\text{dH}_2\text{O}$  with a final volume of  $10 \mu\text{L}$  in each well of a 96-well plate. Bradford Assay Reagent (Thermo) was

diluted 1 in 5 in dH<sub>2</sub>O, where 200µL was added to each well and left to develop at room temperature for 3-5 minutes. The amount of protein was measured using the absorbance at 570nm using an EPOCH plate reader, then quantified from the standard curve generated with the BSA standard.

### **2.3.9 SDS-PAGE:**

25µL final volume reactions were prepared by adding 10-25µg cell lysates, 7.5µL of reducing buffer and topping up with dH<sub>2</sub>O. The samples were denatured by heating for 5 minutes at 95°C and centrifuged for 1 minute at 13000rpm. The samples were loaded into wells on a pre-cast 10% Bis-Tris gel, and run at a constant 100V for 30 minutes, followed by 150V until the Marker reaches the end of the gel.

### **2.3.10 Western Blot**

SDS-PAGE gel was layered between nitrocellulose membrane, filter paper and sponges submerged in transfer buffer. A constant 30V for 75 minutes was applied to allow transfer of the protein onto the membrane. The membrane was removed and blocked with 5% milk for 2 hours. Primary antibody was diluted in BSA-Tween solution (Table 2.4) and left to coat the membrane overnight at 4°C on a rotating platform. The membrane was washed with TBS-Tween before a detection antibody was added in milk, for 1 hour at RT. ECL substrate was prepared at a 1:1 ratio and added to the membrane for 5 minutes at RT, afterwards excess substrate was removed by blotting. In a dark-room, chemiluminescence film is applied to the membrane, and exposed for a length of time before developing using a Xograph Imaging Systems Compact X4. The size ladder is marked onto the developed film for orientation and measurement of bands. To reprobe for another protein, the membrane is stripped for 2 hours at RT in the stripping buffer (Table 2.4).

## **2.4 Functional assays to assess antibody efficacy:**

### **2.4.1 Complement Dependent Cytotoxicity (CDC) assay**

1x10<sup>5</sup> cells in 100µL were opsonised with 100µL of the desired antibody concentration for 15 minutes at RT in a flat-bottomed 96-well plate. Meanwhile, -80°C stored frozen human serum was thawed at 30°C and prepared at a 5x working concentration in cell media. 50µL of the serum working solution was added to the cells and left at 37°C for 30 minutes. Cells were transferred to a FACS tube where propidium iodide (PI) solution (10µg/mL in PBS) was added

prior to data acquisition. 7000 events for each sample was collected for analysis where the percentage cell death was defined as the percentage of PI<sup>+</sup> cells of the total cell population.

$$\% \text{ Cell death} = \left( \frac{\text{Sample} - \text{NoSerum baseline}}{100 - \text{NoSerum baseline}} \right) * 100$$

#### 2.4.2 Antibody dependent Cellular Phagocytosis (ADCP) assay

5x10<sup>4</sup> BMDM per well were plated into 96-well plate the day before the assay was performed. Target cells were labelled with 5μM carboxyfluorescein succinimidyl ester (CFSE) for 10 minutes at room temperature before being washed once in sterile PBS. The CFSE labelled cells were opsonised with antibody for 30 minutes at 4°C before washing once in RPMI media, then the cells were diluted to a density of 2.5x10<sup>6</sup> cells/mL. The BMDM were washed twice with 200μL PBS and once with complete RPMI media. 2.5x10<sup>5</sup> opsonised target cells were added to the BMDM and left to co-culture at 37°C for 1 hour. The BMDM were labelled with 1μL of anti-F4/80-APC (Serotec) for 20 minutes at room temperature. The cells were washed with PBS twice to remove excess antibody and non-phagocytosed cells, and suspended in cold FACS buffer and left on ice for at least 10 minutes to loosen the BMDMs from the well. The wells were scraped with a pipette tip to collect the BMDMs before acquisition on FACS Calibur (BD Biosciences). The percentage phagocytosis was defined as the percentage of CFSE<sup>+</sup> F4/80<sup>+</sup> cells of the total F4/80<sup>+</sup> population.

$$\% \text{ Phagocytosis} = \left( \frac{\text{Sample} - \text{baseline}}{100 - \text{baseline}} \right) * 100$$

#### 2.4.3 Antibody Dependent Cellular Cytotoxicity (ADCC) assay

Target cells were labelled with calcein AM (Life Technologies) (1μL Calcein per 2x10<sup>6</sup> cells) and suspended in RPMI. The calcein labelled cells were opsonised with antibody for 30 minutes at 4°C before washing once in RPMI media. The target cells and PBMC effector cells were co-cultured at a 50:1 (Effector:Target) ratio for 4 hours at 37°C. The cells were pelleted by centrifugation (400g for 5 minutes) and the supernatant was transferred to a white 96-well plate. The plate was read using an excitation wavelength of 485nm and emission wavelength of 530nm using a Varioskan Flash (Thermo Scientific) to measure calcein release. The percentage of maximum lysis was defined as the calcein release compared to the response recorded when cells were treated with 4% Triton-X100 (TX100) solution.



$$\% \text{ Maximum Lysis} = \left( \frac{\text{Sample} - \text{baseline}}{\text{TX100} - \text{baseline}} \right) * 100$$

## 2.5 *In vivo* techniques:

All work was performed in accordance with the Animal (Scientific Procedures) Act 1986, in a Home Office approved facility under the project licence 30/2964. All mice used in these experiments were under 5 months of age when the experiment was initiated. Ear punching (as described by LASA Good Practise Guidelines) was used for identification of individual mice as approved by the project license. All procedures used were recorded as mild severity for each individual by the experiment end point.

### 2.5.1 A20 Cell Passage

$2 \times 10^6$  cells were suspended in 200  $\mu$ L of sterile filtered PBS and administered by either intravenous (i.v.) or intraperitoneal (i.p.) injection into wild type BALB/c mice. Mice were assessed for tumour formation by palpation twice a week, for signs of spleen enlargement.

When mice exhibited visible signs of ill-health which if left would have an adverse impact on the quality of life they were culled, (by exposure to rising concentrations of CO<sub>2</sub> as permitted in Schedule 1 of the 1986 act) and dissected. The spleen, liver, inguinal lymph nodes (LN), blood and bone marrow (along with any additional tumour masses present in the peritoneal cavity) were collected. These were homogenised in 3mL of sterile PBS, into a single cell suspension and passed through a 100  $\mu$ m cell strainer before use in flow cytometry.

### 2.5.2 A20 tumour immunotherapy

$2 \times 10^6$  cells were administered by intravenous injection on day 0, as described in section 2.5.1. On day 3, 100  $\mu$ g of rituximab-mIgG2a or PBS was given by tail i.v. injection. Mice were either left until the control group reached terminal (see section 2.5.1 for criteria), or were culled on day 10, 16 and 24 for time specific comparison between groups.

### 2.5.3 Short term cell transfer

Transfected A20 cells were labelled with 5  $\mu$ M CFSE, and non-transfected cells were labelled with 0.5  $\mu$ M CFSE for 10 minutes at RT. They were mixed at a 1:1 ratio and  $2 \times 10^7$  cells in 200  $\mu$ L were given i.v. into wild type BALB/c mice. At 24 hours, the mice were bled and 50  $\mu$ L of blood was collected for analysis. At 48 hours, the mice were bled and culled, where the LN, spleen and bone marrow was collected for analysis.

## 2.6 Buffer compositions:

All buffers used in the project were prepared following the composition outlined in Table 2.4.

Buffer	Reagents	Other details
FACS wash buffer	PBS 10mM Sodium Azide 1% BSA	Store at 4°C
TBS-Tween	50mM Tris 150mM NaCl	pH 7.4
WB Stripping Buffer	1.9g glycine 1% SDS	pH 2
WB Transfer Buffer	In 2L 100mL 20x NuPage buffer 200mL Methanol 1.7L dH <sub>2</sub> O	-
1° Ab coating buffer for WB	5% BSA 0.05% Sodium Azide (NaN <sub>3</sub> ) Diluted in TBS-Tween	Store at 4°C
Bicarbonate buffer for FITC conjugation	440mM NaHCO <sub>3</sub> 100mM Na <sub>2</sub> CO <sub>3</sub>	pH9.5
MOPS buffer	50mM MOPS 50mM Tris 3.5mM SDS 1mM EDTA	-
RIPA (lysate buffer)	25mM Tris-HCl (pH7.6), 150mM NaCl, 1% NP-40, 1% Sodium deoxycholate, 0.1% SDS	Store at -20°C

**Table 2.4: Composition of Buffers used throughout thesis**

The composition of buffers used for western blotting and flow cytometry are provided in the table.

Unless otherwise stated all buffers are diluted in dH<sub>2</sub>O and stored at room temperature.

## Chapter 3: Generation of Model Antigen Constructs to Investigate Distance on mAb Effector Mechanisms

### 3.1 Introduction:

The aim of this thesis was to develop a range of cell surface target molecules, with differing properties, to determine those which were the most important for conferring potent effector functions in the presence of a mAb. The first property investigated was if the distance an antibody binds from the cell membrane impacts the effector mechanisms engaged. For this to be achieved, a series of fusion proteins containing the same antibody binding epitope, attached to a protein backbone of differing lengths was proposed. Previous work in this area has used a panel of antibodies towards different epitopes at varying distances from the cell surface within a single protein to address this question<sup>150,152</sup>. This approach is not ideal as there would be more than just the position of an antibody binding changing between conditions. By using multiple antibodies, subtle differences with regards to the antibody:antigen binding affinity (variation in on- and off-rates), binding levels and epitope-dependent conformational changes are likely to impact the mechanisms observed, thereby limiting the relevance of conclusions drawn<sup>244,292</sup>. In contrast, the proposed approach, using a single epitope:antibody pair, should not be influenced in this way as these will remain constant throughout. The proposed fusion proteins were to contain an epitope recognised by a clinically relevant antibody – previously shown to engage in the effector mechanisms investigated – attached to a larger protein that contained multiple defined extracellular domains which could be manipulated.

The mature peptide of human CD52 was chosen as an ideal antibody epitope, recognised by the clinically evaluated antibody CAMPATH-1H. Its small mature peptide chain (12 amino acids long) makes it an ideal epitope, as attachment to another protein will not significantly alter the final size of the protein. Although wild type CD52 is attached to a GPI anchor, it has been previously shown that the anti-CD52 antibody CAMPATH-1H can bind a minimal synthetic peptide sequence of QTSSPSADA<sup>237,319</sup>. It was hypothesised that the addition of the –DA group on the C-terminus of the protein serves to mimic the negative charge normally supplied by the GPI anchor.

Human CD137 (also known as 4-1BB), a member of the tumour necrosis factor receptor (TNFR) family, was chosen as the basis for the protein backbone. It contains four defined cysteine rich

domains according to online protein sequence annotations (Uniprot reference: Q07011). Although the four extracellular domains are proposed to confer a similar fold (held together through 2 or 3 disulphide bonds) there is little sequence similarity or clear motifs between them. No crystal structure of CD137 has been resolved, although in 2011 the structure of 4-1BB ligand was resolved, and used to model binding with CD137 (based on the existing structure of the related family member TNFR1, Figure 3.1a<sup>320</sup>). Importantly, previous work on CD137 in the laboratory resulted in the generation of antibodies against the individual extracellular domains of human CD137. These antibodies make CD137 useful as a scaffold, as correct folding of the protein can be confirmed by flow cytometry with these antibodies.

To achieve a range of target proteins where the CAMPATH-1H epitope was expressed at different distances from the cell surface, constructs were designed to contain the modified CD52 peptide attached to the N terminal region of CD137. The CD137 backbone contained different numbers of extracellular cysteine rich domains in order to increase or decrease the distance between the antibody binding site and the cell membrane. These fusion proteins were generated using overlap extension polymerase chain reaction which incorporated the -DA modification detailed above through the primers used to clone the CD52 fragment. Published gene and protein sequences for human CD52 (NM\_001803.2 and P31358) and CD137 (NM\_001561.5 and Q07011) were used to identify sites that could be used to attach CD52 and identify cysteine rich domains. The fusion constructs were designed to contain 1, 2, 3 and 4 extracellular domains, with an additional construct which contained 8 domains (possible through the duplication of the complete CD137 extracellular region) as illustrated in Figure 3.1b.

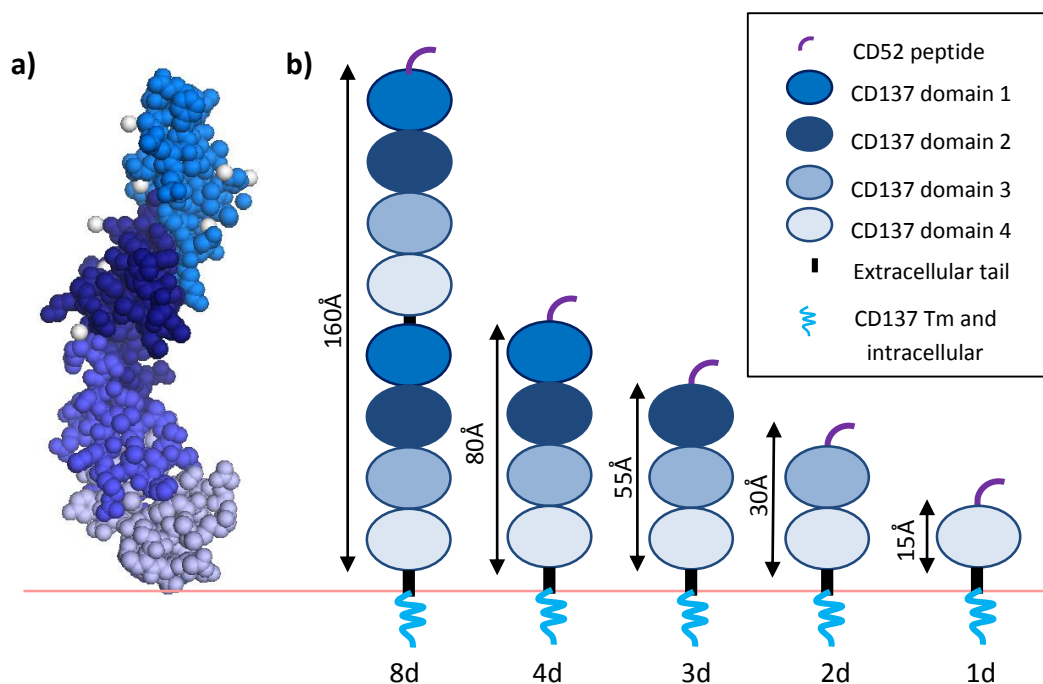


**Figure 3.1: Model of CD137 and the proposed fusion proteins for use throughout thesis project**

a) Proposed structure of extracellular CD137 modelled on the TNFR1 crystal structure,<sup>320</sup> DOI: 10.2210/pdb1tnr/pdb. The four cysteine rich domains have been colour coded and numbered 1-4 for reference, with domain 1 being the furthest away from the cell membrane. b) Schematic of proposed fusion proteins. The CD52 peptide (purple) is attached to the CD137 backbone which has decreasing numbers of cysteine rich domains. Dimensions were estimated using Jsmol viewer provided by the Protein Data Bank (<http://www.jmol.org>), and the extracellular domains coded using PyMOL. For the 8 domain construct (8d), the full length CD137 (4d) molecule was attached to the N-terminus of a second CD137-4d protein resulting in a duplication of each domain.

### 3.2 Cloning of Constructs:

Overlap PCR is a technique that allows the formation of fusion proteins by annealing two separate genes through complementary regions, incorporated via DNA primers<sup>321</sup>. The process of overlap PCR is presented in Figure 3.2. Here the required gene fragments were first amplified by PCR: fragment 1 contained the CD52 signal and peptide sequence (using primers 1 and 2), and fragment two contained the protein-coding CD137 gene (using primers 3 and 4). The initial products were isolated and purified from the PCR reaction by agarose gel electrophoresis, and then used as the template in a second round of PCR (stage 2) without the addition of primers, where the two fragments were able to fuse together. This was possible as primers 2 and 3 (Figure 3.2a) were designed to produce an overlapping fragment which allowed the fragments to anneal (Figure 3.2b). Finally, in stage 3, in order to improve the final yield, the 5' and 3' primers were added along with additional nucleotides and fresh polymerase for a final stage of PCR amplification.

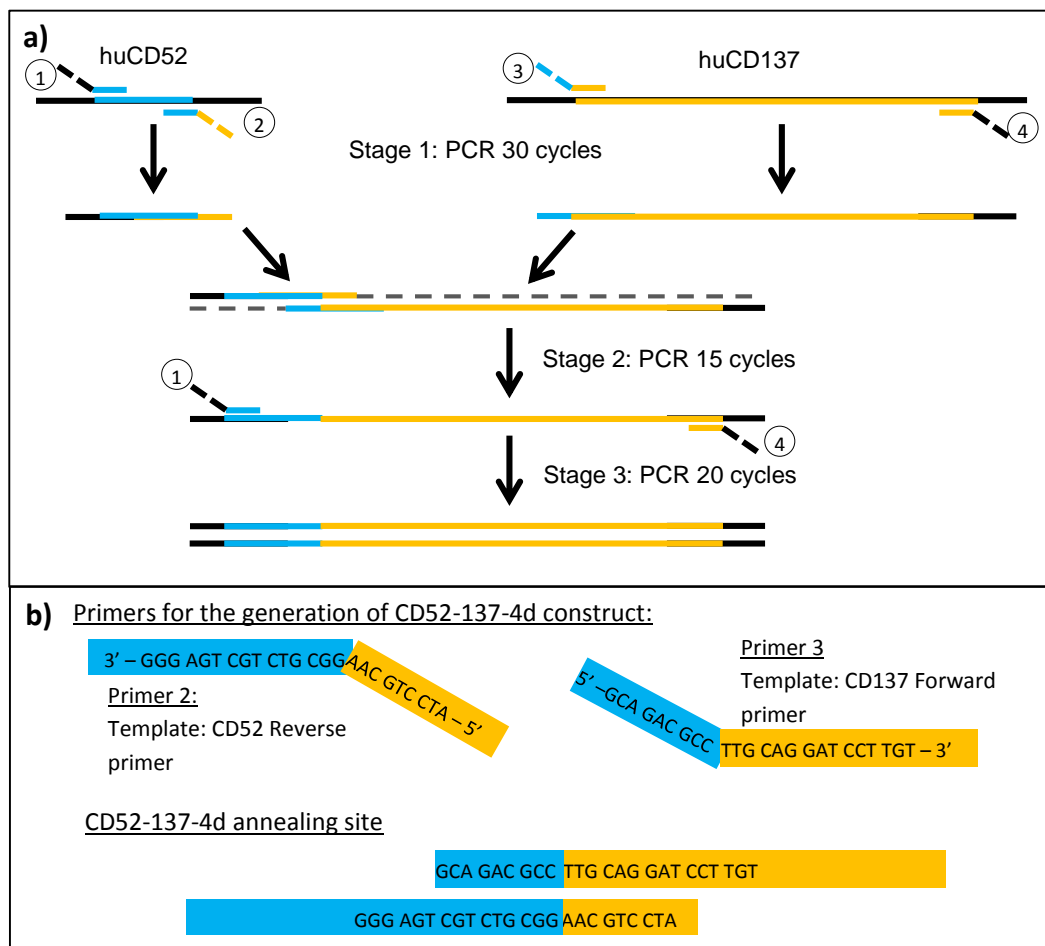


**Figure 3.2: Schematic of overlay PCR technique to produce CD52- CD137 fusion constructs**

a) Stage 1: PCR amplification of the individual CD52 (blue) and CD137 (yellow) gene fragments used four unique primers (numbered 1-4). The 3'-CD52 primer (2) and 5'-CD137 primer (3) contain complementary sections of the other gene to produce a compatible annealing site (see Figure 3.2b). Stage 2: the purified PCR products were combined together in a second PCR reaction, where they were able to anneal at the complementary region and form a single product. Stage 3: Primers 1 and 4 were added to the last PCR reaction in order to improve the yield of the final fusion construct. b) Primers 2 and 3 for the generation of CD52-137-4d are provided showing the annealing site formed as a result of stage one.

The genes of human CD52 and human CD137 had previously been cloned from human lymphocyte cDNA into the expression vector, pcDNA3 (by Dr C. Chan). These plasmids were used as template DNA in order to clone the fusion proteins. PCR products were assessed at stage 1 and 3 for both purity and confirmation of gene size by agarose gel electrophoresis (Figure 3.3). It could be seen that initially the CD52 PCR product was approximately 120bp – based on extrapolation of the DNA ladder migration – and the full length CD137 gene (referred to as CD137-4d) was approximately 700bp (Figure 3.3a). In Figure 3.3b, the sizes of the various gene products for 4, 3, 2 and 1 domain containing constructs were approximately 800bp, 700bp, 600bp and 500bp, respectively, which indicated the correct formation of the intended fusion genes.

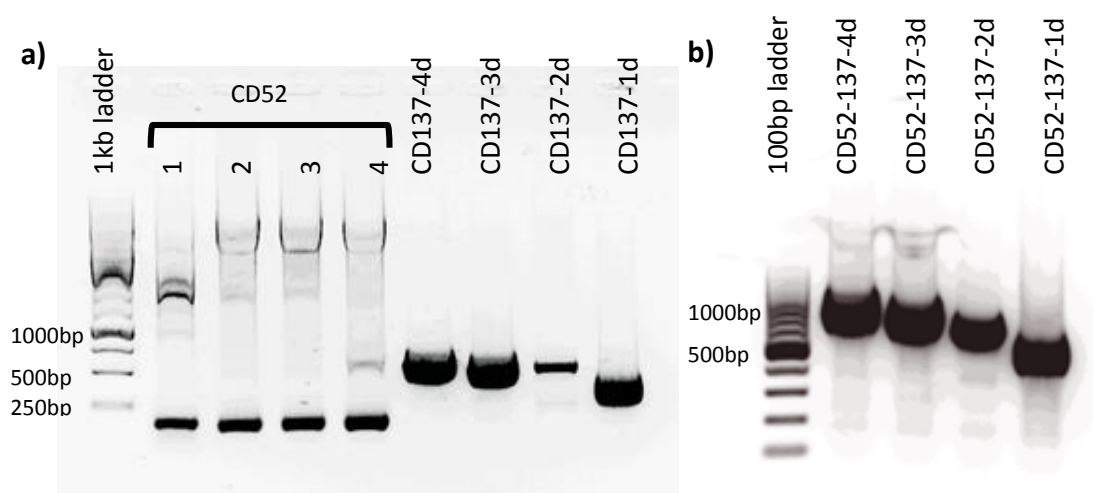


**Figure 3.3: Generation of fusion proteins by overlap PCR**

PCR products assessed by agarose gel electrophoresis at stages 1 and 3 of the overlap PCR method illustrated in Figure 3.2. PCR products were loaded onto a 0.7% agarose gel stained with GelRed and separated under a constant 120V. The DNA was visualised under UV light and an image taken by GelDoc software. a) CD52 signal and peptide sequence (lanes 1-4) were amplified by PCR. Truncated forms of CD137 (as labelled) were amplified from the cDNA of CD137. b) Combining the initial products from a) in another round of PCR (for example CD52 and CD137-4d) followed by further amplification resulted in the formation of a complete fusion gene of the expected sizes.

In order to confirm the identity of each gene, the amplified PCR products visualised in Figure 3.3b were extracted from the gel and ligated into pCR-Blunt II-TOPO vector (herein referred to as TOPO-blunt, Figure 3.4). This vector was chosen as it is pre-linearised with topoisomerase annealed – which mediates the ligation of the gene insert – thereby removing the requirement to further modify the gene insert by A-tailing or phosphatase treatment of the plasmid to prevent self-ligation. As a result of these features, a straightforward ligation of the purified PCR product into the vector without introducing any contaminants or decreasing yield was achieved. As an initial assessment of whether the ligation reaction was successful, plasmid DNA was amplified in transformed pre-competent JM109 cells and the resulting bacteria streaked to provide single colonies for selection.

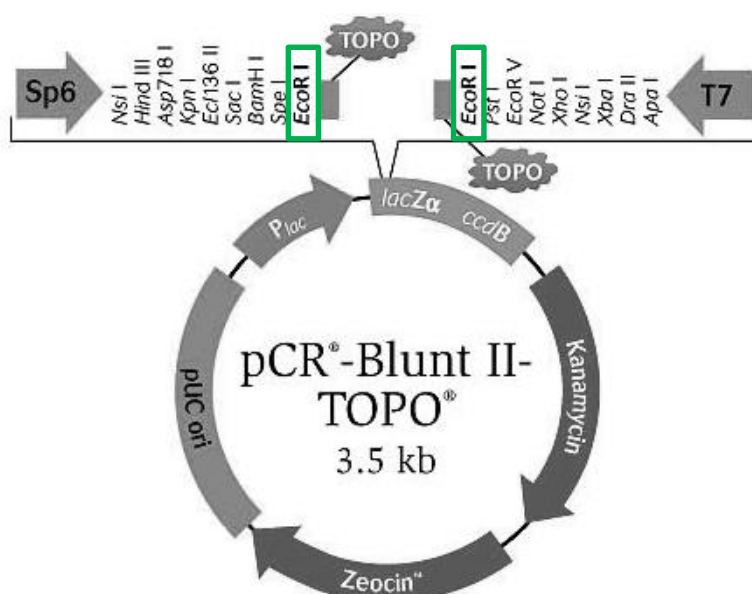


**Figure 3.4: pCR-Blunt II-TOPO cloning vector map**

Annotated vector map for the pCR-Blunt II-TOPO vector used for verification of gene products produced by overlap PCR. This vector contains sites for the T7 and Sp6 primers for DNA sequencing. It also contains two EcoRI sites which flank the multiple cloning site (boxed in green) allowing a straightforward diagnostic restriction digest method to confirm gene insertion. Successful insertion of DNA disrupts the *ccdB* gene, making the cell viable as a method of positive selection. The map was obtained from Life Technologies <sup>322</sup>.

For each construct a minimum of five bacterial colonies were picked from an agar plate, expanded and the plasmid isolated. The plasmid DNA underwent a diagnostic restriction digest with EcoRI to check if the gene was inserted based on its size determined by agarose gel electrophoresis. The TOPO-blunt vector contains two EcoRI sites that flank the multiple cloning site where gene products are inserted (Figure 3.4). Figure 3.5 contains the diagnostic gel for the plasmids isolated from the transformed JM109 cells. Plasmids that contained an insert of the expected gene size are boxed for clarity. The ligation reaction was not 100% efficient; however there was at least one colony which contained a plasmid with the expected gene size for all of the constructs. In order to confirm the identity of these inserts conventional DNA sequencing (short-chain termination method using BigDye Terminator v3.1) was performed. 2-3 colonies were chosen to be sequenced for each construct (only one colony for CD52-137-3d was available for sequencing) using both the T7 and Sp6 primers that are present either side of the gene insertion site in the vector (Figure 3.4).



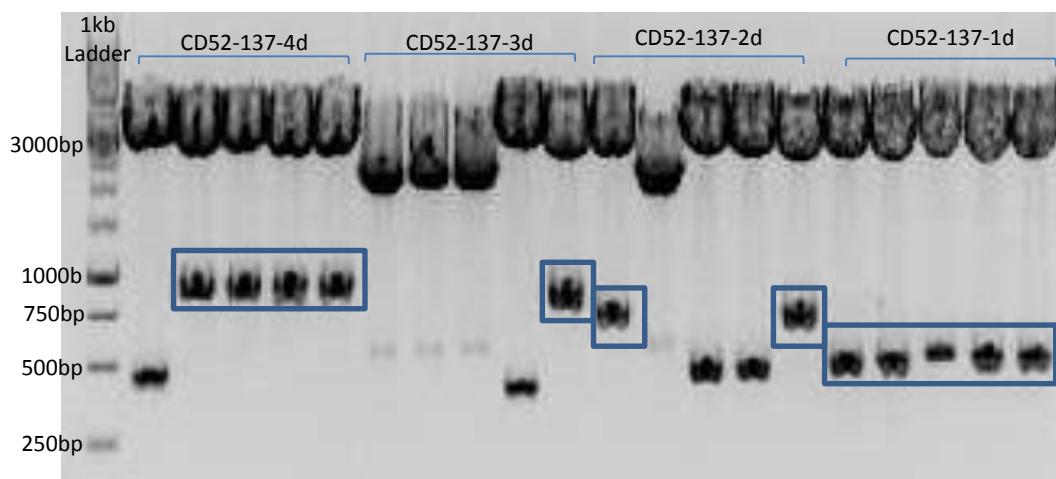


**Figure 3.5: EcoRI digest of JM109 colonies transformed with CD52-137 fusion genes ligated into TOPO-Blunt vector**

CD52-137 fusion genes generated by overlap PCR were ligated into TOPO-Blunt vector. Ligated plasmids were transformed into JM109 cells in order to amplify the plasmids before being isolated using the Qiagen miniprep kit. Isolated plasmids were digested with EcoRI for 1 hour at 37°C, and the products were separated by gel electrophoresis on a 0.7% agarose gel stained with GelRed for DNA visualisation. The boxed bands represent the correct size gene inserts for the corresponding fusion gene.

XbaI and NotI restriction sites were incorporated into the 5' and 3' ends of the fusion gene, respectively, to facilitate directional cloning into an expression vector. pcDNA3.1/- contained the correct orientation of the restriction sites (Figure 3.6) so that the gene inserted was under the control of the cytomegalovirus (CMV) promoter, allowing high protein expression when transfected into mammalian cells. In order to sub-clone the constructs into the expression vector, double restriction digests were performed on the insert containing TOPO-blunt vector as well as empty pcDNA3.1/- to produce compatible ends. The digested products were excised from a 0.7% agarose gel as before, which allowed purification of cut and linearised DNA products, as they migrate differently to uncut circular DNA. A ligation reaction, mediated by T4 ligase, was used to anneal the insert DNA into the pcDNA3.1/- plasmid. The resulting product was then used to transform competent JM109 cells. Colonies were isolated from the resulting culture, as performed previously after TOPO-blunt ligation. Correct insertion of the fusion gene was confirmed by a double restriction digest (using XbaI and NotI) on the isolated plasmids. All constructs produced clear single bands of the correct size as seen previously in Figure 3.5. The identity of the insert was further confirmed with DNA sequencing as before, using the plasmid T7 primer.

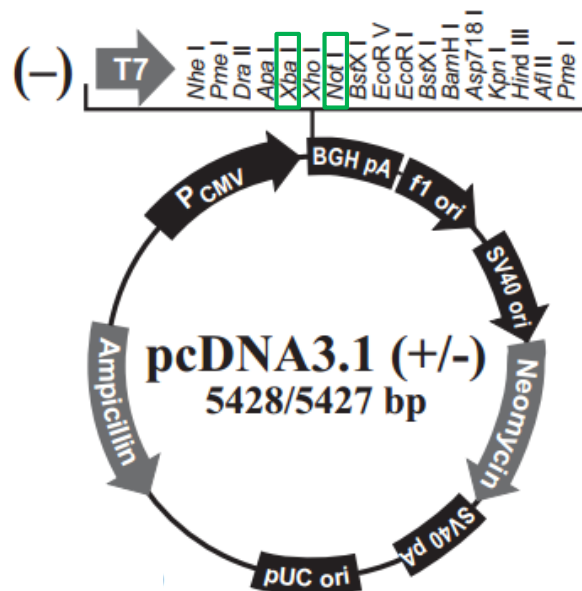


**Figure 3.6: pcDNA3.1/- expression vector map.**

Annotated vector map for the pcDNA3.1/- vector used for protein expression in mammalian cells. This vector contains sites for the T7 primer for DNA sequencing. The orientation of XbaI and NotI (boxed in green) allow for the correct orientation for the gene insert so that it is under the control of the CMV promoter. The map was obtained from Invitrogen <sup>323</sup>.

The CD52-137-8d construct (illustrated in Figure 3.1) was generated by overlap PCR as used previously for the other constructs discussed. However, the process was not as straightforward due to the high homology of the two halves as a result of the direct replication of the CD137 extracellular region. In order to increase the efficiency of this process, the CD52-137-4d gene was used to clone the first half of the construct, using a 3' primer which would join the 4<sup>th</sup> domain seamlessly to the 5' end of the WT CD137 gene. The WT CD137 gene was used to amplify the second half of the gene as done previously in cloning the 4-domain construct. This stage was clean, and produced single products as shown in Figure 3.7a. In order to promote end-to-end joining and not side-to-side (which would result in the formation of another 4-domain construct), the annealing temperature was reduced to 56°C to promote more non-specific binding. When running this product by gel electrophoresis, there is a clear band that corresponds to the size of the 4-domain construct, however there was a lower intensity band at approximately 1400bp which would correspond to the 8-domain construct (highlighted with arrow in Figure 3.7b). This band was excised and ligated into TOPO-blunt in the same manner as previously discussed. DNA sequencing of this gene confirmed that it was the 8-domain construct and not the 4-domain. This gene was then able to be excised using XbaI and NotI and ligated into pcDNA3.1/- in a straightforward ligation reaction as carried out for the other constructs (Figure 3.7c).

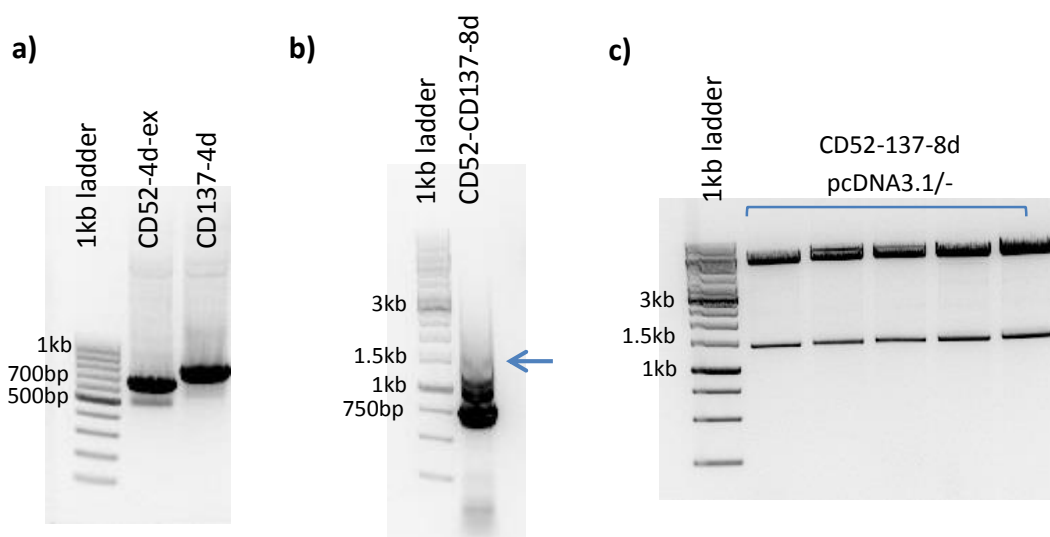


**Figure 3.7: Generation of the CD52-137-8d construct by overlap PCR**

Agarose gel electrophoresis images mapping the generation of CD52-137-8d by overlap PCR. a) The two extracellular fragments consisting of the CD52 peptide attached to the four extracellular domains of CD137 (CD52-4d-ex) and the WT CD137 molecule (CD137-4d) were isolated from the gel and used in a second round of PCR to form an eight domain construct. b) Combining the fragments from a) in another round of PCR (with a lower annealing temperature) resulted in the amplification of multiple fragments. The faint band under 1.5kb (highlighted by arrow) corresponded with the expected size of the CD52-137-8d gene and this was excised and ligated into TOPO-blunt vector. c) Once the CD52-137-8d gene was confirmed by DNA sequencing it was digested and ligated into the pcDNA3.1/- expression vector and transformed into JM109 cells. Plasmids were isolated from 5 colonies and digested with XbaI and NotI to check for gene insertion by agarose gel electrophoresis.

### 3.3 Protein expression in mammalian cells:

Once the gene constructs for the fusion proteins had been cloned, protein expression, correct folding and cell surface detection was assessed. To achieve this, transient transfections of 293F cells were performed and surface expression of the CD137 backbone was assessed by flow cytometry. Prior to this, larger yields of plasmid DNA were prepared from 100mL bacterial cultures, and harvested using the Qiagen Maxiprep protocol.

To detect protein expression a panel of antibodies was employed in order to identify the correct folding of the CD137 backbone. Six anti-CD137 antibodies were chosen based on their ability to bind unique epitopes within CD137 and had previously been demonstrated as binding to different truncated versions of CD137 (Dr. R.French, unpublished data). SAP1-1 and SAP1-3 were able to bind the WT CD137 molecule, SAP3-5 and SAP3-6 were able to bind a 3-extracellular domain CD137 molecule, and SAP3-23 and SAP3-26 were able to bind a 2-extracellular domain CD137 protein. None of these antibodies had previously been tested on truncated construct expressing only one domain (CD52-137-1d), but it was anticipated that at

least one of the six antibodies chosen would bind in order to compare expression profiles between the panel of fusion proteins.

Therefore to assess cell surface expression of the CD52-137 constructs, 293F cells were transfected using Fectin293 reagent (a cationic lipid) which was pre-incubated with the plasmid DNA, before introducing to the cell culture. Initially, 293F cells were transfected with the CD52-137-4d construct and checked at 24 hours for protein expression by flow cytometry. Detection of binding was performed using a secondary phycoerythrin (PE)-labelled anti-mouse IgG polyclonal antibody which fluoresces in the red FL2 channel. Figure 3.8 demonstrates the gating strategy applied to the flow cytometry data of transfected 293F cells in order to determine protein expression. First, cells were gated on the forward and side scatter (FSC and SSC) to exclude debris and dead cells. Subsequently the live gate was verified by adding the viability dye PI to the sample (which fluoresces in the FL2 channel). Next the level of non-specific binding seen with an isotype control mAb was determined as illustrated in Figure 3.8c. Finally the binding of the anti-CD137 mAb was recorded and the geometric mean fluorescence (above the isotype control mAb) was recorded (Figure 3.8d). It was seen that the CD137 backbone for the CD52-137-4d fusion protein was clearly expressed 24 hours after cell transfection (Figure 3.8d). The smeared profile seen for each antibody was a result of a heterogeneous expression throughout the cell population with different expression levels, typical of a transient transfection.

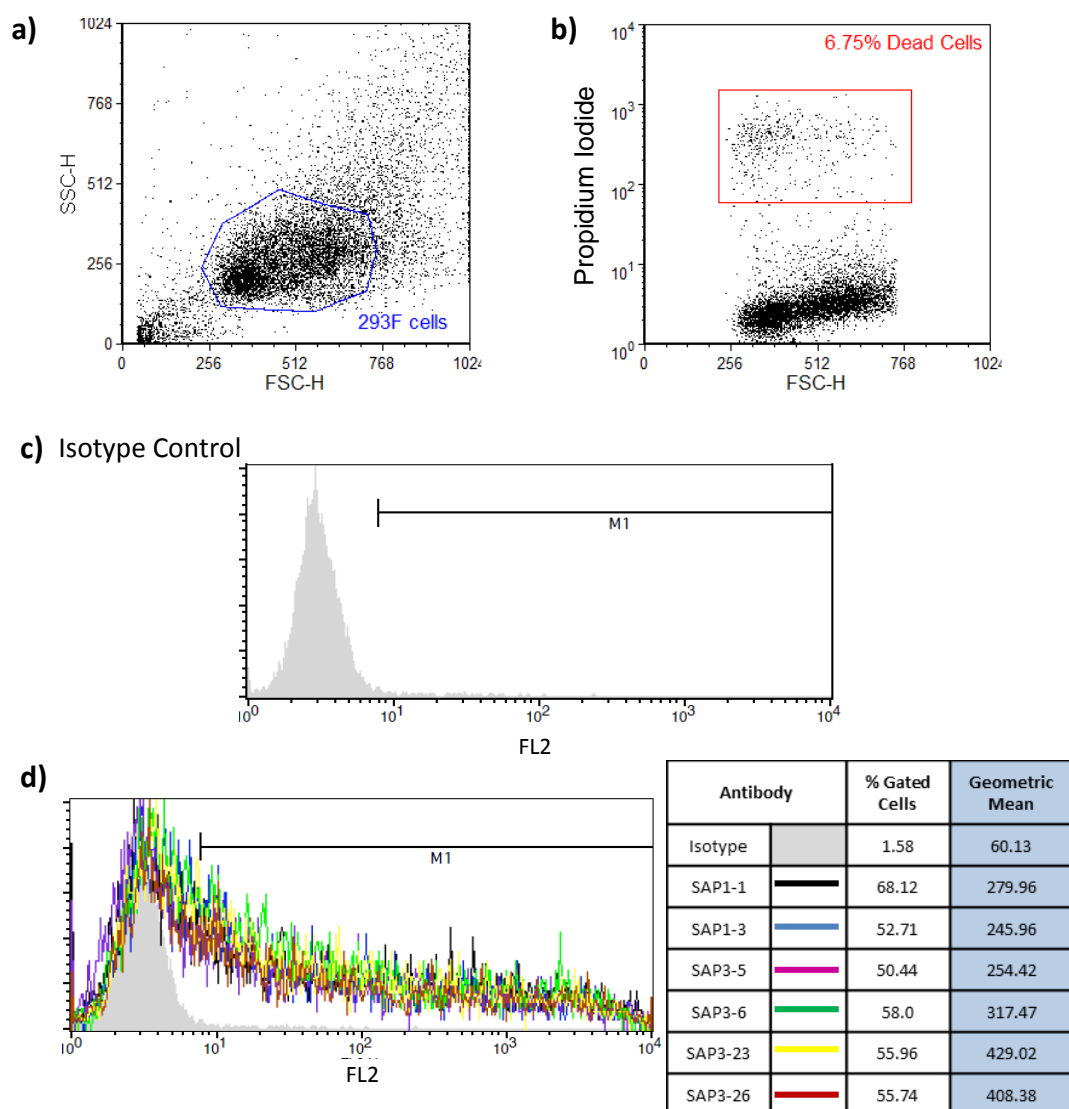


**Figure 3.8: Gating strategy used to analyse cell surface expression of proteins in transfected 293F cells.** 293F cells were transfected with CD52-137-4d construct for 24 hours prior to analysis. Surface protein expression of CD52-137-4d was assessed by flow cytometry using antibodies directed towards the CD137 backbone. All cells were opsonised with 10µg/mL of antibody for 30 minutes at 4°C before washing and detection with a secondary PE-labelled anti-mouse IgG polyclonal antibody. a) Viable cells were identified based on their FSC/SSC profile and gated in order to exclude debris and dead cells from analysis. b) The 293F cell gate was verified using transfected 293F cells stained with the viability stain PI. Dead cells would incorporate the dye and fluoresce in the FL2 channel. In this example, only 4% of the cells present in the 293F gate were dead. c) CD52-137-4d transfected 293F cells were opsonised and labelled with an isotype control mAb in order to determine any non-specific binding or auto-fluorescence. The histogram shows all the cells that are in the 293F gate, and the relative fluorescence in the FL2 channel (which would detect the secondary antibody). A marker is then placed to exclude non-specific binding, and define the range of fluorescence that will reflect a positive result. d) Transfected cells were stained individually for all of the anti-CD137 antibodies and analysed using the same gates as the isotype control. The histogram illustrates the collated data for all of the SAP antibodies, along with a data table which records the percentage of cells positive for the antibody binding and the geometric mean fluorescence. The geometric MFI (in blue) was used to compare the relative antibody binding for all six of the SAP antibodies tested.

Applying the gating strategy presented in Figure 3.8 to 293F cells transfected with the other fusion proteins confirmed that the CD137 backbone was expressed at the cell surface in all of its truncated forms (Figure 3.9a). The binding profiles for the anti-CD137 antibodies seen in Figure 3.9a provided an insight into the exact domain each antibody bound along the CD137 backbone – summarised in Figure 3.9b. SAP3-6 was the only antibody that bound the 1 domain construct (CD52-137-1d). As this domain was present on all of the constructs it can be used to measure the transfection efficiencies and relative expression levels between constructs as an internal control.

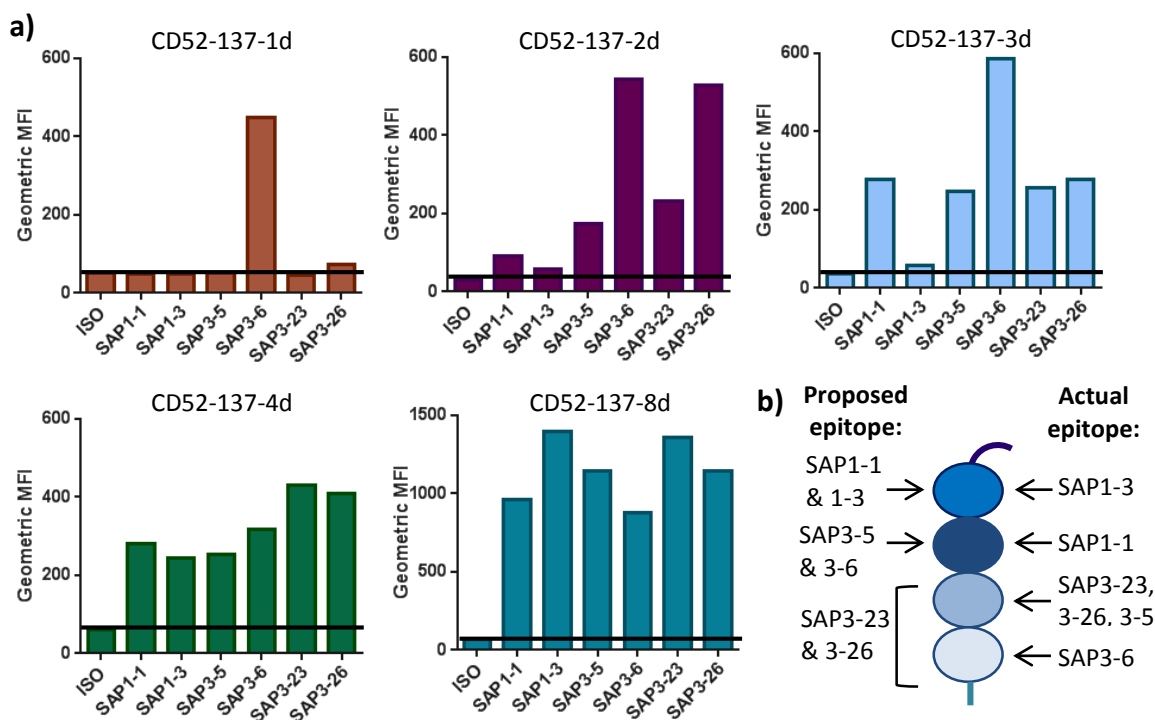


**Figure 3.9: Summary data of fusion protein expression on the surface of 293F cells 24 hours after transfection**

293F cells were transfected with each of the CD52-137 fusion proteins cloned into the pcDNA3.1/- expression vector. 24 hours later the cells were stained with 10µg/mL of the anti-CD137 antibodies or an isotype control (ISO) for 30 minutes at 4°C. The cells were washed before bound antibody was detected using an anti-mouse-IgG-Fc-PE secondary F(ab)<sub>2</sub> for 30 minutes at 4°C. a) The flow cytometry data was analysed using the gating strategy outlined in Figure 3.8. Each graph displays the GeoMFI from a single experiment, and the fusion proteins were not all assessed on the same day. The black line on each graph is set as the threshold of the isotype control; binding above this line indicates specific antibody binding. b) Schematic presenting the original proposed binding sites (left side of the molecule) whilst the summary of the actual binding sites for the panel of anti-CD137 antibodies based on the flow cytometry data in a) are presented on the right. SAP3-6 bound the membrane proximal domain whilst SAP1-3 bound the N-terminal domain, furthest away from the cell membrane.

All of the fusion proteins were able to be expressed and detected on the surface of 293F cells, presumably with the correct folding given their detection using the domain specific anti-CD137 mAbs. Next, the ability of CAMPATH-1H to bind the CD52 peptide was assessed. 293F cells

were transfected with the CD52-137 fusion proteins as before and antibody binding was assessed using a direct FITC conjugated CAMPATH-1H antibody, which fluoresces in the FL1 channel. The gating strategy used to detect the CD137 backbone (in Figure 3.8) was applied; however the FL1 channel was selected instead of FL2 to record CAMPATH-1H binding. CAMPATH-1H was unable to bind any of the fusion proteins expressed in 293F cells, even though surface protein expression was confirmed by SAP3-6 binding to the CD137 backbone (Figure 3.10). The data for CD52-137-1d, -4d and -8d is presented, although the same result was seen for the 2 and 3 domain constructs as well.

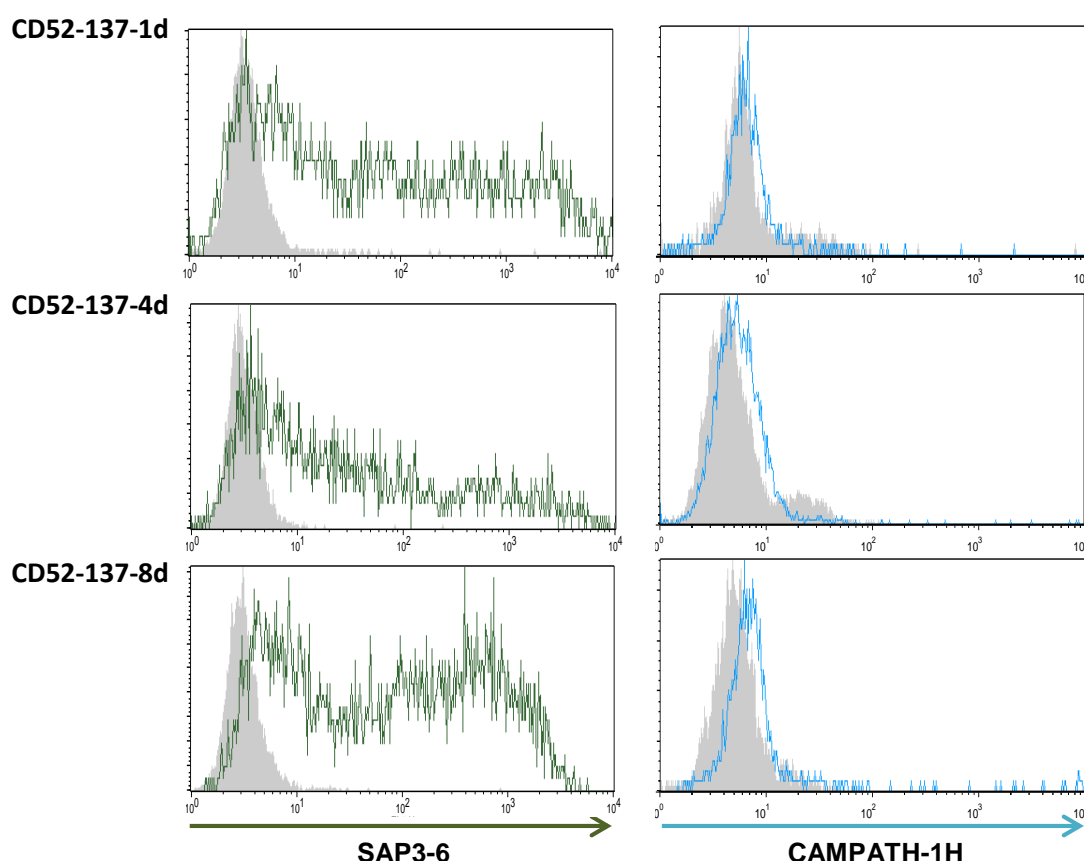


**Figure 3.10: Measuring CAMPATH-1H binding of 293F cells transfected with CD52-137 fusion proteins** 293F cells were transfected with the CD52-137 fusion proteins for 24 hours. Cells were opsonised with 10 $\mu$ g/mL of SAP3-6 (green), CAMPATH-1H (light blue) or an isotype control (grey) for 30 minutes at 4 $^{\circ}$ C, followed by a secondary anti-mouse-IgG-PE. Antibody binding was confirmed by flow cytometry and the data was analysed as previously outlined in Figure 3.8.

Given the negative result, the ability of the CAMPATH-1H antibody to detect wild type CD52 was assessed using two different human cell lines, Raji and Ramos (Figure 3.11). These cells expressed the wild type CD52 antigen which had not been manipulated. CAMPATH-1H was able to bind these cells confirming that the lack of binding observed on the fusion proteins in Figure 3.10 was not a consequence of a defective antibody.

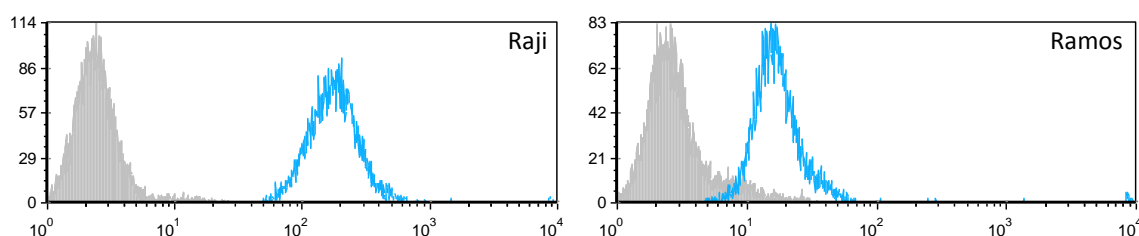


**Figure 3.11: CAMPATH-1H recognises wild type CD52 expressed on Raji and Ramos cell lines**

Raji and Ramos cells were opsonised with 10 $\mu$ g/mL of CAMPATH-1H (blue) or an isotype control (grey) for 30 minutes at 4°C before assessing antibody binding by flow cytometry. The results of a single experiment are presented.

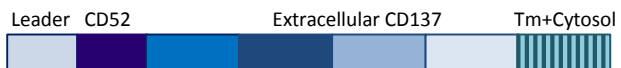
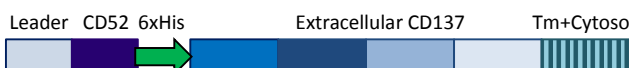
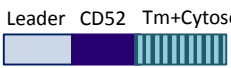
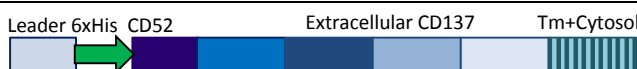
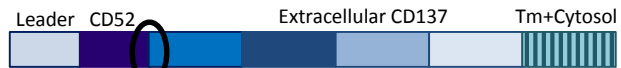
### 3.4 Troubleshooting the CD52 peptide:CAMPATH-1H interaction

Given that CAMPATH-1H was unable to bind the CD52-137 fusion proteins, several hypotheses were considered:

- 1) The CD52 peptide was not accessible to the antibody on the surface of the protein because either it was buried within the protein or the presence of the CD137 backbone was blocking antibody access.
- 2) The CD52 peptide was being cleaved post-translationally and therefore was not present on the surface of the cells.
- 3) The epitope was obscured by the proximity to the CD137 backbone and binding would be improved through the use of linkers or mutations which would alter the display of the peptide, for example using proline to induce bends in the final peptide conformation.

In order to test these hypotheses, structural modifications to the CD52-137-4d construct were generated as summarised in Table 3.1. The CD52-137-4d construct was chosen as the backbone, since it contained the least manipulation of the native protein structure, and any improvements seen for this protein could be applied to the other constructs.



Construct Name	Gene Schematic	Aim of Construct																		
CD52-137-4d		Original Construct																		
CD52-His-4d		To address hypotheses 1 & 3																		
CD52-flush		To address hypothesis 1																		
His-CD52-137-4d		To address hypothesis 2																		
SADPL (V1) and SPDAL (V2) mutants	 <table data-bbox="596 815 979 1016"><tr><td>WT</td><td>S</td><td>A</td><td>D</td><td>A</td><td>L</td></tr><tr><td>V1</td><td>S</td><td>A</td><td>D</td><td>P</td><td>L</td></tr><tr><td>V2</td><td>S</td><td>P</td><td>D</td><td>A</td><td>L</td></tr></table>	WT	S	A	D	A	L	V1	S	A	D	P	L	V2	S	P	D	A	L	To address hypothesis 3
WT	S	A	D	A	L															
V1	S	A	D	P	L															
V2	S	P	D	A	L															

**Table 3.1: Structural modifications made to the CD52-137-4d construct in order to resolve binding of CAMPATH-1H**

In order to resolve the issue with CAMPATH-1H binding the CD52-137 fusion proteins the four domain construct (CD52-137-4d) was modified with the addition of tags or point mutations as detailed above. The colours of the gene segments refer to individual domains of the fusion protein, and relate to the drawing in Figure 3.9b.

In order to assess whether the site chosen to attach CD52 to CD137 resulted in obscuring the binding of the antibody a His-tag was added between the CD52 and CD137 fusion site (CD52-His-4d; Table 3.1). The His-tag – consisting of six histidine amino acids in a row – is a commonly used tool in molecular biology to identify proteins, due to its detectable motif that isn't conformation dependent. Incorporating the tag into the fusion protein provided a second antibody site to confirm whether the fusion site was accessible. The His-tag served the dual purpose of 1) mimicking the position of the CD52 peptide and 2) acting as a spacer to move the CD52 peptide away from the CD137 backbone.

In addition, a second construct was generated (CD52-flush) which consisted of the CD52 modified peptide, attached to the transmembrane and intracellular tail of CD137 (Table 3.1). This construct would determine whether the modified CD52 peptide could be bound in the absence of any extracellular CD137 scaffold protein, indicating whether the peptide could be bound by CAMPATH-1H in a membrane tethered form.

To produce these constructs, the overlap PCR approach was used as before. The His-tag was incorporated into the primers used in the initial PCR, and acted as the annealing site in the subsequent stages. Figure 3.12a shows the initial fragments produced by PCR whilst Figure 3.12b shows the complete product after ligation into the TOPO-blunt cloning vector.

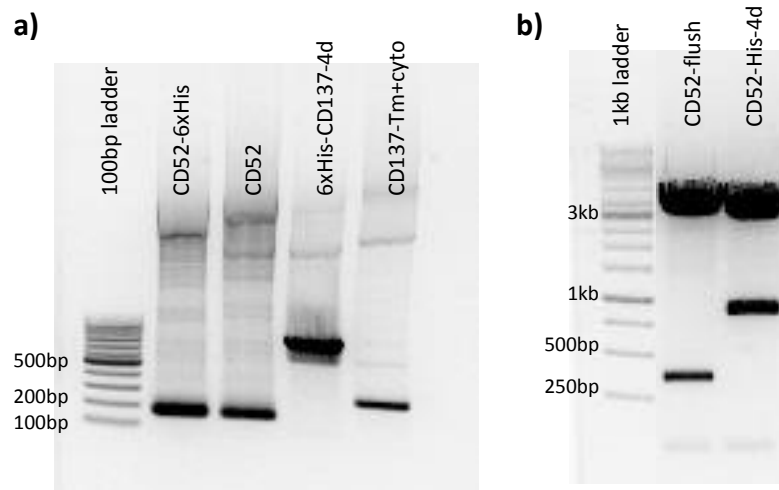


**Figure 3.12: Generation of CD52-flush and CD52-His-4d constructs by overlap PCR**

In order to clone CD52-flush and CD52-His-4d illustrated in Table 3.1, the initial PCR fragments were generated. a) The CD52 peptide was amplified with and without a His-tag and are approximately 150bp in size. Alongside this the CD137 product was generated, either the complete 4 domain construct (6-His-CD137-4d, approximately 700bp in size) or just the transmembrane and intracellular domains (CD137-Tm+cyto) approximately 200bp. b) The products were annealed in order to produce the fusion genes and subsequently ligated into TOPO-Blunt cloning vector and transformed into JM109 cells. A diagnostic restriction enzyme using EcoRI confirmed the fusion genes for CD52-flush and CD52-His-4d were successfully cloned.

As before, each construct was transfected into 293F cells and surface expression was assessed after 24 hours by flow cytometry (Figure 3.13). For the CD52-flush construct, no binding for any of the antibodies tested was seen above the isotype control (Figure 3.13a), confirming that no extracellular CD137 was present on the surface of the cell, but equally no improvement in CAMPATH-1H binding was observed (Figure 3.13b). However, a lack of expression or mis-folding of the fusion protein could not be excluded for this particular construct.

For the CD52-His-4d construct, the anti-His antibody was seen to bind at an equivalent level to the anti-CD137 antibody SAP3-6 (Figure 3.13c) thereby confirming that the CD137 backbone was not obscuring the antibody epitope and that it was accessible on the surface of the protein. For this construct, a minor improvement in CAMPATH-1H binding was seen (Figure 3.13d). However, only a fraction of the total transfected cell population expressing the CD137 scaffold also bound CAMPATH-1H. This improvement was insufficient for use in any subsequent work.

It was considered that an extended linker may further improve the CAMPATH-1H binding, though this approach would go against the rationale of the peptide, as it would increase both the overall distance being investigated, and the flexibility of the peptide which may have unintended consequences when used in the functional assays. It was therefore concluded from these two constructs that the fusion site chosen to attach CD52 was suitable and could be detected on the surface of the cell, and that antibody access was not inhibited by the CD137 backbone.

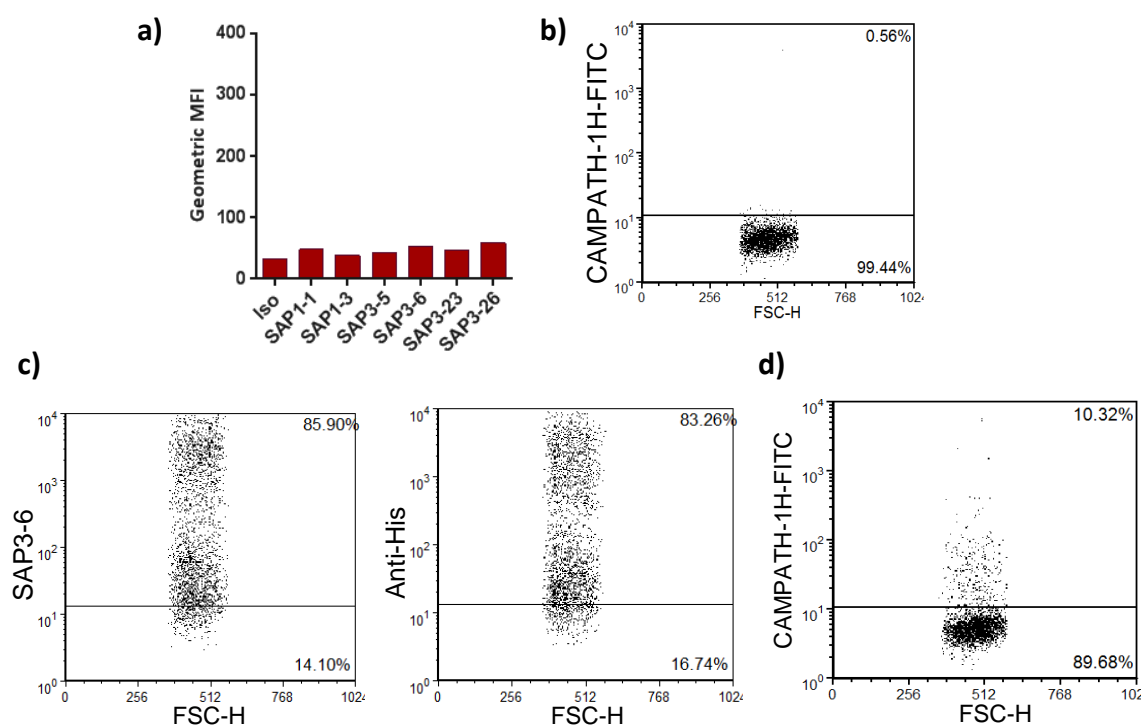


**Figure 3.13: Surface expression of CD52-flush and CD52-His-4d constructs on 293F cells.**

293F cells were transfected with either CD52-flush or CD52-His-4d fusion protein for 24 hours before checking expression by flow cytometry. The transfected 293F cells were opsonised with 10 µg/mL antibody for 30 minutes at 4°C. The anti-CD137 antibodies were then detected using an anti-mouse-IgG-Fc-PE conjugated secondary. a) The GeoMFI for the binding of the anti-CD137-antibody panel for CD52-flush was transfected. No binding was seen as expected due to the lack of extracellular CD137 in this construct. b) Dot plot indicating no CAMPATH-1H binding of CD52-flush cells. c) Dot plots of 293F cells transfected with CD52-His-4d were stained with SAP3-6 and anti-His. d) Dot plot indicating partial CAMPATH-1H binding of CD52-His-4d cells although the positive population does not match the population of cells expressing the His-tag in figure c). The results from a single experiment are presented.

An alternative explanation for why CAMPATH-1H was not efficiently binding the fusion protein, even though the site of attachment was accessible, was that the CD52 peptide was being cleaved post-translationally. To test this hypothesis, a His-tag was attached to the N-terminus of the fusion protein, before the CD52 peptide (His-CD52-137-4d construct; Table 3.1). If the

CD52 peptide was cleaved, then the His-tag would also be cleaved and no longer be detected on the cells.

To achieve this a pcDNA4/HisMaxB expression vector was used. pcDNA4/HisMaxB (Appendix B) is an expression vector which allows the direct attachment of a His-tag to the 5' end of a gene through restriction digest and ligation. CD52-137-4d was digested with KpnI and NotI to remove the insert from the TOPO-Blunt vector, and ligated into pcDNA4 whilst maintaining the open reading frame. This vector was also under the control of the CMV promoter, so the same transfection and expression system in 293F cells could be applied as before. As presented in Figure 3.14, even though CAMPATH-1H was not able to bind the cells, the antibody towards the His-tag was binding, and was comparable to the binding of SAP3-6. It was concluded that the CD52 peptide was not being cleaved after translation of the fusion protein.

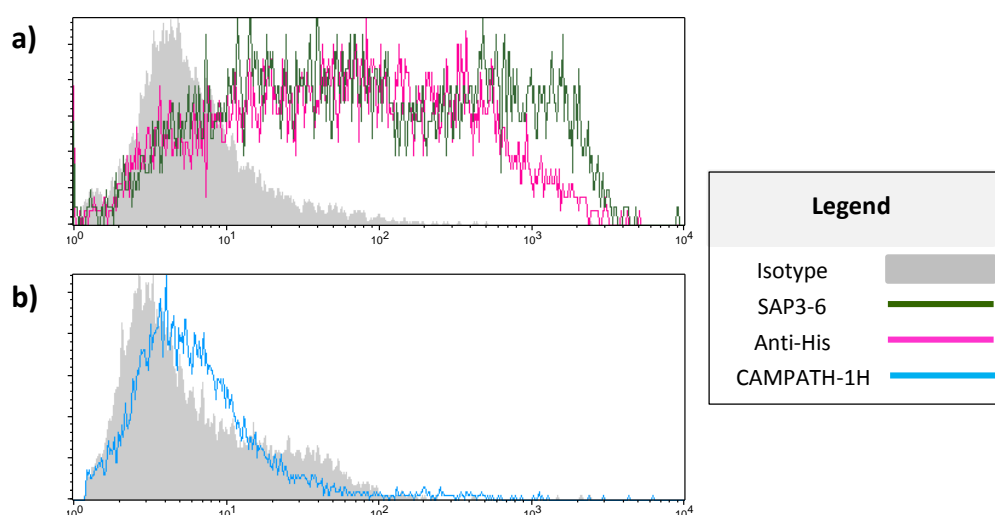


**Figure 3.14: Expression of His-CD52-137-4domain on transfected 293F cells**

293F cells were transfected with His-CD52-137-4d for 24 hours. Cells were stained with a) 10µg/mL anti-His, SAP3-6 or an isotype control followed by an anti-mouse-IgG-PE detection antibody or b) FITC-conjugated CAMPATH-1H.

As the CD52 peptide was apparently expressed and not lost from the surface of the protein it remained possible that specific steric factors were impacting CAMPATH-1H binding. In order to alter the presentation and orientation of the peptide, the use of proline mutations was investigated. Proline is an unusual amino acid structurally, due to the joining of the side chain onto the amine backbone. This structure introduces 'kinks' within a peptide chain changing the conformation as a result. It was reasoned that by switching either of the two alanine residues for proline at the interface of the CD52 and CD137 fusion site, the peptide may be more protruded and better for antibody recognition as a result (the resulting protein sequences are presented in Table 3.1).

To generate these two constructs, a single nucleotide was altered in each case by QuickChange site-directed mutagenesis. This approach uses the principle of PCR to amplify the entire plasmid, rather than just the gene, and incorporates the mutation via the primer used. After the PCR reaction, the original template DNA was digested using DpnI which targets methylated DNA. The remaining plasmid should therefore only be the newly synthesised vector containing the mutation. This plasmid was used to transform *E.coli* and single colonies were isolated for sequencing. Success for the introduction of the mutations was verified by DNA sequencing, and the point mutations were highlighted in Figure 3.15. Following confirmation of the correct sequence the plasmid was maxi-prepped as before to provide enough DNA to allow transient transfections to be performed.

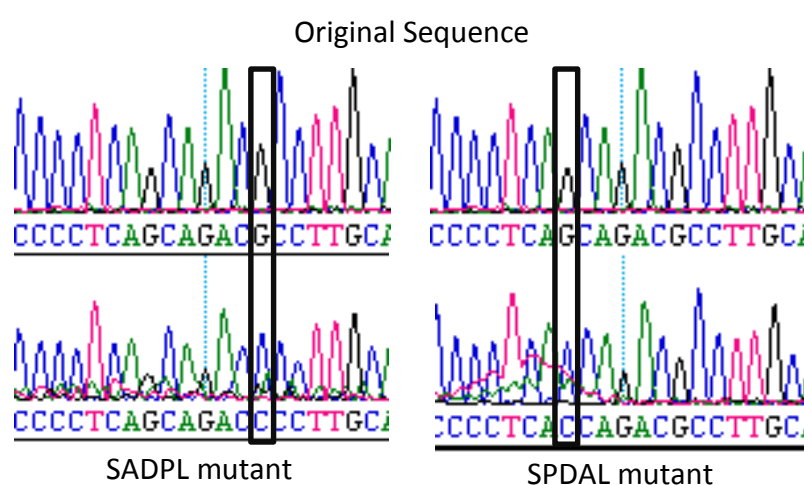


**Figure 3.15: DNA sequencing traces confirming point mutations to create the proline mutants SADPL and SPDAL**

CD52-137-4d underwent site-directed mutagenesis to produce either the SADPL or SDAPL mutants (Table 3.). In order to verify the mutation, the plasmids were transformed into JM109 cells and amplified before undergoing DNA sequencing. The DNA traces were compared against the original DNA sequence (top trace), and the point mutations, G to C for both cases, have been highlighted. The trace is colour coded specifically to each nucleotide as follows: blue = cytosine, red = thymine, black = guanine, green = adenine.

Expression of these two constructs in 293F cells resulted in no improvement in CAMPATH-1H ability to bind (Figure 3.16). The CD137 backbone was once again easily detectable, indicating that the leader sequences and the DNA sequence was correct and functional.

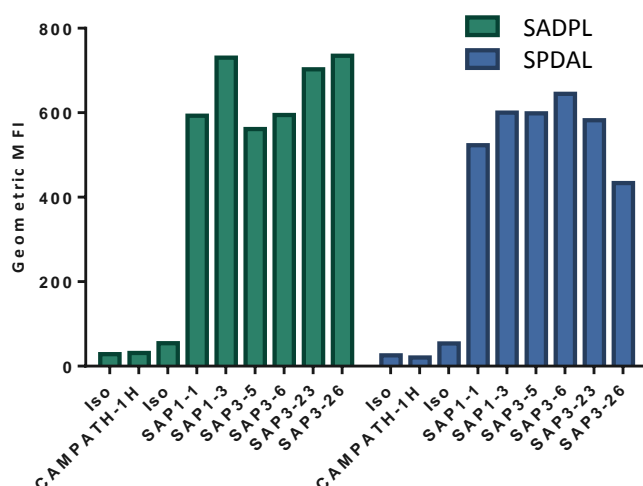


**Figure 3.16: 293F cells transfected with either CD52-SADPL or CD52-SPDAL mutants**

293F cells were transfected with the proline mutants and protein expression was confirmed by flow cytometry after 24 hours, using antibodies towards the CD52 peptide (CAMPATH-1H) and CD137 scaffold (SAP).

In summary, none of these attempts were able to improve CAMPATH-1H binding to the CD52 peptide present in the fusion protein. However, it was concluded that the site of attachment chosen was accessible to antibody binding. Therefore, although previously published as capable of being recognised by CAMPATH-1H when immobilised on cellulose membranes or the carrier protein BSA <sup>319</sup>, it appears that the peptide epitope chosen was not readily recognised by CAMPATH-1H in the context of a mature protein. Therefore an alternative epitope was sought.

### 3.5 Alternative Epitopes:

An alternative epitope that could be bound by CAMPATH-1H was previously identified through phage display technology (termed Cp11) <sup>324</sup>. It consisted of 10 amino acids, which had a disulphide bond between the two cysteine residues to form a cyclic conformation. Table 3.2 compares differences between wild type human CD52, the modified CD52 peptide and the alternative Cp11 peptide. The Cp11 epitope contained the -SPS- motif previously found to be crucial for CAMPATH-1H binding <sup>319</sup>, but apart from that there was relatively little similarity between the two sequences. This epitope had been used by other groups to produce fusion proteins (personal communication, Dr. M.Pule and Dr. B.Philip), making it an attractive alternative to incorporate into the CD137 fusion proteins.

Wild Type Human CD52	G	Q	N	D	T	S	Q	T	S	S	P	S			
CD52 modified peptide	G	Q	N	D	T	S	Q	T	S	S	P	S	A	D	A
Cp11 (CAMPATH-1H epitope)					A	<u>C</u>	G	S	T	S	P	S	S	<u>C</u>	

**Table 3.2: Comparison of human CD52, the modified CD52 peptide present in the fusion protein and the alternative CAMPATH-1H epitope, Cp11**

The SPS motif maintained across both peptides is highlighted, and the cysteine required for the correct fold of the cyclic peptide have been underlined for reference.

These constructs were cloned using overlap PCR as before. The Cp11 was previously attached to a CD8 $\alpha$  stalk by Dr. B.Philip, and provided as a template. This construct was used to amplify the leader sequence and Cp11 epitope, and the CD52-137 fusion genes, consisting of 1, 4 and 8 domains, generated earlier were used to amplify the truncated CD137 domains. An additional, membrane proximal construct was cloned using the same premise as the CD52-flush construct (Table 3.1) referred to as Cp11-flush; this construct consisted of the Cp11 peptide attached to the transmembrane and intracellular domain of CD137. These were chosen as they provided the best coverage of distances from the cell membrane. Once cloned and confirmed by DNA sequencing, the genes were sub-cloned into the expression vector pcDNA3.1 using the restriction sites EcoRI and NotI (Figure 3.17).

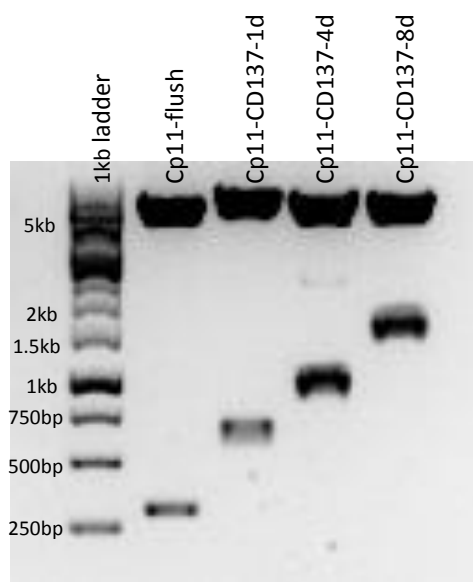


**Figure 3.17: Restriction digest confirming Cp11-CD137 fusion protein ligation into expression vector pcDNA3.1/-**

In order to clone the Cp11-CD137 fusion proteins overlap PCR was used. The Cp11 peptide was amplified from Cp11-CD8 supplied by (Dr. B. Philip) and the CD137 backbone was amplified from the human CD137 cDNA. The genes generated were subcloned into pcDNA3.1/- expression vector, and the ligation of the gene was confirmed by a restriction digest using XbaI and NotI in a diagnostic gel.

The cyclic epitope constructs (Cp11-CD137-) were transfected into 293F cells in order to test both CD137 expression and binding of CAMPATH-1H on the transfected cells. Figure 3.18 shows the flow cytometry data collected for Cp11-flush, Cp11-CD137-1d,-4d and -8d constructs. CAMPATH-1H was able to bind all of the fusion proteins providing us with a set of reagents capable of addressing our hypothesis. This data confirmed the earlier conclusion that the modified CD52 epitope originally used was not capable of being bound by CAMPATH-1H in the context of this fusion protein.

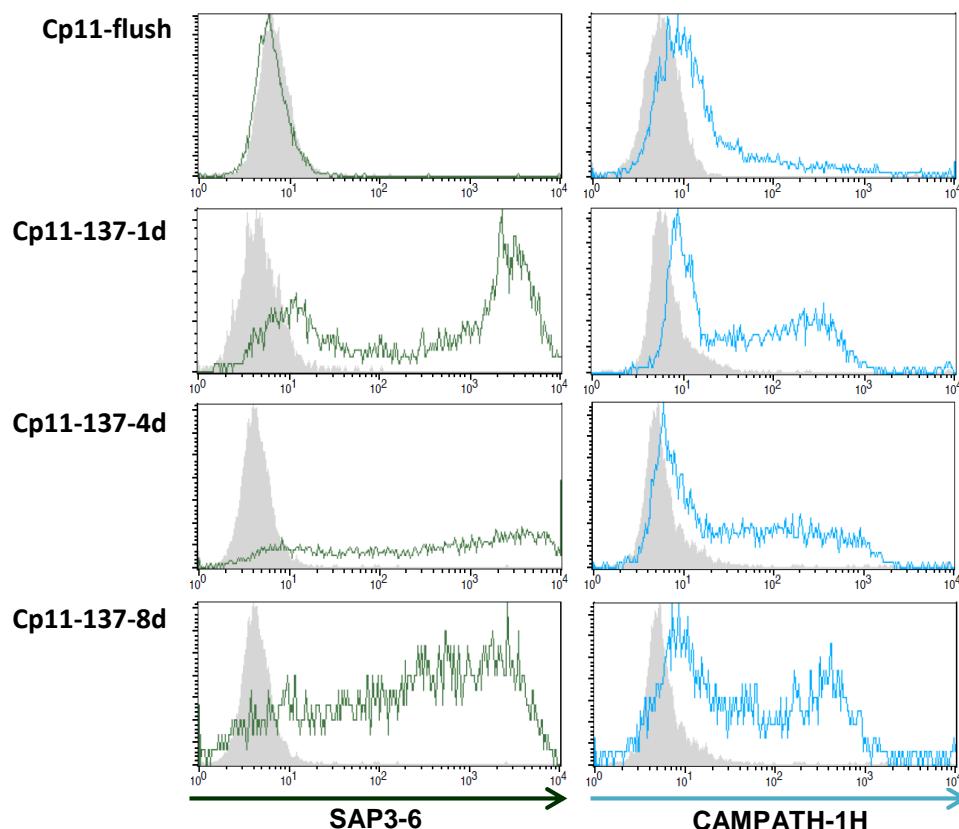


**Figure 3.18: CAMPATH-1H binds Cp11-CD137 fusion proteins expressed in 293F cells.**

293F cells were transfected with the CD52-137 fusion proteins for 24 hours. Cells were opsonised with 10µg/mL of SAP3-6 (dark green), CAMPATH-1H (light blue) or an isotype control (grey) for 30 minutes at 4°C, followed by a secondary anti-mouse-IgG-PE. Antibody binding was confirmed by flow cytometry and the data analysed as previously outlined in Figure 3.8. No SAP3-6 binding was observed for Cp11-flush which was expected as this protein does not contain any extracellular CD137.

### 3.6 Generation of rituximab binding (Rp3-CD137-) constructs:

In order to confirm that any functional results obtained with the constructs generated above were based on the distance an antibody bound and not something specific to CAMPATH-1H an additional set of fusion proteins were also generated. These constructs maintained the same structural properties as the Cp11-CD137 constructs, but contained a different



antibody:epitope combination. For these proteins, a 10 amino acid cyclic epitope recognised by rituximab, previously identified through phage display, was chosen<sup>283</sup>. The epitope chosen (referred to as Rp3) had already been used in the generation of fusion proteins in a similar manner to the Cp11 epitope (Drs M. Pule and B. Philip<sup>142</sup>) and again, minimal impact on the final size of the protein would be seen. These constructs are presented in Figure 3.19.

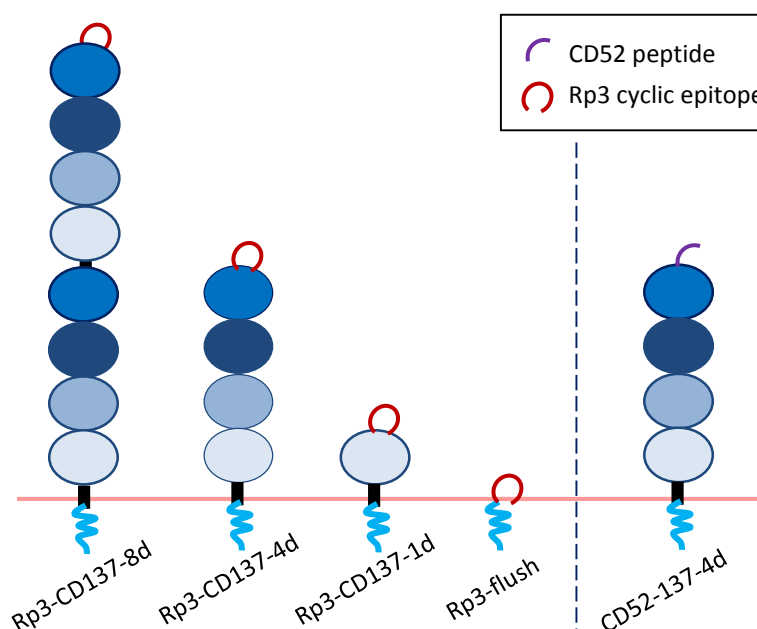


**Figure 3.19: Illustration of rituximab epitope containing constructs, Rp3-CD137**

Shown are the series of fusion proteins expressing the Rp3 rituximab epitope linked to 8, 4, 1 and 0 CD137 extracellular domains with the CD52-137-4d is shown for comparison. To produce these Rp3-CD137- constructs the CD52 peptide (in purple) was mutated for the cyclic CD20 peptide, Rp3 (red). These constructs maintain the same CD137 protein backbone as the previously generated Cp11-CD137 fusion proteins. Alongside this an additional construct which contained no extracellular CD137 was produced (Rp3-flush).

To generate these proteins, the genes for CD52-137-1d, -4d and -8d, were mutated in order to replace the CD52 peptide with the cyclic CD20 epitope. The method of site-directed mutagenesis was the same as that used for the SADPL and SPDAL mutants (Table 3.1) however for the conversion of this epitope, 12 nucleotides were deleted and another 10 nucleotides were mutated in a single reaction as highlighted in Table 3.3.

G	Q	N	D	T	S	Q	T	S	S	P	S	A	D	A
GGA	CAA	AAC	GAC	ACC	AGC	CAA	ACC	AGC	AGC	CCC	TCA	GCA	GAC	GCC
...	...	...	...	<b>G</b> CC	<b>T</b> GC	<b>C</b> CA	<b>T</b> AC	AGC	<b>A</b> AC	CCC	TCA	<b>C</b> TA	<b>T</b> GC	GCC
				A	<u>C</u>	P	Y	S	N	P	S	L	<u>C</u>	A

**Table 3.3: Alignment of gene sequence for the CD52 peptide and Rp3 peptide used to design the mutagenesis primer**

The peptide sequence for the original CD52 peptide (top row in grey) and the Rp3 epitope (bottom row in blue) are provided. Between the peptide sequences, are the gene sequences, with mutations emphasised in bold and blue. In order to convert the CD52 peptide to the Rp3 sequence without inducing any changes in the open reading frame or introducing any premature stop codons; 12 nucleotides needed to be removed (...) and 10 point mutations made within the remainder of the gene.

As there was a high degree of mis-match within the mutagenesis primer, a longer compatible region was required compared to a typical PCR, in order to maximise annealing of the primer to the plasmid. Based on this, 24 nucleotides either side of the peptide mutation site were incorporated into the primer so that approximately 70% of the primer sequence matched the plasmid. The total primer length was far greater than that recommended for traditional PCR (usually 15-20 nucleotides in length), but this approach was deemed necessary to successfully convert the CD52 peptide to the Rp3-epitope sequence by site-directed mutagenesis. The nucleotide sequences of the mutagenesis primers used are provided in appendix A.

After the mutagenesis reaction, the newly synthesised plasmid was used to transform JM109 cells. A diagnostic gel was not performed to identify which plasmids contained the new Rp3 peptide rather than the original CD52 sequence, as the 12 nucleotide mutation was not significantly different in size to visualise by agarose gel electrophoresis, and no unique restriction sites were incorporated. Instead, 5 bacterial colonies for each construct were picked and cultured in order to amplify the plasmid, and verified by DNA sequencing (using the plasmid T7 primer).

Once the plasmid sequence was confirmed the expression of the Rp3-CD137 fusion proteins was assessed in 293F cells. The cells were transfected with each plasmid as performed previously and the binding of rituximab compared to an isotype control. All of the constructs (Rp3-CD137-flush, -1d, -4d and -8d) were able to be bound by rituximab (Figure 3.20).

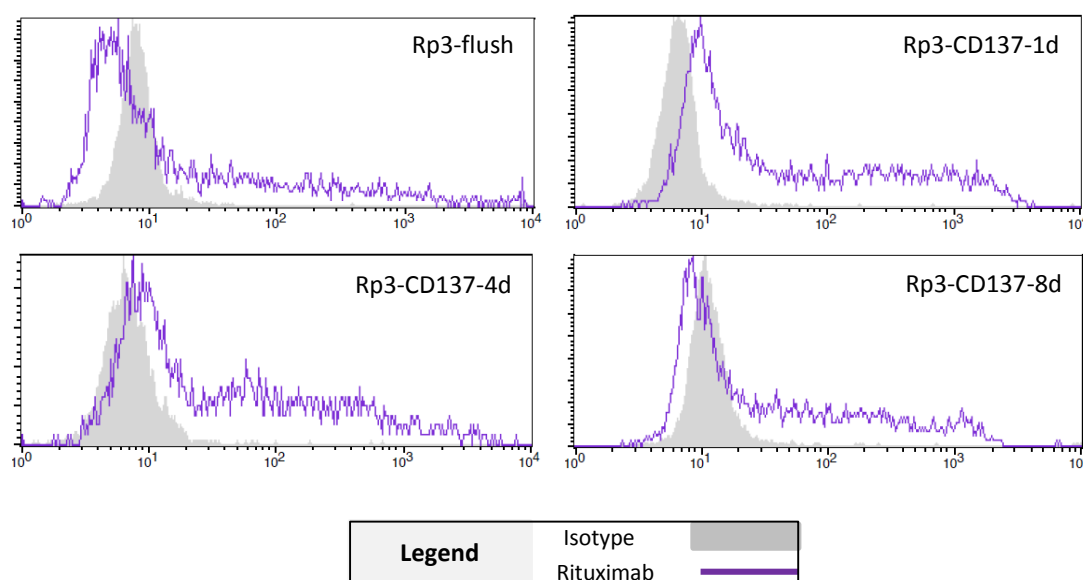


**Figure 3.20: Rp3-CD137 fusion protein surface expression in 293F cells.**

293F cells were transfected with each of the Rp3-CD137 fusion proteins for after 24 hours. The cells were stained with 10 µg/mL of Rituximab-FITC or an isotype control and analysed by flow cytometry using the gating previously described in Figure 3.8.

Finally, to confirm that the fusion genes cloned produced proteins of different sizes, a western blot was carried out. This was required because the flow cytometry data confirmed that CD137 was folded correctly for the expressed fusion proteins, however, was not clear in distinguishing between the four and eight domain proteins (since there is no difference in the binding of anti-CD137 antibodies between them). Whole cell lysates from transfected CHO-S cells were prepared under reducing conditions and separated by SDS-PAGE before the protein was transferred onto a nitrocellulose membrane. A polyclonal antibody directed towards the extracellular CD137 protein (Abcam) was used to detect the fusion proteins by binding the CD137 backbone. As expected bands were visible in Figure 3.21 for the lanes which contained lysates from the Rp3-CD137-1d, -4d and -8d transfected cells whilst no band was seen for Rp3-flush (due to no extracellular CD137 being present for this construct). In most cases there were two bands with the bottom band corresponding to the expected sizes of the fusion proteins. The loading control for Rp3-CD137-8d lane appeared intense due to incomplete stripping of the anti-CD137 polyclonal used prior to the second use of the membrane to detect  $\alpha$ -tubulin.

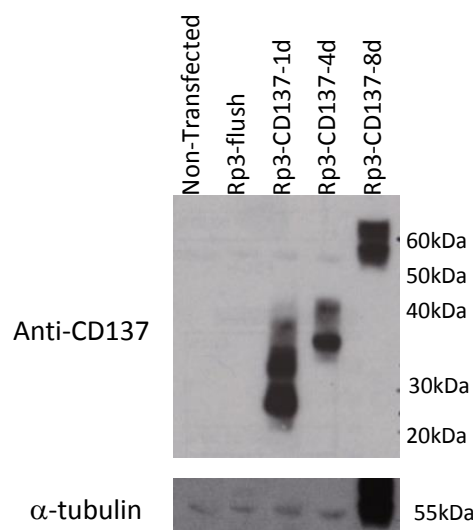


**Figure 3.21: Western Blot for Rp3-CD137 fusion proteins from transfected CHO-S cell lysates**

Whole cell lysates were taken from transfected CHO-S cells and used in a western blot to detect the CD137 scaffold. 10µg of lysate was loaded and separated under reducing conditions at a constant 100V. The protein was transferred to a nitrocellulose membrane, and was probed with anti-CD137 polyclonal antibody and detected with an anti-rabbit-Ig polyclonal.  $\alpha$ -tubulin was used as a loading control.

### 3.7 Chapter Discussion:

In this chapter, a series of fusion proteins were designed to assess the impact distance of antibody binding from the cell membrane has on effector mechanisms and their cell surface expression assessed. Cell surface expression and correct folding of the fusion proteins was confirmed using a panel of antibodies directed against the CD137 backbone. By testing the panel of SAP antibodies to detect CD137, the exact binding domains for each of the antibodies was able to be identified. The six anti-CD137 mAb employed were chosen based on the different abilities to bind the three and two domain CD137 constructs and in their ability to not block each other – therefore indicating unique epitopes within the CD137 scaffold.

The binding data obtained from the anti-CD137 antibodies binding the CD52-137 fusion proteins was different to that expected as presented in Figure 3.9b. The main difference between the two data sets was with the ability of antibodies to bind the second domain of CD137 (present in the wild type and CD137-3d construct). SAP3-23 and SAP3-26 were previously shown to bind the wild type and 2-domain protein only, whereas here they were also able to bind the CD52-137-3d construct (Figure 3.9). The conflict in data could indicate differences between the fusion proteins used. Originally, CD137 was truncated with no additional peptide attachment and then used to test antibody binding by flow cytometry. In this chapter, the truncated CD137 was generated, but further modified with an attachment of

a 12 amino acid peptide at the N-terminus. It is possible that this modification stabilised the truncated CD137 protein, which in turn allowed more/less antibody to bind compared to the original construct. This could be tested by repeating these experiments in 293F cells, where both the CD52-CD137 fusion proteins and CD137-truncated mutants were transfected in parallel and antibody binding assessed side-by-side by flow cytometry. This would allow a direct comparison between the potential variations in these proteins that would not be a consequence of experimental variation – such as fluorochrome intensity, batch variation between antibodies and transfection efficiencies.

The observation that SAP3-6 bound the membrane-proximal domain was important as this allowed for its use as an internal control between all of the constructs (except for the flush construct) facilitating the monitoring of the relative binding and expression of the 'functional' epitope to the complete fusion protein expression. The panel of six antibodies currently used can be reduced to four, one towards each extracellular domain, for the future screening of the CD137 fusion proteins; which are SAP1-3, SAP1-1, SAP3-23 and SAP3-6.

If we wanted to investigate the distance from the cell membrane using different epitopes within a protein, then we could compare the effector mechanisms engaged between SAP1-3 and SAP3-6 – which bind the most distal and proximal epitopes, respectively. Unfortunately this was not possible with these antibodies, as they have a mouse IgG1 heavy chain, which is poor at engaging the Fc mediated effector mechanisms, compared to the IgG2a isotype<sup>325</sup>. Similarly, this approach would need to take into account the differences in binding affinities each antibody has towards the antigen, thereby reducing the relevance of any data gained by this approach.

Originally the proposed proteins were to contain a modified CD52 peptide, identified by Hale *et al.*<sup>319</sup>, attached to a CD137 protein backbone. Unfortunately, the CD52 peptide was unable to be bound by the CAMPATH-1H antibody in this context. It was established that the site of peptide attachment within the fusion protein was accessible to CAMPATH-1H, and there were no steric interactions between the CD137 backbone and the CD52 peptide, precluding binding. Together, this information lead to the conclusion that the inability of CAMPATH-1H to bind the CD52-137 fusion proteins was a consequence of the CD52 peptide chosen and not the design of the fusion protein.

The previously published CD52 peptide was synthesised onto cellulose membranes in the absence of a cell. CAMPATH-1H binding was initially confirmed using an ELISA, and later the synthetic peptide was used as a competitor to block CAMPATH-1H binding to CD52<sup>+</sup> cells

assessed by flow cytometry<sup>319</sup>. These conditions did not assess the use of the peptide as part of a fusion protein, or whether being produced by a cell would work in the same manner. It is possible that the synthetic production of the peptide chain may have resulted in subtle conformational changes or aggregation, either in the orientation of the bonds or that the purification process resulted in alterations that were beneficial to CAMPATH-1 H antigen binding site interactions not possible in a cell-based system.

Given the failure to achieve cell surface binding, changes to the CD52 peptide could be attempted through site directed mutagenesis. As a part of the original work by Hale *et al.*, every amino acid in the last eight residues was switched for each of the other amino acids, in a plate based system, and changes in CAMPATH-1H binding recorded by ELISA<sup>319</sup>. It was concluded that the –SPS– motif was critical for all binding – any substitutions in these residues resulted in a loss of binding – but it was also observed that in other positions a number of substitutions still allowed binding (summarised in Table 3.4). As these were tested as single mutations, testing combinations of these potential amino acids could be applied to the CD52 in the fusion proteins within this project to test whether improvements in the CAMPATH-1H binding could be achieved. Interestingly, the cyclic Cp11 epitope used as a replacement matches the substitutions tested except for one (position 8 in Table 3.4), where it was reported that only Ala or Gly allowed binding.

CD52 peptide	S	Q	T	S	S	P	S	A	D
Alternative Substitution	Not Tested	Any except P	S	L or T	-	-	-	G	A C E F G I L N Q R S T V W Y
Cp11 peptide	C	G	S	T	S	P	S	S	C

**Table 3.4: Viable amino acid substitutions that allow CAMPATH-1H binding**

Table adapted from Hale, 1995<sup>319</sup>. At every position along the minimal CD52 peptide, the amino acid was substituted for each of the remaining 19 amino acids. Each peptide was synthetically produced and attached to a cellulose membrane. The membrane was then probed using CAMPATH-1H for evidence of binding using an ELISA protocol. The above table summarises the results for where a substitution did not impact CAMPATH-1H binding; - indicates no substitution could be tolerated.

The alternative cyclic epitopes for CAMPATH-1H and rituximab (Cp11 and Rp3, respectively) were discovered using phage display libraries. Structurally, both of these peptides fulfil the original requirement for the ‘functional’ epitope, as they allow the binding of clinically relevant antibodies that demonstrate engagement with the key effector mechanisms that will be

investigated (CDC, ADCP and ADCC), and due to the small size of the peptide, they do not interfere substantially with the final size of the protein.

In summary, fusion proteins consisting of a cyclic CAMPATH-1H epitope (Cp11) attached to different forms of human CD137 (flush (no extracellular CD137 present), 1, 4 or 8 domains) were successfully designed and generated. These proteins were able to be expressed transiently in 293F cells and detected by flow cytometry or western blot. To corroborate any functional results obtained, a complementary set of fusion proteins were also cloned, employing a cyclic epitope recognised by rituximab attached to the various CD137 constructs. These constructs were subsequently examined in functional assays in the next chapter.





## Chapter 4: *In vitro* functional assessment of fusion proteins

### 4.1 Expression of constructs in target cells for functional assays:

Fusion proteins containing either a CAMPATH-1H or rituximab epitope attached to a CD137 scaffold were previously generated and expressed in 293F cells (chapter 3). These proteins were subsequently used to assess what impact the distance between an antibody and the cell surface has on the depletion effector mechanisms engaged. CDC was the first mechanism investigated as research indicates that the distance of binding would most likely impact the complement system<sup>230,231</sup>. Work in this laboratory focusses on the use of anti-CD20 mAbs, including rituximab, and as a result we have access to a large range of isotype-switched versions of rituximab, allowing the best isotype to be selected for engagement on either human or murine effector systems. For this reason, constructs containing the CD20 epitope (Rp3-CD137-) were first explored and the CAMPATH-1H binding constructs (Cp11-CD137-) were used to corroborate the data generated.

### 4.2 Complement Dependent Cytotoxicity:

#### 4.2.1 293F cells as targets:

In order to test the effector mechanisms engaged by a mAb, a cell line that was able to express the fusion protein which was compatible with the *in vitro* assays was required. 293F cell line was derived from the adherent human embryonic fibroblast (HEK293) cell line into a suspension line able to grow in serum free media<sup>326</sup>. The 293F cells used previously were able to be transfected efficiently for all of the constructs cloned (Chapter 3) and so their suitability as targets in CDC assays was assessed. The four domain construct (Rp3-CD137-4d) was chosen to validate the assay, as this consistently produced the highest expression range, and was the least manipulated from the initial proteins, therefore ideal for use in defining the assay conditions.

CDC was assessed by recording the percentage of dead cells present after incubation of the target cells with human serum in the presence or absence of a mAb. The gating applied to the flow cytometry data in order to calculate the percentage of complement-dependent cell death is presented in Figure 4.1. Initially, cells were gated on the FSC and SSC to exclude debris and contaminants (Gate 1). This gate was applied to a sample with no PI added, in order to define

the population that refers to viable cells (i.e. PI negative) or dead cells (PI positive). After these populations were set, serum treated samples had PI added and were acquired on the flow cytometer. To analyse the data, the basal level of cell death – defined as the percentage cell death in the absence of human serum (Figure 4.1c) – was removed from all data sets, and re-calculated to 100% using the equation in Figure 4.1e.

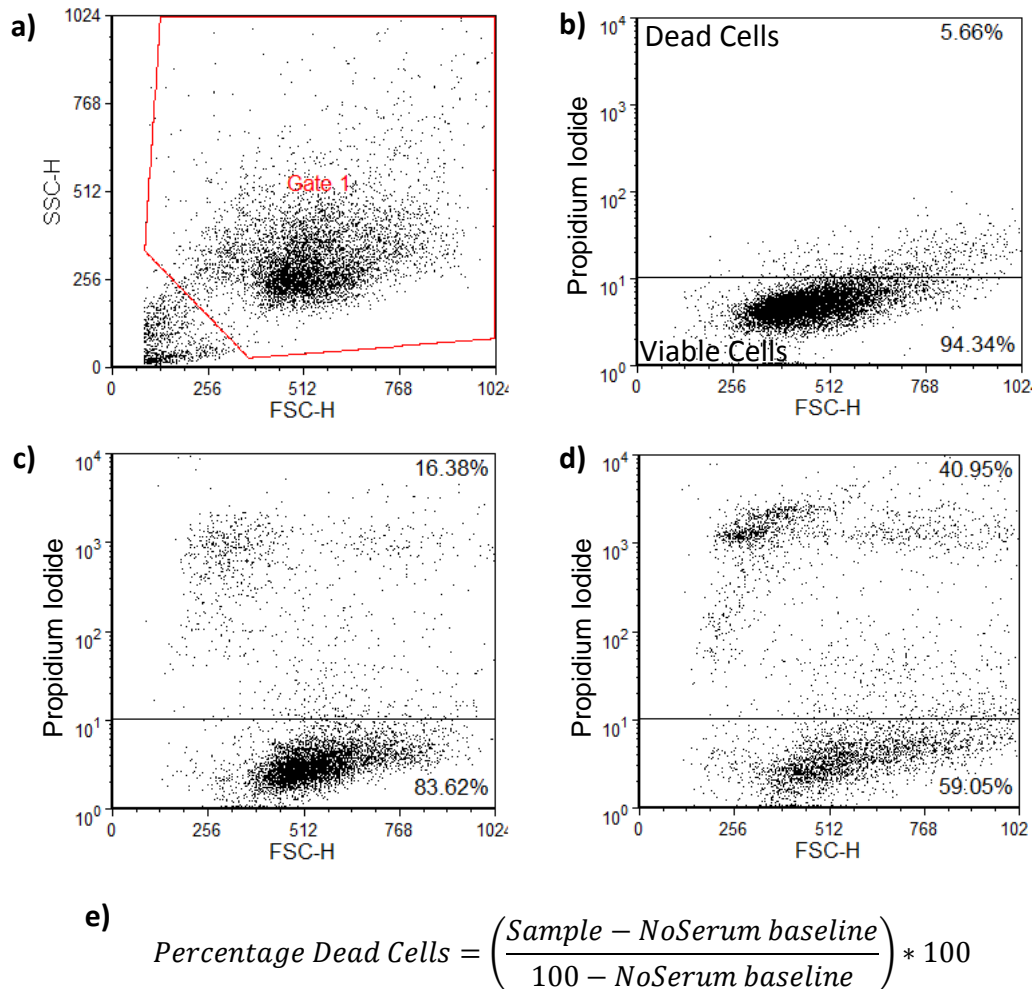


**Figure 4.1: Gating used to analyse flow cytometry data from CDC assay.**

293F cells transfected with Rp3-CD137-4d were incubated with human serum for 30 minutes at 37°C. After serum incubation the serum dependent cell death was assessed by flow cytometry using the following strategy. a) Gate 1 is set to contain all cells but exclude cellular debris based on the FSC/SSC profile and applied to all future plots. b) Cells in Gate 1 were then plotted against the FL2 channel in order to define the PI negative cell population using a sample with no PI added. c) The percentage cell death (defined as PI<sup>+</sup>) of cells incubated in media alone was recorded in order to define the No Serum baseline. d) The percentage cell death of 293F cells incubated with 10% (v/v) human serum was plotted. e) Finally the percentage of dead cells was calculated using the equation to remove the basal cell death in the absence of any serum and readjust to 100% so that only complement dependent cell death was assessed.

A titration of serum concentration was carried out on transfected Rp3-CD137-4d 293F cells in order to determine the optimum serum concentration which provided the best antibody-

dependent lysis and minimal non-specific lysis from the Alternative pathway. A serum titration between 0% and 10% serum (v/v) was performed as presented in Figure 4.2. Although the 293F cells were able to be transfected efficiently, they were sensitive to human complement present in the serum resulting in relatively high levels of death in the absence of antibody opsonisation. This sensitivity to the alternative complement pathway made the 293F cells unsuitable targets for use in the CDC assay.

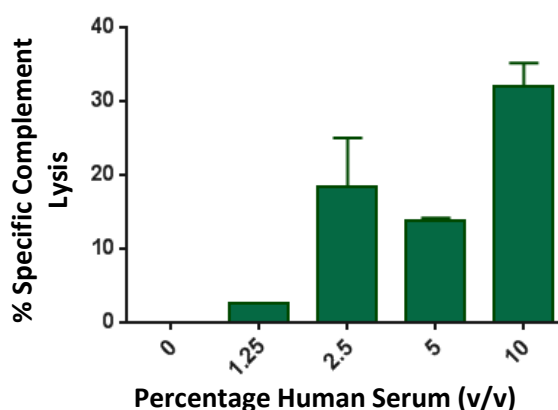


**Figure 4.2: Serum titration of Rp3-CD137-4d transfected 293F cells.**

293F cells were transfected with Rp3-CD137-4d construct for 24 hours. Transfected cells were then incubated with different concentrations of freshly thawed human serum (v/v) for 30 minutes at 37°C. 1 µg/mL of PI was added to each sample prior to data acquisition in order to discriminate between dead and live cells. The data was analysed as presented in Figure 4.1; the mean and range of duplicate results from a single assay plotted.

#### 4.2.2 CHO-S as target cells:

Since 293F cells were sensitive to human serum, CHO-S cells were investigated as an alternative cell line. CHO-S cell line, purchased from Invitrogen, are a derivative of the adherent Chinese Hamster Ovarian (CHO) cell line<sup>327</sup>. Having undergone a similar culturing process to the 293F cells, CHO-S cells have been selected for culture in a serum-free system and in suspension rather than maintain the adherent characteristics of the parental cell-line. As a result of these adaptations, these cells are able to produce high protein expression using a lipid based transfection system<sup>328</sup>. A serum titration was performed on CHO-S cells transfected with a vector control (pcDNA3.1/-) to test their resistance to the Alternative complement pathway. A serum titration between 0% and 20% was performed using the same analysis described previously (Figure 4.1), and the results are presented in Figure 4.3. It was seen that above 7.5% serum there was little change in the basal level of cell death. 15% human serum was chosen for subsequent assays as this concentration would reduce any batch variations in terms of active complement present.

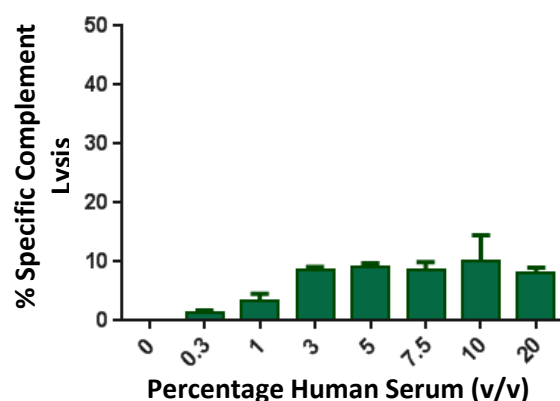


**Figure 4.3: Serum titration of pcDNA3.1/- transfected CHO-S cells.**

CHO-S cells were transfected with empty pcDNA3.1/- vector for 24 hours. Transfected cells were then incubated with different concentrations of freshly thawed human serum for 30 minutes at 37°C. 1µg/mL of PI was added to each sample prior to data acquisition in order to discriminate between dead and live cells. The data was analysed as previously presented in Figure 4.1, the mean and range of duplicate results from a single assay plotted.

CHO-S cells were largely resistant to lysis from the alternative complement pathway, so the ability of these cells to express the Rp3-CD137 fusion proteins was next assessed. The cells were transfected with Rp3-flush, -1d, -4d and -8d for 36 hours and protein expression was assessed by flow cytometry using rituximab-FITC to detect the Rp3 peptide. Figure 4.4 shows the expression profiles obtained confirming that all of the Rp3-CD137 fusion proteins were able to be expressed on the surface of CHO-S cells, and at similar levels to each other.

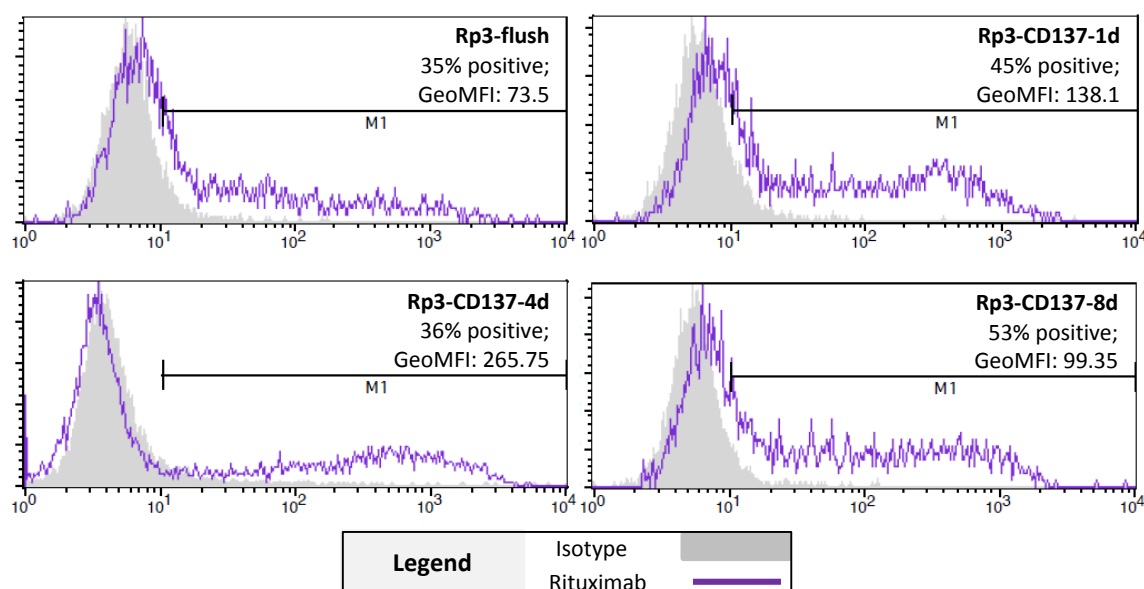


**Figure 4.4: Rp3-CD137 constructs expressed in CHO-S cells.**

CHO-S cells were transfected with the Rp3-CD137 fusion proteins for 36 hours and protein expression was confirmed by flow cytometry, using FITC labelled rituximab to bind the Rp3 peptide. The percentage of positive cells binding rituximab (above the isotype control) and the geometric mean fluorescence intensity (GeoMFI) is recorded for each histogram.

### 4.2.3 Optimising CDC assay:

To optimise the CDC assay conditions for use with these cells, CHO-S cells were transfected with the Rp3-CD137-4d construct for 36 hours prior to analysis. The target cells were opsonised with different concentrations of rituximab (1 in 5 dilutions between 10 $\mu$ g/mL and 0.0032 $\mu$ g/mL) or 10 $\mu$ g/mL of an isotype control mAb (CAMPATH-1H) for 15 minutes prior to the addition of 15% human serum (v/v) for 30 minutes. Flow cytometry data was analysed using the gating strategy presented in Figure 4.1; however the basal cell lysis was defined as the percentage cell death after incubation with 15% serum but in the absence of any antibody. Replicate data from the assay is presented in Figure 4.5. A dose dependent response to antibody concentration was observed with CHO-S cells transfected with Rp3-CD137-4d that was consistent between the duplicate data points collected within the assay. This confirmed that using 15% human serum with cells transfected for 36 hours was a suitable condition for this assay as a clear increase in antibody-mediated cell death was visible above the basal level of cell death.

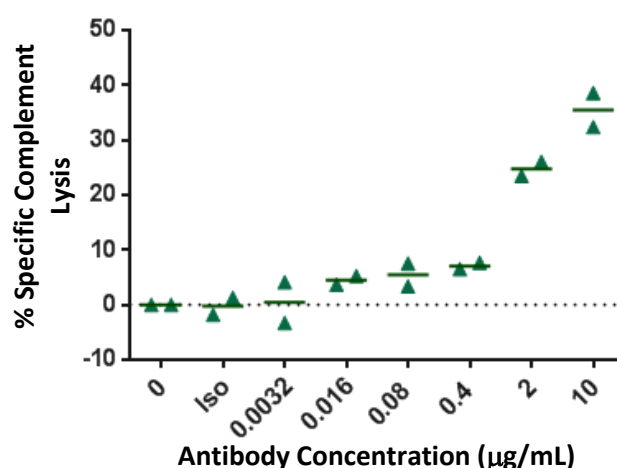


**Figure 4.5: Rp3-CD137-4d transfected CHO-S cells produce an antibody dependent response in CDC assay.**

CHO-S cells were transfected with Rp3-CD137-4d construct and used as targets. The cells were opsonised with varying concentrations of rituximab for 15 minutes at room temperature. 15% human serum was then added to the cells and incubated at 37°C for 30 minutes. The data was analysed as previously described in Figure 4.1. The mean and individual points are plotted from a single experiment.

To provide further confirmation that the dose dependent killing reported in Figure 4.5 was complement dependent, Rp3-CD137-4d transfected CHO-S cells were treated with 10µg/mL rituximab (saturating level) and the serum concentration was titrated. As presented in Figure 4.6, the total amount of cell death diminished as the serum concentration was reduced, confirming that the cell death reported is both dependent on the antibody and human serum being present, and was not a consequence of an alternative depletion mechanism – such as the Alternative complement pathway or direct cell death.

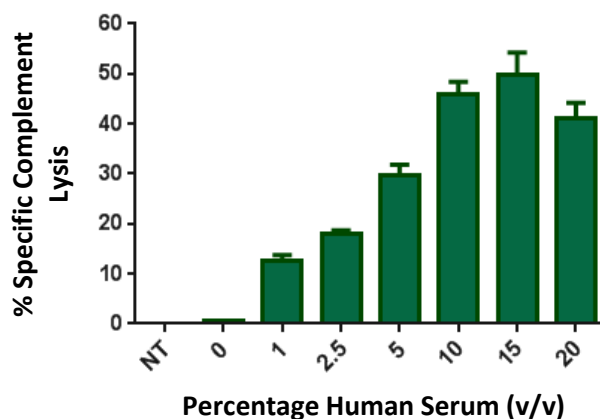


**Figure 4.6: Serum titration of Rp3-CD137-4d transfected CHO-S cells opsonised with rituximab**

CHO-S cells transfected with Rp3-CD137-4d were opsonised with 10µg/mL rituximab, and cultured for 30 minutes at 37°C with different concentrations of human serum. NT refers to transfected CHO-S cells that have no antibody or serum added, to define the basal level of cell death. The mean and range of duplicate results from a single experiment are plotted.

Having validated the assay for the CHO-S cells, these cells were transfected with Rp3-CD137-flush, -1d, -4d or -8d construct for 36 hours in order to assess the CDC engagement of each construct. The transfection efficiency was recorded, by measuring the percentage of cells that bound rituximab compared to an isotype control (as seen previously in Figure 4.4). Transfected cells were then used as targets in the CDC assay conditions described previously. There was high variation in the transfection efficiency between each assay; although the transfection efficiency between constructs within an assay was similar (Figure 4.7). This demonstrated that although the results seen between constructs within an assay were comparable, a form of normalisation was required in order to compare between independent assays.

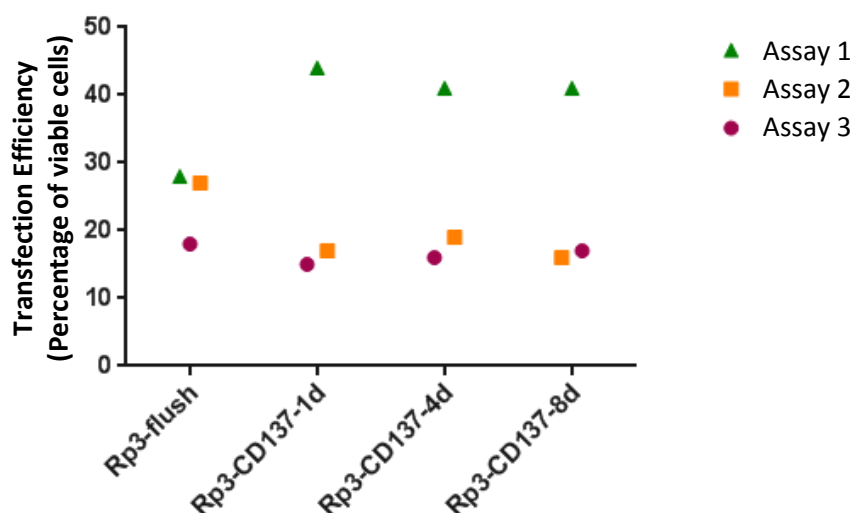
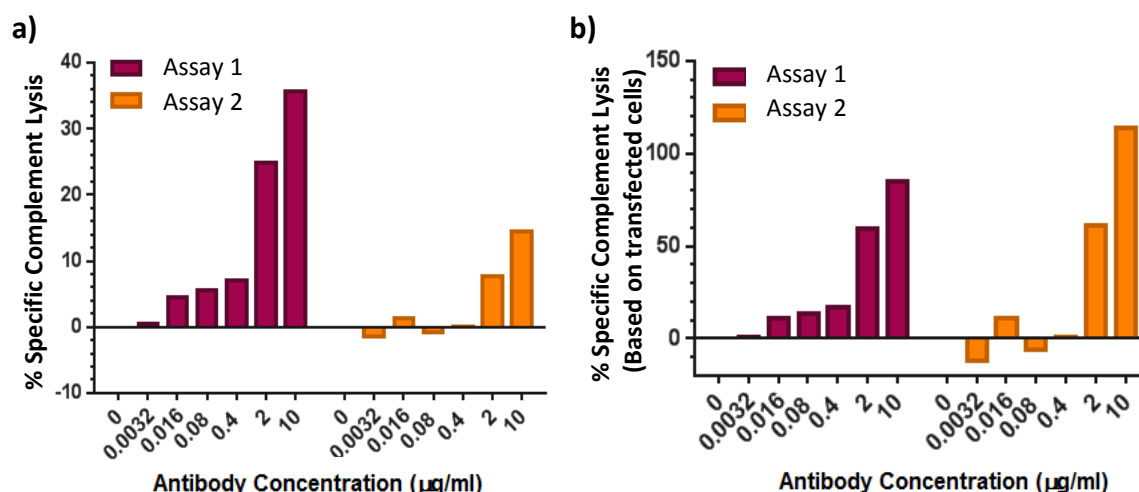


**Figure 4.7: Transfection efficiency for CHO-S cells with each of the Rp3-CD137 fusion proteins.**

CHO-S cells were transfected for approximately 36 hours prior to protein expression. Transfection efficiency defined as the percentage of viable cells that bind 10 $\mu$ g/mL rituximab-FITC. Each point represents an individual transfection.

In order to compare between individual assays, the proportion of rituximab-binding cells present on the day of experimentation was used to relate the percentage cell death to the percentage of transfected cells. For example, in assay 1 presented in Figure 4.8a the maximum cell death recorded was 36%, and within this cell population 42% of cells were able to bind rituximab. Therefore, knowing that the assay is target specific, using the equation in Figure 4.8c the percentage of dead cells can be converted into a percentage of transfected cells, in this case 85% of transfected cells were lysed. The adjustment did not alter the trend for each individual assay, but allowed datasets collected from independent transfections to be displayed on the same axis for straightforward inter-assay comparison (Figure 4.8b).



**c)** 
$$\text{Adjusted \% Specific Complement Lysis} = \left( \frac{\% PI^+ \text{ Cells}}{\% Transfected \text{ cells}} \right) * 100$$

**Figure 4.8: Normalisation of data to allow inter-assay comparison**

CHO-S cells were transfected with Rp3-CD137-4d and used in a CDC assay. a) Removal of the background alone using the analysis described previously (Figure 4.1e) did not take into account the variations between transfection efficiencies; for example, 41% of viable cells were transfected in assay 1, whereas only 14% were transfected in assay 2. b) By accounting for the transfection efficiency (using the equation in c)) it was clear that only the transfected cells were lysed, allowing a more consistent comparison between individual assays to occur. Normalising the data in this manner did not change the trend seen within each individual assay, but allowed both data sets to be compared on the same axis.

All of the fusion proteins were tested in parallel for each independent assay thereby reducing the experimental variation across the complete dataset. In total three independent transfections of CHO-S cells were performed for each fusion protein, and the mean of each assay was calculated and plotted in Figure 4.9. The trends observed were the same within each independent experiment. Statistical significance was assessed for the results at 10ug/mL using a t-test, where a p-value <0.05 was deemed significant.



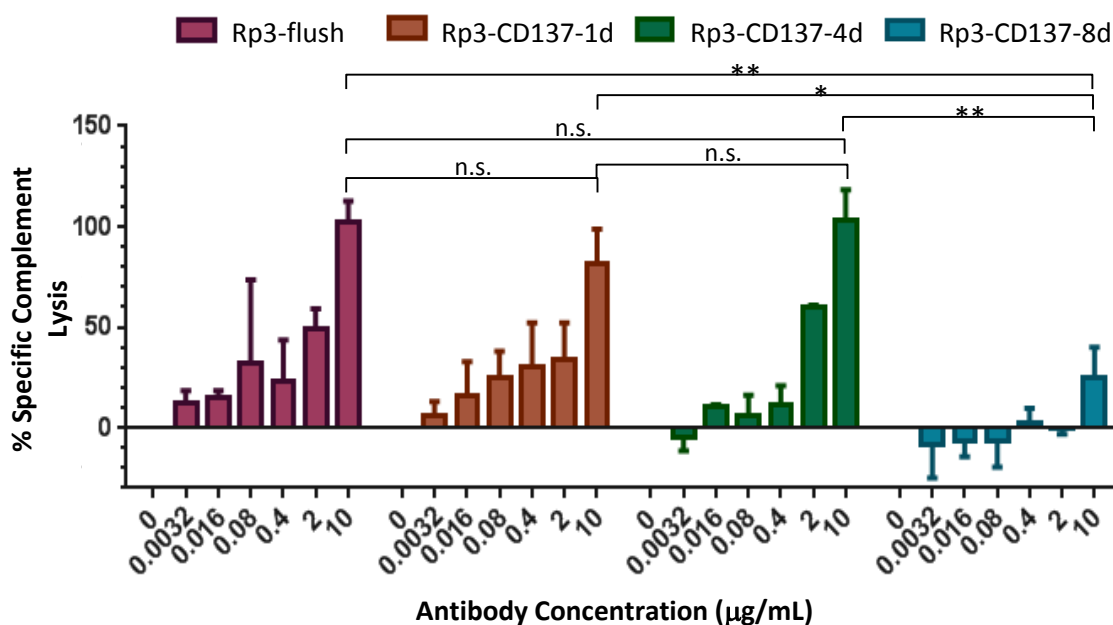


**Figure 4.9: Collated CDC assay results from CHO-S transfected cells after rituximab opsonisation.**

CHO-S cells were transfected with Rp3-CD137 fusion proteins for 36 hours prior to CDC assay. Cells were opsonised at room temperature with different concentrations of rituximab and co-cultured with 15% human serum for 30 minutes at 37°C. The percentage cell death was related to the individual transfection efficiencies as previously discussed Figure 4.8c. The graph presents the mean and standard deviation of three independent experiments. Statistical significance was assessed using an unpaired t test where \* =  $p < 0.05$ , \*\* =  $p < 0.005$ , n.s. = not significant.

The largest construct (Rp3-CD137-8d) was unable to lyse all of the transfected cells present, with a maximum cell death of 30% observed at the highest concentration of antibody only (10 µg/mL). The poorer CDC response was statistically significant at both 10 µg/mL and 2 µg/mL of rituximab when compared to the other three constructs (using an unpaired t test). Conversely, the 1 domain and membrane bound epitope (Rp3-CD137-1d and Rp3-flush, respectively), were best able to lyse all of the transfected cells, even at lower concentrations of antibody (below 0.4 µg/mL) compared to the Rp3-CD137-4d construct. Together these data suggested that the smaller constructs, those where the antibody bound closest to the cell membrane, were able to elicit more potent killing by complement.

### 4.3 Phagocytosis assay:

Having established that there was a difference in the ability of rituximab to engage CDC based on the different target constructs, ADCP was next investigated as the second depletion mechanism for mAb immunotherapy. For the assessment of phagocytosis macrophages were differentiated from the bone marrow of wild type C57BL/6 mice, in the presence of L929 conditioned media for 8 days. Over this time the morphology of the cells changed from small circular suspension cells to elongated adherent cells – light microscope images following these

changes are provided in Figure 4.10a. The macrophages were defined as F4/80 positive, and the expression of the mouse Fc $\gamma$ R are presented for reference, for this example, the BMDM expressed low levels of all receptors (Figure 4.10b).

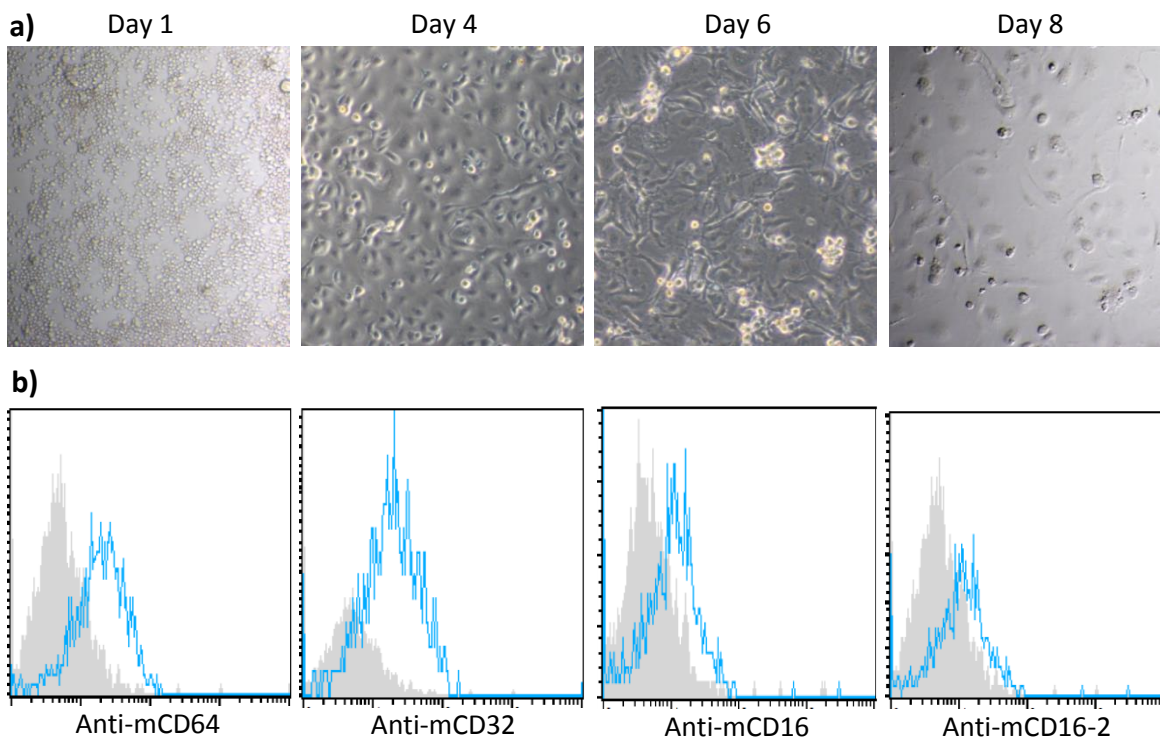


**Figure 4.10: BMDM differentiation from mouse bone marrow**

Bone marrow was collected from the hind legs of WT C57BL/6 mice and cultured for 7 days in 20% L929 conditioned RPMI media. a) Light microscope images of cells at 10X magnification was taken to monitor the morphological changes from small suspension cells at Day 1 to elongated adherent cells at Day 6. On Day 7 the BMDM were replated into 96-well plates and used on Day 8. b) On day of analysis, BMDM were removed from the plate using a cell scraper and phenotyped in order to confirm the expression of the mouse Fc $\gamma$ R using FITC-conjugated F(ab')<sub>2</sub>.

In brief, the phagocytosis assay involved labelling transfected CHO-S cells with the fluorescent green dye, CFSE. These cells were opsonised with varying concentrations of rituximab before co-culturing at a 5:1 Target:Effector (T:E) ratio. The antibodies used in this assay had a mouse-IgG2a isotype in order to best interact with the mFc $\gamma$ R present on the BMDMs. The BMDMs were labelled with an anti-F4/80-APC antibody to identify them from the CHO-S cells, and the percentage of phagocytosis was assessed by flow cytometry – defined as the percentage of macrophages also displaying CFSE-positivity (% dual F4/80<sup>+</sup>CFSE<sup>+</sup> cells) (Figure 4.11).

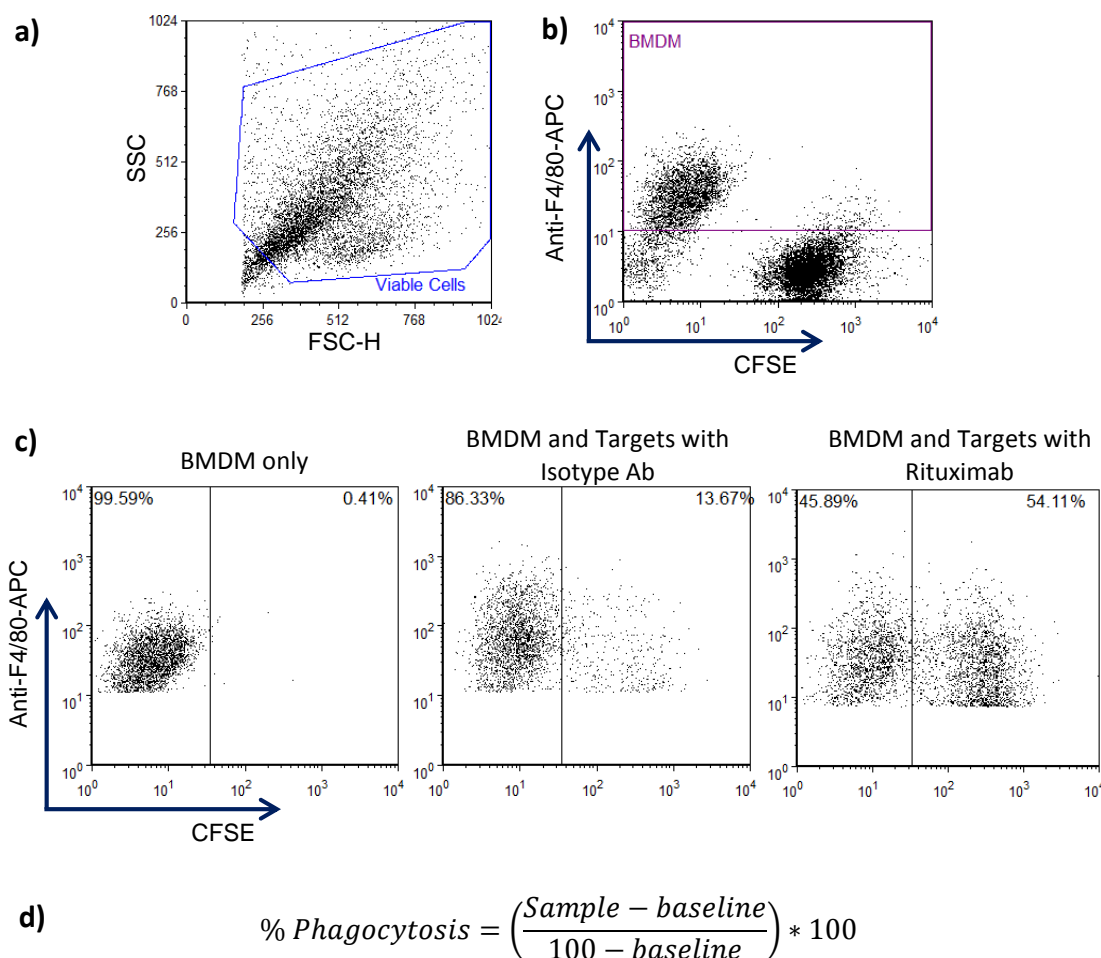


**Figure 4.11: Gating used to analyse flow cytometry data collected from ADCP assay**

CHO-S cells transfected with Rp3-CD137-4d were labelled with 5 $\mu$ M CFSE and opsonised with 10 $\mu$ g/mL rituximab-mIgG2a for 30 minutes at 4°C. The cells were co-cultured in a 96-well plate with BMDM at a 5:1 ratio for 1 hour. The samples were stained with APC-conjugated-anti-F4/80 to identify the BMDM and phagocytosis was assessed by flow cytometry. The analysis of the flow cytometry data is presented above: a) Cells were gated based on FSC/SSC profile to remove cellular debris. b) BMDMs and target cells – without co-culture – were used to set the BMDM gate (defined as F4/80<sup>+</sup> cells). c) BMDMs alone were used to define the phagocytosed and non-phagocytosed cell populations, with an example plot of Isotype treated cells and rituximab treated cells presented. The percentage of cells in for each population was used to define the amount of phagocytosis, based on the F4/80<sup>+</sup>CFSE<sup>+</sup> population. d) The equation used to remove the basal level of phagocytosis – defined as the uptake of CFSE labelled target cells in the absence of antibody opsonisation.

Typically, these assays were designed and optimised to measure the phagocytosis of lymphocytes. Since CHO-S cells are much larger in comparison it was hypothesised that they may take longer to phagocytose than smaller lymphocytes. In order to optimise the assay for CHO-S cells, a co-culture experiment was first performed to define the optimum length of time for transfected cells to be consistently phagocytosed, without increasing non-specific phagocytosis. CHO-S cells, transfected with Rp3-CD137-4d, were opsonised with 10 $\mu$ g/mL rituximab, and left for 30, 60 or 90 minutes with BMDM at a 5:1 T:E ratio. Figure 4.12 shows that the percentage phagocytosis significantly increased from 30 to 60 minutes but there was

little change between 60 and 90 minutes, therefore a 60 minute co-culture was used in subsequent assays.

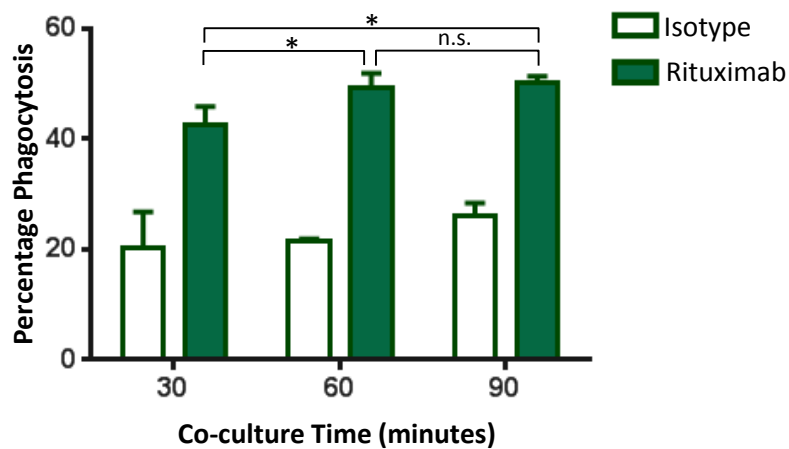


**Figure 4.12: Effect of incubation time on the phagocytosis of Rp3-CD137-4d transfected CHO-S cells.** CHO-S cells were transfected with Rp3-CD137-4d and labelled with the fluorescent dye CFSE. These cells were then opsonised with either 10µg/mL rituximab-mIgG2a or an isotype control for 30 minutes at 4°C. The cells were then co-cultured with BMDM at a 5:1 E:T ratio and incubated for 30, 60 or 90 minutes at 37°C. The BMDMs were subsequently labelled with APC-conjugated anti-F4/80. Percentage phagocytosis was assessed by flow cytometry as previously described (Figure 4.11). The mean and standard deviation (SD) of triplicate results from a single experiment are plotted, and statistical significance was assessed using an unpaired t test where \* = p<0.05 and n.s. = non-significant

Following the establishment of this protocol, Rp3-CD137-4d transfected cells were used to check the dose dependency of the assay. To assess this, the cells were incubated with varying concentrations of rituximab during the opsonisation step. They were added to the BMDMs at a 5:1 ratio and co-cultured for 60 minutes before phagocytosis was measured by flow cytometry. Triplicate samples were plotted within this assay and show good reproducibility within the experiment (Figure 4.13).

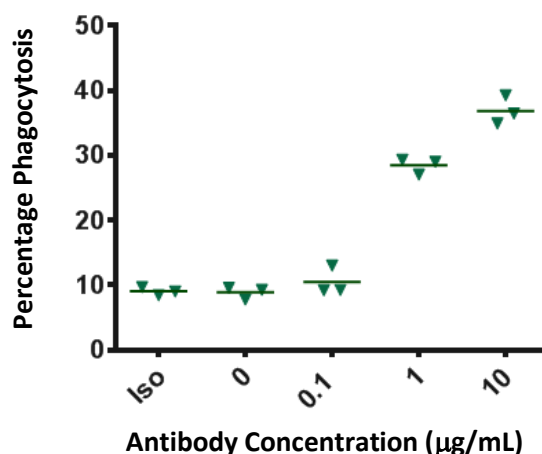


**Figure 4.13: Dose dependent phagocytosis assay using CHO-S cells transfected with Rp3-CD137-4d construct.**

Rp3-CD137-4d transfected CHO-S cells were labelled with 5µM CFSE and opsonised with varying concentrations of rituximab-mIgG2a or an isotype control mAn (ISO) for 30 minutes at 4°C. The cells were co-cultured at 5:1 ratio with BMDM for 60 minutes at 37°C. Flow cytometry was performed to assess phagocytosis using the gating strategy defined in Figure 4.11.

Three independent experiments were performed with the mean phagocytosis plotted for all of the constructs (Figure 4.14). This data has had the background removed – defined as phagocytosis seen in the absence of antibody opsonisation using the equation in Figure 4.11c – but not related to the transfection efficiency. The same trend was seen across all three independent experiments. Rp3-flush was statistically poorer at being phagocytosed compared to the other fusion proteins at saturating concentrations of rituximab. Rp3-CD137-1d, -4d and -8d were able to engage ADCP at 10µg/mL of rituximab but for Rp3-CD137-8d its susceptibility to ADCP was diminished at 1µg/mL, however this was not statistically significant when compared to the phagocytosis seen at 1µg/mL for both Rp3-CD137-1d and -4d constructs.

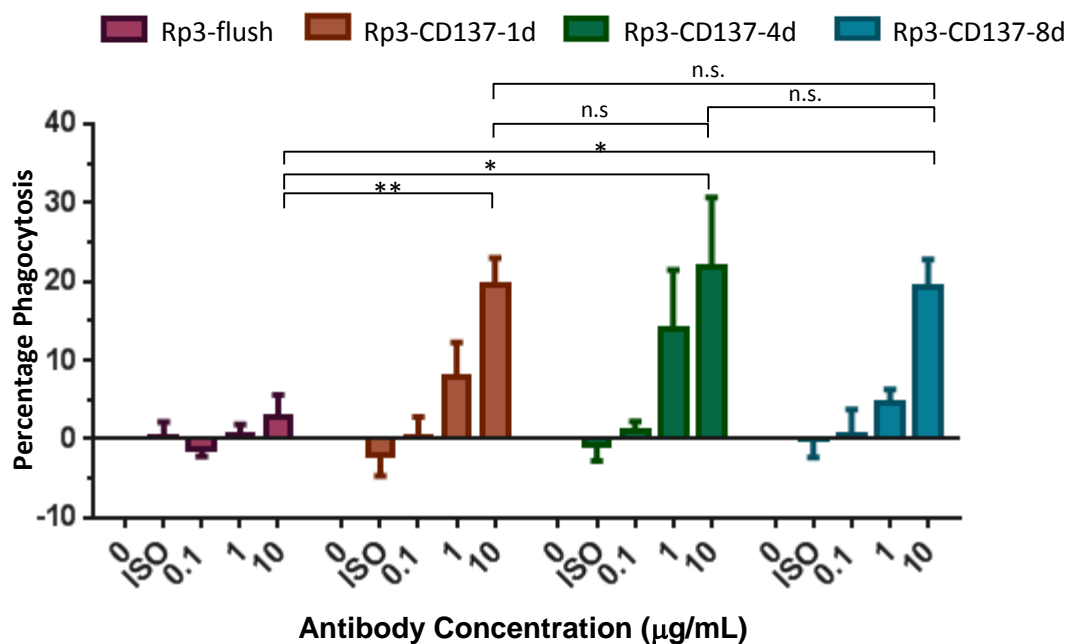


**Figure 4.14: Collated ADCP assay results from CHO-S transfected cells after rituximab opsonisation.** CHO-S cells were transfected with Rp3-CD137 fusion proteins for 36 hours. Transfected cells were labelled with 5µM CFSE and opsonised with rituximab-mIgG2a (0.1, 1 or 10µg/mL) or 10µg/mL isotype control mAb (ISO). These cells were then co-cultured at a 5:1 T:E ratio with BMDM for 1 hour at 37°C. Phagocytosis was measured by flow cytometry as previously described (Figure 4.11). The mean of three independent experiments are plotted. Statistical significance was assessed using an unpaired t test, \* =  $p < 0.05$ , \*\* =  $p < 0.005$ , n.s. = not significant.

#### 4.4 ADCC assay:

The final effector mechanism investigated was ADCC using human PBMC as effectors. As before the Rp3-CD137-4d construct was used to optimise the assay. Transfected CHO-S cells were labelled with the cytoplasmic dye calcein-AM, followed by opsonisation with diluting concentrations of rituximab. The human IgG1 version of the antibody was used in order to best engage the FcγR present on the surface of the NK effector cells. Human PBMC isolated from platelet-depleted whole blood was used as a source of effector cells – these cells contain a mixed population consisting predominantly of monocytes, B, T and NK cells. The target cells were co-cultured with PBMC at a 50:1 E:T ratio; this ratio was chosen as it would be the equivalent to a 5:1 NK:Target ratio deemed necessary through previous work within the group<sup>271</sup>. Cytotoxicity was measured by measuring the fluorescence of calcein-AM released into the culture supernatant compared to the maximum release possible - defined as the calcein-AM released in the presence of 4% Triton-X100 solution.

Each condition was performed in triplicate, in order to assess variability within the assay as presented in Figure 4.15a. The replicates were consistent, providing confidence in the ability

of the PBMCs to kill the cells. The fluorescence units recorded were converted into the percentage of maximum lysis and presented in Figure 4.15b.

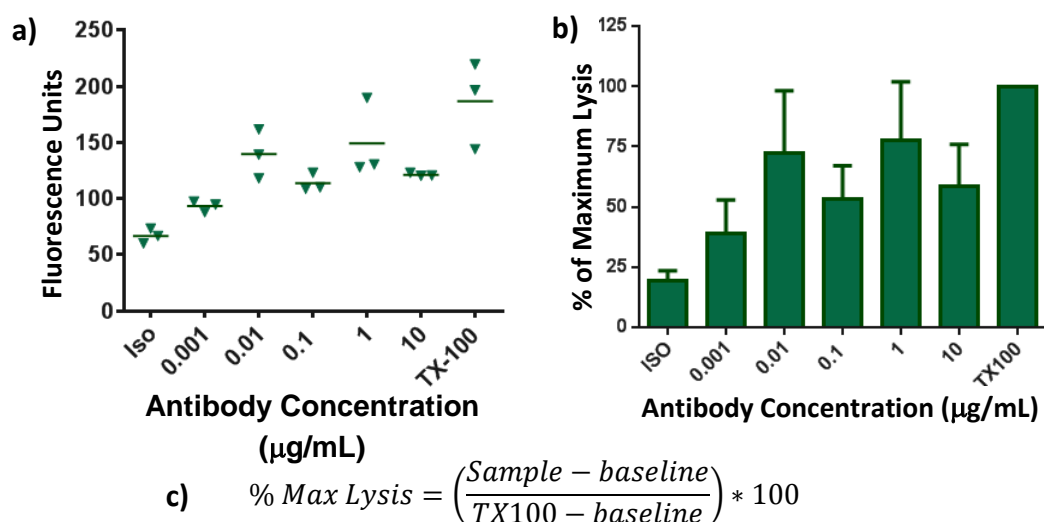


**Figure 4.15: Analysis of ADCC assay data from fluorescence units into percentage of maximum lysis**

CHO-S cells were transfected with Rp3-CD137-4d for 24 hours. Transfected cells were labelled with calcein-AM and diluting concentrations of rituximab before co-culturing at 50:1 E:T ratio with human PBMC. Calcein release from lysed cells into the culture supernatant was measured using an excitation wavelength of 485nm and emission wavelength of 530nm using a Varioskan Flash (Thermo Scientific) to record calcein release. a) The fluorescence units of triplicate data points assessed from a single assay were plotted. b) The fluorescence units were converted into % Maximal lysis using the equation in c) where the calcein release of cells treated with 4% Triton-X100 (TX100) was used to define total lysis. The baseline was defined as the calcein released from target cells in the absence of antibody. The mean and SD of three experimental repeats from a single assay are plotted.

From this data, it was seen that a titration in response to the antibody concentration could be achieved; however, it was a very sensitive assay where not much antibody binding was required to mediate cell death. This observation matches that seen by other groups who have investigated ADCC ability of mAbs<sup>249,271</sup>. Using the assay conditions defined above, the ADCC assay was performed with CHO-S cells transfected with Rp3-CD137-flush, -1d, -4d and -8d constructs. The result of three independent assays was presented in Figure 4.16.

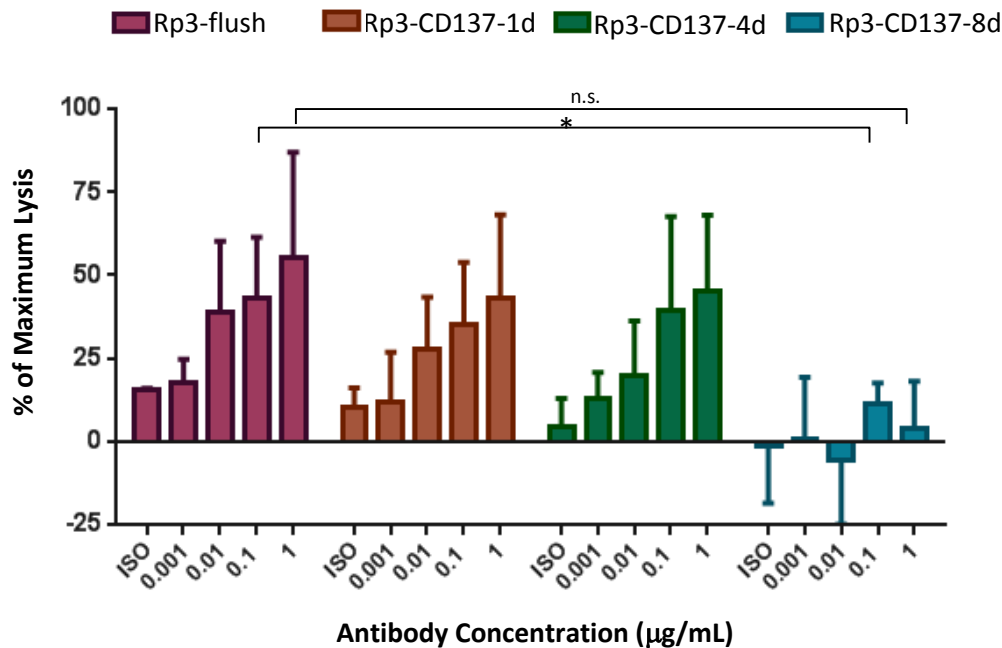


**Figure 4.16: ADCC results for CHO-S cells transfected with Rp3-CD137 fusion proteins**

CHO-S cells were transfected with the Rp3-CD137 fusion proteins 24 hours prior to the assay. The CHO-S target cells were labelled with Calcein-AM and diluting concentrations of rituximab (or 1 µg/mL isotype control) for 30 minutes at 4°C before co-culturing at 37°C with PBMC at 50:1 E:T ratio for 4 hours. Calcein released into the culture supernatant was measured and converted to % Maximal Lysis using Triton-X100 treated cells to define the maximum possible calcein released. The mean and standard deviation of three independent experiments were presented. Statistical significance was assessed using an unpaired t test, \* =  $p < 0.05$ , \*\* =  $p < 0.005$ , n.s. = not significant.

The combined data sets suggest a similar trend to that seen for CDC; that the further away from the cell membrane the antibody binds; the less able it is to engage ADCC. At 0.1 µg/mL there was a statistical significance between cells transfected with Rp3-flush and Rp3-CD137-8d, however at all other concentrations this was not the case. This is most likely due to the variation in maximum lysis achieved between the individual assays, due to the variability in donor PBMCs, even though the trend between the constructs was the same within each assay. This was the opposite trend to that seen for the other FcγR-dependent mechanism, ADCP.

## 4.5 Corroborating datasets – Alternative Antibody:Epitope

Up to this point all of the data presented demonstrates that the depletion mechanisms engaged by a mAb can be altered by the distance an antibody binds from the cell surface. The results so far have used a CD20 epitope and rituximab as the functional mAb. To confirm that the results presented can be applied to antibodies in general, and not specifically to rituximab, a second antibody:epitope pair was chosen. The anti-CD52 antibody CAMPATH-1H was selected as detailed in Chapter 3 using the Cp11 epitope engineered onto the various CD137



scaffolds. Using the same assay conditions established previously for CDC, ADCP and ADCC, CHO-S cells were transfected with the Cp11-CD137 fusion proteins and assessed.

Assessment of CDC for CHO-S cells expressing the Cp11-CD137 constructs is presented in Figure 4.17. It can be seen that the ability to effectively mediate CDC was diminished when targeting Cp11-CD137-8d construct, only partial death was achieved at saturating antibody concentrations. At 2 µg/mL there was a statistically significant difference between Rp3-flush and Rp3-CD137-1d when compared to the Rp3-CD137-8d construct, although the trend at 10 µg/mL looks the same this did not reach significance using a t test. This data corroborates the data previously obtained with the rituximab binding constructs, thereby concluding that CDC can be diminished when targeting an epitope far from the cell membrane.

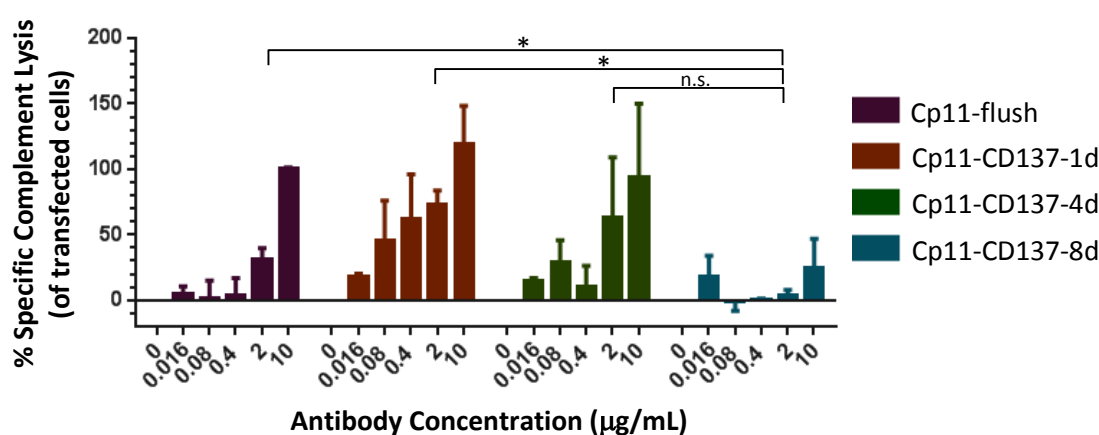


**Figure 4.17: CDC Assay Results for CHO-S cells transfected with Cp11-CD137 fusion proteins.**

CHO-S cells were transfected with the Cp11-CD137 constructs (previously generated in Chapter 3) and tested in the CDC assay optimised for CHO-S cells. Transfected CHO-S cells were opsonised with diluting concentrations of CAMPATH-1H for 15 minutes at room temperature before co-culturing with 15% human serum for 30 minutes at 37°C. Antibody mediated cell death was recorded by flow cytometry using the analysis template outlined in Figure 4.1. The mean and SD of three independent experiments are plotted. Statistical significance was assessed using an unpaired t test, \* =  $p < 0.05$  and, n.s. = not significant.

Mouse BMDM were used as effectors to assess the susceptibility of the Cp11-CD137 constructs towards phagocytosis. CAMPATH-1H antibody (which has a human IgG1 isotype) was used to opsonise the target cells as there was no mouse-IgG2a isotype available. However, previous work has demonstrated that antibodies with a human IgG1 heavy chain are able to engage the mouse FcγR present on the cell surface<sup>271</sup>. The data in Figure 4.18 once again indicates a similar trend to that seen previously in Figure 4.14, where targeting the membrane proximal epitope (Cp11-flush) was unable to effectively engage ADCP compared to the fusion proteins that lie further away from the membrane.

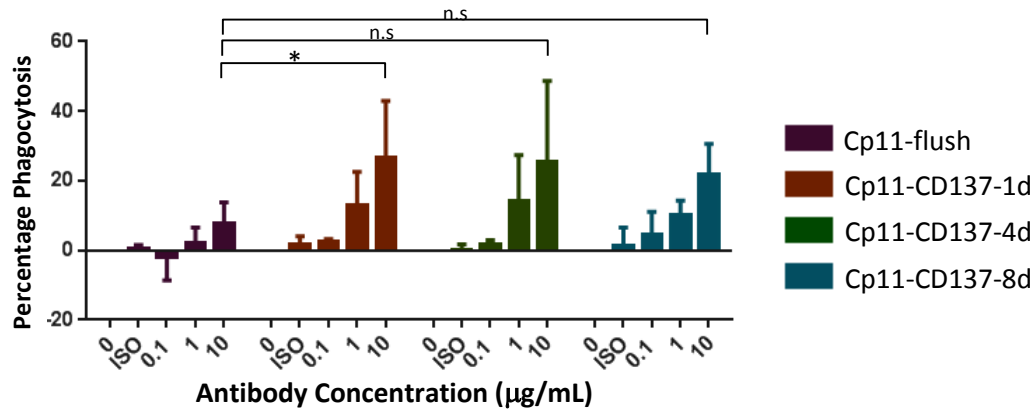


**Figure 4.18: ADCP Assay Results for Cp11-CD137 constructs in CHO-S cells**

CHO-S cells were transfected with Cp11-CD137 fusion proteins for 36 hours. Transfected cells were labelled with 5µM CFSE and opsonised with CAMPATH-1H (0.1, 1 or 10µg/mL) or 10µg/mL isotype control mAb (ISO). These cells were then co-cultured at a 5:1 T:E ratio with BMDM for 1 hour at 37°C. Phagocytosis was measured by flow cytometry as previously described (Figure 4.11). The mean and SD of three independent experiments are plotted. Statistical significance was assessed using an unpaired t test, \* =  $p < 0.05$  and, n.s. = not significant.

Lastly, to complete the data set, CHO-S cells expressing the Cp11-CD137 fusion proteins were tested in the ADCC assay using human PBMC as the effector cells. The ADCC data presented in Figure 4.19 shows a similar trend compared to that seen with Rp3-Cd137 constructs (Figure 4.16). Here, targeting the Cp11-Cd137-8d construct resulted in a diminished engagement of ADCC supporting the observation that effective cell lysis requires an antibody to bind relatively close to the cell membrane.

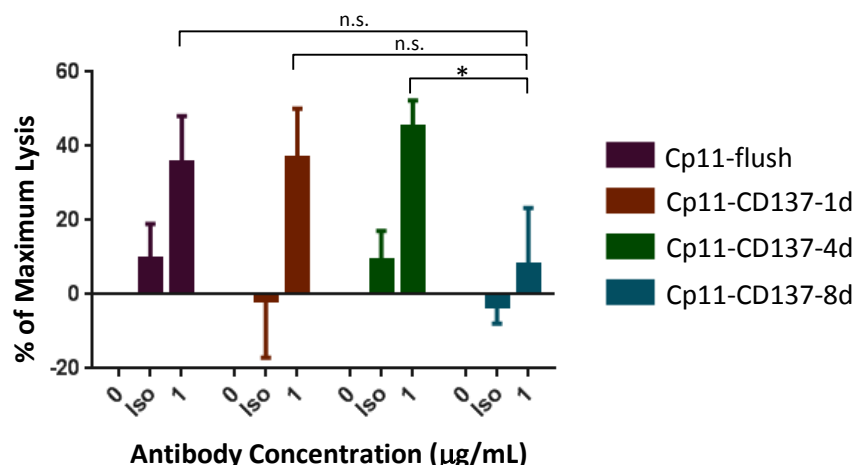


**Figure 4.19: ADCC Assay results for Cp11-CD137 transfected CHO-S cells**

CHO-S cells were transfected with the Cp11-CD137 fusion proteins 24 hours prior to the assay. The CHO-S target cells were labelled with Calcein-AM and diluting concentrations of CAMPATH-1H (or 0.1µg/mL isotype control) for 30 minutes at 4°C before co-culturing at 37°C with PBMC at 50:1 E:T ratio for 4 hours. Calcein released into the culture supernatant was measured and converted to % Maximal Lysis using Triton-X100 treated cells to define the maximum possible calcein released using the equation presented in Figure 4.15c. The mean and SD of three independent experiments are presented. Statistical significance was assessed using an unpaired t test, \* =  $p < 0.05$  and, n.s. = not significant.

## 4.6 Production of Stably Transfected Cell Lines:

All of the data presented so far has utilised transiently transfected CHO-S cells as targets for each assay. As a result of this approach, a heterogeneous cell population (ranging from no expression to very high protein expression) was assessed as a pooled dataset in each experiment. This approach had the advantage of reflecting a potential tumour population where the antigen expression isn't consistent within a population – for example as seen with CD20 levels in CLL or EGFR levels in colon carcinomas<sup>230,249</sup>. Similarly these cells haven't been exposed to antibiotics for selection or extended culture which may alter the phenotype of the cells, allowing the constructs to be tested in cells which have little interference from external conditions. However, the advantages of this approach also has its limitations as more than one variable was being changed between the conditions, and although attempts to normalise the pooled data sets for consistency have been performed, this in itself does not always lead to logical values being approached – for example more than 100% killing was reported for CDC assay using Cp11-flush cells in Figure 4.17 – which was most probably due to a population of low expressing cells that were not clearly identified by flow cytometry. Similarly, it wasn't possible to determine whether the expression level was compensating for the distance being

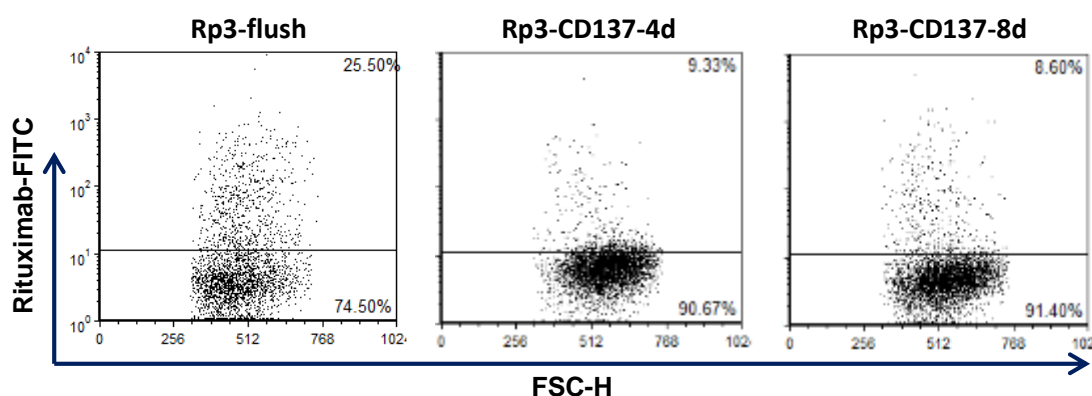
tested between the samples thereby masking the subtleties that the antigen could have on the effector mechanisms being investigated.

Therefore, to support the pooled transient data obtained so far, stably transfected cells which expressed a comparable level of the various fusion proteins was desirable. Ideally the cell line would be of lymphocyte origin, to best mimic the target cells these assays were intended for. Human cell lines, such as Ramos, Raji or Jurkat were not ideal, as they already expressed human CD20 and/or CD52 which would bind the therapeutic antibodies used regardless of the presence of the fusion proteins. Also the use of a human derived cell line would not be easily applied to an *in vivo* investigation in immunocompetent mice. Hence it was decided that a murine derived suspension cell line would be utilised instead.

A number of different mouse suspension cell lines were tested in order to produce stably transfected cells which would express the Rp3-CD137 fusion proteins. These included the plasma cell line J558L, myeloma cell lines – NS-1, NS-0 and BWZ.36 – and lymphoma lines A20 and EL4. All cell lines were transfected using the recommended nucleofection protocols found on the Lonza protocol database (summarised in chapter 2; Table 2.3) – except for BWZ.36 cells which were electroporated instead – with either Rp3-CD137-4d or yellow fluorescent protein (YFP) as a positive control <sup>329</sup>. All of the cells tested were able to express YFP after transfection; however, with the exception of A20 cells, the cell lines were either unable to express the fusion protein after transfection or maintain expression after 1mg/mL geneticin was added to select for clones where the plasmid DNA had been integrated into the genome.

A20 cells (a murine lymphoblastic cell line which has been used as a disseminated lymphoma model in *in vivo* studies <sup>330,331</sup>) were able to be stably transfected using the nucleofection protocol (Figure 4.20a). Rp3-flush, -4d and -8d were used as these three constructs represented the best spread of distance, and would be ideal for testing the effector mechanisms to see if the trends were the same. Although the transfection efficiency after 24 hours was low, by subcloning the cells and culturing in the presence of geneticin; single populations of positive cells were expanded resulting in the similar levels of expression for Rp3-flush, -4d and -8d constructs (Figure 4.20b).

## a) Transient Transfectants:



## b) Stable Transfectants:

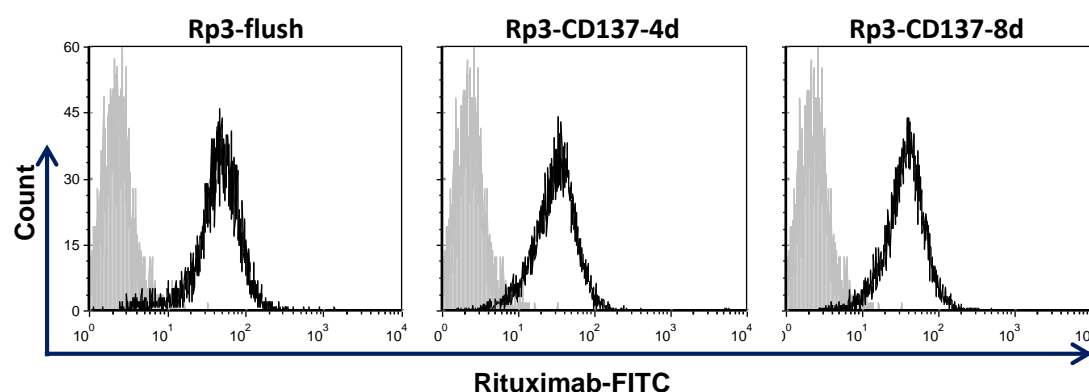


**Figure 4.20: Expression of Rp3-CD137 fusion proteins on A20 cells after transfection and selection**

$5 \times 10^6$  cells were transfected with  $2 \mu\text{g}$  of plasmid DNA using Lonza nucleofection Kit V and programme L-13 a) Protein expression was assessed by flow cytometry 24 hours later using rituximab-FITC to detect expression of the Rp3 peptide. b) 3 weeks after sub-cloning the cells in the presence of  $1 \text{ mg/mL}$  geneticin selection, single populations of cells expressing equivalent levels of each fusion protein were isolated.

To confirm that these fusion proteins were translated properly the CD137 backbone was confirmed by flow cytometry using the anti-CD137 antibodies, SAP1-3 and SAP3-6, (which bind the distal and proximal domains of WT CD137, respectively) Figure 4.21a. In addition a western blot of the cell lysates was carried out and probed with anti-CD137 in order to confirm that the size of the 4- and 8-domain fusion proteins were correct, as presented in Figure 4.21b. As the protein expression has been confirmed, the stably transfected A20 cells these were subsequently used as targets to assess the ability of rituximab in engaging the cell-extrinsic effector mechanisms; CDC, ADPC and ADCC.

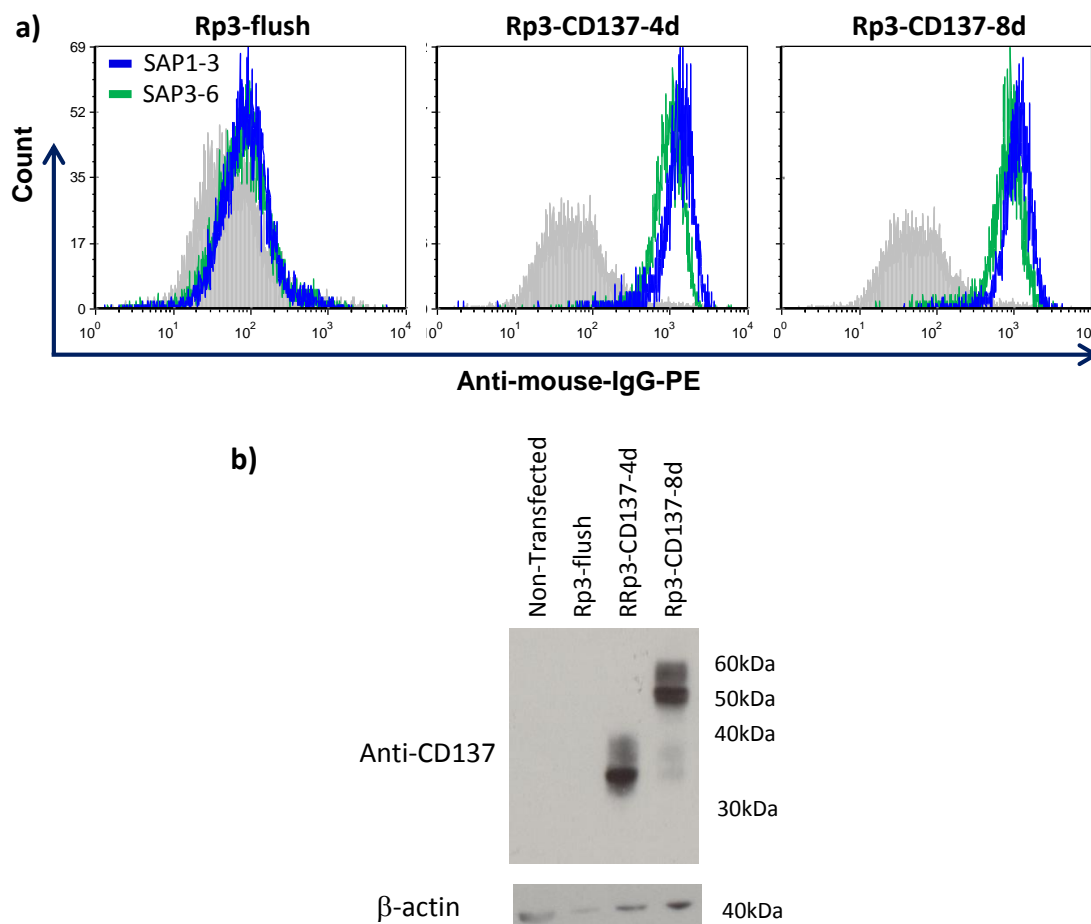


**Figure 4.21: Confirmation of protein expression in A20 stable transfectants.**

a) Flow cytometry confirming the correct folding of the CD137 backbone by SAP3-6 (green) and SAP1-3 (blue). No binding was seen for Rp3-flush as expected due to the absence of any extracellular CD137 in this construct. b) Cell lysates from transfected A20 cells were used in western blot to detect CD137 with a polyclonal anti-human CD137 antibody. As expected Rp3-CD137-8d was observed to run with a higher molecular weight compared to Rp3-CD137-4d construct, thereby confirming the correct translation of the fusion proteins. Non-transfected A20 cells were used as a negative control and β-actin was used as a loading control.

To assess CDC, the same assay conditions with CHO-S cells as targets were used – 15% human serum as the source of complement for 30 minutes at 37°C. The results of three independent experiments are presented in Figure 4.22. Engaging the epitope furthest away from the cell membrane (Rp3-CD137-8d) resulted in a significant decrease of cell lysis where a loss in cell lysis. This data set corroborates the previous observations produced in CHO-S cells, allowing it to be concluded that for effective CDC engagement targeting an epitope that lies close to the cell membrane is favourable, and that a loss in efficacy is achieved when binding an epitope greater than 80Å away.

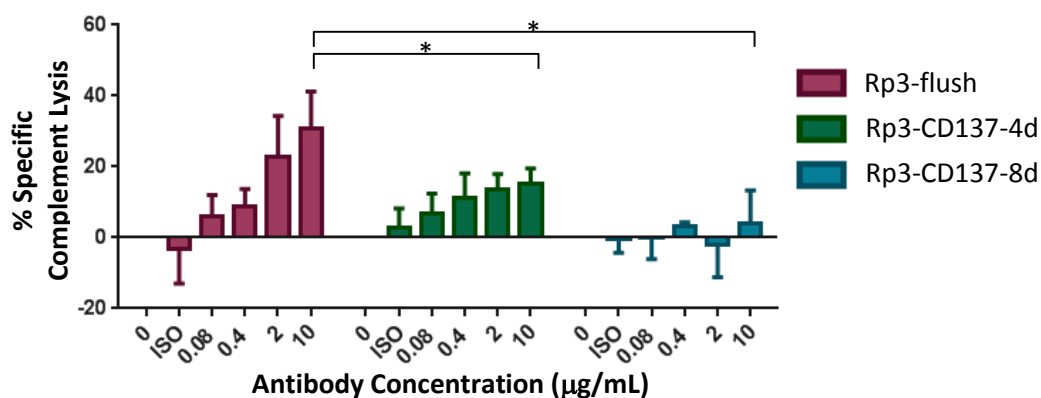


**Figure 4.22: *In vitro* assessment of CDC with stable transfected A20 cells expressing Rp3-CD137 constructs.**

A20 cells which expressed the Rp3-CD137 constructs were used tested in the CDC assay. Transfected A20 cells were opsonised with diluting concentrations of rituximab-hlgG1 for 15 minutes at room temperature before co-culturing with 15% human serum for 30 minutes at 37°C. Antibody mediated cell death was recorded by flow cytometry using the analysis template outlined in Figure 4.1. The mean and SD of three independent experiments are presented. Statistical significance was assessed using an unpaired t test, \* =  $p < 0.05$ .

In order to test ADCP with the A20 cells, BMDM were derived from wild type BALB/c mice in order to reflect the mouse strain of the cell line. The assay conditions were maintained at a 5:1 T:E ratio with 1 hour co-culture for phagocytosis to occur. The results from three independent experiments (each using a different donor of BMDM) are plotted in Figure 4.23. Although the overall phagocytosis is lower than that previously reported, the same trend was observed where targeting the membrane proximal construct resulted in poor phagocytosis. This lower level of phagocytosis may be because of the lower antigen expression level compared to the CHO-S transfections.

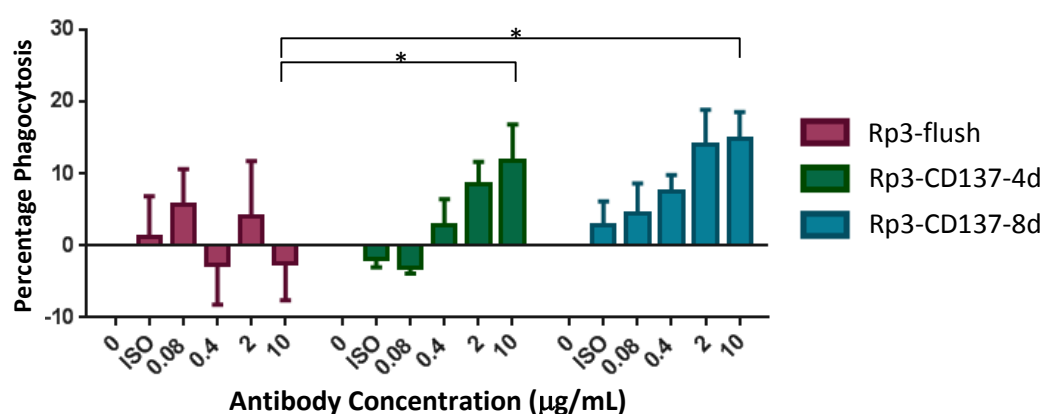


**Figure 4.23: Assessment of ADCP using Rp3-CD137 stable expressing A20 cells**

A20 cells expressing the Rp3-CD137 constructs were labelled with 5µM CFSE and opsonised with diluting concentrations of rituximab-mIgG2a or 10µg/mL isotype control mAb (ISO). These cells were then co-cultured at a 5:1 T:E ratio with BMDM for 1 hour at 37°C. Phagocytosis was measured by flow cytometry as previously described (Figure 4.11). The mean and SD of three independent experiments are plotted. Statistical significance was assessed using an unpaired t-test where a p-value  $< 0.05$  were deemed significant.

In order to assess ADCC the same conditions using human PBMC as a source of effectors was tested for these cells, the results of a single experiment are presented in Figure 4.24. However, the results obtained were unusual and gave the opposite trend to that seen previously with the CHO-S cells (Figure 4.16 and Figure 4.19). This was the mean of two independent experiments and seems consistent, even though the trend matches that for the ADCP data not the CDC data as expected. The background level of lysis in response to human PBMCs alone is high in the raw data – approximately 40-50% – which suggest that these cells are more sensitive to lysis/ADCC compared to the CHO-S cells, in the absence of any antibody opsonisation.

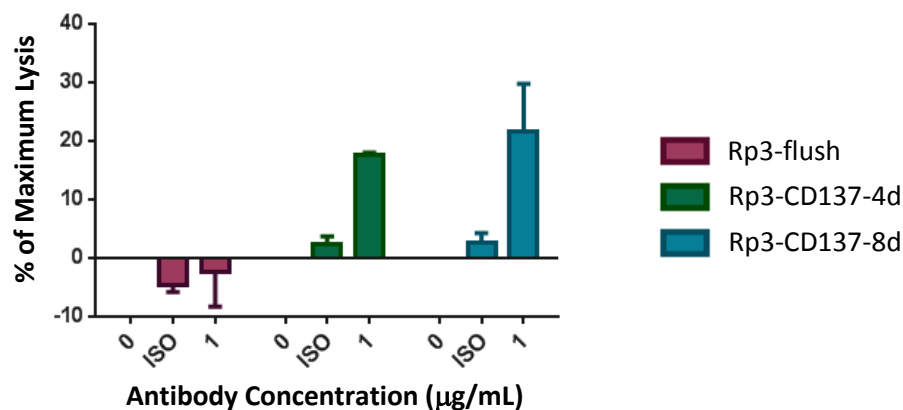


**Figure 4.24: Assessment of ADCC using Rp3-CD137 stable expressing A20 cells**

Rp3-CD137 construct expressing A20 cells were labelled with calcein-AM and rituximab-hIgG1 (or 1µg/mL isotype control) for 30 minutes at 4°C before co-culturing at 37°C with PBMC at 50:1 E:T ratio for 4 hours. Calcein released into the culture supernatant was measured and converted to % Maximum Lysis using Triton-X100 treated cells to define the maximum possible calcein released. The median and range of two independent experiments are plotted.

In order to see whether the same trend seen in Figure 4.24 would be seen if the effector cells were of the same species as the A20 cells, NK cells were isolated from the spleen of a WT BALB/c mouse. These were expanded over 14 days in the presence of IL-2 were they were ready for use in an ADCC assay. Due to the purer cell population in comparison to the human PBMC used previously a lower E:T ratio of 5:1 was used. As presented in Figure 4.25, there seems to be poor killing when rituximab binds the Rp3-CD137-8d construct which would support the original data sets collected using CHO-S cells (Figure 4.16 and Figure 4.19). However, it would seem that cells expressing Rp3-CD137-4d were most sensitive to ADCC. This is only the result of a single experiment, and would require repeating to better draw conclusions on the suitability of these cells for this assay.



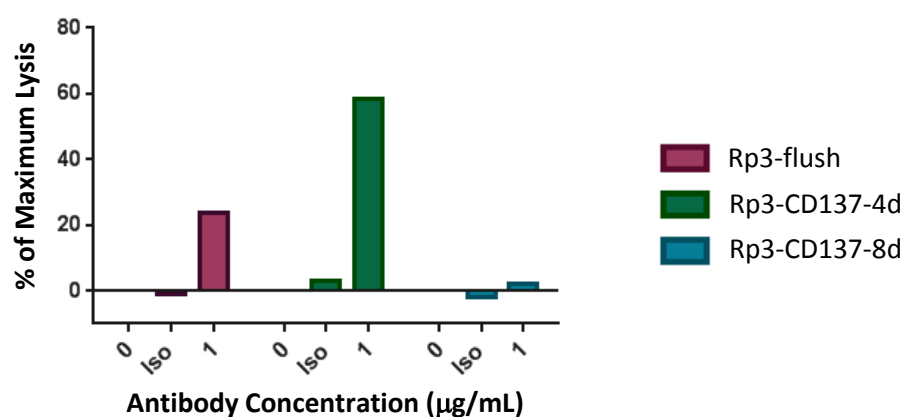


**Figure 4.25: ADCC assay of A20 cells using murine NK cells as effectors**

A20 cells expressing the Rp3-CD137 constructs were labelled with calcein-AM and 1µg/mL of either rituximab-mIgG2a or an isotype control for 30 minutes at 4°C. These cells were co-cultured with mouse NK cells at 5:1 E:T ratio for 4 hours. The supernatant was collected and calcein release measured using a fluorescent plate reader and converted into % Maximum Lysis as previously described in Figure 4.15. The results from a single experiment are plotted.

## 4.7 Chapter Discussion:

In this chapter, the fusion proteins previously generated in Chapter 3 were tested for their sensitivity towards the three cell-extrinsic depletion mechanisms, CDC, ADCP and ADCC. The functional data collected within this chapter has been summarised in Table 4.1. It could be concluded that for the cytotoxic mechanisms, CDC and ADCC, targeting membrane proximal epitopes conferred the best response, whilst targeting the 8-domain construct resulted in a diminished response. In contrast, ADCP engagement was better when targeting epitopes that were positioned, further away from the cell membrane, with the membrane flush epitope resulting in poor ADCP engagement.

	Cell line	Antibody	Effector Mechanism		
			CDC	ADCP	ADCC
Flush	CHO-S	RTX	++	–	++
		CAM	+	–	++
	A20	RTX	++	–	–/+
1 domain	CHO-S	RTX	++	++	++
		CAM	++	++	++
	A20	RTX	N/A	N/A	N/A
4 domains	CHO-S	RTX	+	++	++
		CAM	+	++	++
	A20	RTX	+	+	+
8 domains	CHO-S	RTX	–	+	–
		CAM	–	++	–
	A20	RTX	–	++	+/-

**Table 4.1: Summary of data collated within Chapter 4**

The results of the functional assays performed within this chapter for CDC, ADCP and ADCC are summarised in the table above. ++ = good engagement even at lower antibody concentrations; + = good engagement at saturating levels of antibody; – = poor engagement; N/A = non-applicable as this cell line was not produced for testing. +/- reflects the conflicting results between the human and mouse based ADCC assay used for the A20 cell lines.

These mechanisms were examined using both a heterogeneous cell population as well as a stable expressing cell line. A20 cells were chosen as these were the only cells tested that were able to maintain expression of the fusion protein. Difficulties in establishing a cell line led to questions on the stability of the fusion proteins themselves, and whether there were any particular features in the design of this construct that would explain the inability to be highly expressed across a number of different cell lines.

CD137 is a co-stimulatory molecule found on T cells, whose activation leads to proliferation and cell survival<sup>332</sup>. However, over-activation of T cells eventually leads to an increase in cell death in order to maintain immune homeostasis<sup>333</sup>. Discussions with others within the laboratory revealed technical difficulties in establishing high expressing clones when using wild type human CD137 in mouse cells. It could be that the level of expression achieved with the A20 cells represents the level where the cells are able to survive, but the receptors are not at a density which would cause clustering and self-activation resulting in increased levels of cell death. Potential improvements to the construct for this model to achieve higher expression levels would be to clone the construct with the transmembrane domain present but remove the intracellular tail. This would produce a construct which remained tethered to the cell

membrane but contain no potential signalling domains that would over-activate and kill the higher expressing cells.

Although overall the expression levels of the A20 stable transfectants are low compared to normal human CD20 and CD52 expression levels they are biologically relevant. The human CD20 transgenic mouse B cells have a similar expression level <sup>334</sup>, which is lower than the CD20 levels observed on human B cells. Similarly, low levels of CD20 are reported in CLL, particularly in patients that are more resistant to rituximab therapy <sup>235</sup>. The Rp3-CD137 expressing A20 cells established in this project are more useful as a model of understanding immunotherapy where the antigen isn't highly expressed, rather than as a direct model of established CD20 lymphoma models. Having the A20 cell lines established means that a panel of cells are now available which can be directly compared in terms of morphology and fusion protein expression levels, allowing for a more direct investigation of the impact epitope distance from the cell membrane has on the therapeutic response of a mAb to be performed.

For the engagement of CDC, all of the approaches used within this chapter have repeatedly demonstrated that CDC-mediated lysis is diminished when targeting the 8-domain constructs – and is less sensitive with the 4-domain construct at lower antibody concentrations. This observation fits into what is already known about the half-life of complement components. Once activated, the complement components are susceptible to hydrolysis – cleaving them into inactive forms – unless they are stabilised by complement components (such as factor D, C2) are bound to the cell membrane <sup>221</sup>. Therefore, if activated close to the cell membrane – for example when targeting the Rp3-flush or Rp3-CD137-1d construct – the diffusion distance is smaller, and therefore the components are more likely to form stable complexes on the plasma membrane compared to the distance required if activated at the distance of the 8-domain construct.

This work has looked at the lytic ability of complement in the activation and depletion of the target cells, however, no assessment of its secondary role with regards to recruitment and activation of phagocytes has been investigated <sup>217</sup>. It is possible that the potency of complement is not wholly due to the MAC formation, but on the additional recruitment and activation of other immune effector systems. This could potentially be investigated through the use of a co-culture system where target cells are cultured with C6-9 depleted serum and immune effector cells and the effect of cell death compared heat inactivated serum. Together this information would further our understanding of the role that classical complement plays in antibody immunotherapy.

For an ideal candidate for immunotherapy, the data so far suggests that if effective complement engagement is desired then targeting small membrane proximal proteins/epitopes would be favourable – and would explain the effectiveness of both CD20 and CD52 as therapeutic targets. However, this data also shows that engagement of CDC can be diminished if targeting further away which could be favourable if looking to devise a potent ADCC mechanism approach, as the production of C3b would be far lower and less likely to interfere with the engagement of activatory FcγR <sup>250</sup>.

ADCC dependent cell lysis was diminished when targeting the epitope which was furthest away from the cell membrane (the 8 domain constructs). This trend was consistent when using human PBMCs effectors with CHO-S cells transfected with either the rituximab or CAMPATH-1H binding fusion constructs. Together with the CDC data, this suggests that for the cytotoxic lysis of cells, targeting epitopes close to the cell membrane is preferable.

Human PBMC were isolated from a blood cone on the day of analysis, and used as effectors without isolating the NK cells from the mix. This approach had the advantage of not tampering with the effector cells extensively before using them as cytotoxic effectors, which may have occurred if NK were isolated via magnetic-activated cell sorting (MACS) separation (which could damage the cells due to exposure to strong magnetic fields or antibody activation). The blood was provided from healthy anonymous donors, having the advantage of providing a pooled data set using independent sources of effector cells. No genetic information was available about the FcγR polymorphisms present, which may explain the greater variation seen between the experimental repeats due to different affinities between the effector cells and the mAb. Further repeats of this data using more donors would most likely refine this data set, and strengthen the trends seen when using transfected CHO-S cells as targets.

Curiously, using human PBMC as effectors for the murine A20 cell lines the opposite pattern was seen, with Rp3-flush transfected cells giving a poor response, and the basal levels of lysis was higher and more variable between individual experiments. It was hypothesised that the high level of basal cell death seen with the A20 cells was due to the species difference between the target and effector cells. To assess this, NK cells expanded from the splenocytes of a WT BALB/c mouse were used as effector cells instead. These effectors resulted in another different trend compared to that seen with the CHO-S cells, demonstrating the best lysis was seen when targeting the Rp3-CD137-4d construct compared to the others, although there was a loss of lysis observed when targeting the Rp3-Cd137-8d expressing A20 cells which would corroborate the initial CHO-S findings.

Although commonly classed as a subset of ADCC, ADCP was investigated as a separate mechanism due to the evolving data which indicates that macrophage mediated killing is superior to that of the cytotoxic NK mediated death <sup>242</sup>. Because of this difference in the therapeutic role for these two mechanisms, it was interesting to see whether the FcγR mediated mechanisms responded differently to the fusion proteins developed in this thesis, and whether it revealed key differences which could separate the mechanisms when identifying new potential targets.

Using the panel of fusion proteins to investigate the impact of distance for the engagement of ADCP revealed the opposite trend to that seen with the lytic mechanisms, CDC and ADCC. Targeting the membrane flush epitope resulted in a poor uptake by BMDM whilst those that had at least one extracellular domain present were more efficient at phagocytic engulfment. This observation was reproducible in both the CHO-S cell line and the stably transfected A20, and the same result was seen when using rituximab and CAMPATH-1H. This was not likely a result of the antibody being unable to bind the flush constructs, as protein expression was able to be detected with the same antibodies by flow cytometry.

Although this observation was counter-intuitive at first – it was hypothesised that the engagement of FcγR mediated mechanisms would be the same – it may be explained by looking at the mechanistic differences between ADCC and ADCP. ADCC requires the FcγR to be clustered and in turn downstream signalling events cause the release of cytotoxic granules that are able to lyse the targeted cell <sup>261</sup>. In contrast FcγR signalling events for ADCP result in cytoskeletal rearrangements and phagosome formation before engulfing the targeted cell <sup>270</sup>. Due to these mechanistic differences it is possible that the time for an individual event to occur is variable, and as such they may also have a different dependence on the stability of the epitope:mAb:FcγR complex.

It is possible that endogenous surface proteins present on the cell surface provide a steric barrier which reduces the ability to form a stable complex between the target cell and the macrophage when targeting the membrane flush constructs. Loss of this interaction would make the contact dependent phagocytosis more difficult to complete, resulting in a diminished response. In contrast for ADCC, once the signalling initiates the vesicular release of cytotoxic particles, the requirement to be physically attached may be lower and lysis could still be achieved if this attachment is disrupted <sup>261,268</sup>. It is assumed that that the antibody binding kinetics are the same between the different constructs as the same epitope and antibody are

used. However, it is possible that this is not the case and these subtle differences may be sufficient to impact upon the engagement of the FcγR mediated mechanisms.

The work presented in this chapter demonstrates that the distance between the antibody and the cell membrane is sufficient to alter the mechanisms engaged by a direct targeting antibody. Comparing the three effector mechanisms *in vitro* indicates a cytotoxic trend which favours the membrane proximal epitopes (for CDC and ADCC) and a phagocytic response which favours an epitope further away from the plasma membrane. This indicates that the success of the lymphoma targets CD20 and CD52 may be a result of their small, membrane proximal positioning. For the rituximab antibody the data produced here aligns with what is published with regards to the functions of anti-CD20 mAbs, however for CAMPATH-1H there is a discrepancy with the ability to engage phagocytosis whether it targets the Cp11-flush construct or its wild type antigen, CD52. This will be investigated in the next chapter, to see whether distance is the defining property on the engagement of the effector mechanisms or whether there are other physical properties of an antigen which also influence the engagement of these effector mechanisms engaged.

## Chapter 5: Understanding why human CD52 is an effective target for ADCP

### 5.1 Introduction:

In the previous chapter, it was concluded that the distance an antibody binds from the cell membrane can alter the efficacy of the effector mechanisms engaged. This was best illustrated when comparing the flush and 8 domain constructs (with an approximate distance of 160Å between them). It was also demonstrated that this trend was not specific to the cell type being used, as both CHO-S and A20 cells were similar, and was not a rituximab specific quality as the same result was also seen with a panel of CAMPATH-1H binding antigens.

In relation to *in vivo* function in therapy, CAMPATH-1H is proposed to engage both CDC and FcγR functions<sup>237,238,304</sup>. Whilst the FcγR function for CAMPATH-1H is primarily classed as ADCC, more recent work has demonstrated that macrophages play a large role in FcγR mediated therapeutic response *in vivo*, therefore it is logical to assume CAMPATH-1H is also able to engage ADCP as it is a human IgG1 antibody<sup>277,335,336</sup>. Its antigen, human CD52 (described in more detail in section 1.9.1), is a 12 amino acid mature peptide that is attached to the membrane via a GPI anchor.

GPI anchored proteins exist throughout nature and consists of a glycan core attached to a phospholipid tail which acts as a tether for the phospholipid bilayer<sup>337</sup>. The glycan core consists of phosphoinositol, mannose and glucosamine residues which also provide sites for further modification, as seen with the lipidation isoforms of CD52<sup>296</sup>. The final composition of the GPI anchor is dependent on the biosynthetic pathways available, and as such great heterogeneity exists between species and even cell subsets. Proteins are attached via the carboxy-terminus to a phosphoethanolamine linker present on the glycan core<sup>299</sup>.

Although there are a number of known GPI anchored proteins the role of the anchor and associated proteins are still unclear. This is in part due to difficulties in studying these proteins, particularly in defining structures via conventional approaches of Nuclear Magnetic Resonance and X-ray crystallography<sup>338</sup>. Biochemical approaches have allowed the anchor composition to be defined for an individual protein, but this information alone does not ascertain function. Identified GPI anchored proteins in humans seem to be typically involved in the immune system, for example the complement defence molecules CD55 and CD59<sup>226</sup>, or are found expressed on key immune cells such as CD16b and CD52<sup>252,296</sup>.

Due to the phospholipid tail, GPI anchored proteins do not contain any recognisable signalling motifs (such as ITAM motif), however there have been standalone reports that have observed that crosslinking these proteins (such as CD16b and CD52) increases the activation of a cell in the presence of a mitogen; although a mechanistic explanation for these observations is still required<sup>300</sup>. An alternative role is in the organisation of the phospholipid bilayer<sup>337</sup>. GPI-anchored proteins are able to move across the membrane in an actin-dependent manner. Work by Raghupathy and colleagues propose that this is mediated via phosphoserine residues present on the inner leaflet which facilitate movement of the GPI-anchored proteins and formation of microdomains<sup>339</sup>.

In theory, wild type human CD52 lies close to the cell membrane and as such would be best reflected by the Cp11-flush construct, which has 11 amino acids present in the extracellular domain – as summarised in Figure 5.1. Due to the similarity between these two proteins it was a surprise when the *in vitro* data previously obtained section 4.5 (Figure 4.18) demonstrated that CAMPATH-1H targeting Cp11-flush was inefficient at engaging phagocytosis. These results revealed a contradiction to the mechanisms CAMPATH-1H is reported to engage when targeting its wild type antigen CD52, which is susceptible to phagocytosis.



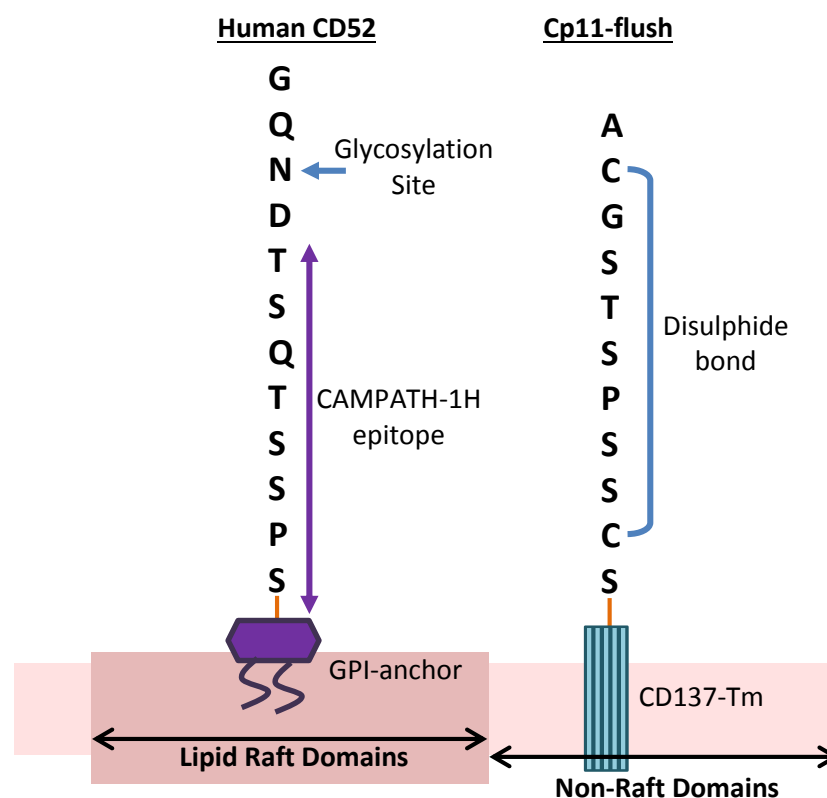


**Figure 5.1: Comparison of Cp11-flush and CD52 mature peptides:**

The peptide sequence of the extracellular domains of CD52 and Cp11-flush with the known post-translational modifications included for reference. Human CD52 contains an N-linked glycosylation site on the Asn at position three, and is attached to a GPI anchor present on the cell surface. Cp11-flush contains a disulphide bond between the two Cys present in the extracellular domain and is attached to the membrane via the transmembrane (Tm) domain of CD137.

## 5.2 CAMPATH-1H is able to phagocytose cells expressing WT-CD52

To confirm that the batch of CAMPATH-1H used throughout this project worked as expected, human PBMC isolated from CLL patients (therefore consisting predominantly of B cells) were used as targets in an ADCP assay. These cells were treated with 2 µg/mL of rituximab, CAMPATH-1H or Herceptin (as an isotype control). As shown in Figure 5.2, CAMPATH-1H was able to effectively engage phagocytosis of CLL PBMCs at a similar level to rituximab, confirming that when targeting its wild type antigen, CAMPATH-1H functions as expected.

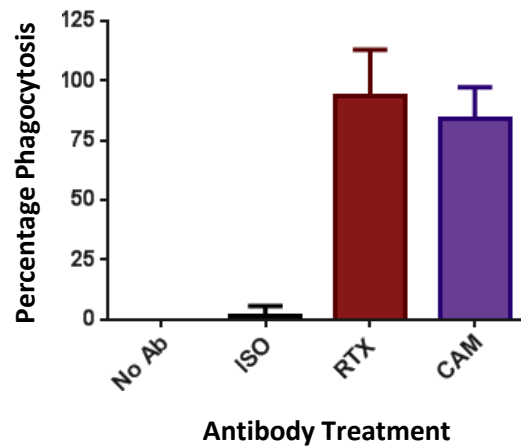


**Figure 5.2: CAMPATH-1H is able to engage ADCP when targeting human B cells**

Human PBMC isolated from whole blood of a CLL patient were labelled with CFSE and opsonised with 2µg/mL of rituximab (RTX), CAMPATH-1H (CAM) or Herceptin (ISO). The cells were co-cultured at a 5:1 T:E ratio with BMDM for 1 hour at 37°C before phagocytosis was measured by flow cytometry. The mean and range of two repeats from a single assay are presented.

One other experimental difference was that the cells used in the previous chapter were not of human origin. To confirm that the CHO-S expression system used previously was not altering the sensitivity to ADCP, CHO-S cells were transfected with either WT-CD52 or Cp11-flush and tested in parallel in an ADCP assay (Figure 5.3c). Once again, when compared to CD52, targeting Cp11-flush was unable to engage an effective ADCP response, even though the transfection efficiency was similar between the constructs (Figure 5.3a-b).

Together these data indicated that there was something inherently different between the wild type protein and the Cp11-flush construct that significantly impacts the ability to engage the phagocytosis mechanism. Comparing the two peptide sequences it was clear that the glycosylation status between the two proteins was different. CD52 contains an N-linked glycosylation site on position 3 of the mature peptide, whereas the Cp11-flush construct does not contain any motif that is susceptible to glycosylation (highlighted in Figure 5.1). The X-ray crystal structure of the CAMPATH-1H F(ab) found that the glycosylation of CD52 did not form part of the epitope; however, it may have a secondary role in stabilising the interaction by binding a second site <sup>340</sup>.

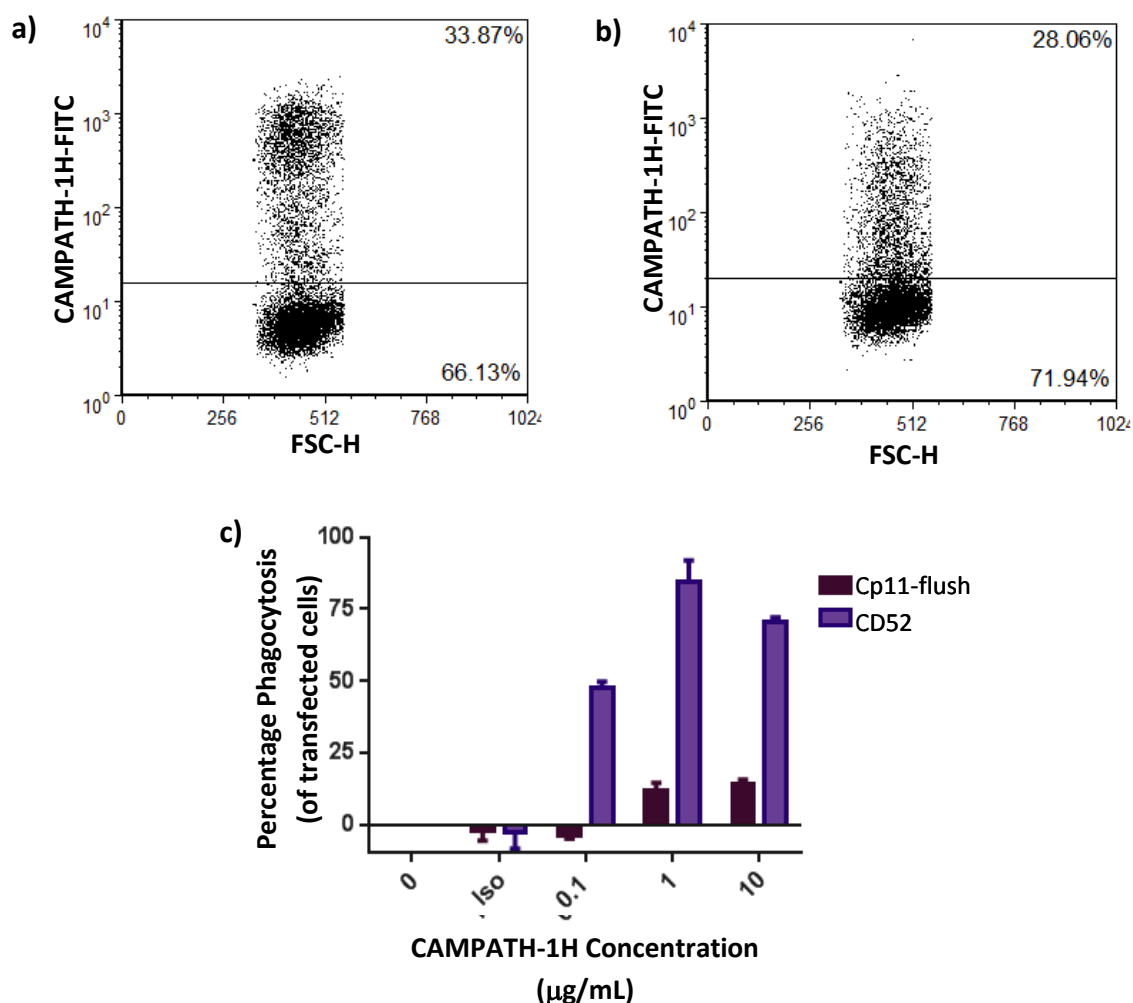


**Figure 5.3: Susceptibility for ADCP is different between CD52 and Cp11-flush**

CHO-S cells were transfected with a) wild type CD52 or b) Cp11-flush and cell surface expression was confirmed by flow cytometry using FITC conjugated CAMPATH-1H. c) The transfected CHO-S cells were then used as targets in an ADCP assay where they were labelled with varying concentrations of CAMPATH-1H or 10 μg/mL of an isotype control mAb (ISO). Following antibody opsonisation the cells were co-cultured with BMDM at a 5:1 T:E ratio for 1 hour at 37°C before phagocytosis was assessed by flow cytometry. The mean and range of two repeats from a single assay are plotted.

### 5.3 Investigating the contribution CD52 glycosylation has on the susceptibility to ADCP

A non-glycosylated mutant of CD52 (CD52-NQ) was therefore generated in order to investigate this hypothesis. Using the human CD52 gene, previously cloned (by Dr C. Chan) into the pcDNA3 expression vector as a template, the Asn at position three was mutated to a Gln by site-directed mutagenesis and confirmed by DNA sequencing (Figure 5.4a). As this was a small two nucleotide mutation, no modification to the basic mutagenesis programme outlined in the methods section was required. Gln was chosen as the surrogate residue, as it contained the

same charge as Asn and was of a similar side chain structure, so in theory would have less of an impact on the final peptide structure in terms of bond rotation, flexibility and conformation. The CD52-NQ mutant was able to be expressed in CHO-S cells, and recognised by CAMPATH-1H (Figure 5.4b).

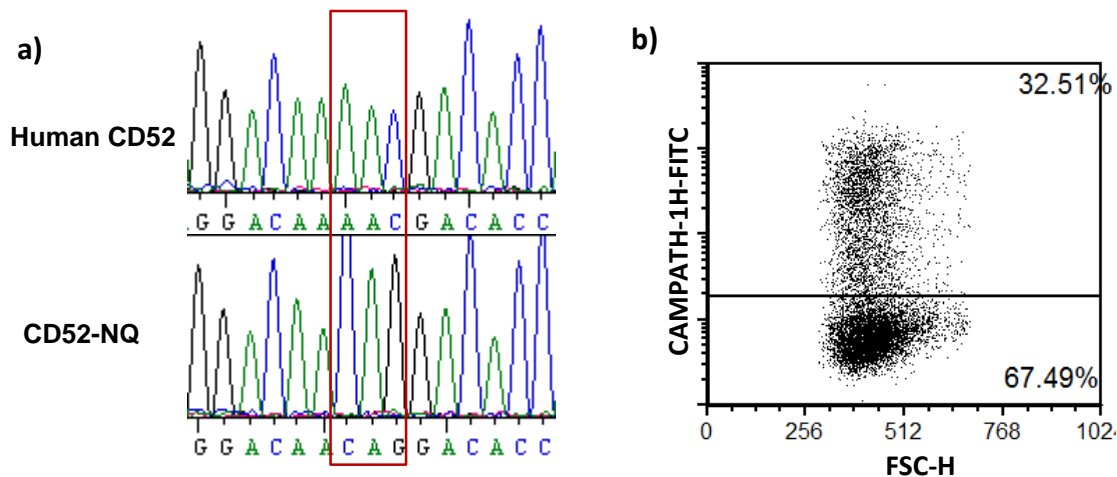


**Figure 5.4: Generation and expression of CD52-NQ in CHO-S cells.**

a) DNA sequencing traces confirming the presence of the two nucleotide mutations required to convert the Asn to Gln in human CD52. The trace is colour coded specifically to each nucleotide as follows: blue = cytosine, red = thymine, black = guanine, green = adenine. b) CHO-S cells were transfected with CD52-NQ and cell surface expression was confirmed by flow cytometry 24 hours later using CAMPATH-1H-FITC.

When these cells were tested in the transient CHO-S ADCP assay, presented in Figure 5.5, no difference in the ability to engage phagocytosis was found between the non-glycosylated and wild type versions of CD52, whilst the Cp11-flush construct (used as a control) was still unable to achieve equivalent activity. Together these data indicate that the presence of an N-linked oligosaccharide did not explain the enhanced ADCP seen with WT-CD52 compared to the model antigen Cp11-flush; therefore an alternative hypothesis was required.

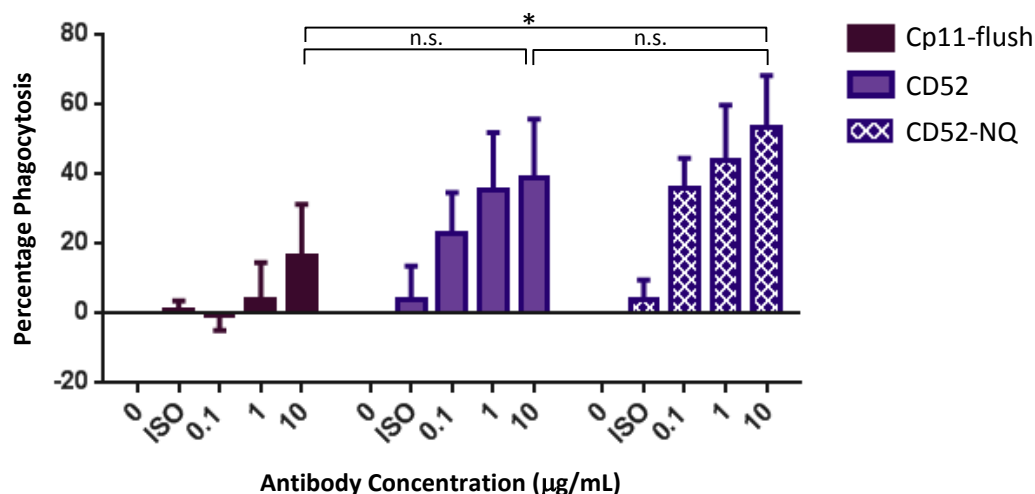


**Figure 5.5: ADCP assay results of Cp11-flush, CD52 and CD52-NQ transfected CHO-S cells following CAMPATH-1H opsonisation**

CHO-S cells transfected with Cp11-flush, CD52 or CD52-NQ were tested in parallel in an ADCP assay using BMDM as effector cells at a 5:1 E:T ratio as previously described (Chapter 4.3, Figure 4.11). Rituximab-hIgG1 was used at 10 µg/mL as the Isotype control (ISO). The mean and standard deviation of three independent experiments are presented. Statistical significance was assessed using an unpaired t test where \* =  $p < 0.05$  and n.s. = non-significant

## 5.4 Investigating the contribution of the GPI anchor on the susceptibility of CD52 to engage ADCP

One other difference between the two constructs is in the method of attachment to the cell membrane. Cp11-flush contains the transmembrane domain of CD137, whereas CD52 is tethered to the surface of the cell by a GPI anchor. Unfortunately, attaching the CD52 peptide to the same transmembrane domain as Cp11-flush was unable to result in either expression or recognition by CAMPATH-1H, even with the Asp-Ala modification incorporated from the synthetic mimotope for CAMPATH-1H (Figure 5.6)<sup>319</sup>. Therefore a GPI linked Cp11 peptide was generated instead. Although there is no defined recognition sequence for GPI attachment, it is proposed to be dependent on the carboxy-terminal peptide sequence<sup>299</sup>. In particular it was determined that the two amino-acids upstream of the GPI attachment site along with the cleavable carboxy-terminal sequence were required. This approach was used by Bournazos and colleagues in 2009 to produce a GPI-linked CD32a chimera using CD55 as the source of the GPI attachment signal<sup>260</sup>.

To mimic these findings, the wild type CD52 peptide was used as a scaffold. The mature peptide sequence of CD52 was switched for Cp11, however the final Pro-Ser of the CD52 mature peptide was kept in place for GPI attachment (summarised in Figure 5.6). This was

achieved by site-directed mutagenesis and confirmed by DNA sequencing. The GPI linked Cp11 peptide (Cp11-GPI) was able to be expressed on the surface of transfected CHO-S cells where it was recognised by CAMPATH-1H by flow cytometry (Figure 5.6).

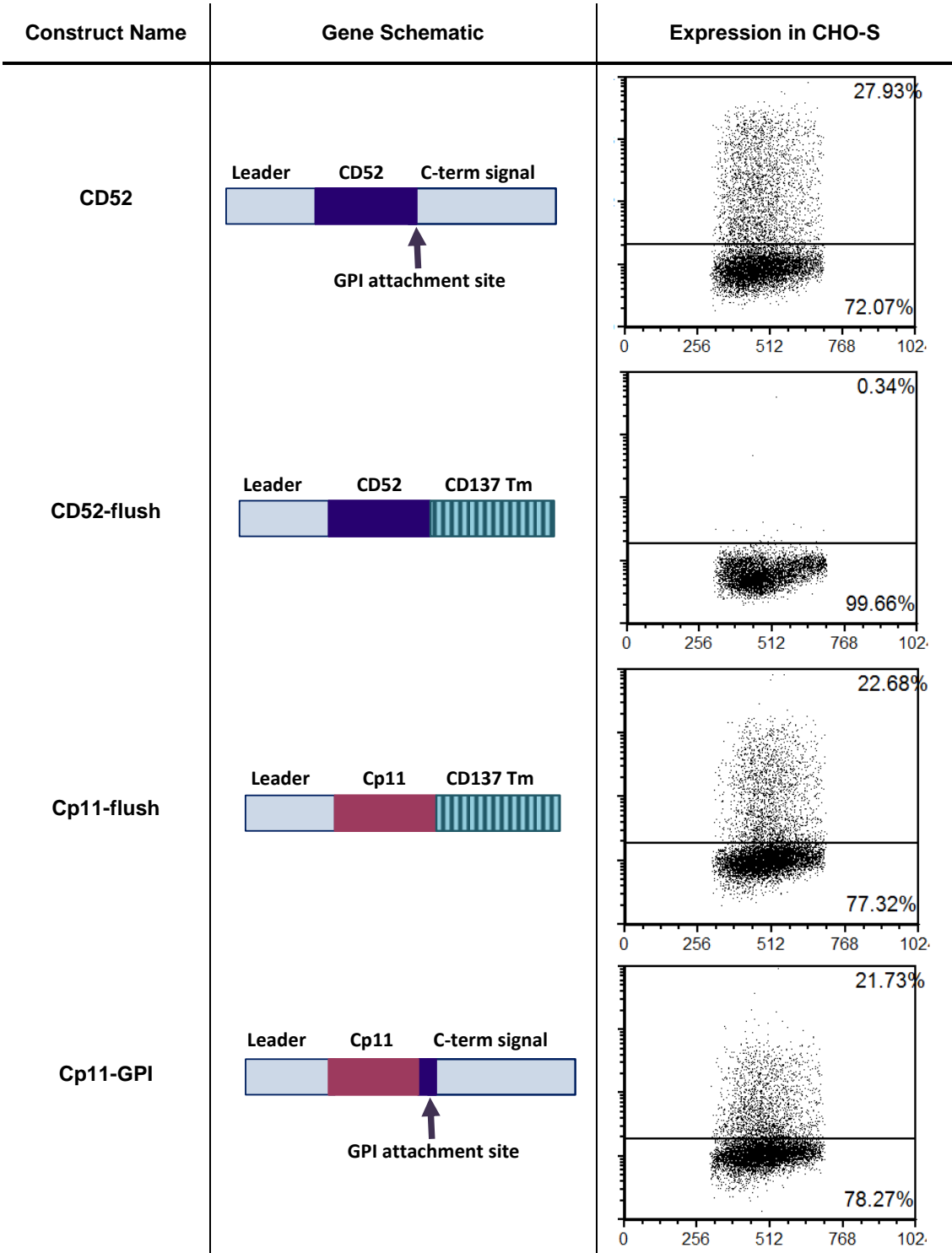


**Figure 5.6: Generation and expression of Cp11-GPI construct in CHO-S cells:** Schematic illustrating the Cp11-GPI construct based on the parental constructs of wild type human CD52 and Cp11-flush. CHO-S cells were transfected for 24 hours with each construct and protein expression was assessed by flow cytometry looking for CAMPATH-1H-FITC binding. Cp11-GPI was cloned by site-directed mutagenesis using CD52 as the template DNA.

Before assessing the role of the GPI anchor on the Cp11 epitope with regards to its susceptibility towards phagocytosis, confirmation of GPI-membrane attachment was required. CHO-S cells transfected with Cp11-GPI were treated with PI-PLC, which would cleave GPI anchored proteins, and the amount of CAMPATH-1H binding was assessed by flow cytometry<sup>260</sup>. A loss in antibody binding between non-treated and treated cells would indicate that the protein was attached by the GPI-anchor thereby confirming that a successful GPI anchored fusion protein was produced. The results presented in Figure 5.7 confirmed that approximately 60% of the total Cp11-GPI protein expressed was cleaved in the presence of PI-PLC indicating the presence of the GPI linkage.

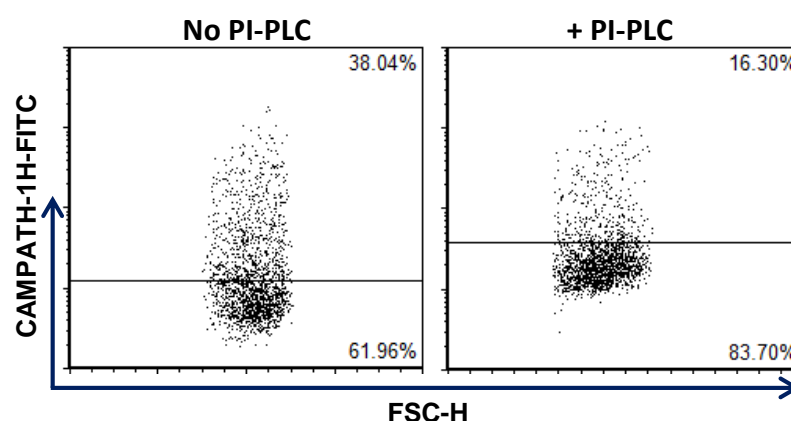


**Figure 5.7: Confirmation of Cp11-GPI anchoring by PI-PLC treatment**

CHO-S cells were transfected with Cp11-GPI for 24 hours prior to experiment. Transfected CHO-S cells were treated with PI-PLC for 30 minutes at 37°C before staining with CAMPATH-1H-FITC at 4°C for 30 minutes. Flow cytometry data for cells treated with or without PI-PLC is presented, showing a reduction in the total amount of antibody binding. The gates were set based on an isotype control stained sample and the same number of events are presented in both plots; data from a single experiment presented.

Having confirmed that the Cp11-GPI construct was able to be expressed on CHO-S cells and attached to the plasma membrane via the GPI anchor; CHO-S cells transfected with Cp11-GPI were compared to wild type human CD52 and Cp11-flush in an ADCP assay (Figure 5.8). It can be seen that Cp11-GPI was far better phagocytosed compared to Cp11-flush, highlighting that it was the method of attachment to the membrane that was responsible for the enhanced phagocytosis seen when targeting wild type CD52 compared to the Cp11-flush construct.

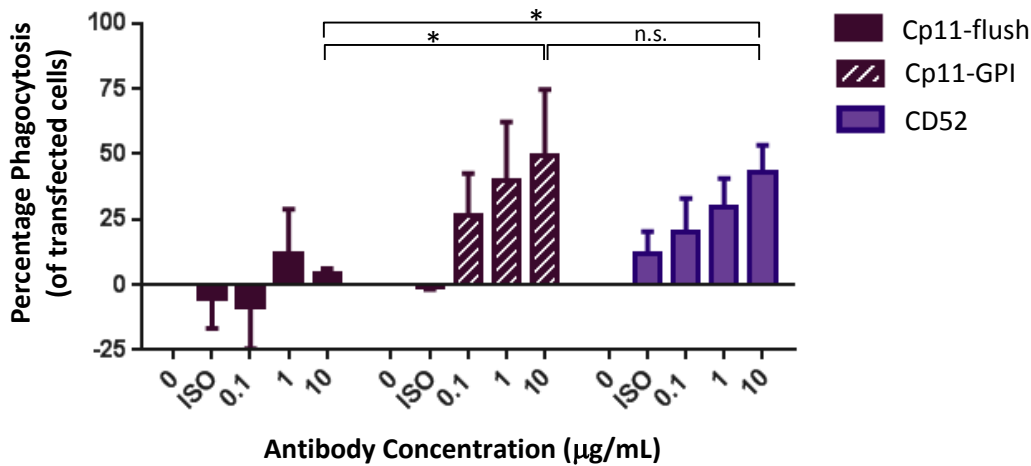


**Figure 5.8: Attaching Cp11 peptide to GPI anchor is able to restore ADCP engagement.**

CHO-S cells were transfected with Cp11-flush, Cp11-GPI or CD52 for 24 hours prior to the ADCP assay. Transfected CHO-S cells were labelled with CFSE and dilutions of CAMPATH-1H. These cells were co-cultured with BMDM at 5:1 T:E ratio for 1 hour before phagocytosis was assessed by flow cytometry. The mean and standard deviation of three independent experiments is presented. Statistical significance was assessed using an unpaired t test where \* =  $p < 0.05$  and n.s. = non-significant.

Finally to confirm that the dependence on the GPI anchor for efficient ADCP engagement wasn't just specific to CAMPATH-1H, a rituximab binding version of the protein was generated (Rp3-GPI). This construct was produced commercially as an extended oligonucleotide to specification (the gene is illustrated in Figure 5.9a), and subcloned into the pcDNA3.1/- expression vector, using the XbaI and NotI restriction sites incorporated into the design. As illustrated in Figure 5.9b, rituximab was able to bind the Rp3-GPI construct when transfected into CHO-S cells, and was sensitive to PI-PLC treatment (Figure 5.9c). Rp3-GPI transfected CHO-S cells were tested in the ADCP assay using BMDM as effectors and found that the ability to engage phagocytosis was restored when compared with Rp3-flush (Figure 5.9d). Together this provided further evidence that the GPI attachment was the reason that wild type CD52 efficiently engaged phagocytosis compared to the membrane tethered constructs.



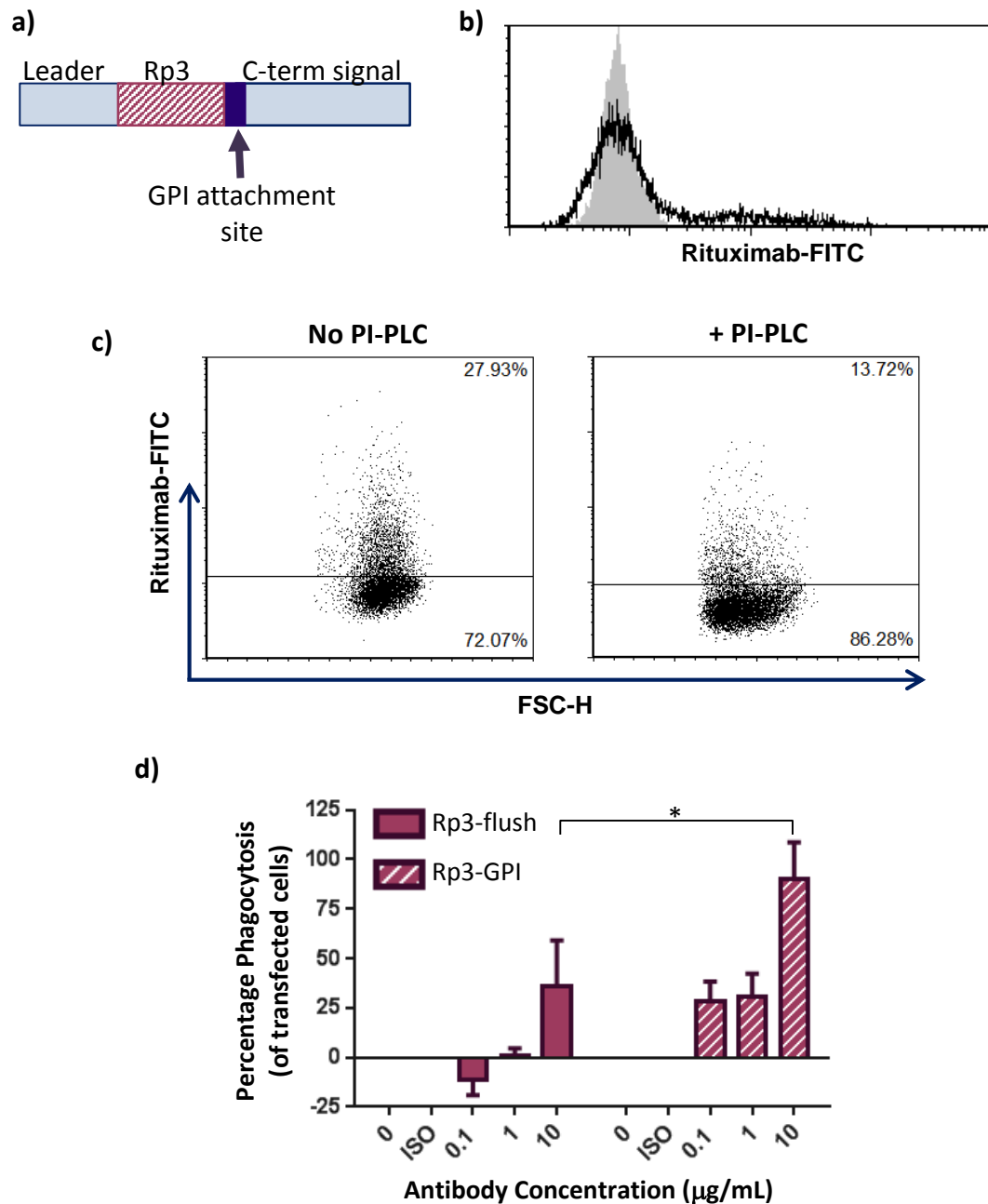


**Figure 5.9: Attachment of the Rp3 peptide to a GPI anchor also restores susceptibility towards ADCP.**

a) Rp3-GPI was designed to incorporate the CD52 leader and GPI attachment signal – as used previously for Cp11-GPI in Figure 5.6. b) CHO-S cells were transfected with Rp3-GPI for 24 hours and tested for rituximab-FITC binding by flow cytometry. c) Rp3-GPI transfected CHO-S cells were treated with PI-PLC, followed by rituximab-FITC to confirm GPI attachment. d) CHO-S cells transfected for 24 hours with either Rp3-flush or Rp3-GPI were assessed in an ADCP assay using the analysis detailed previously in Chapter 4. The mean and standard deviation of three independent experiments is presented. Statistical significance was assessed using an unpaired t test where \* =  $p < 0.05$ .

## 5.5 Chapter Discussion:

In this chapter, the difference in phagocytosis susceptibility between two similar antigens, Cp11-flush and wild type CD52, was investigated. At the peptide sequence level, these two proteins were similar as they both contained a small peptide exposed on the extracellular surface of the cell, and therefore would be of a similar distance from the cell membrane. However their response after CAMPATH-1H treatment in an ADCP assay, revealed very different responses, which went against the overall hypothesis that the distance between an antibody and the cell membrane defined the mechanisms engaged. Therefore a more thorough investigation was required to clarify the observations made in chapter 4 which fitted into our current understanding of how direct targeting antibodies work.

The first property investigated was the presence of the glycosylation site in CD52. Glycan modification of proteins has been reported to have a number of biological roles including regulating protein function and structure. For wild type CD52, its glycosylation has been proposed to act as an immune defence mechanism where it masks the cell from the innate immune system <sup>297</sup>. Work defining the CAMPATH-1H synthetic epitope (which was devoid of the glycosylation site) reported a lower binding affinity compared to that of wild type CD52, as determined through competitive inhibition assays <sup>319</sup>. This suggested that the presence of a glycan on wild type CD52 may have a secondary stabilising effect for the antibody binding.

Stabilisation of the protein:protein interactions by glycans have been reported in work looking at the interactions between the Fc and FcγR, and also with the ability to activate complement; both of these occurrences are ablated when the glycan is removed from the Fc even though it does not directly form part of the binding site <sup>163</sup>. If the glycan present on CD52 was having a stabilising role on CAMPATH-1H binding it could feasibly improve the overall formation of the Ag:Ab:FcγR complex allowing it to remain stable enough for the phagocytic uptake of the cell to be completed. Based on this hypothesis and the notable absence of any glycosylation in the Cp11-flush construct, the role of this modification was investigated further.

Site-directed mutagenesis – leading to the removal of the Asn linkage – was chosen instead of deglycosylating the protein using an enzyme such as PNGase-F as a 100% removal wouldn't be guaranteed for the assay. Similarly, treating the whole cell with the enzyme would remove any N-linked glycans attached to the endogenous membrane bound proteins present which could impact the cells viability, and other unknown functions. It was assumed that by mutating the Asn residue in CD52, a protein-specific deglycosylation would be achieved, allowing the variability between experimental repeats to be minimal. Confirmation of deglycosylation by

Western blot was not performed due to difficulties detecting the protein from cell lysates – there is no extracellular CD137 that could be used to detect the constructs – however mass spectrometry could be performed to confirm that no glycosylation of the mutant occurred if required <sup>296,341</sup>. Since no Asn was present anywhere within the mature peptide for N-linked glycosylation to occur, we were confident that the CD52-NQ construct would be non-glycosylated. Removing the glycosylation site in CD52 did not impact the ability to be recognised by CAMPATH-1H or the ability to engage phagocytosis after antibody treatment *in vitro*. An alternative explanation was therefore required.

The method of membrane attachment to the cell surface was also investigated. Wild type human CD52 is tethered to the plasma membrane via a GPI anchor, whilst Cp11-flush is attached via a protein transmembrane domain. It was demonstrated that by switching the mature CD52 peptide to either a CAMPATH-1H or rituximab binding epitope, an improvement in ADCP activity was achieved compared to the membrane flush version (Figure 5.8 and Figure 5.9d). This data demonstrated that attachment to a GPI anchor was favourable for phagocytosis, but it did not provide an explanation as to why.

Previous work has demonstrated how protein localisation can alter the effector mechanisms engaged. An example of this is by comparing the ability of the type I and II anti-CD20 mAb to localise CD20 into lipid raft domains. The type I mAbs, which are able to localise into the raft domains, are more able to effectively initiate CDC and the FcγR mediated mechanisms <sup>200</sup> whilst the type II favour the cell-intrinsic mechanisms. The need for clustering and/or mobilisation throughout the plasma membrane is also required for effective FcγR engagement. A polymorphism present in the transmembrane domain of CD32a diminishes its ability to move into lipid raft domains, and as such it is less effective in engaging the FcγR mechanisms due to inefficient receptor clustering <sup>342</sup>. Similarly, activation of FcγR signalling is achieved with clustering of immune complexes rather than with monoclonal Fc, so having the antigen densely clustered in these micro-domains will favour efficient FcγR activation <sup>160,242</sup>.

GPI anchored proteins are traditionally more likely to be found in lipid rafts, which are thicker due to the increased presence of cholesterol in these micro-domains <sup>291,343</sup>. Therefore it is feasible to assume that the GPI anchored proteins generated within this chapter are more likely to be found in these raft domains compared to the membrane tethered versions. If true, by having an increased concentration of antigen in these domains, antibody (and in turn FcγR) clustering would be more efficient and achieved quicker, which in turn would favour efficient activation of the phagocytic pathway <sup>270</sup>.

It is currently unclear what proportion of the membrane flush constructs are present in these lipid raft micro-domains following antibody opsonisation. Attempts to assess raft localisation by flow cytometry has been unsuccessful using the transiently transfected CHO-S cells (data not presented). Similarly, assessment of raft localisation by combining sucrose density centrifugation and western blotting would not work for these proteins as there are no antibodies available for blotting (as no extracellular CD137 is present in the Cp11- and Rp3-flush constructs)<sup>233</sup>. One potential solution would be to incorporate a His-tag or similar tag for use in a Western blot; however, this would alter the final peptide composition extensively and may skew findings if these cells were subsequently used in an ADCP assay to directly compare localisation with function.

As the GPI anchor seems to be important for engaging the ADCP mechanism it seems prudent to compare this observation with the other therapeutically approved targets for mAb immunotherapy. With the exception of CD52, the targets – CD20, CD33 and EGFR family – are not GPI linked, yet they are found either endogenously in the raft domains or localise into them following antibody opsonisation. It is possible that localisation into these domains is an underlying property which makes these so effective as antigens for engaging the FcγR-mediated mechanisms, hypothesised as being critical for efficacious tumour cell depletion<sup>271,344,345</sup>.

One assumption made in the description of GPI anchored proteins was that they tether proteins close to the cell membrane and specifically with regards to this project that it would be held at a similar distance as the Rp3-flush or Cp11-flush constructs. There are few resolved crystal structures for membrane anchored proteins – most have just the extracellular domains resolved. Within those structures none include the GPI anchor itself – partially due to the heterogeneity of this structure and difficulties producing ordered crystals of membrane proteins for diffraction. A resolved structure is available for the complement defence molecule CD59 where the authors have modelled the attached GPI anchor<sup>226</sup>. Based on the size estimations the anchor is far larger than anticipated at approximately 10-15Å in size, however, how much of this anchor protrudes above the cell membrane is uncertain. Assuming CD52 binds a similar sized anchor – that is not buried within the membrane – the CD52 peptide would be at an equivalent distance from the cell membrane as the Rp3-CD137-1d construct generated in this thesis. Rp3-CD137-1d was able to engage ADCP, which would support the original conclusion presented in chapter 4, that the distance an antibody binds from the cell membrane can determine which depletion mechanisms are engaged.

## Chapter 6: *In vivo* investigation of the mAb distance from the cell surface hypothesis

### 6.1 Introduction:

The work hereto presented in this thesis has investigated the role of distance on antibody depletion mechanisms, by looking at the mechanisms individually *in vitro*. As alluded to in the literature review, the current understanding is that the FcγR dependent mechanisms are most important for mAb-mediated cell depletion *in vivo*, and mostly mediated by macrophages rather than cytotoxic NK cells<sup>242,271</sup>. However, how these mechanisms work together (whether synergistically or antagonistically) in the context of a complete immune system is still widely debated, with evidence towards different perspectives<sup>248,250,251</sup>. For example, the relationship between CDC and NK activation is complex, where the activation of complement has been shown to inhibit NK activation therefore preventing ADCC from occurring<sup>251</sup>.

In terms of the distance between an antibody and the cell membrane it was found in Chapter 4 that the cytotoxic mechanisms CDC and ADCC favoured smaller distances (such as targeting the flush and 1-domain construct) since the 8-domain constructs were less able to engage these mechanisms. ADCP required at least one extracellular domain to be present (distance of approximately 10-15Å from the plasma membrane) for the effective engagement of phagocytosis. The data collected so far does not provide an understanding of which construct (and therefore distance from the membrane) would be favourable *in vivo* for the clearance of tumours. Using the constructs generated in chapter 3 in a biologically relevant model provides an opportunity to determine whether CDC, ADCC or ADCP is most important for the clearance of tumour cells in the context of a complete immune system. One hypothesis is that the ability of the Rp3-flush construct to activate the complement system, could promote more effective phagocytosis via the complement components, which in turn overcomes the limitation of activating phagocytosis directly via the FcγR.

In order to test if the mechanistic differences presented earlier *in vitro* translate into differences in the therapeutic efficacy of an antibody *in vivo*, the stably transfected A20 cells were used to establish a tumour model in wild type BALB/c mice. The establishment of a tumour model could then be used to directly compare the response to one of the clinically relevant antibodies when targeting the different sized antigen constructs.

## 6.2 Short Term Tracking of A20 cells:

Initially, it was investigated whether i.v. injected A20 cells could be tracked in the blood over 48 hours if labelled with CFSE. If this was possible, then a direct comparison of antibody depletion between two different cell lines (differentially labelled with CFSE) within the same mouse would be possible. This would be advantageous, as fewer mice would be required overall to compare these cell lines, as well as further reduce experimental variation by having the same immune system present. Therefore there would be no difference in the activation state or environmental variation between individual mice, providing a highly robust comparison of cells expressing different antigen constructs.

Non-transfected (WT-A20) and Rp3-CD137-4d transfected A20 cells were labelled with either 0.5 $\mu$ M or 5 $\mu$ M CFSE, respectively. They were mixed at a 1:1 ratio and a total of  $2 \times 10^7$  cells were injected intravenously (i.v.) into a wild type BALB/c mouse (Figure 6.1a). A blood sample was taken at 24 hours and 48 hours after cell transfer, labelled with B220-PerCP (to identify the B cell population) and screened for CFSE labelled cells. Unfortunately, as presented in Figure 6.1b no CFSE labelled cells were able to be identified in the blood during this time. This result indicates that the A20 tumour cells did not remain in the periphery and are unable to be tracked using this approach.

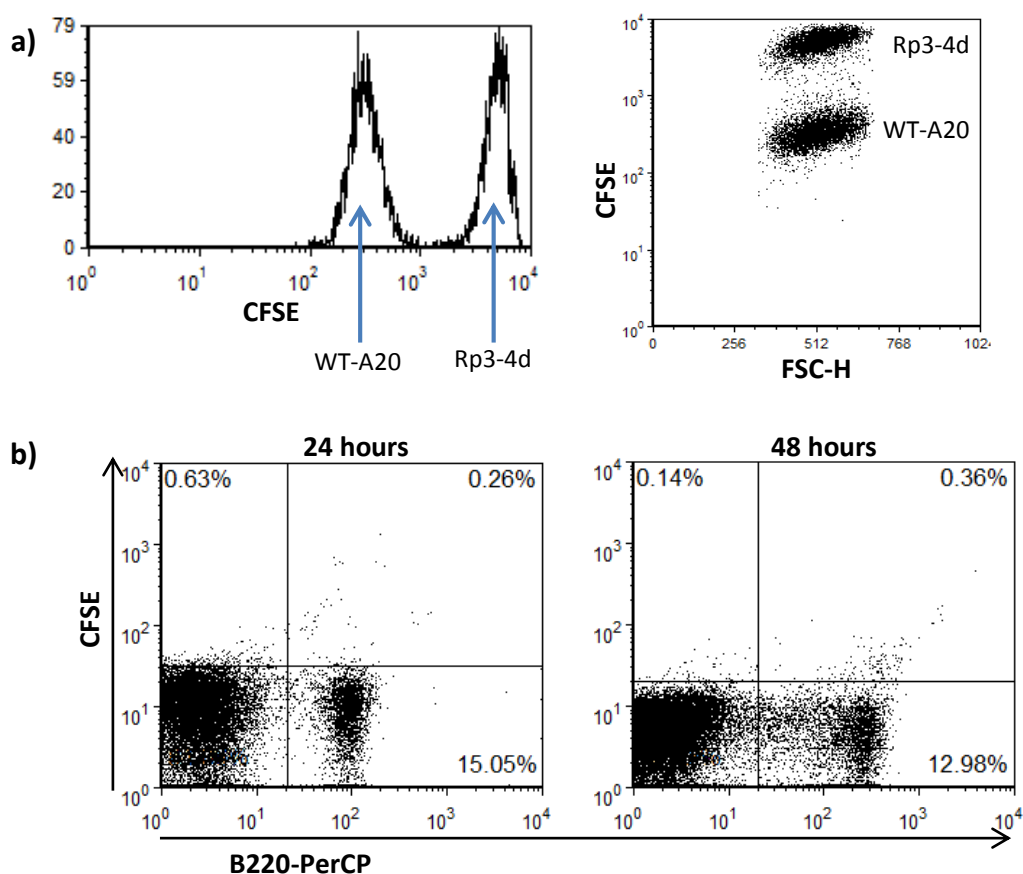


**Figure 6.1: Short term Tracking of CFSE labelled A20 cells in whole blood**

a) Non-transfected A20 (WT-A20) cells labelled with  $0.5\mu\text{M}$  CFSE were mixed at a 1:1 ratio with  $5\mu\text{M}$  CFSE labelled A20 cells expressing Rp3-CD137-4d (Rp3-4d). Histogram and dot plot showing the CFSE labelled cell populations b)  $2 \times 10^7$  cells were administered i.v. into wild type female BALB/c mouse, and blood was taken at 24 and 48 hours, labelled with anti-B220-PerCP and screened by flow cytometry for CFSE labelled cells. No clear CFSE labelled populations (upper quadrants) were present in the samples.

### 6.3 A20 tumour passage:

As it was not possible to track these cells in the blood over 48 hours, an alternative method to investigate antibody therapy was required. A20 cells have been used by other research groups as a disseminated tumour model, where they are found to localise in the liver, spleen and lymph nodes therefore the stably transfected cells were transferred into wild type BALB/c mice to see whether they could proliferate and develop into tumours<sup>330,346</sup>.

Although the A20 cells are lymphocyte-like, they are also larger than endogenous B cells allowing them to be identified based on the FSC/SSC profile. In order to confidently differentiate the A20 cells from the endogenous B-cells additional markers were required, without relying on the scatter profile or the fusion protein (in case the fusion protein was down-regulated when passaged). For this, two markers were chosen: B220 (CD45R) to isolate

the B cell population in conjunction with an anti-idiotype for the BCR of A20 cells (gifted by Prof. R. Levy<sup>347</sup>). Initially, this antibody panel was tested in addition to rituximab by flow cytometry to confirm that the transfected A20 cells could be detected clearly, before transferring into the mouse (presented in Figure 6.2). This provided a method to identify these cells that did not rely solely on the expression of the fusion protein.

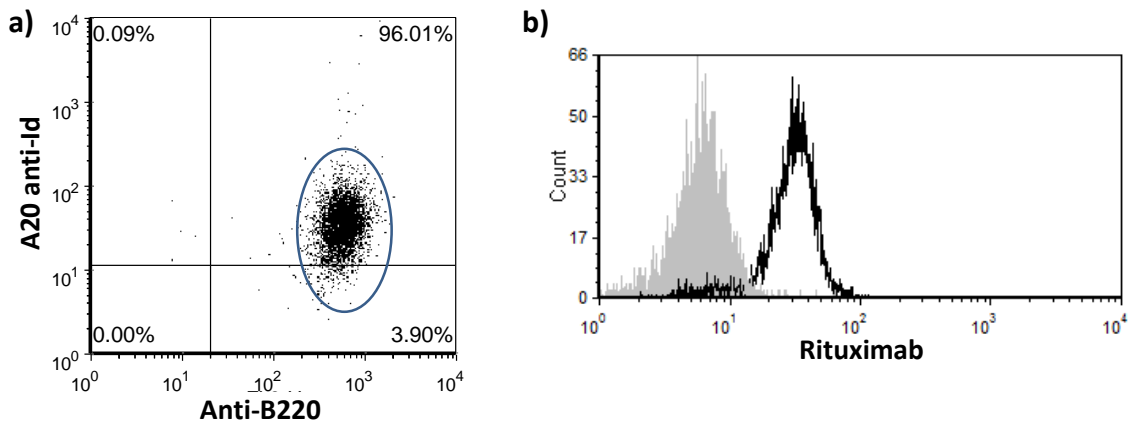


**Figure 6.2: Phenotype of Rp3-CD137-4d transfected A20 cells by flow cytometry**

A20 cells expressing Rp3-CD137-4d were stained with antibodies towards B220, A20 anti-Idiotypic (Id) and rituximab. a) The A20 cells form the Id<sup>+</sup>B220<sup>+</sup> population – circled in the upper right quadrant. b) These cells were gated to define the population where rituximab binding of the fusion protein can be confirmed. This gating strategy was then used in the subsequent analysis of tumour samples collected from future experiments.

Using this antibody panel, it was investigated whether the stably transfected A20 cells were able to proliferate and develop terminal tumours within a wild type BALB/c mouse. Since published work using these cells has reported that it is a disseminated tumour model, a comparison of where the tumour – if established – localised, and whether this was similar between the different transfectants was required. For this set of experiments  $2 \times 10^6$  cells were administered either i.v. or intraperitoneally (i.p.) and the mice were monitored for signs of tumour formation or ill-health.

Mice injected with Rp3-CD137-8d cells developed terminal tumours between 16-18 days, whereas those given either Rp3-flush or Rp3-CD137-4d cells developed terminal tumours between 22-25 days. The spleen, inguinal lymph nodes, liver and any additional tumour masses present were collected from the mice and analysed by flow cytometry using the three-colour panel defined in Figure 6.2. Figure 6.3a presents the gating template used to identify the mononuclear cells based on the FSC/SSC, followed by the proportion of A20 cells present within this gate. Back-gating the B220<sup>+</sup>1G6<sup>+</sup> cells onto the FSC/SSC plot (Figure 6.3b) confirmed the different scatter pattern for the A20 cells previously mentioned compared to the endogenous lymphocytes, providing a third method of identifying and corroborating the



analysis. The raw data from a mouse who received A20 cells expressing Rp3-flush by i.v. injection is presented in Figure 6.3c, to demonstrate the difference in cell localisation between the liver, lymph node and spleen. For the mouse presented in Figure 6.3c, the A20 tumour cells expressing the Rp3-flush construct localised predominantly to the liver and spleen, with very few cells present in the lymph node.

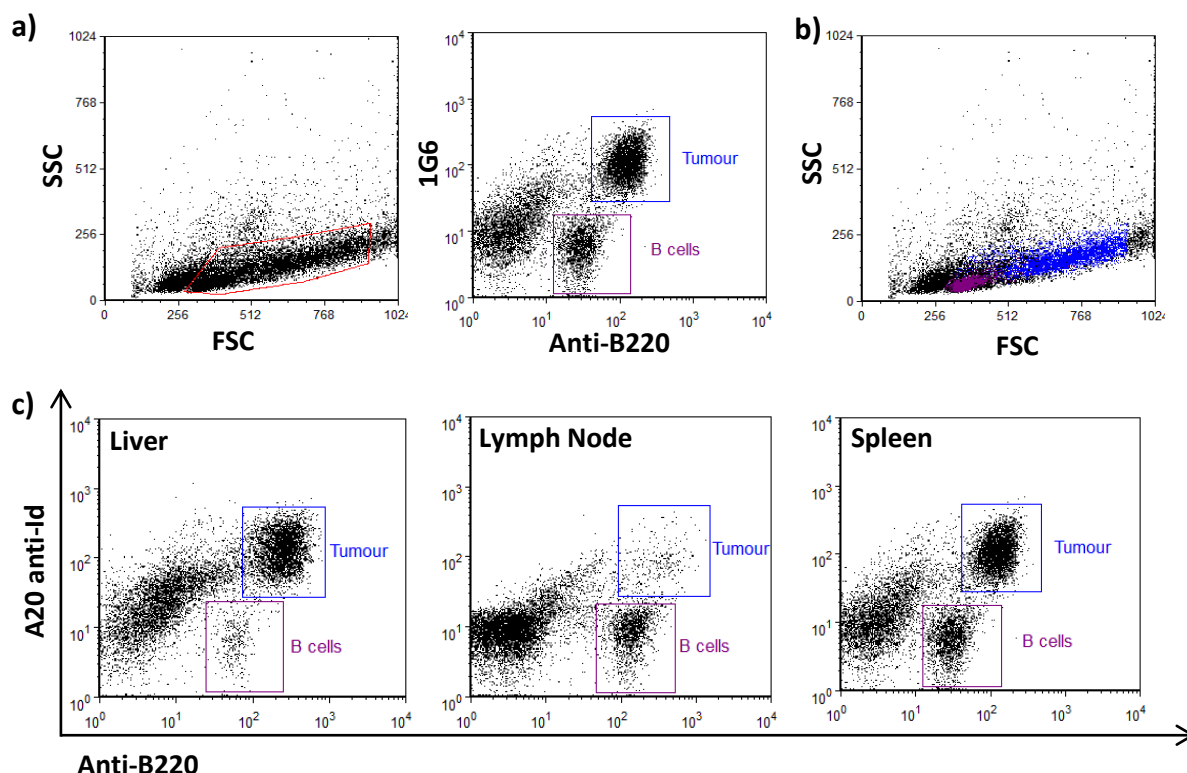


**Figure 6.3: Example of flow cytometry analysis used to quantify A20 cell line passage**

WT BALB/c mouse was received Rp3-flush cells by i.v. injection and monitored for tumour terminal tumour formation. a) Gating analysis template used to identify the presence of Rp3-flush expressing A20 cells from the spleen. The lymphocytes were identified based on the FSC/SSC before identifying the B220<sup>+</sup> Id<sup>+</sup> population (blue gate). b) The A20 cell population (in blue) has a distinct FSC/SSC profile compared to endogenous B cells (purple). c) The data obtained from the liver, inguinal lymph nodes and spleen of a mouse who received Rp3-flush i.v. is presented.

Secondly, these samples were analysed to see if they were still expressing the Rp3-CD137 fusion constructs after growth *in vivo*. For this, the samples were additionally labelled with rituximab or an isotype control. Figure 6.4 displays the results from three individual mice who received A20 cells by i.v. injection expressing the Rp3-flush, Rp3-CD137-4d or Rp3-CD137-8d constructs. In all cases, the A20 cells (defined as B220<sup>+</sup> Id<sup>+</sup> cells) were able to still bind rituximab indicating that the fusion proteins were not lost after growth *in vivo* for 16-22 days.

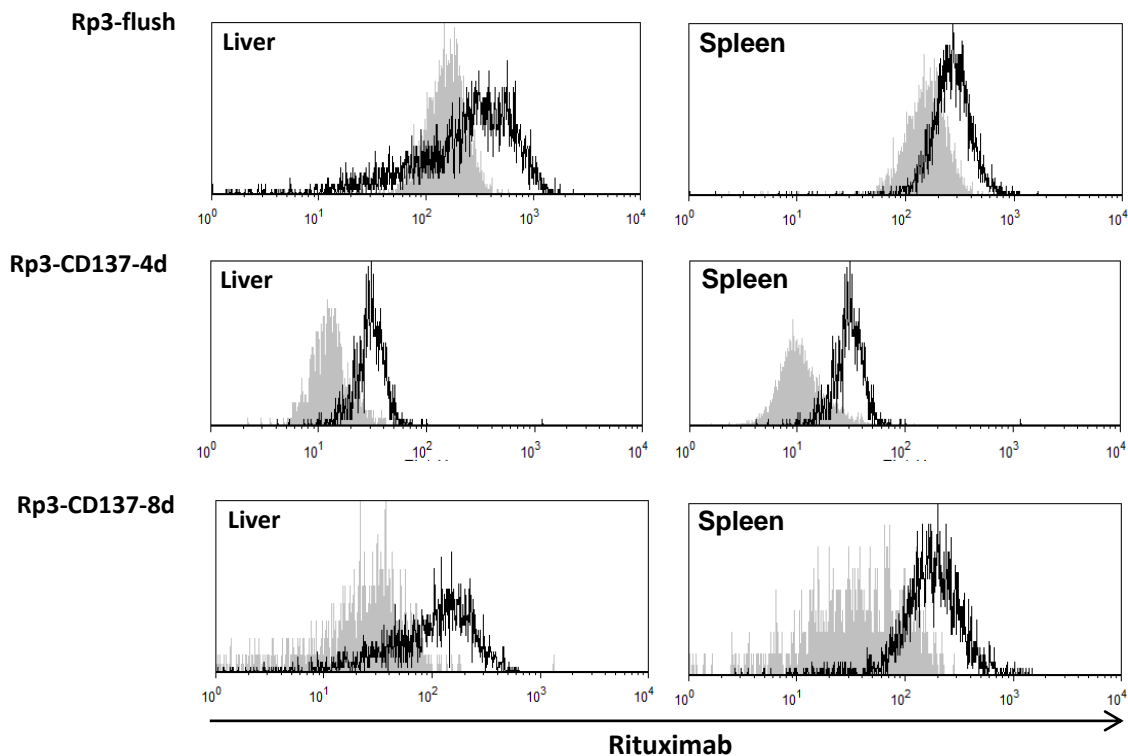


**Figure 6.4: Surface expression of Rp3-CD137 fusion constructs on A20 tumour cells following *in vivo* passage**

Wild type BALB/c mice were injected i.v. with A20 cells expressing either Rp3-flush, Rp3-CD137-4d or Rp3-CD137-8d constructs. Following formation of terminal tumours, the liver and spleen samples were labelled with B220 and anti-Id to identify the A20 cells (using the blue gate from Figure 6.3a). This double positive cell population was then analysed for binding of rituximab (black) or an isotype control (grey) and is presented in the histograms above. There were too few A20 tumour cells from the inguinal lymph node to assess and therefore this data is not shown.

Collating all of the data from the mice given either Rp3-flush, Rp3-CD137-4d or Rp3-CD137-8d cells was presented in Figure 6.5. The main cause of ill-health was due to the tumour colonisation and expansion in the liver, where the majority of the A20 cells localised regardless of the route of administration. Rp3-CD137-4d tumour cells were the most variable in presentation and were more likely to present additional tumour masses within the peritoneal cavity. It could be concluded that cells administered by i.v. tend to localise to the spleen and the liver, whilst those administered i.p. were more likely to form additional tumours within the peritoneal cavity.

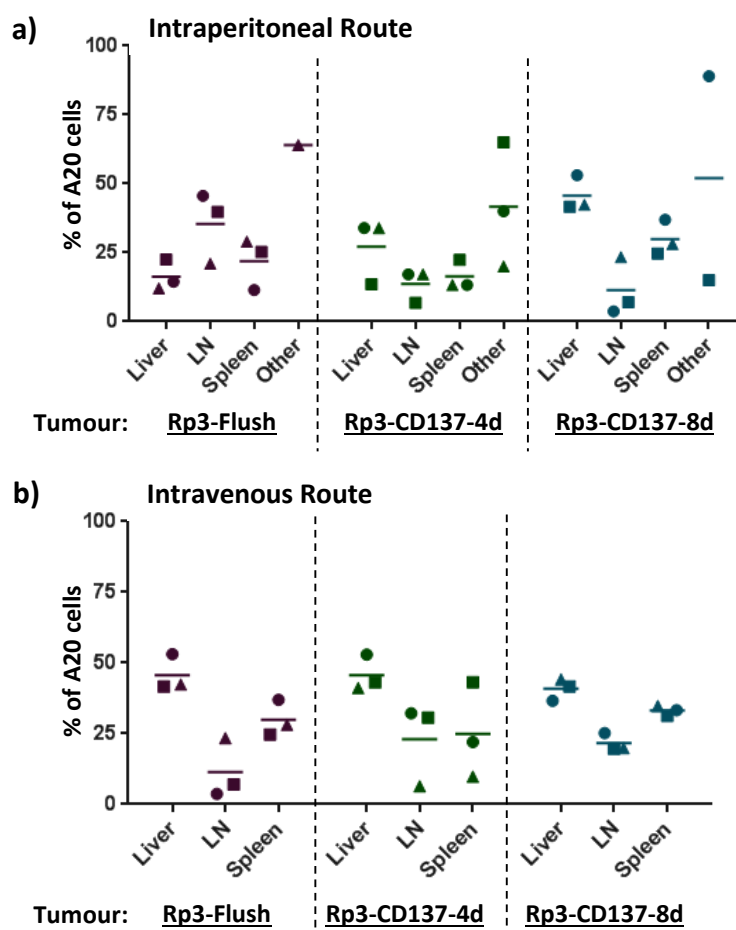


**Figure 6.5: A20 tumour formation after passage into WT BALB/c mice**

$2 \times 10^6$  cells were given by either a) i.p. or b) i.v. injection into wild type female BALB/c mice. Mice were culled when they displayed signs of ill-health/organ enlargement. The spleen, liver, inguinal lymph nodes (LN) and other visible tumour masses (Other) were collected. The organs were processed into single cell suspension and stained with B220-PerCP, Anti-Id-FITC for analysis by flow cytometry using the template presented in Figure 6.3. The percentage of A20 cells present in the lymphocyte gate is presented for all of the mice. Three mice per group from a single experiment are presented, where each individual is presented by a square, circle or triangle. Not all mice had additional tumours therefore there are fewer than three samples for the Other column in Figure 6.5a).

## 6.4 Antibody Immunotherapy Model:

So far it had been demonstrated that although unable to track in the blood over 48 hours, the stably transfected A20 cells were able to develop into tumours *in vivo* that localised primarily in the liver and spleen when given by the i.v. route. Rp3-flush and Rp3-CD137-8d transfected A20 cells were chosen to investigate the response to rituximab therapy – as these two constructs presented the extremes in response to the depletion effector mechanisms investigated *in vitro* in chapter 4.

To observe whether any responses to rituximab therapy were achieved, mice received the transfected A20 cells on day 0 followed by 100µg of rituximab (mIgG2a isotype) 3 days later – as previously done by other groups (Figure 6.6a) <sup>330</sup>. Mice were then monitored for visible signs of ill health, and palpated to assess spleen enlargement; the mice were culled when they reached a humane end point.

The survival of mice given A20 cells expressing either the Rp3-flush or Rp3-CD137-8d construct – with or without 100µg/mL rituximab on day 3 was investigated (Figure 6.6a). Within each tumour cell type, there was no difference between the groups receiving PBS or rituximab in survival (Figure 6.6b). Although no difference in survival was achieved, analysing the tissue collected revealed that the mice who received Rp3-flush tumour cells and rituximab had very little tumour present in the spleen compared to the PBS treated controls (Figure 6.6c). This difference was not seen in mice who received the Rp3-CD137-8d tumour cells. However, regardless of the group, there was a high percentage of tumour cells in the enlarged liver, which resulted in the cause of ill health for all of the mice.

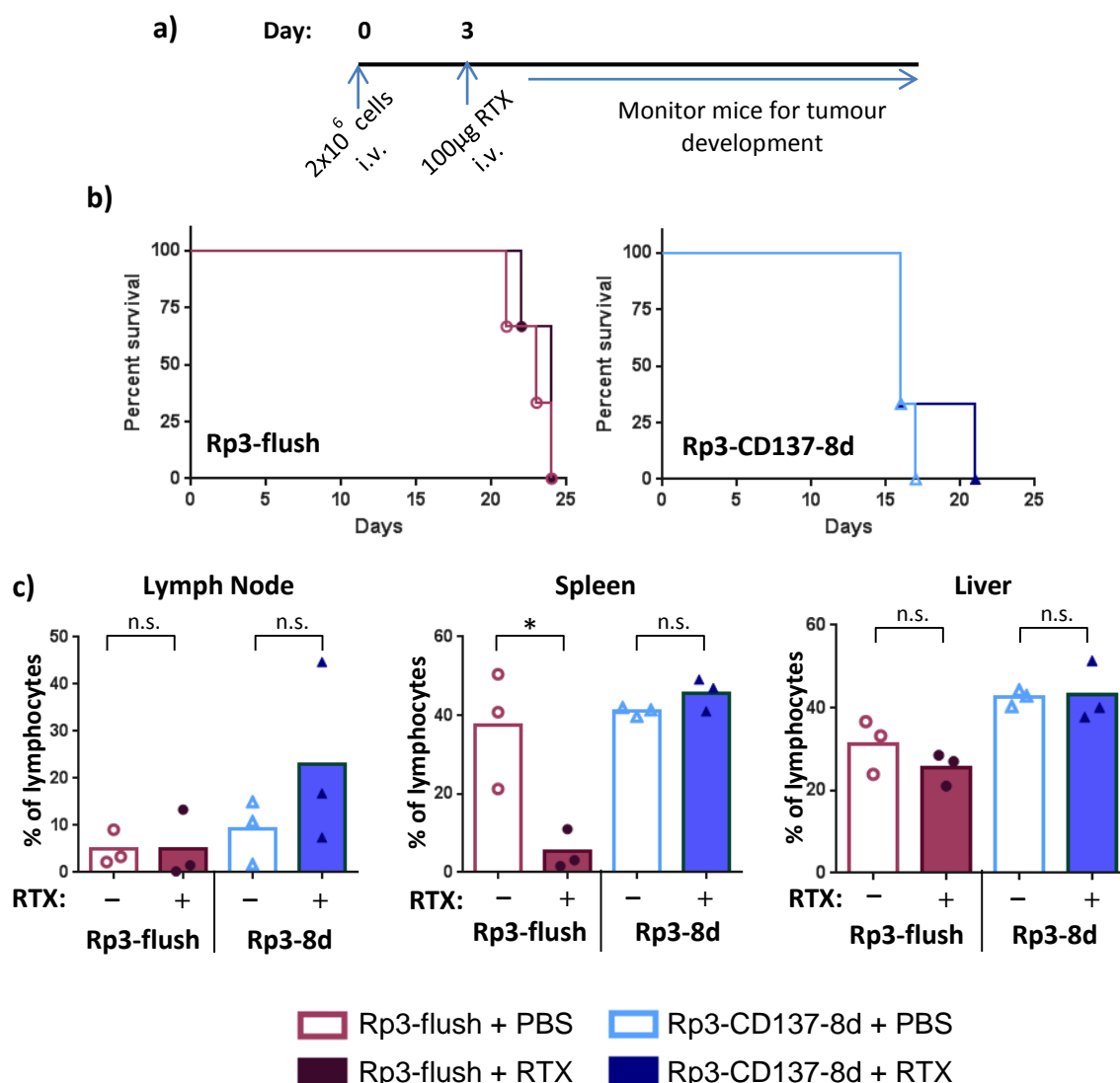


**Figure 6.6: Transfected A20 cells response to rituximab therapy in WT BALB/c mice**

a) Experiment plan; Rp3-flush or Rp3-CD137-8d transfected A20 cells were given to WT BALB/c mice on day 0 followed by 100µg of RTX (rituximab-mIgG2a) or PBS on day 3. Mice were monitored over the next 3 weeks for signs of tumour development. b) No difference in the survival between the mice who received PBS (○) or rituximab (●) was observed for either of the A20 tumour lines. c) Once mice reached terminal tumour load, they were culled and the inguinal lymph nodes, spleen and liver were collected. The percentage of A20 cells present in each tissue were analysed by flow cytometry using the gating template illustrated in Figure 6.3a. Statistical significance was assessed using an unpaired t test where \* =  $p < 0.05$  and n.s. = non-significant

As there was approximately 7 days between the end point of mice that received either the Rp3-flush or Rp3-CD137-8d cells (with the Rp3-CD137-8d tumours becoming terminal more rapidly) an ideal side-by-side comparison was not possible. A comparison of tumour progression and response to therapy at the same time points was required. For this experiment, mice were grouped the same as before and received antibody on day 3; however, 3 mice from each group were culled on day 10 (7 days post-therapy), 16 (end point of Rp3-8d

mice) and day 24 (end point of Rp3-flush mice) – a timeline of the experiment is presented in Figure 6.7a and c.

On day 10 there seems to be no difference between the Rp3-flush and Rp3-CD137-8d tumour cells in the lymph node and spleen, although in the liver mice who received Rp3-CD137-8d cells had a higher percentage of A20 cells present (Figure 6.7b). By day 16 the difference between the two cell lines was most notable, confirming the previous observations that the Rp3-CD137-8d transfected A20 cells develop into terminal tumours quicker than the Rp3-flush A20 tumour. Although this approach did not provide a better means of comparing the responses to therapy between these two cell lines, it did again confirm that rituximab was able to impair tumour growth within the spleen for the Rp3-flush expressing tumours but not the A20 tumours bearing the Rp3-CD137-8d construct.

Together these preliminary experiments indicate that targeting the smaller fusion protein (Rp3-flush) results in an improved clearance of tumour cells in the spleen. Unfortunately this clearance was not sufficient to cure the animals, resulting in no improvement in survival between the groups, as the A20 tumour cells present in the liver seemed untouched by the antibody. Increasing the dose of antibody to 250µg may further improve this clearance however; more work on refining this model is required.

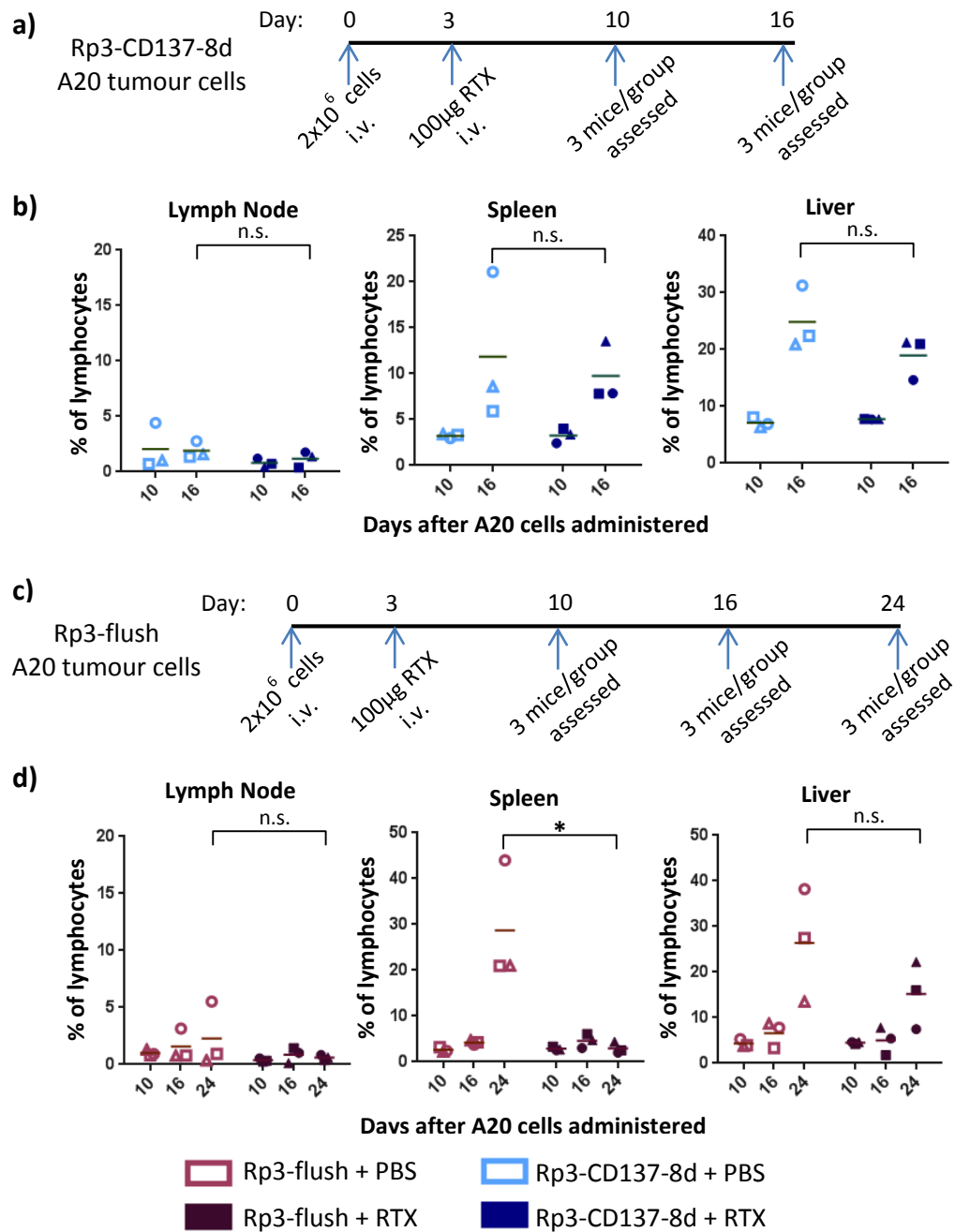


**Figure 6.7: Tracking A20 clearance in response to rituximab therapy at days 10, 16 and 24**

Experiment plan for a) Rp3-CD137-8d and c) Rp3-flush transfected A20 cells given to WT BALB/c mice on day 0 followed by 100µg of rituximab (mIgG2a) or PBS on day 3. The percentage of A20 cells present in the lymph node, spleen and liver from each experiment was analysed by flow cytometry and the results for b) Rp3-CD137-8d (blue) and d) Rp3-flush (pink) expressing tumours is presented. The samples were analysed by flow cytometry using the gating template illustrated in Figure 6.3a. Three mice per group from a single experiment are presented, where each individual is presented by a square, circle or triangle. Statistical significance was assessed using an unpaired t test where \* = p < 0.05 and n.s. = non-significant.

## 6.5 Chapter Discussion:

In this chapter, the ability of rituximab to deplete A20 cells stably transfected with different fusion proteins *in vivo* was investigated. All of the transfected A20 cell lines generated previously (section 4.6) were able to proliferate and develop into terminal tumours when passaged into wild type BALB/c mice. Importantly, following tumour formation, all of the cell lines maintained the expression of the Rp3-fusion proteins. In the therapy model, mice who received rituximab and Rp3-flush expressing tumour cells had an improved clearance in the spleen compared to Rp3-CD137-8d expressing cells, although no improvement in survival was achieved due to the presence of liver metastases.

Although both the Rp3-flush and Rp3-CD137-8d expressing A20 cells were able to form tumours there were differences in the disease presentation between the cell lines. The Rp3-CD137-8d expressing A20 cells were more aggressive resulting in terminal disease approximately a week earlier than the cells transfected with the Rp3-flush construct. This may be a consequence of expanding different clones during the transfection stage (section 4.6) which have different expression levels of receptors controlling migration *in vivo*. Repeating the initial transfection of wild type A20 cells and selecting a number of different clones may allow the isolation of cell lines expressing the fusion proteins which would develop at similar rates when passaged into mice.

There was no difference in the survival following antibody therapy in mice given A20 cells expressing either of the constructs. However, in all of the cases the cause of ill-health was the expansion of tumour within the liver, resulting in an increased pressure within the peritoneal cavity and at least a doubling of the liver mass (data not shown). Due to the tendency of this particular cell line to always migrate towards the liver, developing a more 'splenic' model would be favourable. This could be achieved by collecting the spleen from mice given the transfected A20 cells; isolating the B cell compartment (using a negative selection method such as MACS) and give these cells back into a wild type mouse. Repeated selection in this manner may select for the A20 cells which already express receptors favouring migration to the spleen, thereby resulting in a more splenic model for use in the therapy experiments used in this chapter, which may result in an improvement in survival when liver metastasis are not present (or are at least reduced). However, the extensive culture of transfected cells may alter the morphology and would need to be monitored in order to confirm the expression of the transfected fusion constructs remains.



Based upon the *in vitro* data obtained previously in chapter 4, the difference in the ability of rituximab to delete the cells expressing Rp3-flush and Rp3-CD137-8d could be explained by the effector mechanisms that they engage. Rituximab binding the Rp3-flush construct was best able to engage CDC and ADCC whereas targeting the Rp3-CD137-8d construct was able to engage ADCP and to a lesser extent, ADCC. These data indicate that efficient CDC and/or ADCC were important for the deletion of A20 tumour cells in wild type BALB/c mice.

Previous work which interrogated the mechanisms involved in rituximab clearance of CD20<sup>+</sup> cells demonstrated a dependence on complement being activated <sup>232,241</sup>. These groups used a similar experimental set up to that used in this chapter where CD20<sup>+</sup> cells were injected i.v. into mice followed by rituximab a few days later, therefore the observation that the A20 clearance was witnessed when targeting cells which were susceptible to CDC would corroborate this. However, our own studies using fully syngeneic human CD20 transgenic mouse models indicated that complement was not important for anti-CD20 mediated killing <sup>244,271,293</sup>. This earlier work examined the depletion of endogenous CD20<sup>+</sup> cells throughout the whole mouse, which isn't replicated in the system utilised here <sup>244</sup>, where only relatively few rituximab-epitope positive cells are being targeted. Other differences include the fact that the A20 cells used are a cell-line and malignant. Whether the same trend in the rituximab response can be achieved, when targeting either Rp3-flush or Rp3-CD137-8d constructs, if the A20 tumour is already established, or expressed on endogenous B cells (for example by setting up a retro-transgenic mouse) remains to be determined.

In these immunotherapy experiments A20 tumour cell clearance was only observed in the spleen of mice expressing the Rp3-flush antigen. No significant difference was seen in response to rituximab therapy in the liver of mice given either of the A20 tumour cell lines (Figure 6.6c and Figure 6.7d). The liver is responsible for fighting infection and as such possesses a vast number of macrophages known as Kupffer cells <sup>348</sup>. As macrophages are necessary for the engagement of ADCP, it was expected that although unable to effectively target Rp3-flush for phagocytosis (Chapter 4.3), targeting Rp3-CD137-8d expressing cells with rituximab should have elicited some clearance within this organ <sup>242,349</sup>. One possible reason for the lack of effect was insufficient antibody. Increasing the dose of rituximab given from 100µg to 250µg (as used in other models <sup>244</sup>) may provide better systemic distribution of antibody. Alternatively, repeated doses may deliver more optimal levels of antibody better.

The therapy model used in this chapter has demonstrated that changing the antigen targeted by the same antibody is sufficient to alter the therapeutic response. Further interrogation and refinement of this system is required in order to draw firm conclusions with regards to which

effector mechanisms are most important in defining the overall response. For example, the data so far indicates that CDC and ADCC are important for Rp3-flush cells to be able to be depleted from the spleen of wild type BALB/c mice. Therefore knocking out either of these two pathways should remove this response thereby corroborating the data obtained here. For example the use of Nonobese diabetic (NOD) mice, who exhibit impaired NK function <sup>350</sup>, or C1q<sup>-/-</sup> mice, unable to engage CDC <sup>232</sup>, should distinguish between these two mechanisms for the Rp3-flush expressing tumour cells to define which mechanism is important in the clearance of these cells.

In summary, the impact that distance between an antibody epitope and the cell membrane was investigated in the context of a complete immune system. For this, A20 tumour lines expressing either Rp3-flush or Rp3-CD137-8d were treated with 100µg rituximab (mouse IgG2a isotype) and assessed for evidence of therapeutic benefit. Although no improvement in survival was evident following antibody therapy, tumour clearance from the spleen was apparent in mice that had tumours expressing the Rp3-flush construct only.

## Chapter 7: Discussion and Future Work

This thesis set out to investigate and understand the influence the antigen has on the cell-extrinsic effector mechanisms engaged by direct targeting antibodies. Work in the field has discussed the success of the currently approved targets for immunotherapy and proposed physical features which could explain their success. One particular feature repeatedly mentioned is the overall size of the antigen – particularly when discussing the success of CD20 and CD52 as antigens<sup>237,351</sup> – where small protein targets are preferable compared to larger proteins, such as CD22. For effective lysis via CAR-expressing T cells, binding these smaller proteins (or membrane proximal epitopes within larger proteins) is optimal and implies that the distance between the binding site and the target cell is important, but this property has not been investigated directly with regards to monoclonal antibody immunotherapy<sup>150,152,315</sup>. Previous work which has investigated the role of the antigen in mAb immunotherapy has focussed on the relationship between antigen density and CDC engagement<sup>235</sup>, or compared the function of different antibodies directed towards the same antigen<sup>231,351,352</sup>. What has not been investigated is whether the three cell-extrinsic mechanisms of CDC, ADCP and ADCC, have a similar dependence on the antigen targeted.

The fusion constructs cloned to investigate the distance hypothesis all incorporated the same epitope for a clinically relevant mAb, the same expression vector – therefore translation is under the control of the same promoter – and leader sequence, therefore they should interact with the intracellular trafficking system in a similar manner. Adopting this approach allowed the translation of each individual fusion protein to be as alike as possible. Combining the gene sequence, flow cytometry and Western blot results for the expression of these constructs confirmed that the fusion proteins when expressed were of different sizes.

Their relative distance from the cell membrane was estimated based on the model of CD137 and the TNFR1<sup>320</sup>. In addition, the conformation of the 8-domain construct was assumed to result in a straight extension of the molecule, moving the epitope further away from the cell membrane. This assumes that the molecule does not fold back on itself. Ideally, X-ray crystallography would have been performed for each fusion protein to confirm the size and shape of the various molecules and the presentation of the epitope. In the absence of this, adopting a method which could define the relative size differences between these constructs would provide further confidence in the conclusions drawn based on this panel of fusion proteins. One approach which could confirm that these constructs were holding the functional epitope at different distances from the cell membrane is FRET (Förster resonance energy

transfer). This method has been used by other groups to compare the conformational changes of a receptor, and can usually differentiate between distances of approximately 100Å<sup>353</sup>.

Whilst this window is too large to compare between the 4-domain and 8-domain constructs directly (which has an estimated difference of 80Å), comparing the FRET analysis between the flush or 1-domain construct with the 8-domain would further confirm the distance and orientation of the panel of fusion proteins. As super-resolution microscopy techniques improve, such as those used by Needham *et al.*, are likely to resolve this issue further, allowing the measurement between the 4- and 8-domain constructs to be achieved<sup>354</sup>.

Comparing the engagement of the cytotoxic mechanisms, CDC and ADCC, revealed that the cell lysis reported was diminished as a consequence of targeting the rituximab or CAMPATH-1H epitopes which were more distal from the cell surface. Therefore it suggests that for effective cell lysis to occur, close proximity between the targeted cell and the lytic components (complement or NK cells) is favourable. This observation fits with the current understanding of how the classical complement pathway occurs. Activated complement components have a short half-life in solution unless stabilised, in order to protect the host against self-recognition, therefore being activated in proximity to the targeted cell would be beneficial<sup>210</sup>. As a result of diffusion, more proximal activation of complement would be expected to be more efficient for lysis. As for ADCC mediated death, the release and subsequent uptake of both perforin and granzymes are required<sup>268</sup>. Perforin forms pores in the membrane of a cell, which can allow the influx of granzymes to enter the cell, but also initiate endocytosis of the perforin and granzymes present in close proximity to the targeted cell; they are then released from the endocytic vesicles and initiate apoptosis<sup>264</sup>. These immune synapses are discussed as being similar to that seen in cytotoxic T cells, and the gap between the two cells is small<sup>355</sup>. The work of Choudhuri *et al.* demonstrate that anything larger than 140Å resulted in poor activation due to the synapse being too large<sup>356</sup>. This would support the poor engagement of ADCC observed when targeting the 8-domain constructs as they are estimated to be approximately 160Å in size – not to mention the added distance as a result of the inclusion of both the antibody and FcγR which would make this far larger.

One unexpected result from the investigation of the individual mechanisms was that there were differences in the engagement between the two FcγR-mediated mechanisms, ADCC and ADCP. It was found that for effective ADCP the targeted epitope should be removed from the target cell surface by at least one extracellular domain indicating that the antibody Fc domain is required to be presented further from the cell membrane in order to effectively engage the FcγR, in contrast to the situation with ADCC. Therefore alternative explanations relating the

epitope, mAb and FcγR interactions are required in order to understand how these mechanisms work in the context of the fusion proteins generated.

As discussed previously (in section 4.7) and above, the effector mechanisms following engagement of the FcγR are different for ADCC and ADCP. NK release of cytotoxic granules occurs in a similar process to that seen in T cells, where immunological synapses are formed and the granzymes are released into the synapse between the cells<sup>268,355</sup>. For ADCP, activation of FcγR results in cytoskeletal rearrangements, however rather than forming a comparatively small synapse, they must be able to completely engulf the targeted cell<sup>270,285,345</sup>. This fundamental difference in mechanism provides a potential explanation for the observed distance dependence of the targeted epitope. For example, it is possible, that there is a different dependence in the strength of interaction between the epitope, mAb and the FcγR for these mechanisms. Potentially ADCP requires the FcγR interaction to be maintained during the process of phagocytosis, whilst for ADCC once the FcγR has been activated and the vesicles have started to migrate it may not need to be maintained.

Although it is assumed that by using the same antibody and epitope the binding affinities (in terms of on and off rates) are the same for all constructs; this has not been tested directly. This could be measured using surface plasmon resonance to look at the binding interactions between the mAb and the fusion proteins<sup>160,357</sup>. Assessing the binding kinetics in this manner could confirm that the original hypothesis that the affinities are the same between the constructs. However, this approach looks at the protein:protein interaction on a chip and not in the context of the cell membrane, therefore it wouldn't confirm whether there are other factors that could affect the stability of the bound mAb<sup>357</sup>. For example, binding the membrane-flush constructs will bring the antibody into closer interaction with neighbouring proteins on the cell surface which could alter the stability of the interaction between the mAb and the epitope. These potential differences could be assessed through a competition assay using labelled and unlabelled antibodies towards each fusion protein to compare the relative strength of interactions<sup>319</sup>. A similar level of complexity can be considered for when two cell types (target and effector) become engaged. For example, a membrane proximal epitope will likely bring the target and effector cell more closely together than the membrane distal 8-domain constructs.

The distance hypothesis was challenged in terms of ADCP when comparing the data obtained from the membrane-flush constructs to the wild type CD52 molecule. Wild type CD52 is attached to a GPI anchor and facilitated efficient ADCP, whereas the membrane-flush

constructs (both rituximab and CAMPATH-1H binding) did not. It was concluded that attaching the small peptide epitope to a GPI anchor was required to engage efficient ADCP compared to being attached to the cell membrane via a transmembrane protein domain. Being tethered by a GPI anchor would increase the localisation of the antigen in lipid raft microdomains, therefore promoting clustering of the FcγR within the macrophage for efficient activation<sup>270,337</sup>. However, Type I and II anti-CD20 mAbs are able to engage phagocytosis similarly, suggesting that localisation into these raft domains is not an essential requirement for ADCP<sup>271</sup>.

An alternative hypothesis is that the GPI anchor in CD52 presents the peptide at a more favourable distance from the plasma membrane to engage the FcγR required for phagocytosis. This arises from the observation that ADCP ability was restored when targeting the fusion constructs when at least one extracellular domain is present (section 4.3) and that the proposed size of the GPI anchor in CD59 modelled by Rudd *et al.* is equivalent to 10-15Å<sup>226</sup>. This hypothesis would fit with the recently published observations by Church *et al.* who compared the *in vitro* phagocytosis of CLL cells following treatment with a panel of anti-CD20 mAbs or CAMPATH-1H<sup>358</sup>. CAMPATH-1H was consistently shown to engage ADCP better than ofatumumab (which binds CD20 very close to the cell membrane in the so-called “small loop”<sup>288</sup>) under similar conditions used here. Therefore, assuming that the final distance that ofatumumab binds CD20 from the plasma membrane is comparable with the membrane-flush constructs generated in this thesis; the superior ADCP observed when targeting CD52 may be the result of being presented slightly further away from the cell membrane.

The functional differences between the anti-CD20 mAbs, rituximab and tositumomab, indicate that even when binding at the same distance from the cell membrane there are more factors that dictate how effectively different effector mechanisms are engaged by a mAb<sup>244</sup>. For example, as already discussed in section 1.10, complement activation is facilitated by receptor clustering and raft redistribution of CD20. This suggests that there is a complex relationship between multiple factors of the antigen which work either in synergy or are antagonistic to one another to determine the overall efficacy of the effector mechanisms engaged. Within this thesis the distance between the cell membrane and the bound antibody and, to a lesser extent, the mode of attachment to the cell membrane were investigated. All of the fusion proteins generated in this project position the clinically relevant epitope at the N-terminus of the protein, and are not embedded at different distances within the same antigen. Therefore as an extension to the distance hypothesis, would be to consider whether the position of the epitope within a protein functions the same way as the overall distance from the cell

membrane. For example would an antibody that bound the membrane-proximal domain of WT-CD137, function in the same manner to the 1-domain construct produced in this thesis, or more like the 4-domain construct. One approach to interrogate this would be to produce a panel of fusion proteins which all contained four extracellular domains; however they could be shuffled so that the position of one of the domains moved closer towards the cell membrane. Using human CD137 as a scaffold (and the associated antibodies used to confirm protein in expression as detailed in section 3.3.) would allow the existing validated anti-domain antibodies to be used thereby maintaining consistency between the different constructs. However, the production of a fusion protein in this manner would require further refinement and validation to ensure that the proteins expressed are stable, with no increase in the turnover or mis-folding<sup>359</sup>.

A limitation to the *in vitro* work presented is that it investigates the effector mechanisms in isolation to each other. This has the advantage of depicting and directly monitoring the mechanisms individually, but does not take into account any cross-talk between them. The main point of conflict is with regards to whether complement engagement is beneficial or antagonistic to ADCC<sup>248,250,251</sup>. Further to this is the question of whether the efficient engagement of complement by the membrane-flush construct, is able to engage ADCP via the complement receptors in an FcγR-independent manner. To investigate this question *in vitro* the ADCP assay could be performed in co-culture in the presence of fresh serum containing the lytic complement components. However to be sure that ADCP and not cell-death initiated phagocytosis was measured, MAC-depleted serum (for example lacking in the pore forming components, C8 or C9) may be more suitable. In this situation, the anaphylatoxins, and opsonins (such as iC3b) would still be able to be produced to activate the macrophages, but complement dependent lysis and death would not occur.

One issue in the development of new mAbs for immunotherapy is the high attrition rates between the identification of antibodies in the laboratory and those that demonstrate clinical efficacy<sup>174</sup>. Therefore it was important to confirm whether the differential engagement of the effector mechanisms *in vitro* related to viable differences *in vivo*. In Chapter 6 it was shown that targeting the Rp3-CD137-8d expressing cells with rituximab resulted in no tumour cell clearance whilst targeting the Rp3-flush construct demonstrated clearance within the spleen (although no improvement in survival was achieved due to tumour colonisation of the liver). Relating this finding to the *in vitro* data presented in Chapter 4 implicates CDC and ADCC being involved in the tumour cell clearance in this model, although this has not been directly shown in this therapy model. This observation counters the more recent *in vivo* work which has been

investigating the mechanisms behind the anti-CD20 mAbs<sup>271</sup>. Dissecting antibody effector mechanisms in response to immunotherapy has been achieved through a combination of knock-out mice, or by inhibiting the function of individual components (such as clodronate to deplete macrophages or CVF to inhibit C3)<sup>232,242</sup>. These papers have shown that the therapeutic responses seem to be context dependent and apply a different importance to which effector mechanisms are engaged dependent on whether the cells being depleted are endogenous or present as a transplant model<sup>243</sup>. As discussed previously in section 6.5, applying further methods to the mouse therapy model (such as using NOD mice, C1q<sup>-/-</sup> mice) would provide further evidence towards whether the depletion of Rp3-flush from the spleen was complement or NK cell mediated.

An application of the results from this thesis was to provide an understanding of what would constitute an 'ideal' antigen or epitope to elicit cell depletion in response to mAb immunotherapy. Based on the data generated it could be stated that, in order to best engage all three cell-extrinsic mechanisms, targeting an antigen that is similar in size and position to the 1-domain constructs cloned would be favourable. Reflecting on the clinically approved targets for the direct targeting antibodies (summarised in section 1.10), this pattern is consistent as they are all either a small protein or bind an epitope that lies close to the cell membrane<sup>187,351,360</sup>.

It has been proposed that to improve the safety of CAR-T cells a suicide gene, or protein, needs to be incorporated so that they can be depleted following transplantation into patients<sup>141</sup>. Work by Philip *et al.* proposed and designed a fusion protein which could be targeted by rituximab to remove T cells following antibody treatment, as B cell depletion has proven safe for patients<sup>63,142</sup>. Within this project, the panel of fusion proteins generated have been used as a surrogate for tumour antigens in order to investigate the antibody effector mechanisms engaged for tumour clearance. As it has been shown that the 1-domain construct is best at engaging all three of the antibody effector mechanisms, using a protein of this size would provide efficient clearance of expressing cells. Substituting the rituximab epitope for one that is unique, for example anti-mouse CD20 mAb, would allow the endogenous cells to be untouched, allowing highly specific deletion of the CAR-T cells.

A current avenue for immunotherapy being investigated is the immunomodulation or depletion of regulatory T cells from the tumour microenvironment. Success in this approach removes the requirement to identify tumour specific antigens, therefore (assuming the T cell marker is carefully chosen) this could be used to treat a number of different diseases where infiltrating T<sub>reg</sub> cells are present (such as melanoma and ovarian cancer<sup>361,362</sup>). One potential



target for  $T_{reg}$  depletion is OX40 and CTLA-4. Although they are not unique to  $T_{reg}$  cells, these proteins are upregulated in tumour associated  $T_{regs}$ , and have been investigated as targets for both direct targeting and immunomodulatory mAbs therapies in lymphoma and melanoma<sup>363</sup>. To elicit clearance, rather than activation of these cells, using an antibody directed towards the membrane proximal domains should provide superior clearance compared to other agonistic antibodies. Although whether this approach is best when trying to deplete cells already present in an immune-suppressive environment remains to be seen.

In summary, the work presented within this thesis clearly demonstrates that the antigen can alter the effector mechanisms engaged by an antibody. Effective engagement of CDC and ADCC was diminished when binding the large 8-domain constructs, whilst for effective ADPC at least one domain was required; these findings have been summarised in Figure 7.1. Together, it highlights the importance of understanding and defining the exact epitope bound by an antibody in order to predict the effector mechanisms engaged, as well as providing an alternative approach in altering the therapeutic efficacy *in vivo*. With regards to the therapeutic efficacy, the data suggests that targeting membrane proximal epitopes (or small antigens) are favourable in order to facilitate the depletion mechanisms required to enable clearance in the spleen.

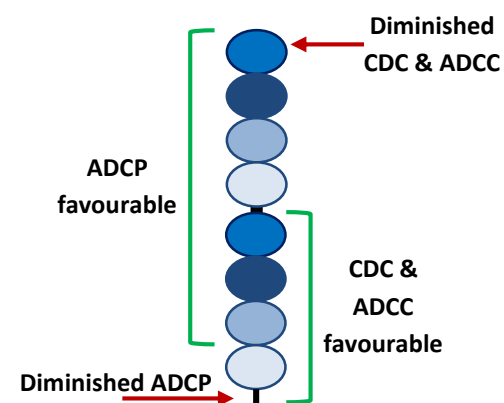


**Figure 7.1: Summary of how distance from the cell membrane impacts the mAb effector mechanisms engaged**

A diagram of the CD137 backbone of the 8-domain construct is presented. The left side of the fusion protein is a summary of the favourable epitope positions for engagement of ADCP; on the right side are the positions for CDC and ADCC (which have similar trends). The green lines depict the range of distances which are efficient at engaging the effector mechanisms. The red arrows depict the position from the cell membrane which results in the diminished engagement of the antibody effector mechanisms.



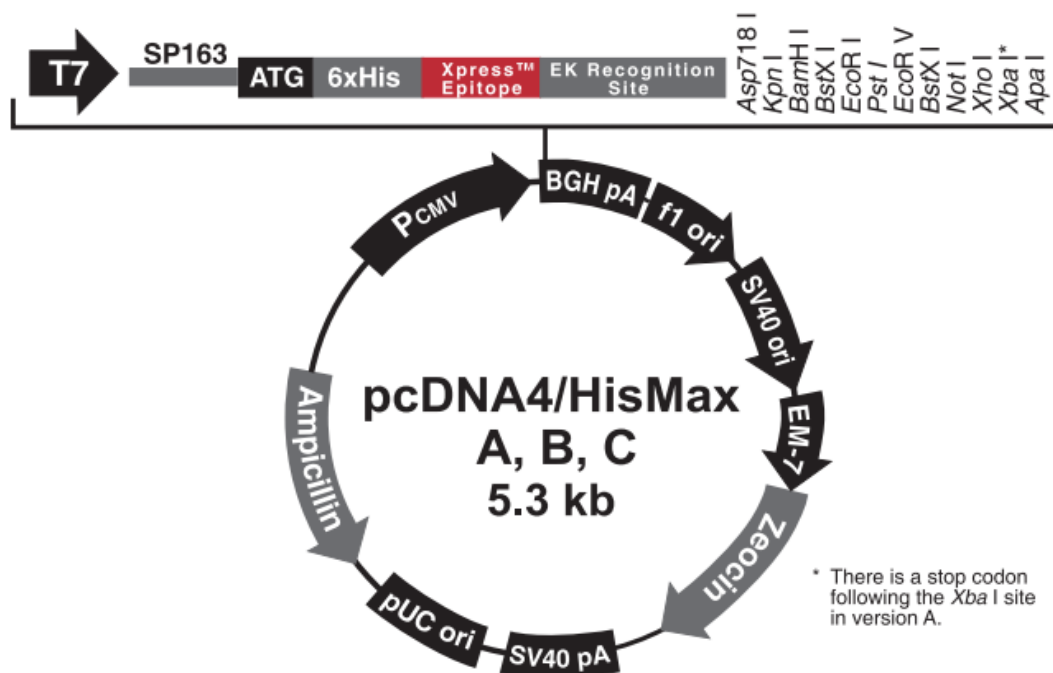
## Appendices:

### Appendix A: Primer sequences used for the generation and DNA sequencing of fusion constructs

Primer Name	Template	Primer Sequence
CD52 -5-XbaI	Human CD52	CAT CTA GAT ACT ACC AAA ATG AAG CGC TTC CTC
HuCD137-R-NotI	Human CD137	AAG CGG CCG CTT GAC TTC CAT TTC ACA GTT
HuCD52-137wt-F	Human CD137	CCC TCA GCA GAC GCC TTG CAG GAT CCT TGT AGT AAC
HuCD52-137wt-R	Human CD137	GTT ACT ACA AGG ATC CTG CAA GGC GTC TGC TGA GGG
HuCD52-137-3d-F	Human CD137	AGC AGC CCC TCA GCA GAC GCC CCC TGT CCT CCA AAT
HuCD52-137-3d-R	Human CD137	ATT TGG AGG ACA GGG GGC GTC TGC TGA GGG GCT GCT
HuCD52-137-2d-F	Human CD137	AGC AGC CCC TCA GCA GAC GCC GAC TGC ACT CCA GGG
HuCD52-137-2d-R	Human CD137	CCC TGG AGT GCA GTC GGC GTC TGC TGA GGG GCT GCT
HuCD52-137-1d-F	Human CD137	AGC AGC CCC TCA GCA GAC GCC GAC TGT TGC TTT GGG
HuCD52-137-1d-R	Human CD137	CCC AAA GCA ACA GTC GGC GTC TGC TGA GGG GCT GCT
CD137-double-F	CD52-137-4d	GAG CCA GGA CAC TCT CCG CAG TTG CAG GAT CCT TGT AGT AAC
CD137-double-R	Human CD137	GTT ACT ACA AGG ATC CTG CAA CTG CGG AGA GTG TCC TGG CTC
CD52-His-F	Human CD137	GAC GCC CAT CAT CAT CAT CAT TTG CAG GAT CCT TGT AGT
CD52-His-R	Human CD52	CTG CAA ATG ATG ATG ATG ATG GGC GTC TGC TGA GGG GCT
CD137-Tm-F	Human CD137	CCC TCA GCA GAC GCC ATC ATC TCC TTC TTT
CD137-Tm-R	Human CD52	AAA GAA GGA GAT GAT GGC GTC TGC TGA GGG

Primer Name	Template	Primer Sequence
SADPL-mut	CD52-137-4d	AGC CCC TCA GCA GAC CCC TTG CAG GAT CCT TGT
SPDAL-mut	CD52-137-4d	ACC AGC AGC CCC TCA CCA GAC GCC TTG CAGGAT
Rp3-CD137-4d	CD52-137-4d or CD52-137-8d	CTG GGT ATG GTA CAG ATA CAA ACT GGA CTC TCA GCC TGCCCA TAC AGC AAC CCC TCA CTA TGC GCC TTG CAG GAT CCT TGT AGT AAC
Rp3-CD137-1d	CD52-137-1d	CTG GTT ATG GTA CAG ATA CAA ACT GGA CTC TCA GCC TGC CCA TAC AGC AAC CCC TCA CTA TGC GCC GAC TGT TGC TTT GGG ACA TTT
Cp11-CD137-4d-F	Human CD137	TGC AGC GGT GGC GGT GGC AGC TTG CAG GAT CCT TGT AGT AAC
Cp11-CD137-4d-R	Cp11-CD8	GTT ACT ACA AGG ATC CTG CAA GCT GCC ACC GCC ACC GCT GCA
Cp11-CD137-1d-F	Human CD137	TGC AGC GGT GGC GGT GGC AGC GAC TGT TGC TTT GGG
Cp11-CD137-1d-R	Cp11-CD8	CCC AAA GCA ACA GTC GCT GCC ACC GCC ACC GCT GCA
Cp11-flush	Rp3-flush	GAC CAC GCC GAT GCC TGC GGC AGC ACC AGC CCC AGC AGC TGC CCA GCC GCC GGC
Cp11-GPI	Rp3-GPI	GGA CTC TCA GCC TGC AGC ACC AGC CCC AGC AGC TGC CCC TCA GCA
CD52-NQ-mut	Human CD52	CTC TCA GGA CAA CAG GAC ACC AGC CAA

## Appendix B: pcDNA4/HisMaxB vector map





## References:

- 1 UK, C. R. Lifetime risk for all cancers combined,  
<<http://www.cancerresearchuk.org/health-professional/cancer-statistics/risk/lifetime-risk#heading-Zero>> (
- 2 Chan, A., Diamandis, E. P. & Blasutig, I. M. Strategies for discovering novel pancreatic cancer biomarkers. *Journal of proteomics* 81, 126-134, doi:10.1016/j.jprot.2012.09.025 (2013).
- 3 CRUK. Melanoma Symptoms, <<http://www.cancerresearchuk.org/about-cancer/type/melanoma/about/melanoma-symptoms>> (2014).
- 4 Katz, S. a. E.-D., W.S. in *Systems Biology of Cancer* (ed Sam Thiagalingham) Ch. 31, 476 (Cambridge University Press, 2015).
- 5 Campo, E. et al. The 2008 WHO classification of lymphoid neoplasms and beyond: evolving concepts and practical applications. *Blood* 117, 5019-5032, doi:10.1182/blood-2011-01-293050 (2011).
- 6 Shanafelt, T. D., Geyer, S. M. & Kay, N. E. Prognosis at diagnosis: integrating molecular biologic insights into clinical practice for patients with CLL. *Blood* 103, 1202-1210, doi:10.1182/blood-2003-07-2281 (2004).
- 7 Vardiman, J. W. et al. The 2008 revision of the World Health Organization (WHO) classification of myeloid neoplasms and acute leukemia: rationale and important changes. *Blood* 114, 937-951, doi:10.1182/blood-2009-03-209262 (2009).
- 8 Jaffe, E. S. The 2008 WHO classification of lymphomas: implications for clinical practice and translational research. *Hematology / the Education Program of the American Society of Hematology. American Society of Hematology. Education Program*, 523-531, doi:10.1182/asheducation-2009.1.523 (2009).
- 9 UK, C. R. Non-Hodgkin lymphoma statistics,  
<<http://www.cancerresearchuk.org/health-professional/cancer-statistics/statistics-by-cancer-type/non-hodgkin-lymphoma#heading-Six>> (2015).
- 10 UK, C. R. Leukaemia (all subsets combined) statistics,  
<<http://www.cancerresearchuk.org/health-professional/cancer-statistics/statistics-by-cancer-type/leukaemia>> (2015).
- 11 WHO. Noncommunicable diseases factsheet,  
<<http://www.who.int/mediacentre/factsheets/fs355/en/>> (2015).
- 12 Tyczynski, J. E., Bray, F. & Parkin, D. M. Lung cancer in Europe in 2000: epidemiology, prevention, and early detection. *The Lancet. Oncology* 4, 45-55 (2003).
- 13 Berman, D. W. & Crump, K. S. A meta-analysis of asbestos-related cancer risk that addresses fiber size and mineral type. *Critical reviews in toxicology* 38 Suppl 1, 49-73, doi:10.1080/10408440802273156 (2008).
- 14 Marks, R. Epidemiology of melanoma. *Clinical and experimental dermatology* 25, 459-463 (2000).
- 15 Baccarelli, A. & Bollati, V. Epigenetics and environmental chemicals. *Current opinion in pediatrics* 21, 243-251 (2009).
- 16 NIH. BRCA1 and BRCA2: Cancer Risk and Genetic Testing,  
<<http://www.cancer.gov/about-cancer/causes-prevention/genetics/brca-fact-sheet>> (2015).
- 17 Pal, T. et al. BRCA1 and BRCA2 mutations account for a large proportion of ovarian carcinoma cases. *Cancer* 104, 2807-2816, doi:10.1002/cncr.21536 (2005).
- 18 Gronwald, J. et al. Tamoxifen and contralateral breast cancer in BRCA1 and BRCA2 carriers: an update. *International journal of cancer. Journal international du cancer* 118, 2281-2284, doi:10.1002/ijc.21536 (2006).

- 19 Chan, H. L. et al. High viral load and hepatitis B virus subgenotype cc are associated with increased risk of hepatocellular carcinoma. *Journal of clinical oncology : official journal of the American Society of Clinical Oncology* 26, 177-182, doi:10.1200/JCO.2007.13.2043 (2008).
- 20 Wheeler, C. M. et al. Cross-protective efficacy of HPV-16/18 AS04-adjuvanted vaccine against cervical infection and precancer caused by non-vaccine oncogenic HPV types: 4-year end-of-study analysis of the randomised, double-blind PATRICIA trial. *The Lancet. Oncology* 13, 100-110, doi:10.1016/S1470-2045(11)70287-X (2012).
- 21 Hanahan, D. & Weinberg, R. A. The hallmarks of cancer. *Cell* 100, 57-70 (2000).
- 22 Hanahan, D. & Weinberg, R. A. Hallmarks of cancer: the next generation. *Cell* 144, 646-674, doi:10.1016/j.cell.2011.02.013 (2011).
- 23 Kastan, M. B. & Bartek, J. Cell-cycle checkpoints and cancer. *Nature* 432, 316-323, doi:10.1038/nature03097 (2004).
- 24 Massague, J. G1 cell-cycle control and cancer. *Nature* 432, 298-306, doi:10.1038/nature03094 (2004).
- 25 Nurse, P. A long twentieth century of the cell cycle and beyond. *Cell* 100, 71-78 (2000).
- 26 Alberts, B. J., A.; Lewis, J.; Raff, M; Roberts, K.; Walter, P. *Molecular Biology of the Cell*. 4th edn, (Garland Science, 2002).
- 27 Murphy, K. *Janeway's Immunobiology*. 8th edn, (Garland Science, 2012).
- 28 Ryan, K. M., Phillips, A. C. & Vousden, K. H. Regulation and function of the p53 tumor suppressor protein. *Current opinion in cell biology* 13, 332-337 (2001).
- 29 Young, K. H. et al. Structural profiles of TP53 gene mutations predict clinical outcome in diffuse large B-cell lymphoma: an international collaborative study. *Blood* 112, 3088-3098, doi:10.1182/blood-2008-01-129783 (2008).
- 30 Amado, R. G. et al. Wild-type KRAS is required for panitumumab efficacy in patients with metastatic colorectal cancer. *Journal of clinical oncology : official journal of the American Society of Clinical Oncology* 26, 1626-1634, doi:10.1200/JCO.2007.14.7116 (2008).
- 31 Prior, I. A., Lewis, P. D. & Mattos, C. A comprehensive survey of Ras mutations in cancer. *Cancer research* 72, 2457-2467, doi:10.1158/0008-5472.CAN-11-2612 (2012).
- 32 Tsao, M. S. et al. Prognostic and predictive importance of p53 and RAS for adjuvant chemotherapy in non small-cell lung cancer. *Journal of clinical oncology : official journal of the American Society of Clinical Oncology* 25, 5240-5247, doi:10.1200/JCO.2007.12.6953 (2007).
- 33 Ouyang, L. et al. Programmed cell death pathways in cancer: a review of apoptosis, autophagy and programmed necrosis. *Cell proliferation* 45, 487-498, doi:10.1111/j.1365-2184.2012.00845.x (2012).
- 34 Elmore, S. Apoptosis: a review of programmed cell death. *Toxicologic pathology* 35, 495-516, doi:10.1080/01926230701320337 (2007).
- 35 Kischkel, F. C. et al. Apo2L/TRAIL-dependent recruitment of endogenous FADD and caspase-8 to death receptors 4 and 5. *Immunity* 12, 611-620 (2000).
- 36 Pezzella, F., Ralfkiaer, E., Gatter, K. C. & Mason, D. Y. The 14;18 translocation in European cases of follicular lymphoma: comparison of Southern blotting and the polymerase chain reaction. *British journal of haematology* 76, 58-64 (1990).
- 37 Vaux, D. L., Cory, S. & Adams, J. M. Bcl-2 gene promotes haemopoietic cell survival and cooperates with c-myc to immortalize pre-B cells. *Nature* 335, 440-442, doi:10.1038/335440a0 (1988).
- 38 Sartorius, U. A. & Krammer, P. H. Upregulation of Bcl-2 is involved in the mediation of chemotherapy resistance in human small cell lung cancer cell lines. *International journal of cancer. Journal international du cancer* 97, 584-592 (2002).
- 39 Monni, O. et al. BCL2 overexpression associated with chromosomal amplification in diffuse large B-cell lymphoma. *Blood* 90, 1168-1174 (1997).



- 40 Bensinger, S. J. & Christofk, H. R. New aspects of the Warburg effect in cancer cell biology. *Seminars in cell & developmental biology* 23, 352-361, doi:10.1016/j.semcdb.2012.02.003 (2012).
- 41 Kim, J. W. & Dang, C. V. Cancer's molecular sweet tooth and the Warburg effect. *Cancer research* 66, 8927-8930, doi:10.1158/0008-5472.CAN-06-1501 (2006).
- 42 Gordan, J. D. & Simon, M. C. Hypoxia-inducible factors: central regulators of the tumor phenotype. *Current opinion in genetics & development* 17, 71-77, doi:10.1016/j.gde.2006.12.006 (2007).
- 43 Kolaczowska, E. & Kubes, P. Neutrophil recruitment and function in health and inflammation. *Nature reviews. Immunology* 13, 159-175, doi:10.1038/nri3399 (2013).
- 44 Kim, R., Emi, M. & Tanabe, K. Cancer immunoediting from immune surveillance to immune escape. *Immunology* 121, 1-14, doi:10.1111/j.1365-2567.2007.02587.x (2007).
- 45 Hunter, K. W., Crawford, N. P. & Alsarraj, J. Mechanisms of metastasis. *Breast cancer research : BCR* 10 Suppl 1, S2, doi:10.1186/bcr1988 (2008).
- 46 Shankaran, V. et al. IFN $\gamma$  and lymphocytes prevent primary tumour development and shape tumour immunogenicity. *Nature* 410, 1107-1111, doi:10.1038/35074122 (2001).
- 47 Watson, N. F. et al. Immunosurveillance is active in colorectal cancer as downregulation but not complete loss of MHC class I expression correlates with a poor prognosis. *International journal of cancer. Journal international du cancer* 118, 6-10, doi:10.1002/ijc.21303 (2006).
- 48 Dunn, G. P., Old, L. J. & Schreiber, R. D. The three Es of cancer immunoediting. *Annual review of immunology* 22, 329-360, doi:10.1146/annurev.immunol.22.012703.104803 (2004).
- 49 Candando, K. M., Lykken, J. M. & Tedder, T. F. B10 cell regulation of health and disease. *Immunological reviews* 259, 259-272, doi:10.1111/imr.12176 (2014).
- 50 Corthay, A. How do regulatory T cells work? *Scandinavian journal of immunology* 70, 326-336, doi:10.1111/j.1365-3083.2009.02308.x (2009).
- 51 Ruffell, B., Affara, N. I. & Coussens, L. M. Differential macrophage programming in the tumor microenvironment. *Trends in immunology* 33, 119-126, doi:10.1016/j.it.2011.12.001 (2012).
- 52 Dunn, G. P., Old, L. J. & Schreiber, R. D. The immunobiology of cancer immunosurveillance and immunoediting. *Immunity* 21, 137-148, doi:10.1016/j.immuni.2004.07.017 (2004).
- 53 Coussens, L. M. & Werb, Z. Inflammation and cancer. *Nature* 420, 860-867, doi:10.1038/nature01322 (2002).
- 54 Smyth, M. J., Dunn, G. P. & Schreiber, R. D. Cancer immunosurveillance and immunoediting: the roles of immunity in suppressing tumor development and shaping tumor immunogenicity. *Advances in immunology* 90, 1-50, doi:10.1016/S0065-2776(06)90001-7 (2006).
- 55 Grivennikov, S. I., Greten, F. R. & Karin, M. Immunity, inflammation, and cancer. *Cell* 140, 883-899, doi:10.1016/j.cell.2010.01.025 (2010).
- 56 Medzhitov, R. & Janeway, C., Jr. Innate immunity. *The New England journal of medicine* 343, 338-344, doi:10.1056/NEJM200008033430506 (2000).
- 57 Fugmann, S. D., Lee, A. I., Shockett, P. E., Villey, I. J. & Schatz, D. G. The RAG proteins and V(D)J recombination: complexes, ends, and transposition. *Annual review of immunology* 18, 495-527, doi:10.1146/annurev.immunol.18.1.495 (2000).
- 58 Melchers, F. et al. Repertoire selection by pre-B-cell receptors and B-cell receptors, and genetic control of B-cell development from immature to mature B cells. *Immunological reviews* 175, 33-46 (2000).

- 59 Edwards, J. C. & Cambridge, G. B-cell targeting in rheumatoid arthritis and other autoimmune diseases. *Nature reviews. Immunology* 6, 394-403, doi:10.1038/nri1838 (2006).
- 60 Krumbholz, M., Derfuss, T., Hohlfeld, R. & Meinl, E. B cells and antibodies in multiple sclerosis pathogenesis and therapy. *Nat Rev Neurol* 8, 613-623, doi:10.1038/nrneurol.2012.203 (2012).
- 61 Muramatsu, M. et al. Class switch recombination and hypermutation require activation-induced cytidine deaminase (AID), a potential RNA editing enzyme. *Cell* 102, 553-563 (2000).
- 62 Crotty, S. Follicular helper CD4 T cells (TFH). *Annual review of immunology* 29, 621-663, doi:10.1146/annurev-immunol-031210-101400 (2011).
- 63 Gurcan, H. M. et al. A review of the current use of rituximab in autoimmune diseases. *International immunopharmacology* 9, 10-25, doi:10.1016/j.intimp.2008.10.004 (2009).
- 64 Vitoria, G. D. & Nussenzweig, M. C. Germinal centers. *Annual review of immunology* 30, 429-457, doi:10.1146/annurev-immunol-020711-075032 (2012).
- 65 Stavnezer, J., Guikema, J. E. & Schrader, C. E. Mechanism and regulation of class switch recombination. *Annual review of immunology* 26, 261-292, doi:10.1146/annurev.immunol.26.021607.090248 (2008).
- 66 Stevenson, F. K. & Caligaris-Cappio, F. Chronic lymphocytic leukemia: revelations from the B-cell receptor. *Blood* 103, 4389-4395, doi:10.1182/blood-2003-12-4312 (2004).
- 67 Iwata, Y. et al. Characterization of a rare IL-10-competent B-cell subset in humans that parallels mouse regulatory B10 cells. *Blood* 117, 530-541, doi:10.1182/blood-2010-07-294249 (2011).
- 68 Kalampokis, I., Yoshizaki, A. & Tedder, T. F. IL-10-producing regulatory B cells (B10 cells) in autoimmune disease. *Arthritis research & therapy* 15 Suppl 1, S1, doi:10.1186/ar3907 (2013).
- 69 Zhang, N. & Bevan, M. J. CD8(+) T cells: foot soldiers of the immune system. *Immunity* 35, 161-168, doi:10.1016/j.immuni.2011.07.010 (2011).
- 70 Zhu, J., Yamane, H. & Paul, W. E. Differentiation of effector CD4 T cell populations (\*). *Annual review of immunology* 28, 445-489, doi:10.1146/annurev-immunol-030409-101212 (2010).
- 71 Korn, T., Bettelli, E., Oukka, M. & Kuchroo, V. K. IL-17 and Th17 Cells. *Annual review of immunology* 27, 485-517, doi:10.1146/annurev.immunol.021908.132710 (2009).
- 72 Szabo, S. J., Sullivan, B. M., Peng, S. L. & Glimcher, L. H. Molecular mechanisms regulating Th1 immune responses. *Annual review of immunology* 21, 713-758, doi:10.1146/annurev.immunol.21.120601.140942 (2003).
- 73 Josefowicz, S. Z., Lu, L. F. & Rudensky, A. Y. Regulatory T cells: mechanisms of differentiation and function. *Annual review of immunology* 30, 531-564, doi:10.1146/annurev.immunol.25.022106.141623 (2012).
- 74 Fontenot, J. D., Gavin, M. A. & Rudensky, A. Y. Foxp3 programs the development and function of CD4+CD25+ regulatory T cells. *Nature immunology* 4, 330-336, doi:10.1038/ni904 (2003).
- 75 Madden, D. R., Gorga, J. C., Strominger, J. L. & Wiley, D. C. The three-dimensional structure of HLA-B27 at 2.1 Å resolution suggests a general mechanism for tight peptide binding to MHC. *Cell* 70, 1035-1048 (1992).
- 76 Neefjes, J., Jongsma, M. L., Paul, P. & Bakke, O. Towards a systems understanding of MHC class I and MHC class II antigen presentation. *Nature reviews. Immunology* 11, 823-836, doi:10.1038/nri3084 (2011).
- 77 Sallusto, F., Geginat, J. & Lanzavecchia, A. Central memory and effector memory T cell subsets: function, generation, and maintenance. *Annual review of immunology* 22, 745-763, doi:10.1146/annurev.immunol.22.012703.104702 (2004).

- 78 Chen, S. et al. Structure-based design of altered MHC class II-restricted peptide ligands with heterogeneous immunogenicity. *Journal of immunology* 191, 5097-5106, doi:10.4049/jimmunol.1300467 (2013).
- 79 Cooper, M. A., Fehniger, T. A. & Caligiuri, M. A. The biology of human natural killer-cell subsets. *Trends in immunology* 22, 633-640 (2001).
- 80 Hart, O. M., Athie-Morales, V., O'Connor, G. M. & Gardiner, C. M. TLR7/8-mediated activation of human NK cells results in accessory cell-dependent IFN-gamma production. *Journal of immunology* 175, 1636-1642 (2005).
- 81 Vivier, E., Tomasello, E., Baratin, M., Walzer, T. & Ugolini, S. Functions of natural killer cells. *Nature immunology* 9, 503-510, doi:10.1038/ni1582 (2008).
- 82 Hatjiharissi, E. et al. Increased natural killer cell expression of CD16, augmented binding and ADCC activity to rituximab among individuals expressing the Fc gamma RIIIa-158 V/V and V/F polymorphism. *Blood* 110, 2561-2564, doi:10.1182/blood-2007-01-070656|10.1182/blood-2007-01-070656 (2007).
- 83 Bendelac, A., Savage, P. B. & Teyton, L. The biology of NKT cells. *Annual review of immunology* 25, 297-336, doi:10.1146/annurev.immunol.25.022106.141711 (2007).
- 84 Geissmann, F. et al. Blood monocytes: distinct subsets, how they relate to dendritic cells, and their possible roles in the regulation of T-cell responses. *Immunology and cell biology* 86, 398-408, doi:10.1038/icb.2008.19 (2008).
- 85 Ziegler-Heitbrock, L. The CD14<sup>+</sup> CD16<sup>+</sup> blood monocytes: their role in infection and inflammation. *Journal of leukocyte biology* 81, 584-592, doi:10.1189/jlb.0806510 (2007).
- 86 Auffray, C., Sieweke, M. H. & Geissmann, F. Blood monocytes: development, heterogeneity, and relationship with dendritic cells. *Annual review of immunology* 27, 669-692, doi:10.1146/annurev.immunol.021908.132557 (2009).
- 87 Geissmann, F. et al. Development of monocytes, macrophages, and dendritic cells. *Science* 327, 656-661, doi:10.1126/science.1178331 (2010).
- 88 Mosser, D. M. The many faces of macrophage activation. *Journal of leukocyte biology* 73, 209-212 (2003).
- 89 Gratchev, A. et al. Mphi1 and Mphi2 can be re-polarized by Th2 or Th1 cytokines, respectively, and respond to exogenous danger signals. *Immunobiology* 211, 473-486, doi:10.1016/j.imbio.2006.05.017 (2006).
- 90 Martinez, F. O. & Gordon, S. The M1 and M2 paradigm of macrophage activation: time for reassessment. *F1000prime reports* 6, 13, doi:10.12703/P6-13 (2014).
- 91 Mantovani, A. et al. The chemokine system in diverse forms of macrophage activation and polarization. *Trends in immunology* 25, 677-686, doi:10.1016/j.it.2004.09.015 (2004).
- 92 Anderson, C. F. & Mosser, D. M. A novel phenotype for an activated macrophage: the type 2 activated macrophage. *Journal of leukocyte biology* 72, 101-106 (2002).
- 93 Park-Min, K. H., Antoniv, T. T. & Ivashkiv, L. B. Regulation of macrophage phenotype by long-term exposure to IL-10. *Immunobiology* 210, 77-86, doi:10.1016/j.imbio.2005.05.002 (2005).
- 94 Adams, S., O'Neill, D. W. & Bhardwaj, N. Recent advances in dendritic cell biology. *Journal of clinical immunology* 25, 177-188 (2005).
- 95 Barchet, W., Blasius, A., Cella, M. & Colonna, M. Plasmacytoid dendritic cells: in search of their niche in immune responses. *Immunologic research* 32, 75-83, doi:10.1385/IR:32:1-3:075 (2005).
- 96 Siegal, F. P. et al. The nature of the principal type 1 interferon-producing cells in human blood. *Science* 284, 1835-1837 (1999).
- 97 Cerutti, A., Qiao, X. & He, B. Plasmacytoid dendritic cells and the regulation of immunoglobulin heavy chain class switching. *Immunology and cell biology* 83, 554-562, doi:10.1111/j.1440-1711.2005.01389.x (2005).

- 98 Aguzzi, A., Kranich, J. & Krautler, N. J. Follicular dendritic cells: origin, phenotype, and function in health and disease. *Trends in immunology* 35, 105-113, doi:10.1016/j.it.2013.11.001 (2014).
- 99 Cyster, J. G. et al. Follicular stromal cells and lymphocyte homing to follicles. *Immunological reviews* 176, 181-193 (2000).
- 100 Nesargikar, P. N., Spiller, B. & Chavez, R. The complement system: history, pathways, cascade and inhibitors. *European journal of microbiology & immunology* 2, 103-111, doi:10.1556/EuJMI.2.2012.2.2 (2012).
- 101 Amulic, B., Cazalet, C., Hayes, G. L., Metzler, K. D. & Zychlinsky, A. Neutrophil function: from mechanisms to disease. *Annual review of immunology* 30, 459-489, doi:10.1146/annurev-immunol-020711-074942 (2012).
- 102 Yu, Y. & Su, K. Neutrophil Extracellular Traps and Systemic Lupus Erythematosus. *Journal of clinical & cellular immunology* 4, doi:10.4172/2155-9899.1000139 (2013).
- 103 Demers, M. & Wagner, D. D. Neutrophil extracellular traps: A new link to cancer-associated thrombosis and potential implications for tumor progression. *Oncoimmunology* 2, e22946, doi:10.4161/onci.22946 (2013).
- 104 Balog, J. et al. Intraoperative tissue identification using rapid evaporative ionization mass spectrometry. *Science translational medicine* 5, 194ra193, doi:10.1126/scitranslmed.3005623 (2013).
- 105 Baskar, R., Lee, K. A., Yeo, R. & Yeoh, K. W. Cancer and radiation therapy: current advances and future directions. *International journal of medical sciences* 9, 193-199, doi:10.7150/ijms.3635 (2012).
- 106 Begg, A. C., Stewart, F. A. & Vens, C. Strategies to improve radiotherapy with targeted drugs. *Nature reviews. Cancer* 11, 239-253, doi:10.1038/nrc3007 (2011).
- 107 DeVita, V. T., Jr. & Chu, E. A history of cancer chemotherapy. *Cancer research* 68, 8643-8653, doi:10.1158/0008-5472.CAN-07-6611 (2008).
- 108 Fleming, R. A. An overview of cyclophosphamide and ifosfamide pharmacology. *Pharmacotherapy* 17, 146S-154S (1997).
- 109 van Maanen, J. M., Retel, J., de Vries, J. & Pinedo, H. M. Mechanism of action of antitumor drug etoposide: a review. *Journal of the National Cancer Institute* 80, 1526-1533 (1988).
- 110 Tacar, O., Sriamornsak, P. & Dass, C. R. Doxorubicin: an update on anticancer molecular action, toxicity and novel drug delivery systems. *The Journal of pharmacy and pharmacology* 65, 157-170, doi:10.1111/j.2042-7158.2012.01567.x (2013).
- 111 Wada, S. et al. Cyclophosphamide augments antitumor immunity: studies in an autochthonous prostate cancer model. *Cancer research* 69, 4309-4318, doi:10.1158/0008-5472.CAN-08-4102 (2009).
- 112 van Moorsel, C. J. et al. Combination chemotherapy studies with gemcitabine and etoposide in non-small cell lung and ovarian cancer cell lines. *Biochemical pharmacology* 57, 407-415 (1999).
- 113 Coiffier, B. et al. CHOP chemotherapy plus rituximab compared with CHOP alone in elderly patients with diffuse large-B-cell lymphoma. *The New England journal of medicine* 346, 235-242, doi:10.1056/NEJMoa011795 (2002).
- 114 Habermann, T. M. et al. Rituximab-CHOP versus CHOP alone or with maintenance rituximab in older patients with diffuse large B-cell lymphoma. *Journal of clinical oncology : official journal of the American Society of Clinical Oncology* 24, 3121-3127, doi:10.1200/JCO.2005.05.1003 (2006).
- 115 Bosch, F. X. et al. Prevalence of human papillomavirus in cervical cancer: a worldwide perspective. *International biological study on cervical cancer (IBSCC) Study Group. Journal of the National Cancer Institute* 87, 796-802 (1995).
- 116 Brody, J., Kohrt, H., Marabelle, A. & Levy, R. Active and passive immunotherapy for lymphoma: proving principles and improving results. *Journal of clinical oncology :*

- official journal of the American Society of Clinical Oncology 29, 1864-1875, doi:10.1200/JCO.2010.33.4623 (2011).
- 117 Freedman, A. et al. Placebo-controlled phase III trial of patient-specific immunotherapy with mitumprotimut-T and granulocyte-macrophage colony-stimulating factor after rituximab in patients with follicular lymphoma. *Journal of clinical oncology : official journal of the American Society of Clinical Oncology* 27, 3036-3043, doi:10.1200/JCO.2008.19.8903 (2009).
- 118 Gao, J., Bernatchez, C., Sharma, P., Radvanyi, L. G. & Hwu, P. Advances in the development of cancer immunotherapies. *Trends in immunology*, doi:S1471-4906(12)00142-1 [pii] 10.1016/j.it.2012.08.004 (2012).
- 119 Redfern, C. H. et al. Phase II trial of idiotype vaccination in previously treated patients with indolent non-Hodgkin's lymphoma resulting in durable clinical responses. *Journal of clinical oncology : official journal of the American Society of Clinical Oncology* 24, 3107-3112, doi:10.1200/JCO.2005.04.4289 (2006).
- 120 Levy, R. et al. Active idiotypic vaccination versus control immunotherapy for follicular lymphoma. *Journal of clinical oncology : official journal of the American Society of Clinical Oncology* 32, 1797-1803, doi:10.1200/JCO.2012.43.9273 (2014).
- 121 Guo, C. et al. Therapeutic cancer vaccines: past, present, and future. *Advances in cancer research* 119, 421-475, doi:10.1016/B978-0-12-407190-2.00007-1 (2013).
- 122 Rice, J., Ottensmeier, C. H. & Stevenson, F. K. DNA vaccines: precision tools for activating effective immunity against cancer. *Nature reviews. Cancer* 8, 108-120, doi:10.1038/nrc2326 (2008).
- 123 Sahota, S. S. et al. PASD1 is a potential multiple myeloma-associated antigen. *Blood* 108, 3953-3955, doi:10.1182/blood-2006-04-014621 (2006).
- 124 Joseph-Pietras, D. et al. DNA vaccines to target the cancer testis antigen PASD1 in human multiple myeloma. *Leukemia* 24, 1951-1959, doi:10.1038/leu.2010.196 (2010).
- 125 Rice, J., Elliott, T., Buchan, S. & Stevenson, F. K. DNA fusion vaccine designed to induce cytotoxic T cell responses against defined peptide motifs: implications for cancer vaccines. *Journal of immunology* 167, 1558-1565 (2001).
- 126 Gilboa, E. DC-based cancer vaccines. *The Journal of clinical investigation* 117, 1195-1203, doi:10.1172/JCI31205 (2007).
- 127 Dillman, R. O. From personalized to patient-specific treatment of metastatic melanoma. *Melanoma Management* 2, 193-197, doi:10.2217/mmt.15.20 (2015).
- 128 Hanna, J. M. G. Cancer vaccines. *Human Vaccines & Immunotherapeutics* 8, 1161-1165, doi:10.4161/hv.21660 (2012).
- 129 Clark, J. & Margolin, K. in *Immunotherapy of Cancer Cancer Drug Discovery and Development* (ed MaryL Disis) Ch. 20, 355-364 (Humana Press, 2006).
- 130 Smith, F. O. et al. Treatment of metastatic melanoma using interleukin-2 alone or in conjunction with vaccines. *Clinical cancer research : an official journal of the American Association for Cancer Research* 14, 5610-5618, doi:10.1158/1078-0432.CCR-08-0116 (2008).
- 131 Yu, A. L. et al. Anti-GD2 antibody with GM-CSF, interleukin-2, and isotretinoin for neuroblastoma. *The New England journal of medicine* 363, 1324-1334, doi:10.1056/NEJMoa0911123 (2010).
- 132 Schwartzentruber, D. J. Guidelines for the safe administration of high-dose interleukin-2. *Journal of immunotherapy* 24, 287-293 (2001).
- 133 Panelli, M. C. et al. Forecasting the cytokine storm following systemic interleukin (IL)-2 administration. *Journal of translational medicine* 2, 17, doi:10.1186/1479-5876-2-17 (2004).
- 134 Rosenberg, S. A., Spiess, P. & Lafreniere, R. A new approach to the adoptive immunotherapy of cancer with tumor-infiltrating lymphocytes. *Science* 233, 1318-1321 (1986).

- 135 Dudley, M. E. et al. Adoptive cell transfer therapy following non-myeloablative but lymphodepleting chemotherapy for the treatment of patients with refractory metastatic melanoma. *Journal of clinical oncology : official journal of the American Society of Clinical Oncology* 23, 2346-2357, doi:10.1200/JCO.2005.00.240 (2005).
- 136 Labarriere, N. et al. Therapeutic efficacy of melanoma-reactive TIL injected in stage III melanoma patients. *Cancer immunology, immunotherapy : CII* 51, 532-538, doi:10.1007/s00262-002-0313-3 (2002).
- 137 Arina, A. et al. Adoptively Transferred Immune T cells Eradicate Established Tumors Despite Cancer-Induced Immune Suppression. *Journal of immunology*, doi:10.4049/jimmunol.1202498 (2013).
- 138 Ho, W. Y., Blattman, J. N., Dossett, M. L., Yee, C. & Greenberg, P. D. Adoptive immunotherapy: engineering T cell responses as biologic weapons for tumor mass destruction. *Cancer cell* 3, 431-437 (2003).
- 139 Grupp, S. A. et al. Chimeric antigen receptor-modified T cells for acute lymphoid leukemia. *The New England journal of medicine* 368, 1509-1518, doi:10.1056/NEJMoa1215134 (2013).
- 140 Porter, D. L., Levine, B. L., Kalos, M., Bagg, A. & June, C. H. Chimeric antigen receptor-modified T cells in chronic lymphoid leukemia. *The New England journal of medicine* 365, 725-733, doi:10.1056/NEJMoa1103849 (2011).
- 141 Ertl, H. C. et al. Considerations for the clinical application of chimeric antigen receptor T cells: observations from a recombinant DNA Advisory Committee Symposium held June 15, 2010. *Cancer research* 71, 3175-3181, doi:10.1158/0008-5472.CAN-10-4035 (2011).
- 142 Philip, B. et al. A highly compact epitope-based marker/suicide gene for easier and safer T-cell therapy. *Blood* 124, 1277-1287, doi:10.1182/blood-2014-01-545020 (2014).
- 143 Weiner, L. M., Murray, J. C. & Shuptrine, C. W. Antibody-based immunotherapy of cancer. *Cell* 148, 1081-1084, doi:S0092-8674(12)00234-6 [pii]10.1016/j.cell.2012.02.034 (2012).
- 144 Reichert, J. M. Therapeutic monoclonal antibodies approved or in review in the European Union or the United States <<http://www.tandf.co.uk/journals/pdf/announcements/kmab-antibodies.pdf>> (2015).
- 145 Weiner, L. M., Surana, R. & Wang, S. Z. Monoclonal antibodies: versatile platforms for cancer immunotherapy. *Nature Reviews Immunology* 10, 317-327, doi:Doi 10.1038/Nri2744 (2010).
- 146 Hodi, F. S. et al. Improved survival with ipilimumab in patients with metastatic melanoma. *The New England journal of medicine* 363, 711-723, doi:10.1056/NEJMoa1003466 (2010).
- 147 Walter, R. B., Raden, B. W., Kamikura, D. M., Cooper, J. A. & Bernstein, I. D. Influence of CD33 expression levels and ITIM-dependent internalization on gemtuzumab ozogamicin-induced cytotoxicity. *Blood* 105, 1295-1302, doi:10.1182/blood-2004-07-2784 (2005).
- 148 von Mehren, M., Adams, G. & Weiner, L. Monoclonal antibody therapy for cancer. *Annual Review of Medicine-Selected Topics in the Clinical Sciences* 54, 343-369, doi:10.1146/annurev.med.54.101601.152442 (2003).
- 149 Beckman, R. A., Weiner, L. M. & Davis, H. M. Antibody constructs in cancer therapy: protein engineering strategies to improve exposure in solid tumors. *Cancer* 109, 170-179, doi:10.1002/cncr.22402 (2007).
- 150 James, S. et al. Antigen sensitivity of CD22-specific chimeric TCR is modulated by target epitope distance from the cell membrane. *Journal of immunology* 180, 7028-7038 (2008).

- 151 Holliger, P., Prospero, T. & Winter, G. "Diabodies": small bivalent and bispecific antibody fragments. *Proceedings of the National Academy of Sciences of the United States of America* 90, 6444-6448 (1993).
- 152 Bluemel, C. et al. Epitope distance to the target cell membrane and antigen size determine the potency of T cell-mediated lysis by BiTE antibodies specific for a large melanoma surface antigen. *Cancer Immunology Immunotherapy* 59, 1197-1209, doi:10.1007/s00262-010-0844-y (2010).
- 153 Todorovska, A. et al. Design and application of diabodies, triabodies and tetrabodies for cancer targeting. *Journal of immunological methods* 248, 47-66 (2001).
- 154 White, A. L. et al. Conformation of the human immunoglobulin G2 hinge imparts superagonistic properties to immunostimulatory anticancer antibodies. *Cancer cell* 27, 138-148, doi:10.1016/j.ccell.2014.11.001 (2015).
- 155 Fagarasan, S. Evolution, development, mechanism and function of IgA in the gut. *Current opinion in immunology* 20, 170-177, doi:10.1016/j.coi.2008.04.002 (2008).
- 156 Bruggemann, M. et al. Comparison of the effector functions of human immunoglobulins using a matched set of chimeric antibodies. *The Journal of experimental medicine* 166, 1351-1361 (1987).
- 157 Boes, M. Role of natural and immune IgM antibodies in immune responses. *Molecular immunology* 37, 1141-1149 (2000).
- 158 Edholm, E. S., Bengten, E. & Wilson, M. Insights into the function of IgD. *Developmental and comparative immunology* 35, 1309-1316, doi:10.1016/j.dci.2011.03.002 (2011).
- 159 Gould, H. J. et al. The biology of IGE and the basis of allergic disease. *Annual review of immunology* 21, 579-628, doi:10.1146/annurev.immunol.21.120601.141103 (2003).
- 160 Bruhns, P. et al. Specificity and affinity of human Fcγ receptors and their polymorphic variants for human IgG subclasses. *Blood* 113, 3716-3725, doi:10.1182/blood-2008-09-179754 (2009).
- 161 Vidarsson, G., Dekkers, G. & Rispens, T. IgG subclasses and allotypes: from structure to effector functions. *Frontiers in immunology* 5, 520, doi:10.3389/fimmu.2014.00520 (2014).
- 162 Arnold, J. N., Wormald, M. R., Sim, R. B., Rudd, P. M. & Dwek, R. A. The impact of glycosylation on the biological function and structure of human immunoglobulins. *Annual review of immunology* 25, 21-50, doi:10.1146/annurev.immunol.25.022106.141702 (2007).
- 163 Rankin, C. T. et al. CD32B, the human inhibitory Fc-γ receptor IIB, as a target for monoclonal antibody therapy of B-cell lymphoma. *Blood* 108, 2384-2391, doi:10.1182/blood-2006-05-020602 (2006).
- 164 Mimura, Y. et al. The influence of glycosylation on the thermal stability and effector function expression of human IgG1-Fc: properties of a series of truncated glycoforms. *Molecular immunology* 37, 697-706 (2000).
- 165 Lively, M. R., Hale, C., Boyce, S., Keen, M. J. & Phillips, J. Glycosylation and biological activity of CAMPATH-1H expressed in different cell lines and grown under different culture conditions. *Glycobiology* 5, 813-822 (1995).
- 166 Sadofsky, M. J. The RAG proteins in V(D)J recombination: more than just a nuclease. *Nucleic acids research* 29, 1399-1409 (2001).
- 167 Wagner, S. D. & Neuberger, M. S. Somatic hypermutation of immunoglobulin genes. *Annual review of immunology* 14, 441-457, doi:10.1146/annurev.immunol.14.1.441 (1996).
- 168 Shulman, Z. et al. T follicular helper cell dynamics in germinal centers. *Science* 341, 673-677, doi:10.1126/science.1241680 (2013).
- 169 Kohler, G. & Milstein, C. Continuous cultures of fused cells secreting antibody of predefined specificity. *Nature* 256, 495-497 (1975).

- 170 Kearney, J. F., Radbruch, A., Liesegang, B. & Rajewsky, K. A new mouse myeloma cell  
line that has lost immunoglobulin expression but permits the construction of antibody-  
secreting hybrid cell lines. *Journal of immunology* 123, 1548-1550 (1979).
- 171 Vatsan, R. S. et al. Regulation of immunotherapeutic products for cancer and FDA's  
role in product development and clinical evaluation. *Journal for immunotherapy of  
cancer* 1, 5, doi:10.1186/2051-1426-1-5 (2013).
- 172 Tjandra, J. J., Ramadi, L. & McKenzie, I. F. Development of human anti-murine antibody  
(HAMA) response in patients. *Immunology and cell biology* 68 ( Pt 6), 367-376,  
doi:10.1038/icb.1990.50 (1990).
- 173 Goldenberg, D. M. The role of radiolabeled antibodies in the treatment of non-  
Hodgkin's lymphoma: the coming of age of radioimmunotherapy. *Critical reviews in  
oncology/hematology* 39, 195-201 (2001).
- 174 Johnson, P. W. & Glennie, M. J. Rituximab: mechanisms and applications. *Br J Cancer*  
85, 1619-1623, doi:S0007092001921275 [pii]10.1054/bjoc.2001.2127 (2001).
- 175 Morrison, S. L., Johnson, M. J., Herzenberg, L. A. & Oi, V. T. Chimeric human antibody  
molecules: mouse antigen-binding domains with human constant region domains.  
*Proceedings of the National Academy of Sciences of the United States of America* 81,  
6851-6855 (1984).
- 176 Riechmann, L., Clark, M., Waldmann, H. & Winter, G. Reshaping human antibodies for  
therapy. *Nature* 332, 323-327, doi:10.1038/332323a0 (1988).
- 177 Sheeley, D. M., Merrill, B. M. & Taylor, L. C. Characterization of monoclonal antibody  
glycosylation: comparison of expression systems and identification of terminal alpha-  
linked galactose. *Analytical biochemistry* 247, 102-110, doi:10.1006/abio.1997.2036  
(1997).
- 178 Jakobovits, A., Amado, R. G., Yang, X., Roskos, L. & Schwab, G. From XenoMouse  
technology to panitumumab, the first fully human antibody product from transgenic  
mice. *Nature biotechnology* 25, 1134-1143, doi:10.1038/nbt1337 (2007).
- 179 Lonberg, N. Human antibodies from transgenic animals. *Nature biotechnology* 23,  
1117-1125, doi:10.1038/nbt1135 (2005).
- 180 Murphy, A. J. et al. Mice with megabase humanization of their immunoglobulin genes  
generate antibodies as efficiently as normal mice. *Proceedings of the National  
Academy of Sciences of the United States of America* 111, 5153-5158,  
doi:10.1073/pnas.1324022111 (2014).
- 181 Hoogenboom, H. R. Selecting and screening recombinant antibody libraries. *Nature  
biotechnology* 23, 1105-1116, doi:10.1038/nbt1126 (2005).
- 182 Soderlind, E. et al. Recombining germline-derived CDR sequences for creating diverse  
single-framework antibody libraries. *Nature biotechnology* 18, 852-856,  
doi:10.1038/78458 (2000).
- 183 Hammers, C. M. & Stanley, J. R. Antibody phage display: technique and applications.  
*The Journal of investigative dermatology* 134, e17, doi:10.1038/jid.2013.521 (2014).
- 184 Reichert, J. M. Antibodies to watch in 2014. *mAbs* 6, 5-14, doi:10.4161/mabs.27333  
(2014).
- 185 Kern, D. J. et al. GA101 induces NK-cell activation and antibody-dependent cellular  
cytotoxicity more effectively than Rituximab when complement is present. *Leukemia &  
lymphoma*, doi:10.3109/10428194.2013.781169 (2013).
- 186 Dalle, S. et al. Preclinical studies on the mechanism of action and the anti-lymphoma  
activity of the novel anti-CD20 antibody GA101. *Molecular cancer therapeutics* 10,  
178-185, doi:10.1158/1535-7163.MCT-10-0385 (2011).
- 187 Oldham, R. J., Cleary, K. L. S. & Cragg, M. S. CD20 and Its Antibodies: Past, Present, and  
Future. *Forum on Immunopathological Diseases and Therapeutics* 5, 7-23,  
doi:10.1615/ForumImmunDisTher.2015014073 (2014).



- 188 Ribas, A. Anti-CTLA4 Antibody Clinical Trials in Melanoma. Update on cancer therapeutics 2, 133-139, doi:10.1016/j.uct.2007.09.001 (2007).
- 189 Blumenthal, G. M. et al. First FDA approval of dual anti-HER2 regimen: pertuzumab in combination with trastuzumab and docetaxel for HER2-positive metastatic breast cancer. *Clinical cancer research : an official journal of the American Association for Cancer Research* 19, 4911-4916, doi:10.1158/1078-0432.CCR-13-1212 (2013).
- 190 Agus, D. B. et al. Targeting ligand-activated ErbB2 signaling inhibits breast and prostate tumor growth. *Cancer cell* 2, 127-137 (2002).
- 191 Shan, D., Ledbetter, J. A. & Press, O. W. Apoptosis of malignant human B cells by ligation of CD20 with monoclonal antibodies. *Blood* 91, 1644-1652 (1998).
- 192 Lavrik, I., Golks, A. & Krammer, P. H. Death receptor signaling. *Journal of cell science* 118, 265-267, doi:10.1242/jcs.01610 (2005).
- 193 Ichikawa, K. et al. Tumoricidal activity of a novel anti-human DR5 monoclonal antibody without hepatocyte cytotoxicity. *Nature medicine* 7, 954-960, doi:10.1038/91000 (2001).
- 194 Yagita, H., Takeda, K., Hayakawa, Y., Smyth, M. J. & Okumura, K. TRAIL and its receptors as targets for cancer therapy. *Cancer science* 95, 777-783 (2004).
- 195 Li, F. & Ravetch, J. V. Apoptotic and antitumor activity of death receptor antibodies require inhibitory Fcγ receptor engagement. *Proceedings of the National Academy of Sciences of the United States of America* 109, 10966-10971, doi:10.1073/pnas.1208698109 (2012).
- 196 Younes, A. et al. A Phase 1b/2 trial of mapatumumab in patients with relapsed/refractory non-Hodgkin's lymphoma. *Br J Cancer* 103, 1783-1787, doi:10.1038/sj.bjc.6605987 (2010).
- 197 Forero-Torres, A. et al. Phase 2, multicenter, open-label study of tigatuzumab (CS-1008), a humanized monoclonal antibody targeting death receptor 5, in combination with gemcitabine in chemotherapy-naïve patients with unresectable or metastatic pancreatic cancer. *Cancer medicine* 2, 925-932, doi:10.1002/cam4.137 (2013).
- 198 Byrd, J. C. et al. The mechanism of tumor cell clearance by rituximab in vivo in patients with B-cell chronic lymphocytic leukemia: evidence of caspase activation and apoptosis induction. *Blood* 99, 1038-1043 (2002).
- 199 van der Kolk, L. E. et al. CD20-induced B cell death can bypass mitochondria and caspase activation. *Leukemia* 16, 1735-1744, doi:10.1038/sj.leu.2402559 (2002).
- 200 Chan, H. T. et al. CD20-induced lymphoma cell death is independent of both caspases and its redistribution into triton X-100 insoluble membrane rafts. *Cancer research* 63, 5480-5489 (2003).
- 201 Ivanov, A. et al. Monoclonal antibodies directed to CD20 and HLA-DR can elicit homotypic adhesion followed by lysosome-mediated cell death in human lymphoma and leukemia cells. *The Journal of clinical investigation* 119, 2143-2159, doi:10.1172/JCI37884 (2009).
- 202 Alduaij, W. et al. Novel type II anti-CD20 monoclonal antibody (GA101) evokes homotypic adhesion and actin-dependent, lysosome-mediated cell death in B-cell malignancies. *Blood* 117, 4519-4529, doi:10.1182/blood-2010-07-296913 (2011).
- 203 Wallis, R., Mitchell, D. A., Schmid, R., Schwaebler, W. J. & Keeble, A. H. Paths reunited: Initiation of the classical and lectin pathways of complement activation. *Immunobiology* 215, 1-11, doi:10.1016/j.imbio.2009.08.006 (2010).
- 204 Ziccardi, R. J. Activation of the early components of the classical complement pathway under physiologic conditions. *Journal of immunology* 126, 1769-1773 (1981).
- 205 Diebolder, C. A. et al. Complement is activated by IgG hexamers assembled at the cell surface. *Science* 343, 1260-1263, doi:10.1126/science.1248943 (2014).
- 206 Ziccardi, R. J. & Cooper, N. R. Activation of C1r by proteolytic cleavage. *Journal of immunology* 116, 504-509 (1976).

- 207 Muller-Eberhard, H. J. The membrane attack complex of complement. Annual review of immunology 4, 503-528, doi:10.1146/annurev.iy.04.040186.002443 (1986).
- 208 Fujita, T. Evolution of the lectin-complement pathway and its role in innate immunity. Nature reviews. Immunology 2, 346-353, doi:10.1038/nri800 (2002).
- 209 Matsushita, M. & Fujita, T. Activation of the classical complement pathway by mannose-binding protein in association with a novel C1s-like serine protease. The Journal of experimental medicine 176, 1497-1502 (1992).
- 210 Pangburn, M. K., Schreiber, R. D. & Muller-Eberhard, H. J. Formation of the initial C3 convertase of the alternative complement pathway. Acquisition of C3b-like activities by spontaneous hydrolysis of the putative thioester in native C3. The Journal of experimental medicine 154, 856-867 (1981).
- 211 Thurman, J. M. & Holers, V. M. The central role of the alternative complement pathway in human disease. Journal of immunology 176, 1305-1310 (2006).
- 212 Rawal, N. & Pangburn, M. K. Structure/function of C5 convertases of complement. International immunopharmacology 1, 415-422 (2001).
- 213 Lambris, J. D., Ricklin, D. & Geisbrecht, B. V. Complement evasion by human pathogens. Nat Rev Microbiol 6, 132-142, doi:nrmicro1824 [pii]10.1038/nrmicro1824 (2008).
- 214 Dunkelberger, J. R. & Song, W. C. Complement and its role in innate and adaptive immune responses. Cell Res 20, 34-50, doi:cr2009139 [pii]10.1038/cr.2009.139 (2010).
- 215 Dinarello, C. A. The C3a receptor, caspase-1, and release of IL-1beta. Blood 122, 3394-3395, doi:10.1182/blood-2013-08-518282 (2013).
- 216 Asgari, E. et al. C3a modulates IL-1beta secretion in human monocytes by regulating ATP efflux and subsequent NLRP3 inflammasome activation. Blood 122, 3473-3481, doi:10.1182/blood-2013-05-502229 (2013).
- 217 Dai, S., Rajaram, M. V., Curry, H. M., Leander, R. & Schlesinger, L. S. Fine tuning inflammation at the front door: macrophage complement receptor 3-mediates phagocytosis and immune suppression for Francisella tularensis. PLoS pathogens 9, e1003114, doi:10.1371/journal.ppat.1003114 (2013).
- 218 van Lookeren Campagne, M., Wiesmann, C. & Brown, E. J. Macrophage complement receptors and pathogen clearance. Cellular microbiology 9, 2095-2102, doi:10.1111/j.1462-5822.2007.00981.x (2007).
- 219 Pettigrew, H. D., Teuber, S. S. & Gershwin, M. E. Clinical significance of complement deficiencies. Annals of the New York Academy of Sciences 1173, 108-123, doi:10.1111/j.1749-6632.2009.04633.x (2009).
- 220 Reid, K. B. & Porter, R. R. The proteolytic activation systems of complement. Annual review of biochemistry 50, 433-464, doi:10.1146/annurev.bi.50.070181.002245 (1981).
- 221 Schreiber, R. D., Pangburn, M. K., Lesavre, P. H. & Muller-Eberhard, H. J. Initiation of the alternative pathway of complement: recognition of activators by bound C3b and assembly of the entire pathway from six isolated proteins. Proceedings of the National Academy of Sciences of the United States of America 75, 3948-3952 (1978).
- 222 Weng, W. K. & Levy, R. Expression of complement inhibitors CD46, CD55, and CD59 on tumor cells does not predict clinical outcome after rituximab treatment in follicular non-Hodgkin lymphoma. Blood 98, 1352-1357 (2001).
- 223 Barilla-LaBarca, M. L., Liszewski, M. K., Lambris, J. D., Hourcade, D. & Atkinson, J. P. Role of membrane cofactor protein (CD46) in regulation of C4b and C3b deposited on cells. Journal of immunology 168, 6298-6304 (2002).
- 224 Johnstone, R. W., Loveland, B. E. & McKenzie, I. F. Identification and quantification of complement regulator CD46 on normal human tissues. Immunology 79, 341-347 (1993).

- 225 Ruiz-Arguelles, A. & Llorente, L. The role of complement regulatory proteins (CD55 and CD59) in the pathogenesis of autoimmune hemocytopenias. *Autoimmunity reviews* 6, 155-161, doi:10.1016/j.autrev.2006.09.008 (2007).
- 226 Rudd, P. M. et al. The glycosylation of the complement regulatory protein, human erythrocyte CD59. *The Journal of biological chemistry* 272, 7229-7244 (1997).
- 227 Gorter, A. & Meri, S. Immune evasion of tumor cells using membrane-bound complement regulatory proteins. *Immunol Today* 20, 576-582, doi:S0167-5699(99)01537-6 [pii] (1999).
- 228 Varela, J. C., Atkinson, C., Woolson, R., Keane, T. E. & Tomlinson, S. Upregulated expression of complement inhibitory proteins on bladder cancer cells and anti-MUC1 antibody immune selection. *International journal of cancer. Journal international du cancer* 123, 1357-1363, doi:10.1002/ijc.23676 (2008).
- 229 Shang, Y. et al. Systematic immunohistochemical analysis of the expression of CD46, CD55, and CD59 in colon cancer. *Archives of pathology & laboratory medicine* 138, 910-919, doi:10.5858/arpa.2013-0064-OA (2014).
- 230 Teeling, J. et al. Characterization of new human CD20 monoclonal antibodies with potent cytolytic activity against non-Hodgkin lymphomas. *Blood* 104, 1793-1800, doi:10.1182/blood-2004-01-0039 | 10.1182/blood-2004-01-0039 (2004).
- 231 Teeling, J. et al. The biological activity of human CD20 monoclonal antibodies is linked to unique epitopes on CD20. *Journal of immunology* 177, 362-371 (2006).
- 232 Cragg, M. S. & Glennie, M. J. Antibody specificity controls in vivo effector mechanisms of anti-CD20 reagents. *Blood* 103, 2738-2743, doi:2003-06-2031 [pii]10.1182/blood-2003-06-2031 (2004).
- 233 Cragg, M. S. et al. Complement-mediated lysis by anti-CD20 mAb correlates with segregation into lipid rafts. *Blood* 101, 1045-1052, doi:2002-06-1761 [pii]10.1182/blood-2002-06-1761 (2003).
- 234 Zent, C. et al. Direct and complement dependent cytotoxicity in CLL cells from patients with high-risk early-intermediate stage chronic lymphocytic leukemia (CLL) treated with alemtuzumab and rituximab. *Leukemia Research* 32, 1849-1856, doi:10.1016/j.leukres.2008.05.014 | 10.1016/j.leukres.2008.05.014 (2008).
- 235 Golay, J. et al. CD20 levels determine the in vitro susceptibility to rituximab and complement of B-cell chronic lymphocytic leukemia: further regulation by CD55 and CD59. *Blood* 98, 3383-3389, doi:10.1182/blood.V98.12.3383 (2001).
- 236 Dechant, M. et al. Complement-dependent tumor cell lysis triggered by combinations of epidermal growth factor receptor antibodies. *Cancer research* 68, 4998-5003, doi:10.1158/0008-5472.CAN-07-6226 (2008).
- 237 XIA, M. et al. STRUCTURE OF THE CAMPATH-1 ANTIGEN, A GLYCOSYLPHOSPHATIDYLINOSITOL-ANCHORED GLYCOPROTEIN WHICH IS AN EXCEPTIONALLY GOOD TARGET FOR COMPLEMENT LYSIS. *Biochemical Journal* 293, 633-640 (1993).
- 238 Zent, C. et al. Alemtuzumab (CAMPATH 1H) does not kill chronic lymphocytic leukemia cells in serum free medium. *Leukemia Research* 28, 495-507, doi:10.1016/j.leukres.2003.09.011 | 10.1016/j.leukres.2003.09.011 (2004).
- 239 Hsu, Y. F. et al. Complement activation mediates cetuximab inhibition of non-small cell lung cancer tumor growth in vivo. *Molecular cancer* 9, 139, doi:10.1186/1476-4598-9-139 (2010).
- 240 El-Sahwi, K. et al. In vitro activity of pertuzumab in combination with trastuzumab in uterine serous papillary adenocarcinoma. *Br J Cancer* 102, 134-143, doi:10.1038/sj.bjc.6605448 (2010).
- 241 Di Gaetano, N. et al. Complement activation determines the therapeutic activity of rituximab in vivo. *Journal of immunology* 171, 1581-1587 (2003).

- 242 Uchida, J. et al. The innate mononuclear phagocyte network depletes B lymphocytes through Fc receptor-dependent mechanisms during anti-CD20 antibody immunotherapy. *The Journal of experimental medicine* 199, 1659-1669, doi:10.1084/jem.20040119 (2004).
- 243 Glennie, M. J., French, R. R., Cragg, M. S. & Taylor, R. P. Mechanisms of killing by anti-CD20 monoclonal antibodies. *Molecular immunology* 44, 3823-3837, doi:S0161-5890(07)00262-3 [pii]10.1016/j.molimm.2007.06.151 (2007).
- 244 Beers, S. A. et al. Type II (tositumomab) anti-CD20 monoclonal antibody out performs type I (rituximab-like) reagents in B-cell depletion regardless of complement activation. *Blood* 112, 4170-4177, doi:10.1182/blood-2008-04-149161 [pii]10.1182/blood-2008-04-149161 (2008).
- 245 Byrd, J. C. et al. Rituximab using a thrice weekly dosing schedule in B-cell chronic lymphocytic leukemia and small lymphocytic lymphoma demonstrates clinical activity and acceptable toxicity. *Journal of clinical oncology : official journal of the American Society of Clinical Oncology* 19, 2153-2164 (2001).
- 246 Kennedy, A. D. et al. Rituximab infusion promotes rapid complement depletion and acute CD20 loss in chronic lymphocytic leukemia. *Journal of immunology* 172, 3280-3288 (2004).
- 247 Golay, J. et al. Biologic response of B lymphoma cells to anti-CD20 monoclonal antibody rituximab in vitro: CD55 and CD59 regulate complement-mediated cell lysis. *Blood* 95, 3900-3908 (2000).
- 248 van Meerten, T., van Rijn, R., Hol, S., Hagenbeek, A. & Ebeling, S. Complement-induced cell death by rituximab depends on CD20 expression level and acts complementary to antibody-dependent cellular cytotoxicity. *Clinical Cancer Research* 12, 4027-4035, doi:10.1158/1078-0432.CCR-06-0066 [pii]10.1158/1078-0432.CCR-06-0066 (2006).
- 249 Derer, S. et al. Impact of Epidermal Growth Factor Receptor (EGFR) Cell Surface Expression Levels on Effector Mechanisms of EGFR Antibodies. *Journal of immunology*, doi:jimmunol.1202037 [pii]10.4049/jimmunol.1202037 (2012).
- 250 Wang, S. Y. et al. Depletion of the C3 component of complement enhances the ability of rituximab-coated target cells to activate human NK cells and improves the efficacy of monoclonal antibody therapy in an in vivo model. *Blood* 114, 5322-5330, doi:10.1182/blood-2009-01-200469 (2009).
- 251 Wang, S. Y., Racila, E., Taylor, R. P. & Weiner, G. J. NK-cell activation and antibody-dependent cellular cytotoxicity induced by rituximab-coated target cells is inhibited by the C3b component of complement. *Blood* 111, 1456-1463, doi:10.1182/blood-2007-02-074716 [pii]10.1182/blood-2007-02-074716 (2008).
- 252 Nimmerjahn, F. & Ravetch, J. V. Fcγ receptors as regulators of immune responses. *Nature reviews. Immunology* 8, 34-47, doi:10.1038/nri2206 (2008).
- 253 Shibata-Koyama, M. et al. Nonfucosylated rituximab potentiates human neutrophil phagocytosis through its high binding for FcγRIIIb and MHC class II expression on the phagocytotic neutrophils. *Exp Hematol* 37, 309-321, doi:S0301-472X(08)00524-9 [pii]10.1016/j.exphem.2008.11.006 (2009).
- 254 Li, X. et al. Allelic-dependent expression of an activating Fc receptor on B cells enhances humoral immune responses. *Science translational medicine* 5, 216ra175, doi:10.1126/scitranslmed.3007097 (2013).
- 255 Bruhns, P. Properties of mouse and human IgG receptors and their contribution to disease models. *Blood* 119, 5640-5649, doi:10.1182/blood-2012-01-380121 (2012).
- 256 Gessner, J. E., Heiken, H., Tamm, A. & Schmidt, R. E. The IgG Fc receptor family. *Annals of hematology* 76, 231-248 (1998).

- 257 Kono, H. et al. Fc gamma RIIB Ile232Thr transmembrane polymorphism associated with human systemic lupus erythematosus decreases affinity to lipid rafts and attenuates inhibitory effects on B cell receptor signaling. *Hum Mol Genet* 14, 2881-2892, doi:Doi 10.1093/Hmg/Ddi320 (2005).
- 258 van der Poel, C. E., Spaapen, R. M., van de Winkel, J. G. & Leusen, J. H. Functional characteristics of the high affinity IgG receptor, FcgammaRI. *Journal of immunology* 186, 2699-2704, doi:10.4049/jimmunol.1003526 (2011).
- 259 Clynes, R. A., Towers, T. L., Presta, L. G. & Ravetch, J. V. Inhibitory Fc receptors modulate in vivo cytotoxicity against tumor targets. *Nature medicine* 6, 443-446, doi:10.1038/74704 (2000).
- 260 Bournazos, S., Hart, S. P., Chamberlain, L. H., Glennie, M. J. & Dransfield, I. Association of FcgammaRIIa (CD32a) with lipid rafts regulates ligand binding activity. *Journal of immunology* 182, 8026-8036, doi:10.4049/jimmunol.0900107 (2009).
- 261 Sanchez-Mejorada, G. & Rosales, C. Signal transduction by immunoglobulin Fc receptors. *Journal of leukocyte biology* 63, 521-533 (1998).
- 262 Nimmerjahn, F. & Ravetch, J. V. Antibodies, Fc receptors and cancer. *Current opinion in immunology* 19, 239-245, doi:S0952-7915(07)00008-8 [pii]10.1016/j.coi.2007.01.005 (2007).
- 263 Koncz, G., Gergely, J. & Sarmay, G. Fc gammaRIIb inhibits both B cell receptor- and CD19-induced Ca<sup>2+</sup> mobilization in Fc gammaR-transfected human B cells. *International immunology* 10, 141-146 (1998).
- 264 Cullen, S. P., Brunet, M. & Martin, S. J. Granzymes in cancer and immunity. *Cell death and differentiation* 17, 616-623, doi:10.1038/cdd.2009.206 (2010).
- 265 Cartron, G. et al. Therapeutic activity of humanized anti-CD20 monoclonal antibody and polymorphism in IgG Fc receptor FcgammaRIIIa gene. *Blood* 99, 754-758 (2002).
- 266 Nimmerjahn, F. & Ravetch, J. V. Fcgamma receptors: old friends and new family members. *Immunity* 24, 19-28, doi:10.1016/j.immuni.2005.11.010 (2006).
- 267 Beum, P. V., Lindorfer, M. A. & Taylor, R. P. Within peripheral blood mononuclear cells, antibody-dependent cellular cytotoxicity of rituximab-opsonized Daudi cells is promoted by NK cells and inhibited by monocytes due to shaving. *Journal of immunology* 181, 2916-2924 (2008).
- 268 Cullen, S. P. & Martin, S. J. Mechanisms of granule-dependent killing. *Cell death and differentiation* 15, 251-262, doi:10.1038/sj.cdd.4402244 (2008).
- 269 Lopez-Albaitero, A. et al. Role of polymorphic Fc gamma receptor IIIa and EGFR expression level in cetuximab mediated, NK cell dependent in vitro cytotoxicity of head and neck squamous cell carcinoma cells. *Cancer immunology, immunotherapy : CII* 58, 1853-1864, doi:10.1007/s00262-009-0697-4 (2009).
- 270 Garcia-Garcia, E. & Rosales, C. Signal transduction during Fc receptor-mediated phagocytosis. *Journal of leukocyte biology* 72, 1092-1108 (2002).
- 271 Tipton, T. R. et al. Antigenic modulation limits the effector cell mechanisms employed by type I anti-CD20 monoclonal antibodies. *Blood*, doi:10.1182/blood-2014-07-588376 (2015).
- 272 Lim, S. H. et al. Fc gamma receptor IIb on target B cells promotes rituximab internalization and reduces clinical efficacy. *Blood* 118, 2530-2540, doi:blood-2011-01-330357 [pii]10.1182/blood-2011-01-330357 (2011).
- 273 Williams, E. L. et al. Immunotherapy targeting inhibitory Fcgamma receptor IIB (CD32b) in the mouse is limited by monoclonal antibody consumption and receptor internalization. *Journal of immunology* 191, 4130-4140, doi:10.4049/jimmunol.1301430 (2013).

- 274 Einfeld, D. A., Brown, J. P., Valentine, M. A., Clark, E. A. & Ledbetter, J. A. Molecular cloning of the human B cell CD20 receptor predicts a hydrophobic protein with multiple transmembrane domains. *The EMBO journal* 7, 711-717 (1988).
- 275 Polyak, M. J., Tailor, S. H. & Deans, J. P. Identification of a cytoplasmic region of CD20 required for its redistribution to a detergent-insoluble membrane compartment. *Journal of immunology* 161, 3242-3248 (1998).
- 276 Shan, D., Ledbetter, J. A. & Press, O. W. Signaling events involved in anti-CD20-induced apoptosis of malignant human B cells. *Cancer immunology, immunotherapy : CII* 48, 673-683 (2000).
- 277 Beers, S. A., Chan, C. H., French, R. R., Cragg, M. S. & Glennie, M. J. CD20 as a target for therapeutic type I and II monoclonal antibodies. *Semin Hematol* 47, 107-114, doi:S0037-1963(10)00002-8 [pii]10.1053/j.seminhematol.2010.01.001 (2010).
- 278 Polyak, M. J., Li, H., Shariat, N. & Deans, J. P. CD20 homo-oligomers physically associate with the B cell antigen receptor. Dissociation upon receptor engagement and recruitment of phosphoproteins and calmodulin-binding proteins. *The Journal of biological chemistry* 283, 18545-18552, doi:10.1074/jbc.M800784200 (2008).
- 279 Morsy, D. E. et al. Reduced T-dependent humoral immunity in CD20-deficient mice. *Journal of immunology* 191, 3112-3118, doi:10.4049/jimmunol.1202098 (2013).
- 280 Kuijpers, T. W. et al. CD20 deficiency in humans results in impaired T cell-independent antibody responses. *The Journal of clinical investigation* 120, 214-222, doi:10.1172/JCI40231 (2010).
- 281 Altschul, S. F. et al. Gapped BLAST and PSI-BLAST: a new generation of protein database search programs. *Nucleic acids research* 25, 3389-3402 (1997).
- 282 Uchida, J. et al. Mouse CD20 expression and function. *International immunology* 16, 119-129 (2004).
- 283 Perosa, F., Favoino, E., Caragnano, M. A. & Dammacco, F. Generation of biologically active linear and cyclic peptides has revealed a unique fine specificity of rituximab and its possible cross-reactivity with acid sphingomyelinase-like phosphodiesterase 3b precursor. *Blood* 107, 1070-1077, doi:2005-04-1769 [pii]10.1182/blood-2005-04-1769 (2006).
- 284 Reff, M. E. et al. Depletion of B cells in vivo by a chimeric mouse human monoclonal antibody to CD20. *Blood* 83, 435-445 (1994).
- 285 Wang, S. Y. & Weiner, G. Complement and cellular cytotoxicity in antibody therapy of cancer. *Expert Opin Biol Ther* 8, 759-768, doi:10.1517/14712598.8.6.759 [pii]10.1517/14712598.8.6.759 (2008).
- 286 Molina, A. A decade of rituximab: improving survival outcomes in non-Hodgkin's lymphoma. *Annual review of medicine* 59, 237-250, doi:10.1146/annurev.med.59.060906.220345 (2008).
- 287 Coiffier, B. et al. Long-term outcome of patients in the LNH-98.5 trial, the first randomized study comparing rituximab-CHOP to standard CHOP chemotherapy in DLBCL patients: a study by the Groupe d'Etudes des Lymphomes de l'Adulte. *Blood* 116, 2040-2045, doi:10.1182/blood-2010-03-276246 (2010).
- 288 Du, J., Yang, H., Guo, Y. & Ding, J. Structure of the Fab fragment of therapeutic antibody Ofatumumab provides insights into the recognition mechanism with CD20. *Molecular immunology* 46, 2419-2423, doi:S0161-5890(09)00179-5 [pii]10.1016/j.molimm.2009.04.009 (2009).
- 289 Cragg, M. S. CD20 antibodies: doing the time warp. *Blood* 118, 219-220, doi:118/2/219 [pii]10.1182/blood-2011-04-346700 (2011).

- 290 Nicolson, G. L. The Fluid-Mosaic Model of Membrane Structure: still relevant to  
understanding the structure, function and dynamics of biological membranes after  
more than 40 years. *Biochimica et biophysica acta* 1838, 1451-1466,  
doi:10.1016/j.bbamem.2013.10.019 (2014).
- 291 Pike, L. J. Lipid rafts: bringing order to chaos. *Journal of lipid research* 44, 655-667,  
doi:10.1194/jlr.R200021-JLR200 (2003).
- 292 Niederfellner, G. et al. Epitope characterization and crystal structure of GA101 provide  
insights into the molecular basis for type I/II distinction of CD20 antibodies. *Blood* 118,  
358-367, doi:10.1182/blood-2010-09-305847 (2011).
- 293 Beers, S. A. et al. Antigenic modulation limits the efficacy of anti-CD20 antibodies:  
implications for antibody selection. *Blood* 115, 5191-5201, doi:blood-2010-01-263533  
[pii]10.1182/blood-2010-01-263533 (2010).
- 294 Waldmann, H. A personal history of the CAMPATH-1H antibody. *Med Oncol* 19 Suppl,  
S3-9 (2002).
- 295 Xia, M. Q., Tone, M., Packman, L., Hale, G. & Waldmann, H. Characterization of the  
CAMPATH-1 (CDw52) antigen: biochemical analysis and cDNA cloning reveal an  
unusually small peptide backbone. *European journal of immunology* 21, 1677-1684,  
doi:10.1002/eji.1830210714 (1991).
- 296 TREUMANN, A., LIFELY, M., SCHNEIDER, P. & FERGUSON, M. PRIMARY STRUCTURE OF  
CD52. *Journal of Biological Chemistry* 270, 6088-6099 (1995).
- 297 Kirchhoff, C. & Hale, G. Cell-to-cell transfer of glycosylphosphatidylinositol-anchored  
membrane proteins during sperm maturation. *Mol Hum Reprod* 2, 177-184 (1996).
- 298 Gilleece, M. H. & Dexter, T. M. Effect of Campath-1H antibody on human  
hematopoietic progenitors in vitro. *Blood* 82, 807-812 (1993).
- 299 Chen, R., Knez, J. J., Merrick, W. C. & Medof, M. E. Comparative efficiencies of C-  
terminal signals of native glycoposphatidylinositol (GPI)-anchored proproteins in  
conferring GPI-anchoring. *J Cell Biochem* 84, 68-83, doi:10.1002/jcb.1267 [pii] (2001).
- 300 Rowan, W. C., Hale, G., Tite, J. P. & Brett, S. J. Cross-linking of the CAMPATH-1 antigen  
(CD52) triggers activation of normal human T lymphocytes. *International immunology*  
7, 69-77 (1995).
- 301 Rowan, W., Tite, J., Topley, P. & Brett, S. J. Cross-linking of the CAMPATH-1 antigen  
(CD52) mediates growth inhibition in human B- and T-lymphoma cell lines, and  
subsequent emergence of CD52-deficient cells. *Immunology* 95, 427-436 (1998).
- 302 Hale, G. et al. Removal of T cells from bone marrow for transplantation: a monoclonal  
antilymphocyte antibody that fixes human complement. *Blood* 62, 873-882 (1983).
- 303 Waldmann, H. et al. Elimination of graft-versus-host disease by in-vitro depletion of  
alloreactive lymphocytes with a monoclonal rat anti-human lymphocyte antibody  
(CAMPATH-1). *Lancet* 2, 483-486 (1984).
- 304 Nuckel, H., Frey, U., Roth, A., Duhrsen, U. & Siffert, W. Alemtuzumab induces  
enhanced apoptosis in vitro in B-cells from patients with chronic lymphocytic leukemia  
by antibody-dependent cellular cytotoxicity. *European Journal of Pharmacology* 514,  
217-224, doi:10.1016/j.ejphar.2005.03.024 (2005).
- 305 Alinari, L. et al. Alemtuzumab (Campath-1H) in the treatment of chronic lymphocytic  
leukemia. *Oncogene* 26, 3644-3653, doi:1210380 [pii]10.1038/sj.onc.1210380 (2007).
- 306 Jones, J. L. & Coles, A. J. Mode of action and clinical studies with alemtuzumab.  
*Experimental neurology* 262 Pt A, 37-43, doi:10.1016/j.expneurol.2014.04.018 (2014).
- 307 Coles, A. J. et al. Alemtuzumab versus interferon beta-1a in early relapsing-remitting  
multiple sclerosis: post-hoc and subset analyses of clinical efficacy outcomes. *The  
Lancet. Neurology* 10, 338-348, doi:10.1016/S1474-4422(11)70020-5 (2011).
- 308 Hiscott, R. FDA Approves Alemtuzumab (Lemtrada) for Relapsing-Remitting MS.  
*Neurology Today* (2014).

- 309 Glennie, M. J. & van de Winkel, J. G. Renaissance of cancer therapeutic antibodies. *Drug Discov Today* 8, 503-510, doi:S1359644603027144 [pii] (2003).
- 310 Domagała, A. & Kurpisz, M. CD52 antigen--a review. *Med Sci Monit* 7, 325-331, doi:1632 [pii] (2001).
- 311 Niwa, R. et al. Enhanced natural killer cell binding and activation by low-fucose IgG1 antibody results in potent antibody-dependent cellular cytotoxicity induction at lower antigen density. *Clinical cancer research : an official journal of the American Association for Cancer Research* 11, 2327-2336, doi:10.1158/1078-0432.CCR-04-2263 (2005).
- 312 Kalyankrishna, S. & Grandis, J. R. Epidermal growth factor receptor biology in head and neck cancer. *Journal of clinical oncology : official journal of the American Society of Clinical Oncology* 24, 2666-2672, doi:10.1200/JCO.2005.04.8306 (2006).
- 313 Magdelaine-Beuzelin, C. et al. Structure-function relationships of the variable domains of monoclonal antibodies approved for cancer treatment. *Critical reviews in oncology/hematology* 64, 210-225, doi:S1040-8428(07)00087-X [pii]10.1016/j.critrevonc.2007.04.011 (2007).
- 314 Pawluczko, A. W. et al. Binding of submaximal C1q promotes complement-dependent cytotoxicity (CDC) of B cells opsonized with anti-CD20 mAbs ofatumumab (OFA) or rituximab (RTX): considerably higher levels of CDC are induced by OFA than by RTX. *Journal of immunology* 183, 749-758, doi:jimmunol.0900632 [pii]10.4049/jimmunol.0900632 (2009).
- 315 Haso, W. et al. Anti-CD22-chimeric antigen receptors targeting B-cell precursor acute lymphoblastic leukemia. *Blood* 121, 1165-1174, doi:10.1182/blood-2012-06-438002 (2013).
- 316 Leupin, O., Zaru, R., Laroche, T., Muller, S. & Valitutti, S. Exclusion of CD45 from the T-cell receptor signaling area in antigen-stimulated T lymphocytes. *Current biology : CB* 10, 277-280 (2000).
- 317 James, J. R. & Vale, R. D. Biophysical mechanism of T-cell receptor triggering in a reconstituted system. *Nature* 487, 64-69, doi:10.1038/nature11220 (2012).
- 318 Vaughan, A. T. et al. Inhibitory FcγRIIb (CD32b) becomes activated by therapeutic mAb in both cis and trans and drives internalization according to antibody specificity. *Blood* 123, 669-677, doi:10.1182/blood-2013-04-490821 (2014).
- 319 Hale, G. Synthetic peptide mimotope of the CAMPATH-1 (CD52) antigen, a small glycosylphosphatidylinositol-anchored glycoprotein. *Immunotechnology* 1, 175-187 (1995).
- 320 Won, E. Y. et al. The structure of the trimer of human 4-1BB ligand is unique among members of the tumor necrosis factor superfamily. *The Journal of biological chemistry* 285, 9202-9210, doi:M109.084442 [pii]10.1074/jbc.M109.084442 (2010).
- 321 Horton, R. M., Hunt, H. D., Ho, S. N., Pullen, J. K. & Pease, L. R. Engineering hybrid genes without the use of restriction enzymes: gene splicing by overlap extension. *Gene* 77, 61-68, doi:0378-1119(89)90359-4 [pii] (1989).
- 322 Technologies, L. TOPO® Blunt-End for subcloning, <<http://www.lifetechnologies.com/uk/en/home/life-science/cloning/topo/topo-blunt-subcloning.html>> (2015).
- 323 Invitrogen. (ed Invitrogen) (Invitrogen Corporation, Carlsbad, CA 92008, 2010).
- 324 Sanchez, A. B. et al. A general process for the development of peptide-based immunoassays for monoclonal antibodies. *Cancer Chemother Pharmacol* 66, 919-925, doi:10.1007/s00280-009-1240-1 (2010).
- 325 Hamaguchi, Y., Xiu, Y., Komura, K., Nimmerjahn, F. & Tedder, T. F. Antibody isotype-specific engagement of Fcγ receptors regulates B lymphocyte depletion during



- CD20 immunotherapy. *The Journal of experimental medicine* 203, 743-753, doi:10.1084/jem.20052283 (2006).
- 326 Invitrogen. (ThermoFisher Scientific).
- 327 Invitrogen. (ThermoFisher Scientific, 2015).
- 328 Scientific, T. (ed Life Technologies) (ThermoFisher Scientific, <https://www.lifetechnologies.com/order/catalog/product/R80007>, 2015).
- 329 Lonza. (Lonza, Online at <http://bio.lonza.com/6.html>, 2012).
- 330 Tutt, A. L. et al. T cell immunity to lymphoma following treatment with anti-CD40 monoclonal antibody. *Journal of immunology* 168, 2720-2728 (2002).
- 331 Kim, K. J., Kanellopoulos-Langevin, C., Merwin, R. M., Sachs, D. H. & Asofsky, R. Establishment and characterization of BALB/c lymphoma lines with B cell properties. *Journal of immunology* 122, 549-554 (1979).
- 332 Zhang, X. et al. CD137 promotes proliferation and survival of human B cells. *Journal of immunology* 184, 787-795, doi:jimmunol.0901619 [pii]10.4049/jimmunol.0901619 (2010).
- 333 Green, D. R., Droin, N. & Pinkoski, M. Activation-induced cell death in T cells. *Immunological reviews* 193, 70-81 (2003).
- 334 Hu, C. Y. et al. Treatment with CD20-specific antibody prevents and reverses autoimmune diabetes in mice. *The Journal of clinical investigation* 117, 3857-3867, doi:10.1172/JCI32405 (2007).
- 335 Minard-Colin, V. et al. Lymphoma depletion during CD20 immunotherapy in mice is mediated by macrophage FcγRI, FcγRIII, and FcγRIV. *Blood* 112, 1205-1213, doi:10.1182/blood-2008-01-135160 (2008).
- 336 Hu, Y. et al. Investigation of the mechanism of action of alemtuzumab in a human CD52 transgenic mouse model. *Immunology* 128, 260-270, doi:10.1111/j.1365-2567.2009.03115.x (2009).
- 337 Paulick, M. G. & Bertozzi, C. R. The glycosylphosphatidylinositol anchor: a complex membrane-anchoring structure for proteins. *Biochemistry* 47, 6991-7000, doi:10.1021/bi8006324 (2008).
- 338 Luckey, M. *Membrane Structural Biology: with biochemical and biophysical foundations*. (Cambridge University Press, 2008).
- 339 Raghupathy, R. et al. Transbilayer lipid interactions mediate nanoclustering of lipid-anchored proteins. *Cell* 161, 581-594, doi:10.1016/j.cell.2015.03.048 (2015).
- 340 James, L. C., Hale, G., Waldmann, H., Bloomer, A. C. & Waldman, H. 1.9 A structure of the therapeutic antibody CAMPATH-1H fab in complex with a synthetic peptide antigen. *J Mol Biol* 289, 293-301, doi:S002228369992750X [pii]10.1006/jmbi.1999.2750 (1999).
- 341 Reusch, D. et al. Comparison of methods for the analysis of therapeutic immunoglobulin G Fc-glycosylation profiles-Part 2: Mass spectrometric methods. *mAbs* 7, 732-742, doi:10.1080/19420862.2015.1045173 (2015).
- 342 Garcia-Garcia, E., Brown, E. J. & Rosales, C. Transmembrane mutations to Fc γRIIA alter its association with lipid rafts: Implications for receptor signaling. *Journal of immunology* 178, 3048-3058 (2007).
- 343 Gowrishankar, K. et al. Active remodeling of cortical actin regulates spatiotemporal organization of cell surface molecules. *Cell* 149, 1353-1367, doi:10.1016/j.cell.2012.05.008 (2012).
- 344 Overdijk, M. B. et al. Antibody-mediated phagocytosis contributes to the anti-tumor activity of the therapeutic antibody daratumumab in lymphoma and multiple myeloma. *mAbs* 7, 311-321, doi:10.1080/19420862.2015.1007813 (2015).
- 345 Weiskopf, K. & Weissman, I. L. Macrophages are critical effectors of antibody therapies for cancer. *mAbs* 7, 303-310, doi:10.1080/19420862.2015.1011450 (2015).

- 346 Schliemann, C. et al. In vivo biotinylation of the vasculature in B-cell lymphoma identifies BST-2 as a target for antibody-based therapy. *Blood* 115, 736-744, doi:10.1182/blood-2009-08-239004 (2010).
- 347 Varghese, B. et al. Generation of CD8+ T cell-mediated immunity against idiotype-negative lymphoma escapees. *Blood* 114, 4477-4485, doi:10.1182/blood-2009-05-223263 (2009).
- 348 Naito, M., Hasegawa, G., Ebe, Y. & Yamamoto, T. Differentiation and function of Kupffer cells. *Medical electron microscopy : official journal of the Clinical Electron Microscopy Society of Japan* 37, 16-28, doi:10.1007/s00795-003-0228-x (2004).
- 349 Gul, N. et al. Macrophages eliminate circulating tumor cells after monoclonal antibody therapy. *The Journal of clinical investigation* 124, 812-823, doi:10.1172/JCI66776 (2014).
- 350 Anderson, M. S. & Bluestone, J. A. The NOD mouse: a model of immune dysregulation. *Annual review of immunology* 23, 447-485, doi:10.1146/annurev.immunol.23.021704.115643 (2005).
- 351 Klein, C. et al. Epitope interactions of monoclonal antibodies targeting CD20 and their relationship to functional properties. *mAbs* 5, 22-33, doi:10.4161/mabs.22771 (2013).
- 352 Shim, H. One target, different effects: a comparison of distinct therapeutic antibodies against the same targets. *Experimental & molecular medicine* 43, 539-549, doi:10.3858/emm.2011.43.10.063 (2011).
- 353 Tynan, C. J. et al. Human epidermal growth factor receptor (EGFR) aligned on the plasma membrane adopts key features of Drosophila EGFR asymmetry. *Molecular and cellular biology* 31, 2241-2252, doi:10.1128/MCB.01431-10 (2011).
- 354 Needham, S. R. et al. Measuring EGFR separations on cells with ~10 nm resolution via fluorophore localization imaging with photobleaching. *PloS one* 8, e62331, doi:10.1371/journal.pone.0062331 (2013).
- 355 Dustin, M. L. & Long, E. O. Cytotoxic immunological synapses. *Immunological reviews* 235, 24-34, doi:10.1111/j.0105-2896.2010.00904.x (2010).
- 356 Choudhuri, K., Wiseman, D., Brown, M. H., Gould, K. & van der Merwe, P. A. T-cell receptor triggering is critically dependent on the dimensions of its peptide-MHC ligand. *Nature* 436, 578-582, doi:10.1038/nature03843 (2005).
- 357 McDonnell, J. M. Surface plasmon resonance: towards an understanding of the mechanisms of biological molecular recognition. *Current opinion in chemical biology* 5, 572-577 (2001).
- 358 Church, A. K. et al. Anti-CD20 monoclonal antibody dependent phagocytosis of chronic lymphocytic leukemia cells by autologous macrophages. *Clinical and experimental immunology*, doi:10.1111/cei.12697 (2015).
- 359 George, R. A. & Heringa, J. An analysis of protein domain linkers: their classification and role in protein folding. *Protein Eng* 15, 871-879 (2002).
- 360 Cho, H. S. et al. Structure of the extracellular region of HER2 alone and in complex with the Herceptin Fab. *Nature* 421, 756-760, doi:nature01392 [pii]10.1038/nature01392 (2003).
- 361 Fialova, A. et al. Dynamics of T-cell infiltration during the course of ovarian cancer: the gradual shift from a Th17 effector cell response to a predominant infiltration by regulatory T-cells. *International journal of cancer. Journal international du cancer* 132, 1070-1079, doi:10.1002/ijc.27759 (2013).
- 362 Jacobs, J. F., Nierkens, S., Figdor, C. G., de Vries, I. J. & Adema, G. J. Regulatory T cells in melanoma: the final hurdle towards effective immunotherapy? *The Lancet. Oncology* 13, e32-42, doi:10.1016/S1470-2045(11)70155-3 (2012).
- 363 Marabelle, A. et al. Depleting tumor-specific Tregs at a single site eradicates disseminated tumors. *The Journal of clinical investigation* 123, 2447-2463, doi:10.1172/JCI64859 (2013).